50/1/2018
ISSN 1338-3523
ISSN 0369-2086

Mineralia Slovaca

50. výročie / 50th Anniversary

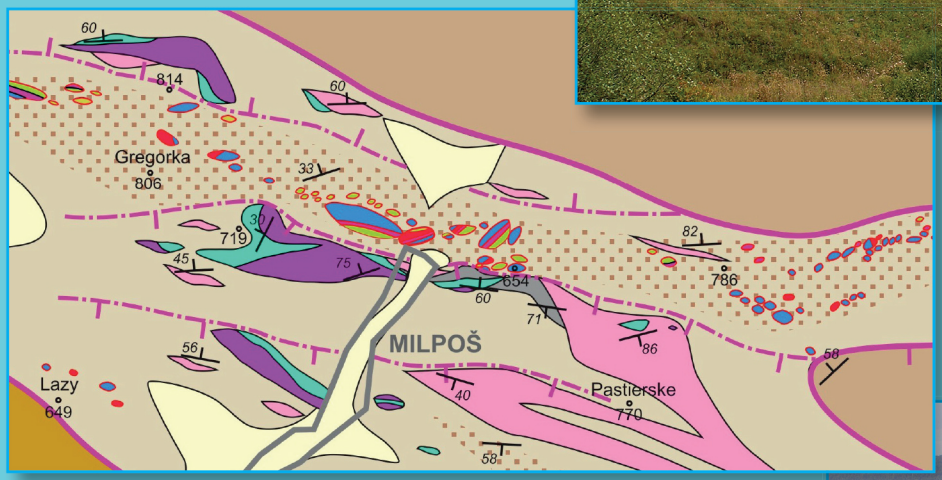

Štátny geologický ústav Dionýza Štúra Bratislava

Mineralia Slovaca

Časopis pre regionálnu a environmentálnu geológiu
a aktivity Slovenskej geologickej spoločnosti a geologických asociácií

PREDSEDA VYDAVATEĽSKEJ RADY – CHAIRMAN OF EDITORIAL BOARD

BRANISLAV ŽEC
Štátny geologický ústav Dionýza Štúra Bratislava

VEDECKÝ REDAKTOR – SCIENTIFIC EDITOR

ZOLTÁN NÉMETH
Štátny geologický ústav Dionýza Štúra
Regionálne centrum Košice
Jesenského 8, 040 01 Košice
zoltan.nemeth@geology.sk

REDAKČNÁ RADA – EDITORIAL BOARD

Igor Broska, Ústav vied o Zemi SAV Bratislava
Klement Fordinál, Štátny geologický ústav D. Štúra Bratislava
Vlasta Jánová, Ministerstvo životného prostredia SR Bratislava
Martin Kováčik, Štátny geologický ústav D. Štúra Bratislava
Peter Malík, Štátny geologický ústav D. Štúra Bratislava
Jozef Michalík, Ústav vied o Zemi SAV Bratislava
Ľubomír Petro, Štátny geologický ústav D. Štúra Košice
Dušan Plašienka, Prírodovedecká fakulta UK Bratislava
Marián Putiš, Prírodovedecká fakulta UK Bratislava
Igor Slaninka, Štátny geologický ústav D. Štúra Bratislava
Ján Soták, Ústav vied o Zemi Banská Bystrica
Ladislav Šimon, Štátny geologický ústav D. Štúra Bratislava
Pavel Uher, Prírodovedecká fakulta UK Bratislava

REDAKCIA – EDITORIAL STAFF

Vedúci oddelenia vydavateľstva ŠGÚDŠ a propagácie – Head of the Department of ŠGÚDŠ Publishers and Promotion

LADISLAV MARTINSKÝ
ladislav.martinsky@geology.sk

Jazykoví redaktori – Lingual editors

Janka Hrtusová – Zoltán Németh
janka.hrtusova@geology.sk

Grafická úprava a technické spracovanie – DTP processing

Slávka Žideková
slavka.zidekova@geology.sk

Mineralia Slovaca (Web ISSN 1338-3523, ISSN 0369-2086), EV 3534/09, vychádza dvakrát ročne. Vydavateľ a tlač: Štátny geologický ústav Dionýza Štúra, Mlynská dolina 1, 817 04 Bratislava, IČO 31 753 604. Dátum vydania čísla 50/1/2018: jún 2018.
Predplatné v roku 2018 vrátane DPH, poštovného a balného pre jednotlivcov 16,50 €, pre členov SGS a geologických asociácií 15,40 €, pre organizácie v SR 22,00 €. Cena jednotlivého čísla pri osobnom nákupe v predajniach ŠGÚDŠ v Bratislave a v Košiciach je 5,50 € vrátane DPH. Časopis možno objednať v redakcii a v knižnici regionálneho centra v Košiciach.
Adresa redakcie: Štátny geologický ústav D. Štúra – RC Košice (Mineralia Slovaca), Jesenského 8, 040 01 Košice. Telefón: 055/625 00 43; fax: 055/625 00 44, e-mail: mineralia.slovaca@geology.sk, e-mail knižnica: secretary.ke@geology.sk

Mineralia Slovaca (Web ISSN 1338-3523, ISSN 0369-2086) is published twice a year by the State Geological Institute of Dionýz Štúr Bratislava, Slovak Republic. The date of issuing of the number 50/1/2018: June 2018.
Subscription for the whole 2018 calendar year (two numbers of the journal): 33.00 € (Europe), 45.00 € (besides Europe), including VAT, postage and packing cost. Claims for nonreceipt of any issue will be filled gratis.
Order send to address of the Editorial office: Štátny geologický ústav D. Štúra – RC Košice (Library), Jesenského 8, SK-040 01 Košice, Slovak Republic. Phone: +421/55/625 00 43; fax: +421/55/625 00 44, e-mail: mineralia.slovaca@geology.sk, library: secretary.ke@geology.sk

© Štátny geologický ústav Dionýza Štúra Bratislava

www.geology.sk/mineralia

Obsah – Content

Mineralia Slovaca 50 (2018) • 1

PÔVODNÉ ČLÁNKY – ORIGINAL PAPERS

Plašienka, D.
The Carpathian Klippen Belt and types of its klippen – an attempt at a genetic classification
Karpatské bradlové pásmo a typy jeho bradiel – pokus o genetickú klasifikáciu 1

Pelech, O., Józsa, Š. & Fajdek, P.
Fold deformation of the Fatricum – a case study from the Banka section (Považský Inovec Mts., Slovakia)
Vrásová deformácia fatrika – prípadová štúdia z profilu Banka (Považský Inovec, Slovensko) 25

Csibri, T., Lačný, A., Putiška, R., Dostál, I. & Kušnirák, D.
The depth range and possible continuation of the Havranická jaskyňa cave system revealed by geological methods and electrical-resistivity tomography (ERT), the Malé Karpaty Mts., Slovakia
Hĺbkový rozsah a možné pokračovanie jaskynného systému Havranickej jaskyne, zistené geologickými metódami a elektrickou odporovou tomografiou (ERT), Malé Karpaty 37

Teťák, F.
Simple processing and retilting of the oriented lineations and its application in paleocurrent analysis
Jednoduché spracovanie a sklápanie usmernených lineácií a jeho aplikácia pri paleoprúdovej analýze 47

Radvanec, M. & Németh, Z.
Variscan epidote-eclogite, blueschists and pumpellyite-actinolite facies Cpx/Sr-rich epidote-metagabbro blocks exhumed in Carboniferous, with Permian amphibolite facies overprint (Gemeric unit, Western Carpathians)
Variská metamorfóza exhumovaných blokov metagabra bohatého na Cpx a Sr epidot v karbónskej epidotovo-eklogitovej fácii, fácii modrých bridlíc a pumpellyitovo-aktinolitovej fácii s permským prepracovaním v amfibolitovej fácii (gemerikum, Západné Karpaty) 55

OBÁLKA:
Genetické typy bradiel v bradlovom pásme Západných Karpát

Vľavo hore: Pohľad na východ od Kyjova na rad strmo uložených bradiel pieninskej jednotky budovaných doskovitými vápencami pieninského súvrstvia a rádiolaritmi czajakowského súvrstvia – typ bradiel B1Y („kozí chrbát", resp. kvesta). V popredí Kosova skalka (pozri obr. 3 v článku Plašienku v tomto čísle).

Vpravo hore: Bradlo Zadné skálie (obr. 3 v práci Plašienku) je typom kompozitného sedimentárneho bradla – megaolistolitu (typ A2XY) – zloženého z viacerých šupín subpieninskej jednotky, ktoré leží uprostred brekcií, pieskovcov a bridlíc pročského súvrstvia šarišskej jednotky.

V strede: Výsek z geologickej mapy zobrazujúcej rôzne typy bradiel v okolí obce Milpoš na východnom Slovensku (pozri obr. 4 v článku Plašienku v tomto čísle).

Vpravo dole: Bradlo Zámok s ruinami Kamenického hradu (cf. obr. 4 v článku Plašienku v tomto čísle) tvorené czorsztynskou sukcesiou subpieninskej jednotky – veľké izolované tektonické bradlo typu A1Y, modifikované eróziou a ľudskou činnosťou.

COVER:
Genetic types of individual klippes in Carpathian Klippen Belt

Top left: View to the east of Kyjov village on the row built of steeply dipping klippen of the Pieniny Unit, composed of bedded limestones of the Pieniny Formation and radiolarites of the Czajakowa Formation – klippen type B1Y ("goat back" or cuesta). The Kosova skalka klippe is in the foreground (cf. Fig. 3 in the paper of Plašienka, this issue).

Top right: The Zadné skálie klippe (Fig. 3 in Plašienka, this issue) is a composite sedimentary klippe – megaolistolith (type A2XY) – composed of several slices of the Subpieniny Unit, which are resting amidst breccias, sandstones and shales of the Proč Formation of the Šariš Unit.

In the middle: Section of the geological map showing klippen of various types in the surroundings of Milpoš village in eastern Slovakia (see Fig. 4 in Plašienka, this issue).

Right below: Klippe Zámok with ruins of the Kamenica Castle (see Fig. 4 in Plašienka, this issue) formed by the Czorsztyn succession of the Subpieniny Unit – a big isolated tectonic klippe of the A1Y type shaped by erosion and human activities.

Mineralia Slovaca, Web ISSN 1338-3523, ISSN 0369-2086
50 (2018), 1 – 24, © Author 2018. CC BY 4.0

The Carpathian Klippen Belt and types of its klippen – an attempt at a genetic classification

DUŠAN PLAŠIENKA

Department of Geology and Paleontology, Faculty of Natural Sciences, Comenius University, Mlynská dolina, Ilkovičova 6, 842 15 Bratislava, Slovakia; dusan.plasienka@uniba.sk.

Abstract: Based on the literature examinations and field investigations in various parts of the Pieniny Klippen Belt of the Western Carpathians, a tentative classification of the klippen forms and types is presented. The mode of the klippen separation (genetic aspect), inclination of klippen long axes (structural factor), and alterations impressed by superimposed surface processes like erosion, gravitational movements or human activities (morphologic factor) are the three major criteria considered. By their combination, the klippen are categorized to the primary types whose origin was dominantly controlled by the endogenous tectonic, or by the exogenous sedimentary processes (olistoliths), and to the secondary forms influenced by the superficial modifications.

Keywords: Klippen Belt, tectonic concepts, block-in-matrix structures, olistoliths, typology of klippen forms, Western Carpathians

Graphical abstract

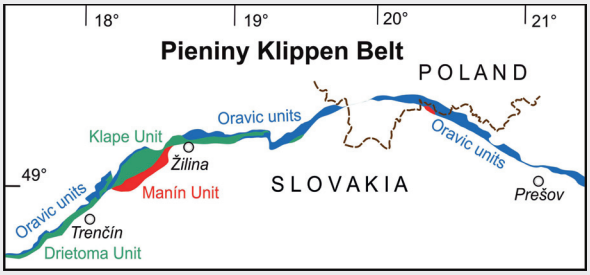

Highlights

- Klippen of the Carpathian Klippen Belt are rigid inclusions embedded in a soft matrix – predominantly Jurassic to Lower Cretaceous limestones within Upper Cretaceous – Eocene shales marls and sandstones;
- In general, klippen of two main categories are distinguished – sedimentary klippen, i.e. olistoliths, and tectonic klippen, i.e. fragments of sedimentary successions dismembered by deformation processes;
- Classification of klippen forms considers the mode of their separation (genetic factor), shape and attitude of klippen (structural factor), and superimposed surface processes (morphological factor).

Introduction

The Carpathian Pieniny Klippen Belt (PKB) is an exceptional Carpathian structural zone, only a few km wide, but up to 600 km long, as far as only the "true" Oravic units with the characteristic Czorsztyn-type successions are considered (Fig. 1). The PKB was formed by the latest Cretaceous to Middle Eocene thrust stacking and by superimposed Late Eocene–Early Miocene out-of-sequence thrusting and wrenching. It separates the Cenozoic accretionary prism of the External Western Carpathians (EWC, Flysch Belt) from the Cretaceous basement/cover thrust stack of the Austroalpine Central Western Carpathians (CWC). The PKB is exceptional by its scenic humped landscape, being formed by numerous, variously large "klippen", which are often isolated cliffy hills surrounded by a mild relief. The majority of klippen is composed of relatively competent, Middle Jurassic to Lower Cretaceous limestones, enclosed by the "klippen mantle" – incompetent Lower Jurassic and Upper Cretaceous to Middle Eocene shales, marls and sandstones. Beside of composition, the extraordinary complex PKB structure resulted from a long-termed deformation in a backstop position between the EWC accretionary wedge and the bulldozing CWC thick-skinned thrust stack (e.g. Plašienka and Soták, 2015 and references therein). As a result, some parts of the PKB show a disorganized, nearly chaotic block-in-matrix structure, having been often described as a megabreccia, or mélange – either tectonic, or sedimentary, or both.

Various concepts of the structure and evolution of the PKB have been developing and modified through time from the early ideas in the second half of 19th century (e.g. Neumayr, 1871; Uhlig, 1890), which was reflected also by changing opinions about the origin of peculiar klippen

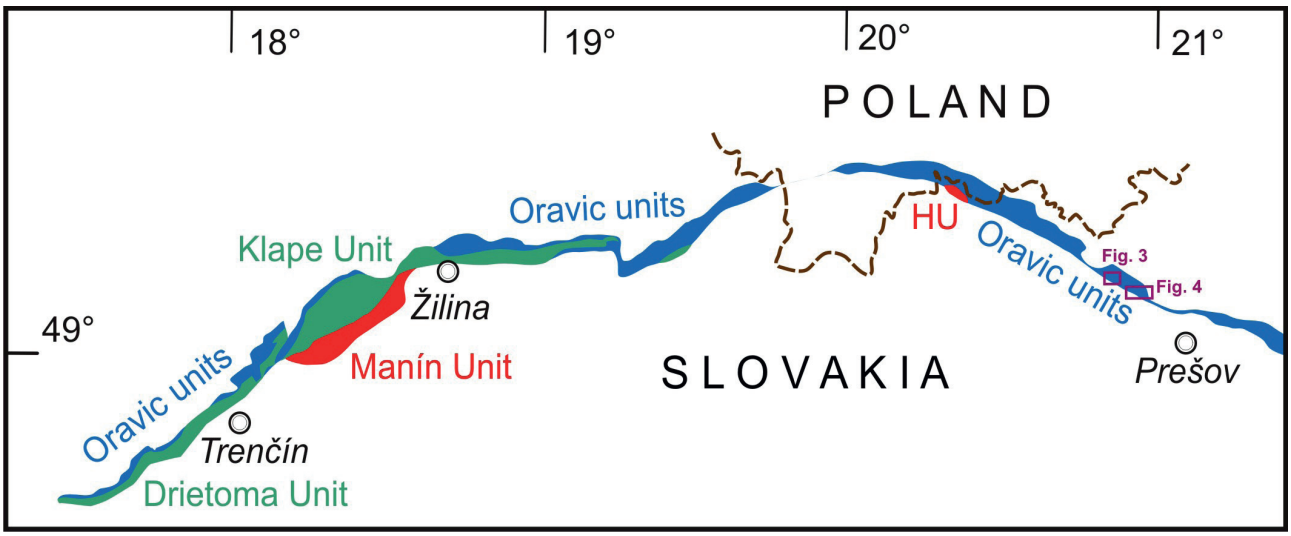

Fig. 1. The course of the Považie–Pieniny Belt (sensu Plašienka, 1999). The Oravic units (blue) compose the Klippen Belt proper, while nappe units of the Central Carpathian origin (Fatric according to Plašienka, 1995, 1999, 2012a and references therein – Manín, Klape, Drietoma, Haligovce HU) plus their Gosau (Senonian to Middle Eocene) post-thrusting cover form the Peri-Klippen Zone (Plašienka and Soták, 2015).

forms. Based on a combination of structural and morphological factors, the latest comprehensive classifications were published by Andrusov and Scheibner (1968) and Andrusov (1974). However, these classifications do not comply with the actual views on the tectonic and sedimentary development of the PKB that offer a more dynamic approach. Therefore, the purpose of this paper is to review older and current concepts about the origin of PKB and its klippen and to present a novel categorization of the klippen forms and types.

Derivation of the term klippe

The German word *die Klippe* (pl. *die Klippen*) designates the rock cliff, crag or reef. In the Alpine geological literature, the term has been used for about two centuries to denote the more-or-less isolated, weathering-resistant, variously sized block of rocks surrounded by softer strata that are prone to be easily removed by erosion. In a tectonic sense, the klippe means a block of rocks that is physically separated from the host strata by fault plane(s). Following introduction of the nappe theory in structure of the Alps, it has been frequently used for isolated nappe outliers, especially if they form morphologically distinct, isolated hard rock cliffs overlying soft rocks forming a mild relief (e.g. the Klippen nappe of the Western Alpine Préalpes – cf. Trümpy, 2006; Pfiffner, 2014 and references therein). In the international literature and geological dictionaries (e.g. Allaby, 2008), the terms klippe and klippen are used mainly in this specific meaning. To avoid possible misunderstandings in using the term klippe, already Suess (1885) introduced the notion of "klippen of the Carpathian type" for those that typically occur in the PKB. Vice versa, Andrusov and Scheibner (1960) named the morphologically expressive nappe remains as "klippen of the Swiss type".

However, the term klippe itself has no genetic connotation; generally it refers to any morphologically positive rocky form. In the Carpathians, it had been coined much earlier than the nappe theory was formulated in the Alps and Carpathians (Pusch, 1836 ex Andrusov, 1974). Klippen may have various sizes from a few metres to several hundred metres. Uhlig (1904) estimated the number of klippen up to five thousand, Maheľ (1989) to more than two thousand, and Andrusov (1938) counted 125 klippen in the Orava segment of PKB.

A terminological note – in the English-written text, the idioms klippe and klippen are not used consistently, due to their various transcriptions from German. This particularly refers to plural – terms like Klippen, klippen, klippes and even klippens can be found in the literature. To keep consistency with the historical prejudice and the most common practice, we shall use the term "klippe" for singular and "klippen" for plural throughout this paper.

In the Western Carpathians, the term klippe become to be widely used starting from the first half of 19th century and the zone of klippen was designated as the "*Klippenkalkzug*" or "*Klippenkalk-Gruppe*" (e.g. Stur, 1860; see the historical overviews by Andrusov, 1938, 1964; Scheibner, 1968; or Birkenmajer, 1977, 1986). Afterwards, Neumayr (1871) was the first who introduced the name "*Pieninische Klippenzug*" for the peculiar Carpathian zone characterized by the widespread presence of chaotically dispersed blocks of stiff rocks of various sizes and origin – the klippen, embedded in a soft matrix – the klippen man-

tle or cover. Uhlig (1907) and several other authors used also the term "*Südliche Klippenzone*" and its analogues. At present, this zone is most commonly entitled as the Pieniny Klippen Belt in the current English-written texts, but terms Carpathian Klippen Belt or simply Klippen Belt have been frequently used as well. In the local Carpathian languages, the terms *klippe* and *Klippen Belt* have names of similar meanings – Slovak *bradlo* and *bradlové pásmo*, Polish *skałka* and *pas skałkowy*, or Ukrainian *utes* and *zona utesov*.

Structure of the Klippen Belt – earlier and present views

The Pieniny Klippen Belt (PKB) is perhaps the most outstanding regional tectonic structure of the Western Carpathians that has attracted the interest of variously specialized geologists for a long time. It was marked like a "tectonic megabreccia", "raisins in cake", "chaotic mélange", or "wonder of nature", which names themselves pertinently express the character of this extremely complex zone. Despite the comparatively small area extent, a great number of tectonic units, nappes, sedimentary series, successions, developments, formations or morphological klippen types have been distinguished and innumerable opinions about their paleogeographic settings and tectonic affiliations have been expressed (e.g. Andrusov, 1965, 1974; Birkenmajer, 1977, 1986; Mišík et al., 1996; Mišík, 1997).

Essential thoughts about the composition, structure and evolution of the PKB were formulated in the late 19th and early 20th century by Austrian geologist Viktor Uhlig (1890, 1903, 1904, 1907) who studied mainly the northern – Pieniny part of the PKB. The tectonic style of the PKB in western Slovakia (Považie, Kysuce and Orava regions) was described in detail by the excellent PKB expert Dimitrij Andrusov in 1930-ties (e.g. Andrusov, 1931, 1938). An essence of these early Andrusov´s views, which largely followed the conclusive Uhlig´s idea about the primary nappe structure of the PKB (Uhlig, 1907), inhered in a concept of two-phase development of the PKB: 1) Cretaceous (pre-Albian) thrusting of three principal PKB nappes (Subpieniny, Pieniny and Manín); 2) post-Paleogene deformation of PKB along with thrusting of nappes of the Flysch Belt. Later on, Andrusov (Andrusov and Scheibner, 1960; Andrusov, 1965, 1968, 1974) modified especially the timing of the first thrusting phase – from the mid-Cretaceous (Austrian resp. Pieniny or Manín phase), through Late Cretaceous pre-Gosauian (Subhercynian or Ilsedian phase), up to the Cretaceous Paleogene boundary (Laramian phase). Nevertheless, the Oligocene – Early Miocene disintegration of the PKB nappe edifice by additional folding, reverse faulting and tectonic separation of klippen, was still regarded as the main "klippen-producing" event.

Prominent Polish geologist Krzysztof Birkenmajer published a number of fundamental works concerning the litho-biostratigraphy, sedimentology and tectonic relationships of PKB units in the Polish Pieniny Mts (e.g. Birkenmajer, 1960, 1970, 1977, and 1986 as his milestone papers). He ultimately distinguished nine principal evolutionary stages of the PKB formation (Birkenmajer, 1986): (A) initial Triassic extension, and (B) oceanic rifting and spreading (Eocimmerian phase, latest Triassic – Early Jurassic); (C) pelagic stage with individualization of the fault bounded Czorsztyn ridge (Neocimmerian phase, Jurassic – Early Cretaceous); (D) initial compression due to partial subduction of the Klippen basin below the so-called Exotic ridge (Lower Cretaceous Manín phase); (E) three principal successive Late Cretaceous – Early Tertiary deformation phases generated by subduction of the northern Grajcarek trough below the Czorsztyn ridge and the central Pieniny oceanic trough below the Exotic ridge (late Subhercynian phase) with development of north-verging nappes, early and late Laramian refolding of nappes with flysch and molasse deposits, and retro-arc thrusting of the northern Grajcarek unit southwards; (F) Paleogene extensional collapse and south-directed transgression; (G) Early Miocene (Savian) compressional stage due to collision of the North European plate and Central Carpathian-Pannonian microplate with fragmentation of the nappes and their Czorsztyn autochthonous substratum, backthrusting and development of diapiric structures; (H) late Savian transpression resulting from differential rotation of the Inner Carpathians with respect to the Outer Carpathian zones with development of longitudinal sinistral strike-slips limiting the PKB from both sides, prolonging mega-brecciation and oroclinal bending of the PKB; (I) Middle Miocene (Styrian) compression with strike-slipping along transversal faults, intrusion of andesite dykes.

There are many other works dealing with the PKB composition and structure in its individual segments which mostly follow the principal views of Uhlig, Andrusov and Birkenmajer. With a few exceptions describing deformation structures in the Pieniny Mts. (Birkenmajer, 1983; Ratschbacher et al., 1993; Jurewicz, 1994), these views were solely based on litho-biostratigraphic and sedimentological observations expressed by geological maps constructed on the lithostratigraphic principles and overlooked the structural record, however. Owing to the essentially brittle deformation of the PKB units and with development of the paleostress analytical techniques, numerous works interpreting kinematics of fault structures have appeared since the 1990s also in the western Slovakian branch of PKB (Nemčok and Nemčok, 1994; Marko et al., 1995, 2005; Kováč and *Hók, 1996*; Pešková et al., 2009, 2012; Bučová et al., 2010; Šimonová and Plašienka, 2011, 2017; Beidinger and Decker, 2016).

Recent investigations of the PKB composition, structure and evolution in its western (Považie, Kysuce and Ora-

va regions) and eastern (Pieniny, Ľubovnianska vrchovina and Čergov Mts.) Slovakian segments strongly modified the previous opinions (Plašienka, 2003, 2010, 2012a, b; Schlögl et al., 2008; Plašienka in Froitzheim et al., 2008; Plašienka and Mikuš, 2010; Plašienka and Soták, 2015; Plašienka et al., 2010, 2012, 2013, 2017; Spišiak et al., 2011; Márton et al., 2013; Kováč et al., 2016). The main points of this new conception can be briefly characterized as follows: (i) PKB in a broader sense (Považie-Pieniny Belt; Fig. 1) involves units of two groups – Oravic Superunit (PKB s.s.) and Central Carpathian units forming the inner Peri-Klippen zone (Maheľ, 1980); (ii) three Oravic thrust units include the lowermost Šariš Unit (deep-water Jurassic – Middle Eocene succession) overridden by the Subpieniny Nappe (Jurassic-Cretaceous intra-oceanic ridge and slope successions like Czorsztyn, Niedzica, Czertezik, Pruské) and by the Pieniny Nappe (Jurassic-Cretaceous deep-marine successions Pieniny, Kysuca, Branisko); (iii) the Oravic sedimentary basin originated by broad rifting of the European continental lithosphere during the earliest Jurassic, followed by Middle Jurassic asymmetric rifting and breakup of the South Pennine oceanic zone (Piemont–Váh Ocean) with uplift of the Czorsztyn ridge as the upper-plate rift shoulder, the Pieniny-Kysuce basin neighboured the ridge from the inner side and the northern Tatric margin formed the lower plate break-away zone on the other side of the expanding Váh Ocean; (iv) individualization of the Czorsztyn ridge as an intra-oceanic continental ribbon was completed by the Early Cretaceous uplift of the rift shoulder during oceanic rifting of the North Pennine Valais–Rhenodanubian–Magura Ocean; (v) sequential shortening, detachment and nappe emplacement of Oravic units is recorded by syn-thrusting, coarse-grained wildflysch deposits containing material from the overriding nappe – latest Cretaceous in the Subpieniny Unit (Jarmuta flysch basin with Gregorianka breccias composed of clasts from the Pieniny nappe), and Paleocene – Early Eocene in the Šariš Unit (Proč flysch basin with Milpoš olistostromes containing blocks of Czorsztyn-type successions); (vi) the Central Carpathian ("non-Oravic") units consist of the frontal Fatric (Krížna) nappe units – Drietoma, Manín and Klape in western and Haligovce in eastern Slovakia (sensu Plašienka, 1995, 1999, 2012a and references therein; Fig. 1), which were emplaced during the Late Cretaceous over the inner Oravic zones and subsequently incorporated into the PKB structure; (vii) during the early Paleogene (Paleocene–Lutetian) the detached PKB units formed an accretionary wedge growing by frontal accretion and experiencing alternating contractional and extensional events that controlled sedimentation in both - the foreland trench and the wedge-top, Gosau-type piggyback basins; (viii) throughout the Paleogene, the western PKB segment was affected by NW–SE compression and gradual transfer of Oravic units from the front to the rear of the wedge, where their original nappe structure was disintegrated by forward out-of-sequence thrusting, then backtilting and backthrusting, whereas extensive dextral transpression affected the eastern segment; (ix) further important deformation occurred in the Early Miocene, when the SW–NE compression lead to narrowing of the eastern segment and sinistral transtension in the western one; (x) by the Early-Middle Miocene, the PKB became welded to both the Central and External Carpathian zones which rotated as a unity by some 50° CCW relative to Europe.

Origin of klippen – historical overview

The earliest views in the first half of 19th century considered klippen as stratigraphically concordant synsedimentary inclusions in the klippen mantle. Later on, Stur (1860) recognized that many limestone klippen have abnormal positions and cannot form generic formations with the surrounding sediments, and Mojsisovics (1867) wrote that each klippe is a tectonic individuality. This notion was then followed by a majority of authors working in the PKB. However, the mechanical mode of their disconnection from originally continuous strata successions and mixing with the contiguous matrix formations has remained unclear for a long time. The most popular conceptions that concern the entire PKB, its parts or individual klippen types include:

The initial **archipelago hypothesis** presumed that PKB was formed on ruins of older, disintegrated and eroded mountains ("Inselgebirge" of Uhlig, 1890), which compose the present klippen that were covered by younger rocks of the klippen mantle. Subsequently, the strong lateral contraction produced the current chaotic structure of the PKB (Neumayr, 1871; Uhlig, 1890, 1903, 1904). Soon after, Uhlig (1907) abandoned this hypothesis in favour of the nappe theory. However, the archipelago idea was not dead – it returned, though in a modified form, in the 1950-60s. At that time, the geosynclinal paradigm reached its climax by the most fixistic views on orogenic processes, symptomatically just before the advent of the new plate tectonics paradigm. Maheľ (in Buday et al., 1960) questioned the nappe concept and supposed that individual klippen originated from shallow-water successions deposited on submarine elevations and islands (Czorsztyn-type formations) amidst the deep-water geosynclinal sea (Pieniny-type successions). In his view, development of the "mature klippen style" was controlled by the material variability and heterogeneity caused by rapid vertical and horizontal facies changes that conditioned a mechanical differentiation during deformation controlled by the relative competence. Later he attributed the lateral facies changes to differences in crustal thickness and characterized the PKB as a former island arc (Maheľ, 1981, 1986).

The equally fixistic **lineament model** looked upon the PKB as the surface expression of a deep-seated, crustal-scale fault zone, which was indicated by geophysical methods and inferred from differences between the age and composition of the pre-Mesozoic Bohemian Massif and the "Slovak Block". This deep fault zone was named the Peripieniny lineament by Máška and Zoubek (in Buday et al., 1960), or Pieniny lineament by Scheibner (1969). Based on the supposed differences in structure and age of the Bohemian Massif and the "Slovak Block", these authors presumed even the Precambrian origin of this fault zone, which opinion was criticized by many authors (e.g. Biely, 1975; Sikora, 1976; Książkiewicz, 1977). Its intermittent activity should have controlled the vertical differentiation of the Pieniny geosyncline, as well as development of the klippen tectonic style. Nevertheless, also at that time the earlier dynamic idea of Uhlig (1907), who considered the Klippen and Flysch belts as zones of extensive shortening associated with flat underthrusting of the autochthonous European foreland below the Carpathian orogen, was not fully forgotten and accentuated by e.g. Stille (1953). The mobilistic approach was also kept for instance by Andrusov (1968) or Roth (1963, 1964), still before the plate tectonic principles were fully taken on in the Western Carpathians.

Despite the concept of lineaments has been abandoned together with the geosynclinal theory, it is obvious that the PKB apparently follows and sometimes coincides with an important crustal-scale boundary zone indicated by various geophysical methods (see e.g. Šefara et al., 1998 and Bielik et al., 2004 for the reviews). This zone is commonly interpreted as the deep boundary between the North European Platform (NEP) and the Central Carpathian block (e.g. Tomek, 1993; Tomek and Hall, 1993), whereby PKB represents its surface expression. However, as pointed out by Plašienka et al. (2008), notwithstanding that PKB seems to be fixed to this boundary and often exhibits steep structures, it cannot be rooted deep in this boundary zone. Steep up to vertical structures are related to development of tight fold-thrust and transpressional flower structures that mostly originated late in the tectonic evolution, and PKB is lacking rock complexes that would record considerable tectonic burial and associated metamorphism, or other signs of deep crustal processes. Nevertheless, from a paleogeographic point of view, the Oravic units represent an independent continental crustal fragment bounded by oceanic domains (Czorsztyn Ridge – e.g. Birkenmajer, 1986), i.e. the PKB margins delineate former plate boundaries. In view of this, PKB appears to be in a collisional **suture position**, i.e. it should be linked to a boundary of different crustal blocks. This peculiarity was explained by an early detachment of the Oravic cover units from their subducted substratum to form a shallow fold-thrust "float" in the rear part of the developing accretionary wedge of the External Carpathian Flysch Belt that was thrust over the NEP margin (Plašienka and Soták, 2015). After all, the late Cenozoic collision of NEP and the CWC at deep crustal levels was in part expressed in near-surface PKB structures. For instance, the importance of pre-existing weakness zones in the subducted margin of NEP in the Pieniny Mts. area was accentuated by Jurewicz (2005, 2018). The NNW-SSE trending fracture zones in the deep basement affected structure of the PKB and adjoining zones by dextral shearing (e.g. along the Dunajec Fault) and block rotations.

With the first applications of the plate tectonics principles, the deep-seated boundary between the North European Platform and the Carpathian orogen, formerly known as the Peripieniny lineament, became to be interpreted as a witness of an ancient subduction zone, i.e. the oceanic suture, and the PKB as a tectonic, **suture-related mélange** complex (e.g. Maheľ, 1974, 1977; Andrusov, 1975; Szádecky-Kardoss, 1975; Stegena, 1975; Grecula and Roth, 1976; Birkenmajer, 1976; Horváth et al., 1977; Leško and Varga, 1980). This view was chiefly inspired by the presence of various ophiolitic and blueschist detritus in the Cretaceous "exotic" Wildflysch formations. However, these initial thoughts were incredibly changeable. There were very different opinions about the age, links and subduction direction of the corresponding oceanic or "quasi-oceanic" crust, timing of subduction and collision, as well as their impacts on the PKB structure. Since the PKB does not contain typical oceanic elements and ophiolitic material in a primary position, attention was paid to the provenance of ophiolitic detritus. Then, the character and position of the source area, variously named as the Exotic, (Ultra)Pieniny or Andrusov Ridge ("cordillera"), has become one of the most discussed issues in the Western Carpathian geology and no generally accepted interpretation has been achieved yet (see Mišík et al., 1977, 1981; Mišík, 1978, 1979; Mišík and Sýkora, 1981; Maheľ, 1981; Birkenmajer, 1988; Soták, 1992; Plašienka, 1995, 2012a; Dal Piaz et al., 1995; Faryad and Schreyer, 1997; Rakús and Marschalko, 1997; Kissová et al., 2005).

The peculiar **diapiric model** in part developed the former archipelago concept and was applied on the entire PKB (Andrusov, 1938), but especially on groups of the Czorsztyn-type blocky klippen emerging from below the overlying Pieniny nappe in tectonic windows in the Pieniny Mts. (Birkenmajer, 1959, 1986; Andrusov and Scheibner, 1968 called them the "Czerwona skala type"), or klippen of the Kysuca (Pieniny) unit protruding upwards through the Manín (Klape) unit in the Middle Váh Valley (Scheibner, 1963a; Andrusov, 1974). In contrast to classic diapirs formed by vertical extrusion of less dense material, these are kinds of "pseudodiapirs" or "false diapirs" generated by inversion of mechanical properties, whereby competent klippen rocks were separated from the substra-

tum and protruded upwards into the less competent strata due to the strong lateral contraction (e.g. Scheibner, 1963a, 1968). As a result, lots of the faulted blocky klippen were totally individualized and could float passively in the soft klippen matrix. This deformation style was called the "mature klippen style" by Maheľ (e.g. 1989), in contrast to the "immature style" developed preferably in the well-bedded Kysuca-Pieniny or Manín successions prone to folding rather than to faulting.

The diapir notion was combined also with the **boudinage model** suggested by Scheibner (1961, 1963a, b). He supposed that during the northward radial translation and orthogonal compression, the PKB was laterally extended by some 60 km according to his calculations. Consequently, the former fold structures, anticlines in particular, were segmented and split into large-scale boudins, i.e. the present klippen.

The **coulisse model** was the forerunner of the transpressional concept; it assumes lateral movements of individual PKB segments along strike-slip faults oblique to the general trend of the PKB. According to Maheľ (1989), some Central Carpathian elements (like the Kozinec klippe near Zázrivá village) might have been translated to the outer PKB margin by this process. The coulisse-like structure of some PKB parts was mentioned also by Andrusov (1938), Scheibner (1963a) or Potfaj et al. (1991).

Tectonic fragmentation, horizontal shortening, vertical extension, lateral shearing and origin of block-in-matrix structures are best explainable by the **transpressional theory**. The along-strike movements related to the activity in the zone of the Peripieniny lineament ("Námestovo Narbe") that influenced the PKB structure were envisaged already by Andrusov (1968 – "Längsgleitungszone"). Maheľ (1989, 1990) related the transpressional deformation to formation of the arc structure of the PKB. In the Pieniny Mts, Birkenmajer (1983, 1986, 1998) postulated sinistral strike-slipping along the PKB boundary faults. A major transform fault with sinistral translation along the northern Tatric edge was deduced by Marschalko (1986) and Rakús and Marschalko (1997) to explain the long-living sources of Cretaceous exotic flysch complexes of the Klape unit. Starting from the 1990s, the dextral and sinistral (western sector) and dextral (eastern sector) transpression and transtension was documented in details by kinematic and paleostress analyses in numerous papers (Ratschbacher et al., 1993; Nemčok and Nemčok, 1994; Marko et al., 1995; Kováč and Hók, 1996; Bučová et al., 2010; Pešková et al., 2009, 2012; Plašienka, 2012b; Šimonová and Plašienka, 2011, 2017; Beidinger and Decker, 2016).

The **olistostrome concept** presumes that at least a part of klippen originated not by primarily tectonic, but sedimentary processes. The occurrence of extraneous blocks emplaced by sedimentary processes was accepted by several authors (e.g. Andrusov and Scheibnerová, 1963; Andrusov and Scheibner, 1968; Andrusov, 1974; Sikora, 1974; Marschalko and Samuel, 1977; Birkenmajer, 1977; Marschalko, 1979; Marschalko and Kysela, 1980; Maheľ, 1989; Salaj, 1991, 1997), but only in a restricted extent related to specific settings and conditions. A large extent of sedimentary klippen was presumed by Muratov (1949). According to him, klippen might have originated as rock masses that slid down from elevated ridges neighbouring the PKB synorogenic basins from the south. However, this view was not accepted at that time (Andrusov, 1968). Afterwards, Nemčok (1980) considered the whole PKB in eastern Slovakia as a sedimentary body – gigantic olistostrome emplaced between the Paleogene flysch complexes of the Magura Unit and Central Carpathian Paleogene Basin. As a consequence, Nemčok (1980) did not make difference between the klippen successions, as well as he did not specify the sources of olistoliths. This view was based on correct observations (Gregorianka Breccia – Nemčok et al., 1989), but erroneously applied to the entire PKB. Later on, the presence of olistostrome breccia bodies with sedimentary klippen occurring in two stratigraphic levels (Maastrichtian and Paleocene) and in two units (Subpieniny and Šariš, respectively) has been substantiated by Plašienka and Mikuš (2010), Plašienka (2012a) and Plašienka et al. (2012). In the Orava region, the Maastrichtian Záskalie Breccia has been considered as an olistostrome body for a long time (e.g. Marschalko et al., 1979 and references therein). In the western Slovakian Middle Váh River Valley, the olistolithic origin has been ascribed to loose blocks of Jurassic and Lower Cretaceous limestones embedded in mid-Cretaceous hemipelagic and turbiditic formations of the Klape Unit (klippe of Klapy Hill, Marschalko, 1986; Marschalko and Rakús, 1997) and Manín Unit (Kostolec klippen, Rakús and Marschalko, 1997). Finally, Golonka et al. (2015) considered many PKB klippen as olistoliths, among others also the klippe Haligovce, as well as Manín and Butkov hills. This view was disapproved by Plašienka et al. (2017), who provided also a classification of olistostromes and olistoliths in the PKB units (see below).

Considering the Klippen Belt as a genuine tectonic phenomenon with nappe structure would imply that the klippen structures originated during the main deformation phases, i.e. during the **thrusting processes**. However, even after recognition of nappes in the PKB (Lugeon, 1903; Limanowski, 1906; Uhlig, 1907), origin of klippen was still chiefly ascribed to the post-thrusting and dominantly post-Paleogene deformation (e.g. Andrusov, 1938, 1968; Stráník, 1965; Birkenmajer, 1986). In addition to "klippen of the Swiss type" (i.e. nappe outliers; e.g. Andrusov and Scheibner, 1968), imbricated, thrusting-related structures were identified by Książkiewicz (1977). He distinguished the post-Paleogene Pieniny nappe and the Czorsztyn nappe with two partial structural units – the

strongly dismembered Czorsztyn blocky subunit and the Czorsztyn imbricated subunit with better preserved and thicker successions. Later on, Plašienka and Mikuš (2010) and Plašienka et al. (2012) came to a similar conclusion about two structural subunits of the Subpieniny (Czorsztyn) nappe – the Maslienka and Jarabina subunits, respectively. However, they dated thrusting and imbrication of the Subpieniny nappe as Paleocene – Early Eocene, similarly as it was inferred by Jurewicz (1994, 2005). Interestingly, the nappe thrusting was closely related to generation of olistostrome bodies in front of advancing nappes and their emplacement in the trench-type foreland flysch basins (Jurewicz, 1994, 2005; Plašienka and Mikuš, 2010; Plašienka, 2012a). Leading edges of nappes were fragmented, liberated and slid down to form brecciated olistostromes carrying megaolistoliths. This process concerns both the Pieniny nappe (Maastrichtian Gregorianka breccias), as well as the Subpieniny nappe (Paleocene Milpoš breccias – Plašienka and Mikuš, 2010).

The **accretionary wedge** concept was referred to several times (e.g. Golonka et al., 2015), but elaborated in detail just recently (Plašienka and Soták, 2015). Accordingly, the PKB occurs presently in a backstop position of the outer Carpathian accretionary complex of the Flysch Belt. After diminishing of the South Pennine Váh Ocean in the Late Cretaceous times, the Central Carpathian orogenic wedge, with already attached units of the present Peri-Klippen zone, prograded by frontal accretion of Oravic units detached from the intra-Pennine continental sliver (Czorsztyn Ridge), which were then gradually transferred from the wedge toe to its rear during the Paleogene. This process was accompanied by nappe stacking, out-of-sequence fore- and backthrusting and backtilting, and then by transpressional and transtensional movements along the boundary zone between the rigid buttress of the Central Western Carpathians and deformable External Carpathian accretionary wedge. Alternations of extensional and compressional events in the wedge controlled also the widespread recycling of the exotic material in the foreland trench and wedge-top (Gosau) synorogenic basins (Plašienka and Soták, 2015). Hence this multi-phase deformation evolution would be responsible for the current structural complexities of the Klippen Belt with all its bizarre klippen forms.

It is ought to be said that most of these klippen-forming processes might have been active in the certain PKB parts and at certain times, some of them may have prevailed and influenced the final structure of individual PKB segments and none of them should be considered as the solely decisive for the final PKB structure.

Earlier classifications of klippen forms

Several authors attempted at categorization of klippen forms, types and subtypes (Birkenmajer, 1958; Andrusov and Scheibner, 1960, 1968; Scheibner, 1968; Andrusov, 1968, 1974), using both - the tectonic and morphologic criteria. Although differing in details, these classifications are very similar. In general, they distinguished the klippen of non-tectonic and tectonic origin. The non-tectonic sedimentary klippen are either autochthonous, like reef bodies projected by erosion from surrounding sediments, or allochthonous older bioherms emplaced in younger deposits by submarine slides, extremely big boulders in conglomerates, olistoliths in slump bodies and blocks in recent landslides.

Klippen related to tectonic processes can be in situ, tectonically predisposed forms like projecting cores of anticlines with continuous sedimentary successions (Drieňovka or Butkov; the "immature klippen style" of Maheľ, 1980), remnants of cordilleras and horsts, and various "pseudoklippen" – these should not be called klippen. The proper klippen are morphologically positive forms, which are tectonically fully individualized from the surrounding sediments (Andrusov, 1974). Klippen of the "Moravian type" form slices of detached rigid rocks at leading edges of flysch nappes, while the "Pieniny type" includes several subtypes. These are the Rudín, Vršatec and Pieniny proper subtypes, differing in relationships between the klippen and surrounding rocks. In addition, Andrusov (1974) distinguished also the diapiric Czerwona skala subtype and several types of compound, mainly fold-related klippen. According to him, large-scale boudins should not be called klippen.

Based on descriptive morphostructural criteria, Plašienka (2012b) differentiated the so-called blocky and ribbon klippen associated with the klippen matrix in the eastern Slovakian PKB segment. Blocky klippen are more-or-less isometric bodies formed by predominantly Jurassic massive limestones of the Czorsztyn-type successions. They occur in two considerably different settings – as olistoliths in Milpoš breccias of the flysch Proč Fm. in the Šariš Unit, or as tectonically constricted lenses or slices in the strongly imbricated Maslienka subunit of the Subpieniny nappe (Plašienka et al, 2012b, their Fig. 3). In the first case, the internal foliations (bedding and cleavage) are randomly oriented, whereas in the second case they show attitudes generally consistent with the surrounding Cretaceous variegated marlstones. The ribbon klippen are typical for the Pieniny Unit, they are formed by well-bedded, in places folded Jurassic to Lower Cretaceous limestone and radiolarite formations preserving the structural trends for longer distances. Nevertheless, large and laterally persistent slabs and imbricates of the Czorsztyn-type successions also form ribbon-type klippen. In essence, the blocky klippen correspond to the Gruppentypus, and ribbon klippen to the Reihentypus of Uhlig (1890, 1903). The marly-shaly klippen matrix encompassing the blocky or ribbon tectonic klippen has often penetrative scaly fabrics, whilst the bloc-

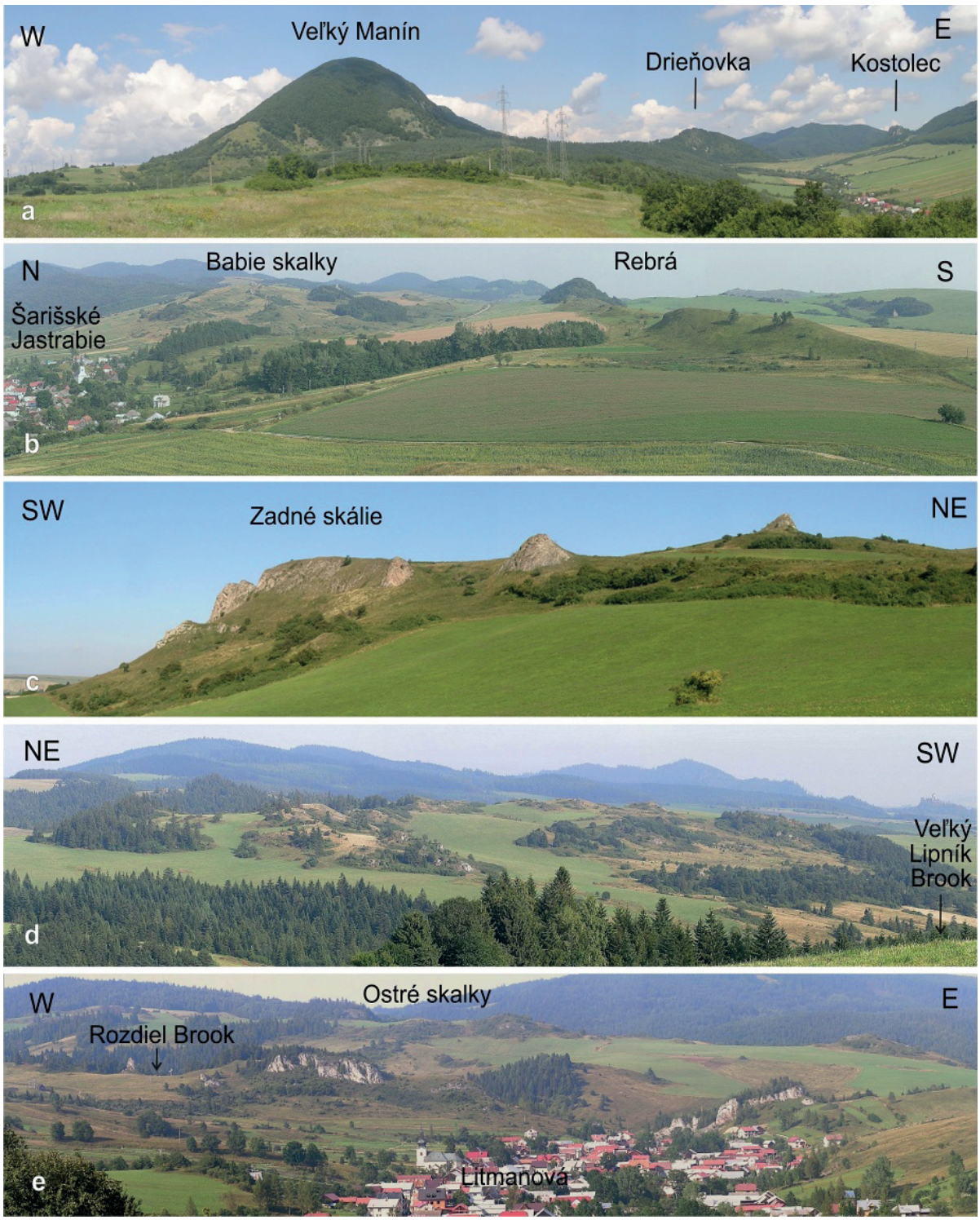

Fig. 2. Panoramic views of the klippen landscape: (a) view of the Manín and Drieňovka anticlines (B1XY type, see below) from the south (Manín Unit, Middle Váh River Valley, western Slovakia); (b) klippen area of Oravic units south-east of village Šarišské Jastrabie in eastern Slovakia; (c) scenery of the Zadné skálie group of olistolithic klippen between Kyjov and Kamenica villages in eastern Slovakia, viewed from the south-east (cf. Fig. 3); (d) smooth ridge between Litmanová and Jarabina villages in eastern Slovakia formed by sandstones of the Proč Fm. (Šariš Unit) overlain by a mosaic of scattered Czorsztyn-type klippen of the Maslienka subunit of the Subpieniny nappe ("carapace" type A-B1X), look to the south-east; (e) row of the olistolithic Litmanová klippen viewed from the south.

ky olistoliths are enclosed by more competent and weakly deformed breccias and sandstones.

The tentative classification presented in this paper is based upon the author´s field experience from practically all PKB parts, but chiefly from the eastern Slovakian Pieniny and Šariš sectors (Plašienka and Mikuš, 2010; Plašienka, 2012b; Plašienka et al., 2012). Thanks to comparatively weak vegetation coverage in this area, the rugged morphology with numerous scattered stony crags – the klippen – attracts for searching the origin of such a peculiar structure (Fig. 2). Although the current morphology is largely an erosional feature, and the relationships of klippen to the enclosing strata are rarely outcropped, the main factors controlling klippen structures can be defined with a sufficient degree of reliability.

Genetic factors controlling the klippen forms

In general, klippen of the PKB are defined here as fully or at least partly isolated, sharply edged blocks of comparatively rigid, mainly Jurassic and Lower Cretaceous limestones of various lithologies embedded in a softer matrix formed locally by Lower Jurassic, but dominantly Cretaceous (from the Aptian onwards) and Paleogene (up to Middle Eocene) marlstones, shales and flysch deposits. Another common attribute of klippen is their morphological expression due to selective erosion of surrounding, less resistant rocks.

As far as the lithostratigraphic composition of klippen is concerned, the simple klippen formed by only one formation or continuous sedimentary succession, and the composite klippen involving a few partial units with repeating successions can be distinguished. Whereas the simple klippen are highly prevalent, the composite klippen can be seldom properly documented. One striking example is the Zadné skálie klippe in the watershed saddle Pusté Pole between Kyjov and Kamenica villages in eastern Slovakia, which consists of three closely packed slices (Figs 3 and 2c) – one with the Niedzica, the other two with the Czorsztyn succession, which rest as a unity within sandstones and breccias of the Proč Fm. It means it is an imbricated slide sheet or composite megaolistolith. Similar, even larger internally imbricated body occurs on the southern slopes of the Lysá hora Hill east of Kyjov village (Figs 3 and 7f).

Characterization of the genetic factors influencing the origin and appearance of various klippen forms is based on definition of processes leading to the individualization of klippen, and to their subsequent final shaping. In principle, there are two fundamental ways how the klippen can be disconnected – the primary mode, i.e. klippen originated during formation of basic features of the PKB structure; and secondary, i.e. formed by surface processes superimposed on the original structures. The primary separation includes the sedimentary (i.e. superficial or exogenous) and tectonic (subsurface or endogenous) processes.

Exogenous sedimentary klippen – olistoliths

The near-surface, exogenous mode of klippen individualization means that the klippen blocks were torn off their original positions in continual sedimentary successions and transported into the neighbouring sedimentary basin by gravity forces, in other words the post-sedimentary separation and then the syn-sedimentary transport and placing as far as the klippen blocks are concerned. There are two types of sedimentarily transported klippen: (i) solitary olistoliths, usually large (many hundreds to several thousand cubic metres), emplaced amidst much younger hemipelagic or flysch deposits (down-slope sliding, rolling or jumping blocks); (ii) variously sized olistoliths (cobbles, boulders or blocks) embedded in younger coarse-grained sandstones or breccia bodies (disorganized mass-transport debrites like grain flows, debris flows, rock avalanches, olistostromes or tectono-sedimentary breccias) associated with turbiditic "Wildflysch" sequences.

In either case, the release, transport and resedimentation of olistoliths are gravity-driven processes. The discharge of olistoliths requires fragmentation of lithified sedimentary formations and freeing of blocks. This may occur either in extensional syn-rift or – more commonly – in compressional syn-orogenic tectonic settings, i.e. the origin of sedimentary klippen is primarily also conditioned by tectonic deformation of the source area. In the PKB, the generally extensional regime is presupposed for the rifting events during the Middle Jurassic and Early Cretaceous (Plašienka, 2003). Uplift of the Czorsztyn ridge as a horst bounded by possibly seismoactive normal faults would have allowed for in-situ disintegration of freshly deposited and in part indurated shallow-water deposits (Krasín Breccia Member – Aubrecht and Szulc, 2006) and resedimentation events on slope escarpments. This is evidenced by beds of calciturbidites and other allodaps deposited on the ridge slopes and foots where they intercalate Middle Jurassic hemipelagites of several Oravic successions (Niedzica, Pruské, Šariš). However, they transported only the contemporaneous fine- or medium-grained shallow-water material and no olistoliths have been documented so far.

On the other hand, huge masses of Jurassic polygenic scarp breccias carrying megaolistoliths of pre-rift complexes were described from the opposite – Tatric margin of the opening South Penninic–Vahic oceanic tract (Plašienka, 2012a and references therein). It is not to be excluded that the Mariková klippen group with exceptional presence of block of Triassic dolomites, described as an outlier of a Czorsztyn-type unit imbricated with the Kysuca succession (Plašienka et al., 2010), might represent a sliding body with olistoliths of Jurassic and Triassic rocks enclosed in mid-Cretaceous marlstones. The olisto-

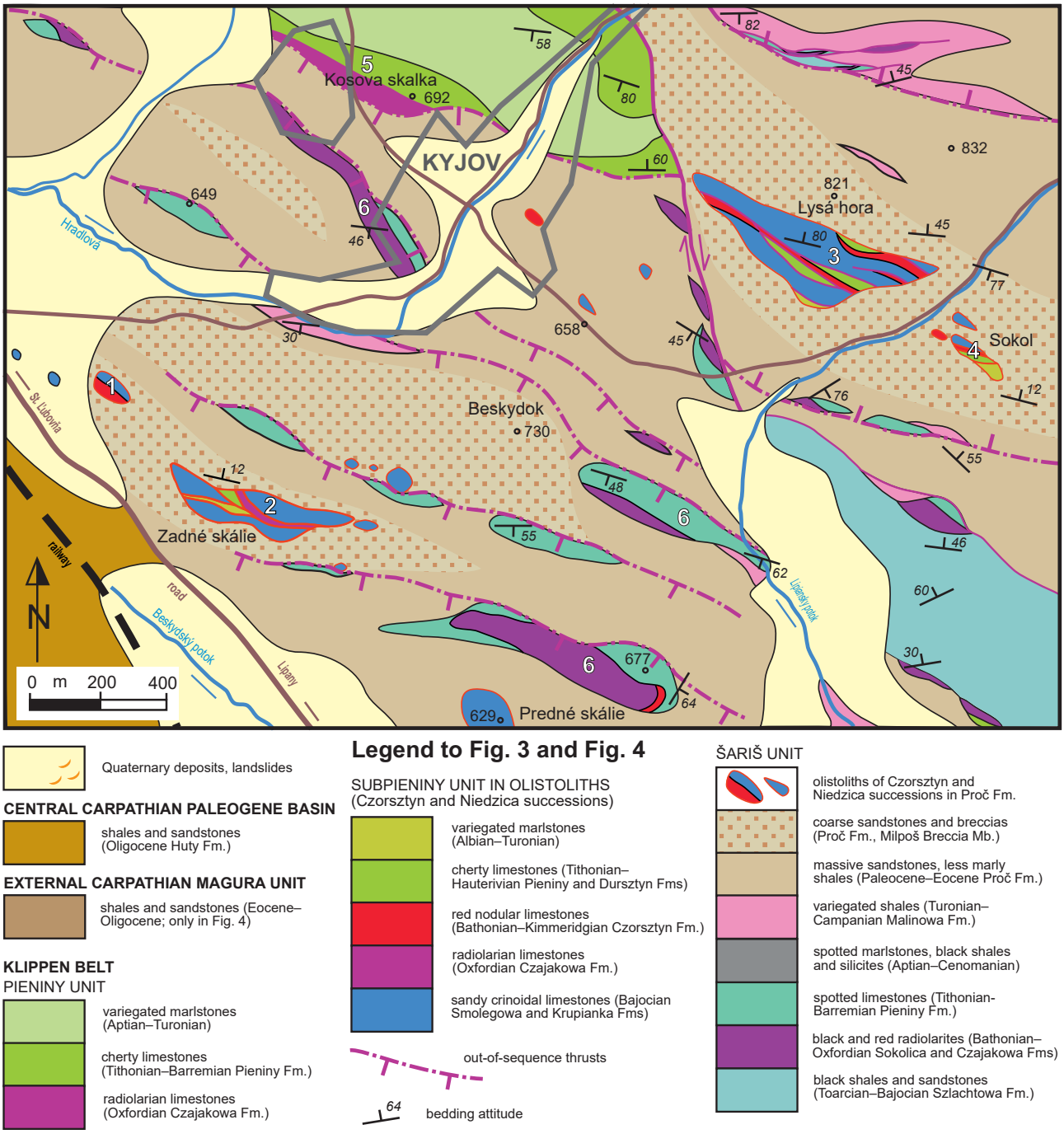

Fig. 3. Geological map of the Klippen Belt in the area around the Kyjov village in eastern Slovakia (for localization see Fig. 1). The map shows various types of klippen: (1) klippe (olistolith) Kyjov-Pusté Pole (studied by Mišík and Sýkora, 1993); composite olistoliths – imbricated slide sheets Zadné skálie (2) and Lysá hora (3); (4) Czorsztyn klippe – olistolith Sokolia skala; (5) klippe of type B1Y – cuesta in the limb of large-scale syncline of the Pieniny Unit; (6) projecting ribbon klippen B1Y of Jurassic – Lower Cretaceous formations of the Šariš Unit.

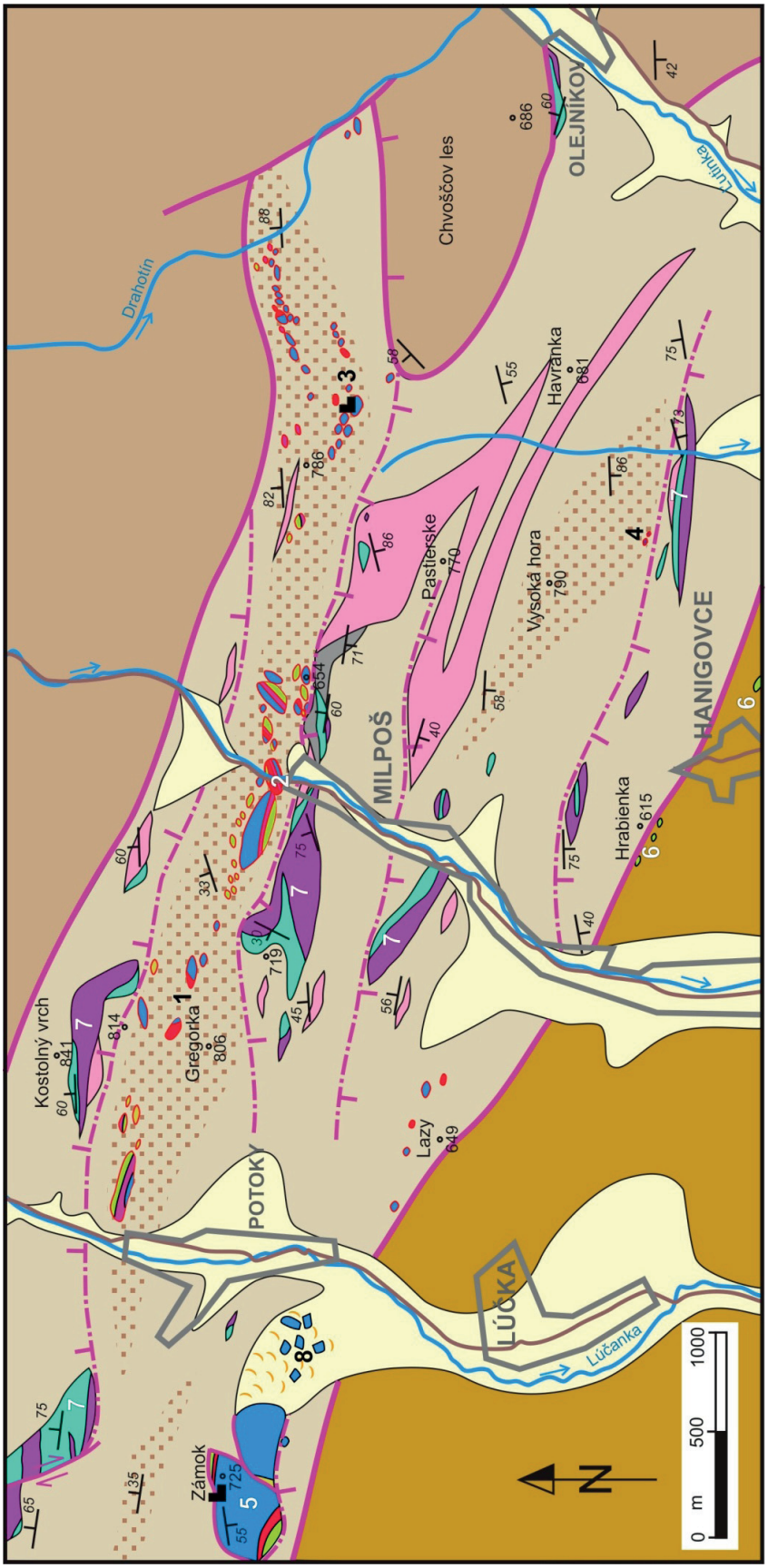

Fig. 4. Geological map of the Klippen Belt between villages of Lúčka, Milpoš and Hanigovce in eastern Slovakia (for localization see Fig. 1). The Klippen Belt area is dominantly composed of the Šariš Unit: (1) type locality of the Milpoš breccia (Nemčok et al., 1989; Plašienka and Mikuš, 2010); (2) klippe (olistolith) of the Niedzica succession described by Wierzbowski et al. (2004); (3) olistoliths embedded in Milpoš breccias of the Proč Fm. around the Hanigovce Castle ruins (A2XY); (4) two blocky olistoliths of alkaline basalts (Spišiak and Sýkora, 2009); (5) Kamenica Castle klippe of A1Y type composed of the Czorsztyn succession of the Subpieniny nappe; (6) button-like klippen of the Pieniny Fm. uncovered by erosion from below the overstepping Oligocene Huty Fm. (special B1Y type); (7) projecting ribbon klippen of Jurassic – Lower Cretaceous formations of the Šariš Unit (B1Y type); (8) loose blocks that gravitationally slid from the Kamenica klippe (type B2XY). For the legend see Fig. 3.

lithic character of Mariková klippen was assumed by Salaj (1991) and Golonka et al. (2015), but they did not provide any reliable evidence and explanation of their origin.

The occurrences of olistostromes and olistoliths in the PKB were reviewed by Plašienka et al. (2017). They distinguished and illustrated five basic types, which are differing in their tectonic position, genesis, sources and age. From structurally higher to lower and from younger to older, these are:

(1) Blocks of Thanetian algal-coral reefs (Kambühel limestone) embedded in contemporaneous or slightly younger calcareous sandstones and marls associated with tempestites, turbidites and slump bodies (Paleocene-Lutetian Myjava-Hričov Group; Mello et al., 2011). They are generally related to shallow-marine environments, where the bioherms were disintegrated by storms or seismic events and transported for a short distance; partly they correspond also to in situ patch reefs. Blocks of Kambühel limestones occur in a narrow, but lengthy strip along the southern boundary of PKB from Austria up to western Ukraine (see e.g. Marschalko and Kysela, 1980; Köhler et al., 1993; Köhler and Buček, 2005; Buček and Köhler, 2017). They can be regarded as intra-formational olistoliths originated from coeval rim and patch reefs, but are associated also with extraneous clasts of Urgonian limestones derived from the adjacent Manín Unit.

Type (2) olistoliths are similar to type (1), but older – Upper Cretaceous (Coniacian–Santonian and Maastrichtian). These are again formed by re-deposited rudists- and orbitoids-bearing bioherms and biostromes associated with conglomerates, allodapic limestones, tempestites and marlstones of nearly the same age (intra-olistoliths), as well as with extra-olistoliths of Lower Cretaceous Urgonian and Middle Triassic Wetterstein platform limestones (Senonian Brezová and Hoštiná groups; Mello et al., 2011).

Types (1) and (2) olistoliths originated probably in syn-orogenic wedge-top depressions in a piggyback position above the deforming accretionary wedge and are affiliated with the Gosau Supergroup (Plašienka and Soták, 2015). In the Middle Váh Valley and in the Pieniny Mts., the Gosau sediments form the post-thrusting cover overstepping the Fatric (Klape, Manín, Haligovce and Krížna; Fig. 1) and Hronic nappes of the Central Carpathian origin in the so-called Peri-Klippen zone (Maheľ, 1980).

The third olistolith type (3) is represented by the Kostolec group of limestone klippen resting within the Albian-Cenomanian hemipelagic and turbiditic deposits (Butkov and Praznov Fms, respectively) of the southernmost partial subunit of the Manín Unit, just below the overriding Central Carpathian Krížna nappe (Fig. 2a). According to Marschalko and Kysela (1980), Marschalko (1986), Rakús and Marschalko (1997) and Rakús and Hók (2005), the Jurassic-Lower Cretaceous sedimentary successions of these klippen are similar to coeval deposits of the Manín Unit and were interpreted as olistoliths.

The most spectacular olistoliths of type (4) occur in the Klape Unit of the Peri-Klippen zone in the Middle Váh Valley. These are solitary slide blocks measuring tens to hundreds of metres in diameter, the distinctive Mt. Klapy klippe being the largest one (e.g. Marschalko, 1986). The Klape olistoliths are embedded in hemipelagic and distal turbiditic sediments of Aptian–Early Albian age, i.e. their emplacement preceded the climax of coarsening-upward, synorogenic deposition of the Upper Albian–Cenomanian "exotic" Klape Flysch (Mello et al., 2011 and references therein).

Genesis and structural settings of the type (5) olistostromes and olistoliths in the Oravic units of the PKB that originated in a contractional regime were described by Plašienka and Mikuš (2010), Plašienka et al. (2012, 2017), Plašienka (2012a) and Plašienka and Soták (2015), partially relying on the work by Nemčok et al. (1989). These were evidently formed by fragmentation of the advancing nappe fronts and downslope transportation of discharged debris and olistoliths into the foreland depressions. The Paleocene olistostromes of the Šariš Unit (Milpoš Breccia Member of the Proč Formation) and Maastrichtian olistostromes of the Subpieniny Unit (Gregorianka Breccia Member of the Jarmuta Formation) represent syn-thrusting mass-flow deposits composed of material released from destructive frontal edges of overriding Subpieniny and Pieniny thrust sheets, respectively. The Milpoš olistostromes carry also huge sedimentary klippen of Jurassic–Lower Cretaceous formations derived from the Subpieniny nappe, including the Czorsztyn-type and also Czertezik and/or Niedzica successions (cf. Wierzbowski et al., 2004). In places, e.g. at the type locality (Nemčok et al., 1989) and in the klippen area around the Hanigovce Castle ruins (Fig. 4), the Milpoš breccias form apparently matrix-free, chaotic blocky accumulations of klippen that resemble huge apron-like rockfalls and debris avalanches inserted within the turbidite fans of the Proč Fm. Due to enormous shortening and reduction of the Oravic units in the western PKB branch, it is difficult to recognize this sort of sedimentary klippen with certainty. One of the possible candidates is the solitary blocky klippe near Plešivá settlement of Zázrivá village affiliated with the Czertezik succession by Haško (1976), which rests within calcareous sandstones of the Proč type. Some Czorsztyn-type klippen between Klieština, Hatné and Brvnište villages in the Middle Váh Valley might also represent olistoliths.

In contrast to olistoliths placed in syn-rift or passive margin settings, the syn-orogenic olistoliths can contain structural record of preceding compressional deformation processes like cleavage sets or small-scale folds (Plašienka, 2012b).

Endogenous tectonic klippen

Endogenous klippen originated by tectonic processes in the higher levels of the Earth´s crust, as revealed by the essentially brittle deformation mechanisms resulting in individualization of klippen, while the enclosing klippen matrix shows signs of a semi-ductile behaviour. Tectonic klippen are usually cut by numerous fractures – faults, slickensides or joints. These might have originated in various deformation regimes from purely extensional (e.g. boudins), through transtensional (rhomboidal blocks) and transpressional (lozenge-shaped blocks), up to entirely compressional (variously shaped imbricated rectangular ribbons, slabs, chunks or lumps). Lens-shaped blocky klippen developed if their competence contrast with respect to the matrix was low and/or if noncoaxial shearing prevailed in the contiguous matrix.

The shaly-marly matrix of typical tectonic klippen often shows scaly fabric with numerous, tightly packed anastomozing shear planes developed by combination of pressure solution and simple shearing. Smooth shear planes are often lustrous like glossy mirrors and are accompanied by tiny syntectonic calcite veinlets and sometimes extremely long slickenfibres. This indicates that the sheared matrix accommodated the major part of bulk deformation that grades into high-strain zones operating as detachment planes. As these planes climb up or down the stratigraphic succession, they truncate the competent strata in a brittle way, which is the basic principle of the klippen separation (cf. Fig. 3 in Plašienka et al., 2012). The larger is throwing along the detachment faults, the larger is separation between klippen.

However, not all klippen are bounded by fault surfaces from all sides, thus they can partly retain the stratigraphic continuity with encircling strata, especially if the competence differences are small and gradual. Large-scale upright folds developed in well-bedded strata, which are cored by more competent formations (e.g. Urgonian limestones in the Butkov or Drieňovka brachyanticlines of the Manín Unit – see e.g. Michalík et al., 2013; Rakús, 1997), may serve as an example. However, these symmetric or slightly asymmetric fold structures do not match the classic definition of klippen (cf. Andrusov and Scheibner, 1968). On the other hand, the immense Manín antiform is different, as its NW limb is cut by a large reverse fault, i.e. it is sharply fault-bounded from at least the NW side (Fig. 2a).

The stratigraphic continuity of klippen rocks with their sedimentary "mantle" is frequently preserved also in the Pieniny Unit. Albeit internally folded, the spectacular klippen composed mainly of the Pieniny Limestone Formation in the Kysuca Gate or in the Pieniny Mts are dominantly the erosional features. Rounded conical towers of these klippen were predominantly shaped by exfoliation processes, similarly as many Czorsztyn-type klippen.

Polygenetic klippen

Several klippen cannot be strictly classified as exogenous or endogenous, since they originated by some transitional or combined processes. In particular, these comprise small gravity gliding nappes and volcanogenic boulder breccias.

Besides olistoliths in Milpoš breccias, the Šariš Unit commonly contains also chaotic slide masses and solitary slide sheets, providing a transition from thrusting-related movements of imbricated allochthonous nappe units towards gravitational sliding of their liberated frontal masses into the foreland trench-type Proč basin. Provided that the sliding sheets maintained their internal integrity, they may be classified as nappes (if they slid for more than five kilometres as required by definition of tectonic nappes). Nice examples from the Subpieniny Unit occur in the Pieniny sector – the outliers of the tightly imbricated Maslienka subunit with blocky klippen (e.g. the area of Ostré skalky north of Litmanová village – maps Fig. 1 in Plašienka, 2012b, Fig. 11 in Plašienka et al., 2012, and photo Fig. 2e herein), as well as of the more compact Jarabina subunit (Homole block in the Polish Małe Pieniny Mts. – Birkenmajer, 1970; Jurewicz, 1994, 2005, 2018). The above illustrated imbricated slide bodies (Zadné skálie and Lysá hora in Fig. 3) represent the end members – composite olistoliths. Accordingly, the genetic links between prograding imbricated thrust nappes, their frontal failure, downslope gliding of more-or-less coherent sheets (slides or gravity nappes) and sliding of incoherent disintegrated masses (rock avalanches or olistostromes) may be inferred for this special case.

Submarine volcanogenic brecciation processes, like shallow intrusions and explosive extrusions, may have generated olistolith-sized blocks of disintegrated sediments mixed with volcanic products and soft matrix deposits. This situation is exceptional, but present in the PKB. In the Manín Unit, the Lower Cretaceous alkaline basaltic volcanism produced submarine hyaloclastic lava flows and shallow intrusions that were in places mixed with fragmented, slightly older and probably yet not fully lithified massive Urgon-type limestones. Afterwards, part of the limestone olistoliths and hyalobasanites were jointly resedimented as olistostrome bodies (possibly in front of the overriding Krížna nappe – Marschalko and Kysela, 1980), inserted in the Albian hemipelagic marls. The opposite situation – olistoliths of massive basalts (in this case substantially older) within the Jarmuta-Proč sandstones – is also present (Biała Woda – e.g. Birkenmajer and Lorenc, 2008; Hanigovce – Spišiak and Sýkora, 2009; Fig. 4). Lower Cretaceous hyaloclastic and pillowed basalts, rarely occurring in the Czorsztyn-type successions, contain only tiny fragments of surrounding limestones and marlstones (Vršatec – Spišiak et al., 2011; Velyky Kamenets – Oszczypko et al., 2012).

Another type of polygenic klippen occurs near Demjata village north of Prešov. There, the morphologically expressive limestone crags named Vápenníky closely remind the common klippen, but a closer inspection reveals that they are formed by the Gregorianka-type breccias with closely packed fragments of Lower Cretaceous cherty limestones, some of them of olistolith size. Hence the klippen rocks are breccias with primary sedimentary klippen, strongly modified by younger tectonic separation of breccia body, and followed by exogenous modifications including limited local mining for lime products.

Discussion – categories and examples of the klippen types

Like in the former classifications, the appraisal presented here takes into account the two basic principles – structural and morphological. However, our attempt is more comprehensive by consideration of some other important aspects – the mode of klippen separation (genetic factor), their bedding attitudes and inclination of long klippen axes with respect to horizontal (structural factor), and post-origin processes modifying the klippen forms like erosion, redistribution by gravitational movements, and anthropogenic impacts. Fig. 5 presents the resulting categorization of klippen forms and types as a combination of these principal factors. It should be noted, however, that this is a very simplified scheme that, for the sake of simplicity, takes into account only a part of the factors characterized above.

Modes of the klippen partitioning are the principal genetic attributes that include the primary and secondary factors. The primary separation modes were characterized in the previous section and are labelled as the factor **A** in Fig. 5. The parting of endogenous tectonic klippen is marked as **A1** and that of exogenous sedimentary olistoliths as **A2**.

Secondary factors (**B** in Fig. 5) that modify the klippen forms and may cause their individualization involve first of all various erosional processes (**B1**) like mechanical abrasion by water streams, chemical dissolution of preferably limestone rocks, exfoliation etc. Equally important is disintegration and down-slope transport of klippen blocks that are triggered by gravitational forces (**B2**). Gravity-driven processes include breakdown of steep cliffs and ridges along vertical fissures, tilting of released blocks, rock falls and avalanches, and sliding, slumping or creeping dependent on the slope inclination and rheology of the underlying or encircling material. Klippen shapes have been often modelled also by the human activities (anthropogenic factor **B3**) – from small excavations and local exploitations as raw materials for various purposes to large quarries in which mostly limestones for the cement and lime factories are mined.

Since bedding is the most common planar anisotropy in the sedimentary rocks, it represents the weakest planar structural predisposition along which a klippe can break and separate. Therefore the surface klippen shapes are largely controlled by their bedding attitude, as the long axes of klippen used to be generally parallel to bedding. In less frequent cases the main anisotropy is represented by other types of pervasive foliation – cleavage, indiscrete layering due to lithological variations, or regular joint systems. For the classification purposes, we distinguish two end members of the foliation attitudes – gently dipping (0–45°; factor **X** in Fig. 5), and steeply oriented (45–90°; **Y** in Fig. 5). However, some massive rocks often do not hold any foliation planes, or the dip factor plays no role in the klippen forms, as well as dips can be variable within an individual klippe due to small- or large-scale folding – this factor is marked as **XY**. These three situations represent the structural aspects for both individual klippen and their linked groups.

Typology of klippen presented in this paper is based on a combination and integration of the above principles (Fig. 5). Hence the principal types can be characterized as follows:

Type A1XY – tectonically individualized klippen, more-or-less isometric and rather small, with insignificant or without foliation, usually fully separated from and floating in a scaly matrix. They typically occur within narrow transpressional shear zones at the outer contact of the PKB (Šariš and Subpieniny units) with the Biele Karpaty or Magura units (e.g. near Zázrivá – Fig. 6b). In eastern Slovakia, such klippen occur also along the inner PKB fault contact with deposits of the Central Carpathian Paleogene Basin (Subpieniny and Pieniny units; e.g. Fig. 2 in Plašienka and Mikuš, 2010; Fig. 1 in Plašienka et al., 2013). These klippen represent the typical "Pienin" type of isolated tectonic slices and fragments (Uhlig, 1904; Andrusov and Scheibner, 1968).

Type A1X – tectonically separated blocks of predominantly Czorsztyn-type klippen with gently dipping bedding which form plateau-like klippen with either normal (e.g. Hatné in the Middle Váh Valley – Aubrecht and Sýkora, 1998; Homole block in the Małe Pieniny Mts. – Birkenmajer, 1970; Jurewicz, 1994; only partly outcropped lower imbrication of the Jarabina subunit of the Subpieniny nappe – Fig. 6a), or with overturned stratification (for instance Ostrá hora near Horné Sŕnie in the Middle Váh Valley – Aubrecht et al., 2006; Erdúdsky kostol klippe near Zázrivá – Jamrichová et al., 2012; Červená skala klippe near Podbiel in the Orava region – Andrusov, 1938). Groups of such clearly related klippen originated by boudinage of originally continuous or imbricated stiff layer and resemble a mosaic or splitting “carapace” in the map view (cf. Plašienka, 2012b). This rare situation occurs in areas where the original subhorizontal nappe structure is preserved, for instance on the low round ridge between Jarabina and Litmanová villages, where flat-lying imbricates of the Maslienka subunit overriding the Šariš Unit

A, B separation modes \ foliation tilt X, Y		foliation missing or unimportant XY	
		gentle dips <45° X	steep dips >45° Y
		areal klippen groups	linear klippen groups
primary A	TECTONIC A1	isolated "floating" blocks A1XY	
		plateaus "carapaces" A1X	rhomboidal blocks "dragon backs" A1Y
	SEDIMENTARY A2	olistoliths, slides olistostromes, mass-flows A2XY	
secondary B	EROSIONAL B1	periclines and "ribs" B1XY	
		table mts, monadnocks mosaics B1X	rock needles and towers "goat backs" – cuestas B1Y
	GRAVITATIONAL B2	separate downslope moving blocks chaotic blocks accumulated at landslide toes B2XY	
	ANTHROPOGENIC B3	quarries, carved crags B3XY	

Fig. 5. Classification of the basic klippen types and forms.

are modified also by gravitational spreading (vicinity of the Jar-1 borehole – Fig. 2 in Plašienka et al., 2012; Fig. 2D in Plašienka, 2012b; and Fig. 5D in Plašienka and Mikuš, 2010; Fig. 2d in this work), or in the Ostré skalky area north of Litmanová village (Fig. 2e in this work; see also Fig. 1 in Plašienka, 2012b). These klippen clusters were previously described as Gruppentypus (Uhlig, 1890), or "diapirs" of the Czerwona skała type (Birkenmajer, 1959; Andrusov and Scheibner, 1968).

Type A1Y – these are archetypal tectonic klippen with steeply inclined up to subvertical and often slightly overturned primary foliation that form the most impressive cliffy landscape of many parts of PKB. Larger klippen are dissected by transversal fractures and form "dragon back" ridges that are present in both the Pieniny (e.g. the famous Trzy Korony klippe in the Polish Pieniny Mts, or the Orava Castle rock – Andrusov, 1931, 1938) and Subpieniny units (e.g. the Lednica Castle klippe – Fig. 6c). In the Subpieniny Unit, large individual klippen of this type are exemplified also by the Krasín klippe near Dolná Súča in the Middle Váh Valley (Aubrecht and Szulc, 2006), Chmeľová and Javorník hills in the Vršatec klippen area in western Slovakia, and Nemecký vrch klippe near Stará Ľubovňa (Fig. 2 in Plašienka and Mikuš, 2010), Kamenica Castle klippe (Fig. 4 herein), or Beňatiná klippe (Schlögl et al., 2004) in eastern Slovakia, as well as the Veliky Kamenets klippe in Ukraine (Lewandowski et al., 2005; Reháková et al., 2011; Oszczypko et al., 2012). Isolated, fault-bounded cores of mesoscale upright tight anticlines constitute a special type of these klippen, like the klippe of the Kysuca succession outcropped in an abandoned quarry near Myjava-Turá Lúka (Scheibner, 1963a, his Fig. 4).

In most cases the klippen rows of the A1Y type are arranged in linear groups of klippen (Reihentypus of Uhlig, 1890) dissected by oblique strike slips into lozenge-shaped blocks. Such a row composed of Czorsztyn-type successions forms for example the amazing craggy chain Krivoklát–Vršatec–Lednica stretching for some 12 km (e.g. Bučová et al., 2010). Similar chains can be more commonly observed in the Pieniny Unit – the discontinuous ridge Chorvátsky vrch–Hrebeň between Podbranč and Turá Lúka villages in the westernmost PKB segment, the massive mountainous ridge Rochovica–Brodnianka (Kysuce Gate)–Vreteno–Veľké Ostré–Steny–Ľadonhora and the Požeha–Panské Zliene ridge near Lysica village in the Kysuce segment, or discontinuous belt of the Pieniny Unit between the Ľubovňa Castle rock, Podsadok and Údol villages NE of Stará Ľubovňa town (Fig. 2 in Plašienka and Mikuš, 2010; ribbon-type klippen in Fig. 4 of Plašienka, 2012b). In the Kysuce segment, the sedimentary succession is more-or-less continuous, thus the Kysuce klippen chain is more an erosive than a tectonic feature ("Rudin" type of Andrusov and Scheibner, 1968).

Type A2XY – sedimentary klippen, i.e. olistoliths and slide sheets, are in a majority of cases composed of the Czorsztyn and "transitional" (Niedzica, Czertezik) succession derived from the Subpieniny nappe and emplaced in the Paleocene Milpoš Breccia Mb. of the Proč Fm. in the Šariš Unit. The Gregorianka Breccia Mb. (Jarmuta Fm.,

Subpieniny Unit) usually contain only minute fragments, clasts of olistolith size occur near Demjata village north of Prešov. Although these breccias have a disorganized chaotic internal structure, they form stratiform bodies within the host flysch deposits. Therefore the large platy megaolistoliths lie generally conformably with bedding of the surrounding strata and their orientation mimics structures of the neighbouring formations. In consequence, morphological forms of olistoliths largely correspond to those of tectonic klippen (see examples in Figs 2, 6 and 7) and their distinguishing depends on identification of the matrix sediments. Only rarely it can be recognized that individual olistoliths in matrix-poor blocky accumulations have different bedding attitudes (such as at the Pieniny Slovak/Polish borderland ridge Rabštín–Šľachovky–Vysoké skalky–Vysoká–Vrchriečky; the Litmanová group of klippen (Fig. 2E), Marmon–Hajtovka klippen area, and the gigantic, up to 5 km long and about 200 m thick body of innumerable, variously sized olistoliths between Kamenica and Milpoš villages and Hanigovce Castle ridge up to the Drahotín stream north of Ľutina village (Fig. 4; see also Plašienka et al., 2013, their Fig. 1), all in eastern Slovakia.

In addition, all klippen appearing on the surface were obviously affected by various secondary processes, mostly by erosion and gravity movements. However, these secondary effects are in most cases clearly dependent on the primary klippen forms described above. Hence it is sometimes problematic to decide whether the primary or the secondary processes were more important in the final shaping of klippen. Notwithstanding these uncertainties, we prefer considering the primary genetic aspects, if still recognizable, and the secondary klippen forms are classified only if they seem not to be directly related to the primary attributes.

The klippen forms modelled dominantly by erosion are marked as **B1** in Fig. 5. Their morphology is very variable. The **B1XY type** concerns first of all projecting cores of large-scale upright dome-like brachyanticlines composed of erosion-resistant formations conformably overlain by more easily washed out shaly or marly strata. The Butkov and Drieňovka periclines of the Peri-Klippen Manín Unit are the most straightforward examples (Fig. 2a). Part of the narrow symmetric linear ridges in the Pieniny Unit (ribbon klippen of Plašienka, 2012b), so-called "ribs" in the local geographic terminology, might also be affiliated with this type. Rib-like klippen are developed also in the Czorsztyn succession on northern slopes of the Červený Kameň village in the Middle Váh Valley. In this case two parallel subvertical cliffy ridges represent two imbricates with repeating succession of massive Jurassic limestones separated by soft marly strata (Fig. 6e).

Large flat-lying A1X klippen are often incised by narrow deep antecedent gorges, such as the Wawóz Homole gorge and Biała Woda valley in the Polish Małe Pieniny Mts (e.g. Birkenmajer, 1970), or Jarabinské tiesňavy canyon (Figs 6a, 7a). The solitary **B1X** klippen have an appearance of small table mountains or columnar monadnocks with subhorizontal stratification, e.g. the Čertova skala twin klippen near Jarabina. The needle-like klippe Skalná ihla (Čertova skala) in the river Poprad valley between Chmeľnica and Hajtovka villages, originally probably an olistolith, has been vigorously modelled by abrasion of the meandering river also recently (Figs 7b and 7c). The B1X klippen groups are closely related to the "carapace" A1X klippen additionally affected by erosion and slumping (Figs 2d and 2e).The isolated klippe Brysztan in the Polish Małe Pieniny Mts nicely illustrates the way how gently dipping thick-bedded limestones of the Czorsztyn succession are gradually degraded by erosional processes – first gravity-induced vertical joints are formed at unconstrained klippe walls exposed by erosion, then joints develop to open fissures widened by water dissolution, and finally tops of separated segments are shaped to conical pikes modelled by exfoliation that resemble small mogotes (Fig. 7d).

The isolated **B1Y type** klippen rise up along steep foliation to build rocky towers or needles. These are often olistoliths (e.g. the Sokolia skala klippe near Kyjov – Fig. 5B in Plašienka and Mikuš, 2010, Figs 3 and 7f, g in this work; Litmanová klippen – Fig. 2e). Some long linear (ribbon-type) klippen are typical cuestas developed in comparatively resistant Upper Jurassic – Lower Cretaceous radiolarites and cherty limestones of the Pieniny Unit underlain and overlain by soft strata. In the area between Šarišské Jastrabie and Kyjov villages in eastern Slovakia, these cuestas follow limbs of large-scale brachyfolds (Fig. 2b). Due to being cut by minor younger oblique-trending reverse faults, cuestas have a humped look of "goat backs" (Fig. 6d). A very special B1Y type klippen occur at the SE margin of the transversal Plaveč "graben" (in reality it is not a graben, but axial depression) filled with Oligocene shales and thin-bedded sandstones of the Oligocene Huty and/or Malcov Formation sealing the PKB structures. Owing to ongoing erosion of Oligocene strata, the buried klippen relief is gradually uncovered in a chain of "buttons" sticking out on a smooth ridge between Plaveč and Ďurková villages in eastern Slovakia (Fig. 7e).

Gravitationally transported klippen are labelled as **B2XY type** (Fig. 5). Detached individual klippen can slowly creep down even along a very gentle slope. Repeated landslides on slopes of river valleys penetrating still deeper into soft sediments (e.g. flysch) accumulate liberated blocks (e.g. olistoliths) in chaotic piles at the base-of-slope (south-eastern foot of the Kamenica Castle klippe – Fig. 4).

Besides large active or smaller abandoned quarries, the klippen rocks were often mined in areas with shortage of other suitable building material. Therefore shaping of klippen by restricted local exploitation is quite common in more settled areas – **B3XY type**. There are numerous

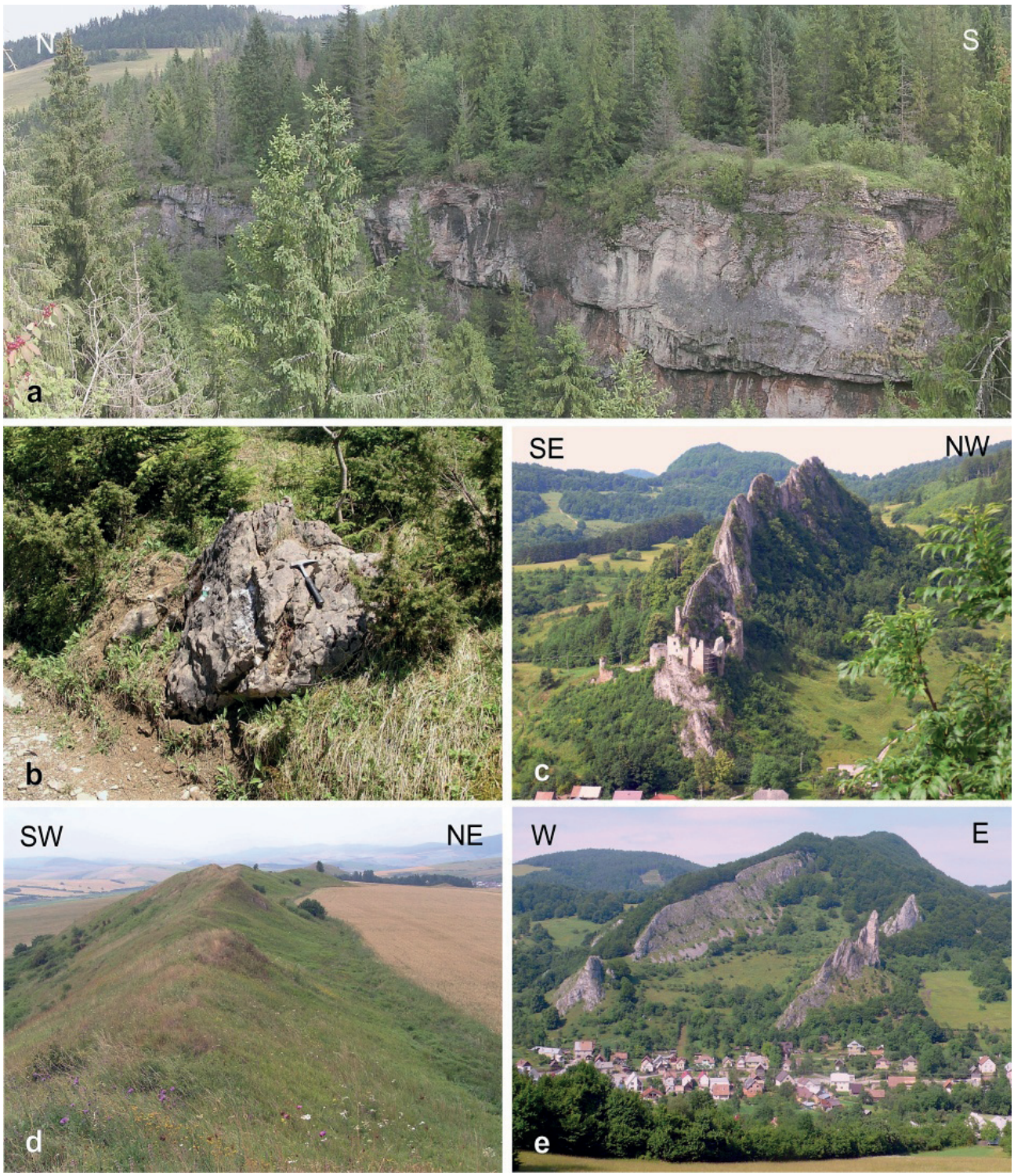

Fig. 6. Examples of various klippen types: (a) eastern wall of the Jarabinské tiesňavy gorge exposing flat-lying Middle Jurassic red nodular and crinoidal limestones of the Subpieniny Unit (Jarabina subunit, Czorsztyn succession, plateau A1X type incised by Malý Lipník stream); (b) isolated block of crinoidal limestones embedded in Upper Cretaceous variegated marls of the Subpieniny Unit, Janíkov vrch near Zázrivá (A1XY type); (c) "dragon back" klippe with the Lednica Castle ruins in western Slovakia (A1Y); (d) typical cuesta in the Pieniny Unit near Šarišské Jastrabie formed by the SW-dipping, erosion-resistant Upper Jurassic and Lower Cretaceous limestones and radiolarites surrounded by marlstones viewed from SE ("goat back" B1Y type); (e) doubled inclined cuestas or "ribs" in the Subpieniny Unit (Czorsztyn succession) above Červený Kameň village in western Slovakia, view to the north.

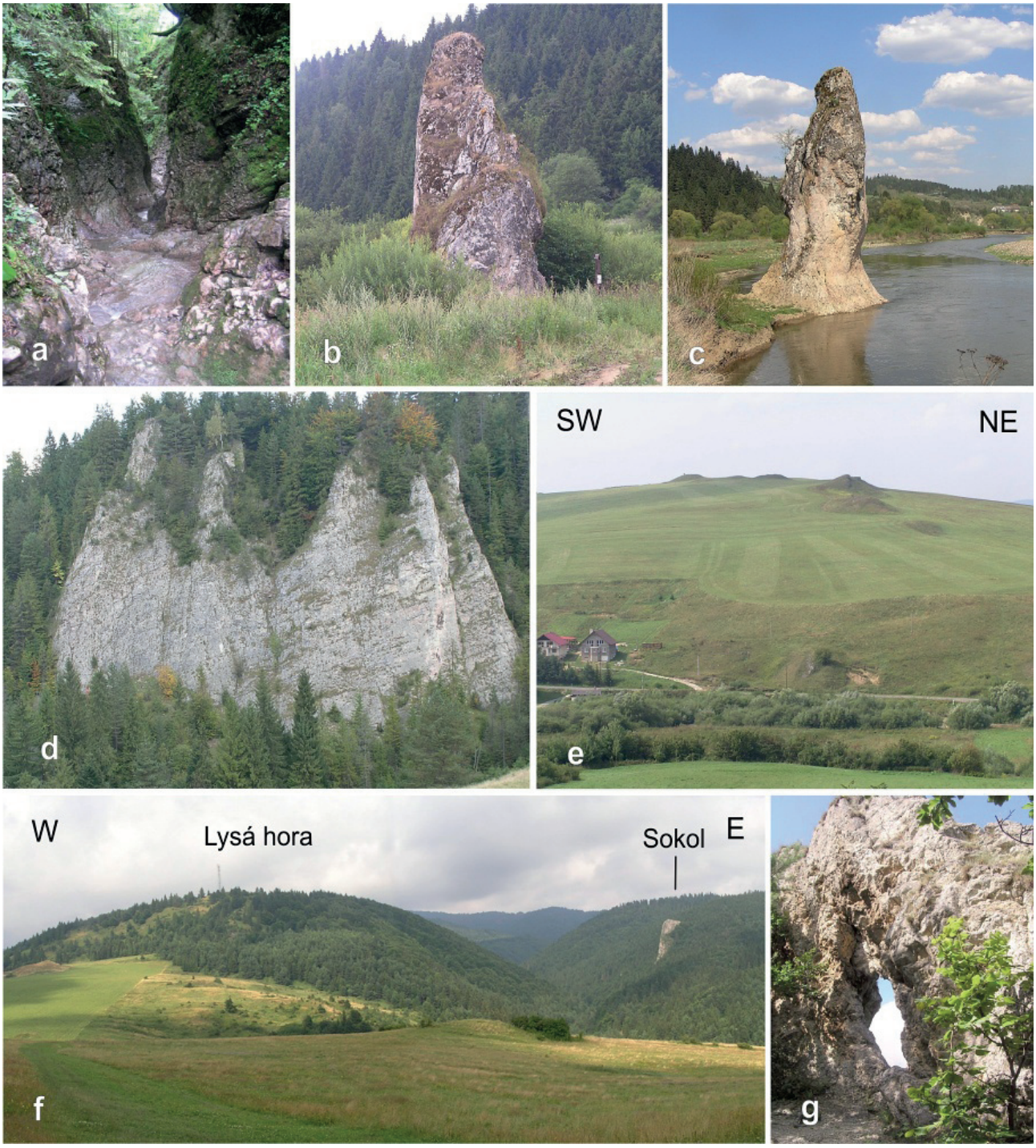

Fig. 7. Examples of various klippen types: (a) Jarabina canyon incised in red nodular limestones of the Czorsztyn succession; (b) and (c) – solitary klippe Skalná ihla in the Poprad River Valley presently affected by abrasion (b – state in 2006, c – in 2012); (d) Brysztan klippe in the Polish Male Pieniny Mts (B1X type); (e) "buttons" of the Pieniny limestones that are gradually uncovered by erosion of the overstepping Oligocene shales of the Huty Fm., ridge Skalka NW of Ďurková village in the foreground; (f) composite olistolith Lysá hora and simple olistolith Sokolia skala east of Kyjov village (see Fig. 3) viewed from the south-west; (g) natural rocky window in the upper part of the Sokol klippe – an example of erosional processes.

small historical quarries and carved crags occurring near Stará Ľubovňa (Marmon, Hajtovka, Údol), where red nodular limestones (Czorsztyn Fm.), chiefly olistoliths in the Milpoš Breccia, were excavated. This Ľubovňa "marble" was used preferably for tombstones especially in the 16th and 17th centuries (Pivko, 2017 and references therein). In places, smaller klippen were almost totally extracted.

It should be noted that the presented classification, although postulated as genetic, is largely empirical and intuitive. With few exceptions, the decisive feature – the contact of a klippe with its matrix, is not accessible to a direct observation. At the same time, the presented klippen types represent the end members, since the majority of klippen exhibit a combination or mixture of various processes shaping their final forms. Nevertheless, it may serve as a guide for distinguishing variable origins and modifications of the endless forms and types of the PKB klippen.

Conclusions

In this work, three basic criteria are applied for distinguishing the various klippen forms and to categorize their genetic and morphologic types. These include: (i) the genetic aspect, i.e. the mode of separation of klippen from original continuous successions; (ii) the structural criterion that differentiates between the gently and steeply dipping primary foliation that largely controls the klippen shapes; (iii) post-origin processes modifying the klippen forms – erosion, fragmentation and transportation by gravity movements, and anthropogenic modifications. The genetic factor considers the primary (A) and secondary (B) modes of klippen individualization. The disconnection by faulting of endogenous tectonic klippen is marked as A1 and that of exogenous sedimentary olistoliths as A2 (Fig. 5). The secondary manners of klippen partition and alterations include various subrecent erosional (B1), gravity-driven (B2) and anthropogenic (B3) processes. The structural factor X marks the gently dipping foliation (bedding, sedimentary layering, cleavage) and Y its steep inclination. For klippen types labelled XY the foliation is insignificant, folded or missing.

By a combination of these factors (Fig. 5), several klippen types are characterized and illustrated: A1XY – tectonically fully separated, variously oriented blocks floating in strongly sheared soft matrix; A1X – plateaus and mosaic-like klippen groups; A1Y – archetypical, steeply inclined tectonic klippen often arranged in rows; A2XY – olistoliths of various sizes and orientations; B1XY – projecting cores of large-scale brachyanticlines; B1X – small table hills and columns; B1Y – cliffy towers and needles, cuestas; B2XY – blocks in landslides; B3XY – quarries, small excavations, road cuts and other artificial alterations of klippen shapes.

Acknowledgements

The present work results from the long-term author´s investigations in the Klippen Belt, which have been supported by a number of research projects, in the last years by APVV-0212-12 and APVV-16-0146. Financial aid from the Slovak Research and Development Agency is gratefully acknowledged. Thorough and constructive reviews by Prof. Edyta Jurewicz (Warsaw) and Dr. Ondrej Pelech (Bratislava) are gratefully acknowledged.

References

Allaby, M., 2008: A Dictionary of Earth Sciences. *Oxford University Press*, 3rd ed., 654 p.

Andrusov, D., 1931: Étude géologique de la zone des Klippes internes des Carpathes Occidentales. I-ière partie: Introduction, II-ième partie: Stratigraphie (Trias et Lias). *Rozpr. St. geol. Úst. Čs. Republ., 6, 167 p.*

Andrusov, D., 1938: Étude géologique de la zone des Klippes internes des Carpathes Occidentales, IIIe partie: Tectonique. *Rozpr. St. geol. Úst. Čs. Republ., 9, 135 p.*

Andrusov, D., 1964: Geologie der tschechoslowakischen Karpaten I. *Berlin, Akademie Verlag; Bratislava, Verlag Slow. Akad. Wiss., 263 p.*

Andrusov, D., 1965: Geologie der tschechoslowakischen Karpaten II. *Berlin, Akademie Verlag; Bratislava, Verlag Slow. Akad. Wiss., 443 p.*

Andrusov, D., 1968: Grundriss der Tektonik der nördlichen Karpaten. *Bratislava, Verlag Slow. Akad. Wiss., 188 p.*

Andrusov, D., 1974: The Pieniny Klippen Belt. In: Maheľ, M. (ed.): Tectonics of the Carpathian-Balkan regions. *Bratislava, Geol. Inst. D. Štúr, 145 – 158.*

Andrusov, D., 1975: Aperçu bref du bati des Carpathes Occidentales. Report of the 10th Jubilee Congress of Carpathian-Balkan Geological Association, General Proceedings. *Bratislava, Geol. Inst. D. Štúr, 95 – 108.*

Andrusov, D. & Scheibner, E., 1960: Prehľad súčasného stavu poznatkov o geológii bradlového pásma medzi Vlárou a Tvrdošínom. *Geol. Sbor., 11, 2, 239 – 279.* (English summary: An outline of the present state of knowledge about the geology of the Klippen Belt between R. Vlára and T. Tvrdošín).

Andrusov, D. & Scheibner, E., 1968: Classification of "Klippes" or "Klippen". Report of the twenty-third International Geological Congress, Proceedings of Section 3 – Orogenic belts. *Prague, Academia, 93 – 102.*

Andrusov, D. & Scheibnerová, V., 1963: On the origin of redepositions of foraminifera in the Cretaceous and Paleogene of Carpathians. *Geol. Sbor., 14, 1, 145 – 148.*

Aubrecht, R. & Sýkora, M., 1998: Middle Jurassic crinoidal shoal complex at Hatné – Hrádok locality (Czorsztyn Unit, Pieniny Klippen Belt, western Slovakia). *Miner. Slov., 30, 157 – 166.*

Aubrecht, R. & Szulc, J., 2006: Deciphering of the complex depositional and diagenetic history of a scarp limestone breccia (Middle Jurassic Krasin Breccia, Pieniny Klippen Belt, Western Carpathians). *Sedimentary Geol., 186, 265 – 281.*

Aubrecht, R., Krobicki, M., Sýkora, M., Mišík, M., Boorová, D., Schlögl, J., Šamajová, E. & Golonka, J., 2006: Early Cretaceous hiatus in the Czorsztyn succession (Pieniny Klippen Belt, Western Carpathians): submarine erosion or emersion? *Ann. Soc. geol. Pol., 76, 161 – 196.*

Beidinger, A. & Decker, K., 2016: Paleogene and Neogene kinematics of the Alpine-Carpathian fold-thrust belt at the Alpine-Carpathian transition. *Tectonophysics, 690, 263 – 287.*

Bielik, M., Šefara, J., Kováč, M., Bezák, V. & Plašienka, D., 2004: The Western Carpathians – interaction of Hercynian and Alpine processes. *Tectonophysics, 393, 63 – 86.*

Biely, A., 1975: Poznámka k termínu „pripieninský lineament". *Geol. Práce, Spr., 63, 205 – 209* (in Slovak: A note to the term "Peripieniny lineament").

Birkenmajer, K., 1958: Przewodnik geologiczny po pienińskim pasie skałkowym. Część I – szkic geologiczny pasa skałkowego. *Warszawa, Wyd. geol., 135 p*. (in Polish: Geological guidebook of the Pieniny Klippen Belt. Part I – geological sketch of the Klippen Belt).

Birkenmajer, K., 1959: Diapiric tectonics in the Pieniny Klippen Belt (Carpathians). *Bull. Acad. pol. Sci., Ser. Sci. Chim., Géol., Géogr., 7, 123 – 128.*

Birkenmajer, K., 1960: Geology of the Pieniny Klippen Belt of Poland. *Jb. Geol. Bundesanst., 103, 1 – 36.*

Birkenmajer, K., 1970: Przedeoceńskie struktury fałdowe w pienińskim pasie skałkowym Polski. *Stud. geol. pol., 31, 81 p.* [English summary: Pre-Eocene fold structures in the Pieniny Klippen Belt (Carpathians of Poland)].

Birkenmajer, K., 1976: Carpathian orogen and plate tectonics. *Publs. Inst. Geophys. Pol. Acad. Sci., A-2 (101), 43 – 53.*

Birkenmajer, K., 1977: Jurassic and Cretaceous lithostratigraphic units of the Pieniny Klippen Belt, Carpathians, Poland. *Stud. geol. pol., 45, 1 – 158.*

Birkenmajer, K., 1983: Uskoki przesuwcze w północnym obrzeżeniu pienińskiego pasa skałkowego w Polsce. *Stud. geol. pol., 77, 89 – 112.* (English summary: Strike-slip faults in the northern boundary zone of the Pieniny Klippen Belt, Carpathians).

Birkenmajer, K., 1986: Stages of structural evolution of the Pieniny Klippen Belt, Carpathians. *Stud. geol. pol., 88, 7 – 32.*

Birkenmajer, K., 1988: Exotic Andrusov Ridge: its role in plate-tectonic evolution of the West Carpathian Foldbelt. *Stud. geol. pol., 91, 7 – 37.*

Birkenmajer, K., 1998: Pieniny Klippen Belt, Carpathians: strike-slip tectonics, terranes and pseudoterranes. *XVI Congress Carpath.-Balkan Geol. Assoc., Aug. 30th – Sept. 2nd, 1998, Abstracts. Vienna, p. 74.*

Birkenmajer, K. & Lorenc, M. W., 2008: Lower Cretaceous exotic intraplate basaltoid olistolith from Biała Woda, Pieniny Klippen Belt, Poland: geochemistry and provenance. *Stud. geol. pol., 131, 237 – 246.*

Buček, S. & Köhler, E., 2017: Palaeocene reef complex of the Western Carpathians. *Slovak Geol. Mag., 17, 1, 3 – 163.*

Bučová, J., Plašienka, D. & Mikuš, V., 2010: Geology and Tectonics of the Vršatec Klippen area (Pieniny Klippen Belt, Western Slovakia). In: Christofides, G., Kantiranis, N., Kostopoulos, D. S. & Chatzipetros, A. A. (eds): Proceedings 19th Congress of the Carpathian-Balkan Geological Association. *Scientific Annals of the School of Geology, Aristotle University, Thessaloniki, Spec. Vol. 100, 197 – 207.*

Buday, T., Kodym, O., Maheľ, M., Máška, M., Matějka, A., Svoboda, J. & Zoubek, V., 1960: Tectonic development of Czechoslovakia. *Praha, Nakl. ČSAV, Ústř. Úst. geol., 226 p.*

Dal Piaz, G. V., Martin, S., Villa, I. M., Gosso, G. & Marschalko, R., 1995: Late Jurassic blueschist facies pebbles from the Western Carpathian orogenic wedge and paleostructural implications for Western Tethys evolution. *Tectonics, 14, 874 – 885.*

Faryad, S. W. & Schreyer, W., 1997: Petrology and geological significance of high-pressure metamorphic rocks occurring as pebbles in the Cretaceous conglomerates of the Klippen Belt (Western Carpathians, Slovakia). *Eur. J. Mineral., 9, 547 – 562.*

Froitzheim, N., Plašienka, D. & Schuster, R., 2008: Alpine tectonics of the Alps and Western Carpathians. In: McCann, T. (ed.): The Geology of Central Europe. Volume 2: Mesozoic and Cenozoic. *London, Geol. Soc. Publ. House, 1 141 – 1 232.*

Golonka, J., Krobicki, M., Waśkowska, A., Cieszkowski, M. & Ślączka, A., 2015: Olistostromes of the Pieniny Klippen Belt, Northern Carpathians. *Geol. Mag., 152, 2, 269 – 286.*

Grecula, P. & Roth, Z., 1978: Kinematický model Západních Karpat v souborném řezu. *Sbor. geol. Věd, Geol., 32, 49 – 73*. (English summary: Kinematic model of the West Carpathians).

Haško, J., 1976: Czertezický vývin bradlového pásma v Zázrivej-Plešivej. *Geol. Práce, Spr., 65, 91 – 95* (in Slovak with English abstract).

Horváth, F., Vörös, A. & Onuoha, K. M., 1977: Plate-tectonics of the Western Carpatho-Pannonian region: a working hypothesis. *Acta geol. Acad. Sci. hung., 21, 4, 207 – 221.*

Jamrichová, M., Józsa, Š., Aubrecht, R. & Schlögl, J., 2012: Lower Cretaceous palaeokarst in a klippe of the Czorsztyn Succession north of Zázrivá (Pieniny Klippen Belt, Orava sector, northern Slovakia). *Acta Geol. Slov., 4, 1, 75 – 90.*

Jurewicz, E., 1994: Analiza strukturalna pienińskiego pasa skałkowego okolic Jaworek. *Stud. geol. pol., 106, 7 – 87.* (English summary: Structural analysis of the Pieniny Klippen Belt at Jaworki, Carpathians, Poland).

Jurewicz, E., 2005: Geodynamic evolution of the Tatra Mts. and the Pieniny Klippen Belt (Western Carpathians). *Acta geol. pol., 55, 3, 295 – 338.*

Jurewicz, E., 2018: The Šariš Transitional Zone, revealing interactions between Pieniny Klippen Belt, Outer Carpathians and European platform. *Swiss J. Geosci.*, *https://doi.org/10.1007/s00015-017-0297-9.*

Kissová, D., Dunkl, I., Plašienka, D., Frisch, W. & Marschalko, R., 2005: The Pieninic exotic cordillera (Andrusov Ridge) revisited: new zircon FT ages of granite pebbles from Cretaceous flysch conglomerates of the Pieniny Klippen Belt (Western Carpathians, Slovakia). *Slovak Geol. Mag., 11, 1, 17 – 28.*

Kováč, P. & Hók, J., 1996: Tertiary development of the western part of Klippen Belt. *Slovak Geol. Mag.*, 2/96, 137 – 149.

Kováč, M., Plašienka, D., Soták, J., Vojtko, R., Oszczypko, N., Less, Gy., Ćosović, V., Fügenschuh, B. & Králiková, S., 2016: Paleogene palaeogeography and basin evolution of the Western Carpathians, Northern Pannonian domain and adjoining areas. *Global Planet. Change*, *140, 9 – 27*.

Köhler, E. & Buček, S., 2005: Paleocene reef limestones near Veľký Lipník (Pieniny Mts., NE Slovakia): Facial environments and biogenic components. *Slovak Geol. Mag., 11, 4, 249 – 267.*

Köhler, E., Salaj, J. & Buček, S., 1993: Paleogeographical development of the Myjava sedimentary area (Western Slovakia) during the existence of the Paleocene reef complex. *Geol. Carpath., 44, 373 – 380.*

Książkiewicz, M., 1977: The tectonics of the Pieniny Klippes Belt. In: Książkiewicz, M., Oberc, J. & Pożaryski, W.: Geology of Poland, Vol. IV Tectonics. *Warsaw, Publ. House Wyd. Geol., 519 – 552.*

Leško, B. & Varga, I., 1980: Alpine elements in the West Carpathian structure and their significance. *Miner. Slov., 12, 2, 97 – 130.*

Lewandowski, M., Krobicki, M., Matyja, B. A. & Wierzbowski, A., 2005: Palaeogeographic evolution of the Pieniny Klippen Basin using stratigraphic and palaeomagnetic data from the Veliky Kamenets section (Carpathians, Ukraine). *Palaeogeogr. Palaeoclimatol. Palaeoecol., 216, 53 – 72.*

Limanowski, M., 1906: Sur la génèse des Klippes des Carpathes. *Bull. Soci. géol. France (4me Sér.), 6, 151 – 169.*

Lugeon, M., 1903: Les nappes de recouvrement de la Tatra et l´origine des Klippes des Carpathes. *Bull. Lab. Géol., Géogr., Phys. Mineral. Petrogr. Univ. Lausanne, 4, 1 – 51.*

Maheľ, M., 1974: Alpidy, hlavne Západné Karpaty, z hľadiska globálnej tektoniky. *Miner. Slov., 6, 2, 97 – 102* (in Slovak: Alpides, mainly Western Carpathians, from the viewpoint of global tectonics).

Maheľ, M., 1977: Development model of the West Carpathians. *Geol. Carpath., 28, 2, 203 – 218.*

Maheľ, M., 1980: Pribradlové pásmo, charakteristika a význam. *Miner. Slov., 12, 3, 193 – 207.* (English summary: The Peri-klippen zone: nearer characterization and significance).

Maheľ, M., 1981: Island character of the Klippen Belt; Vahicum – continuation of Southern Penninicum in West Carpathians. *Geol. Zbor. Geol. carpath., 32, 3, 293 – 305.*

Maheľ, M., 1986: Geologická stavba československých Karpát. 1 – Paleoalpínske jednotky. *Bratislava, Veda, Vyd. Slov. Akad. Vied, 510 s.* (in Slovak: Geological structure of the Czechoslovak Carpathians. 1 – Palaeoalpine units).

Maheľ, M., 1989: Bradlové pásmo z aspektu geodynamického modelu. *Miner. Slov., 21, 99 – 108*. (English summary: The Klippen Belt from the aspect of the geodynamic model).

Maheľ, M., 1990: Strižné zóny, ich prejavy (oblúky a niektoré priečne prelomy) v Západných Karpatoch. *Miner. Slov., 22, 41 – 46*. [English summary: Shear zones, their manifestation (arcs and some transversal rifts) in the West Carpathians].

Marko, F., Plašienka, D. & Fodor, L., 1995: Meso-Cenozoic tectonic stress fields within the Alpine-Carpathian transition zone: a review. *Geol. Carpath., 46, 19 – 27.*

Marko, F., Vojtko, R., Plašienka, D., Sliva, Ľ., Jablonský, J., Reichwalder, P. & Starek, D., 2005: A contribution to the tectonics of the Periklippen zone near Zázrivá (Western Carpathians). *Slovak Geol. Mag., 11, 37 – 43.*

Marschalko, R., 1979: Considerations about Pienide flysch basins and their substratum in the Cretaceous and Paleogene (West Carpathians). In: Maheľ, M. & Reichwalder, P. (eds): Czechoslovak geology and global tectonics. *Bratislava, Veda, Vyd. Slov. Akad. Vied, , 103 – 113.*

Marschalko, R., 1986: Vývoj a geotektonický význam kriedového flyšu bradlového pásma. *Bratislava, Veda, Vyd. Slov. Akad. Vied, 140 s.* (English summary: Evolution and geotectonic significance of the Klippen Belt Cretaceous flysch in the Carpathian megastructure).

Marschalko, R. & Kysela, J., 1980: Geológia a sedimentológia bradlového pásma a manínskej jednotky medzi Žilinou a Považskou Bystricou. *Západ. Karpaty, Sér. Geol., 6, 7 – 79.* (English summary: Geology and sedimentology of the Klippen Belt and Manín Unit between Žilina and Považská Bystrica).

Marschalko, R. & Rakús, M., 1997: Development of the Cretaceous flysch in the Klape unit and the recyclicity problem of the clastic material. In: Plašienka, D., Hók, J., Vozár, J. & Elečko, M. (eds): Alpine evolution of the Western Carpathians and related areas. Internat. Conference, Introductory articles to the excursion. *Bratislava, GS SR, D. Štúr Publ., 71 – 78.*

Marschalko, R. & Samuel, O., 1977: Olistostrómové fácie kriedového flyšu bradlového pásma pri Širokej a Krivej na Orave. *Geol. Práce, Spr., 67, 53 – 71.* (English summary: Olistostrome facies of Cretaceous Flysch in Klippen Belt near Široká and Krivá in Orava).

Marschalko, R., Haško, J. & Samuel, O., 1979: Záskalské brekcie a proces vzniku olistostrómov. *Geol. Práce, Spr., 73, 75 – 88.* (English summary: Záskalie breccias and genesis of olistostromes).

Márton, E., Grabowski, J., Plašienka, D., Túnyi, I., Krobicki, M., Haas, J. & Pethe, M., 2013: New paleomagnetic results from the Upper Cretaceous red marls of the Pieniny Klippen Belt, Western Carpathians: Evidence for general CCW rotation and implications for the origin of the structural arc formation. *Tectonophysics, 592, 1 – 13.*

Mello, J. (ed.), Boorová, D., Buček, S., Filo, I., Fordinál, K., Havrila, M., Iglárová, Ľ., Kubeš, P., Liščák, P., Maglay, J., Marcin, D., Nagy, A., Potfaj, M., Rakús, M., Rapant, S., Remšík, A., Salaj, J., Siráňová, Z., Teťák, F., Zuberec, J., Zlinská, A. & Žecová, K., 2011: Vysvetlivky ku geologickej mape stredného Považia 1 : 50 000. *Bratislava, Št. Geol. Úst. D. Štúra, 378 s.* (English summary: Explanations to the geological map of the Middle Váh Valley).

Michalík, J., Vašíček, Z., Boorová, D., Golej, M., Halásová, E., Hort, P., Ledvák, P., Lintnerová, O., Měchová, L., Šimo, V., Šimonová, V., Reháková, D., Schlögl, J., Skupien, P., Smrečková, M., Soták, J. & Zahradníková, B., 2013: The Butkov Hill – a stone archive of Slovakian mountains and the Mesozoic sea life history. *Bratislava, Veda, 164 p.*

Mišík, M., 1978: Niektoré paleogeografické problémy bradlového pásma. In: Vozár, J. et al. (eds): Paleogeografický vývoj Západných Karpát. *Konferencie – Sympóziá – Semináre, Bratislava, Geol. Úst. D. Štúra, 147 – 159.* (English summary: Some paleogeographical problems concerning Klippen Belt).

Mišík, M., 1979: Pieniny Klippen Belt and the global tectonics model. In: Maheľ, M. & Reichwalder, P. (eds): Czechoslovak geology and global tectonics. *Bratislava, Veda*, *89 – 101.*

Mišík, M., 1997: The Slovak part of the Pieniny Klippen Belt after the pioneering works of D. Andrusov. *Geol. Carpath.*, *48, 209 – 220.*

Mišík, M. & Sýkora, M., 1981: Pieninský exotický chrbát rekonštruovaný z valúnov karbonátových hornín kriedových

zlepencov bradlového pásma a manínskej jednotky. *Západ. Karpaty, Sér. Geol., 7, 7 – 111.* (German summary: Der pieninische exotische Rücken, rekonstruiert aus Geröllen karbonatischer Gesteine kretazischer Konglomerate der Klippenzone und der Manín-Einheit).

Mišík, M. & Sýkora, M., 1993: Jurassic submarine scarp breccia and neptunian dykes from the Kyjov-Pusté Pole klippen (Czorsztyn unit). *Miner. Slov., 25, 411 – 427.*

Mišík, M., Mock, R. & Sýkora, M., 1977: Die Trias der Klippenzone der Karpaten. *Geol. Zbor. Geol. carpath., 28, 1, 27 – 69.*

Mišík, M., Jablonský, J., Mock, R. & Sýkora, M., 1981: Konglomerate mit exotischem Material in dem Alb der Zentralen Westkarpaten – paläographische und tektonische Interpretation. *Acta geol. geogr. Univ. Comen., Geol., 37, 5 – 55.*

Mišík, M., Aubrecht, R., Sýkora, M. & Ožvoldová, L., 1996: New lithostratigraphic units in the Klippen Belt. *Slovak Geol. Mag., 1/1996, 17 – 19.*

Mojsisovicz, E., 1867: Umgebung von Rogoznik und Csorsztyn. Nördliche Tatra-Thäler. *Verh. K.-Kön. geol. Reichsanst., 10, 212 – 214.*

Muratov, M. V., 1949: Tektonika i istorija razvitija aľpijskoj geosynklinaľnoj oblasti juga evropejskoj časti SSSR i sopredeľnych stran. In: Tektonika SSSR, Vol. 2. *Moskva – Leningrad, Izd. AN SSSR, 510 p.* (in Russian: Tectonics and evolution of geosynclinal area of the southern European part of USSR and neighbouring regions).

Nemčok, J., 1980: Non-traditional view of East-Slovakian Klippen Belt. *Geol. Zbor. Geol. carpath., 31, 563 – 568.*

Nemčok, M. & Nemčok, J., 1994: Late Cretaceous deformation of the Pieniny Klippen Belt, West Carpathians. *Tectonophysics, 239, 81 – 109.*

Nemčok, J., Kullmanová, A. & Ďurkovič, T., 1989: Vývoj a stratigrafické postavenie gregorianskych brekcií bradlového pásma na východnom Slovensku. *Geol. Práce, Spr., 89, 11 – 37.* (English summary: Facies- and stratigraphical analyses of Gregorianka breccias in Klippen Belt of East Slovakia).

Neumayr, M., 1871: Jurastudien. 5. Das Pieninische Klippenzug. *Jb. K. -Kön. geol. Reichsanst., 21, 4, 451 – 536.*

Oszczypko, N., Salata, D. & Krobicki, M., 2012: Early Cretaceous intra-plate volcanism in the Pieniny Klippen Belt – a case study of the Velykyi Kamenets'/Vilkhivchyk (Ukraine) and the Biała Woda (Poland) sections. *Geol. Quarterly, 56, 4, 629 – 648.*

Pešková, I., **Vojtko, R.**, Starek, D. & Sliva, Ľ., 2009: Late Eocene to Quaternary deformation and stress field evolution of the Orava region (Western Carpathians). *Acta geol. pol., 59, 1, 73 – 91.*

Pešková, I., Hók, J., Potfaj, M. & Vojtko, R., 2012: Štruktúrna interpretácia varínskeho a oravského úseku bradlového pásma. *Geol. Práce, Spr., 120, 51 – 64.* (English abstract: Structural interpretation of the Varín and Orava segment of the Klippen Belt).

Pfiffner, O. A., 2014: Geology of the Alps. *Sec. ed. Blackwell, Wiley, 376 p.*

Pivko, D., 2017: Jurassic red nodular limestone from NE Slovakia used as the Ľubovňa "marble" during the Renaissance in Slovakia and Poland. *Geol. Quart., 64, 1, 53 – 61.*

Plašienka, D., 1995: Mesozoic evolution of Tatric units in the Malé Karpaty and Považský Inovec Mts.: Implications for the position of the Klape and related units in western Slovakia. *Geol. Carpath., 46, 101 – 112.*

Plašienka, D., 1999: Tektonochronológia a paleotektonický model jursko-kriadového vývoja Centrálnych Západných Karpát. *Bratislava, Veda, 125 p.* (English summary: Tectonochronology and paleotectonic model of the Jurassic – Cretaceous evolution of the Central Western Carpathians).

Plašienka, D., 2003: Dynamics of Mesozoic pre-orogenic rifting in the Western Carpathians. *Mitt. Österr. geol. Gesell., 94 (2001), 79 – 98.*

Plašienka, D., 2010: Structure and evolution of the Pieniny Klippen Belt and its position in the Western Carpathian framework. *J. Alpine Geol., 52, 35 – 40.*

Plašienka, D., 2012a: Jurassic syn-rift and Cretaceous syn-orogenic, coarse-grained deposits related to opening and closure of the Vahic (South Penninic) Ocean in the Western Carpathians – an overview. *Geol. Quart., 56, 601 – 628.*

Plašienka, D., 2012b: Early stages of structural evolution of the Carpathian Klippen Belt (Slovakian Pieniny sector). *Miner. Slov., 44, 1 – 16.*

Plašienka, D. & Mikuš, M., 2010: Geologická stavba pieninského a šarišského úseku bradlového pásma medzi Litmanovou a Drienicou na východnom Slovensku. *Miner. Slov., 42, 155 – 178.* (English summary: Geological structure of the Pieniny and Šariš sectors of the Klippen Belt between Litmanová and Drienica villages in eastern Slovakia).

Plašienka, D. & Soták, J., 2015: Evolution of Late Cretaceous-Palaeogene synorogenic basins in the Pieniny Klippen Belt and adjacent zones (Western Carpathians, Slovakia): tectonic controls over a growing orogenic wedge. *Ann. Soc. geol. Pol., 85, 1, 43 – 76.*

Plašienka, D., Vozár, J. & Bielik, M., 2008: The Pieniny Klippen Belt at the depth – rooted, or unrooted? In: Németh, Z. & Plašienka, D. (eds): SlovTec08. 6th Meeting of the Central European Tectonic Studies Group (CETeG) and 13th Meeting of the Czech Tectonic Studies Group (ČTS), Upohlav, Slovakia, 23 – 26 April 2008. Proceedings and Excursion Guide. *Bratislava, St. Geol. Inst. D. Stur, 104 – 108.*

Plašienka, D., Sýkora, M., Aubrecht, R., Krobicki, M. & Józsa, Š., 2010: Reinterpretation of the lithostratigraphy and tectonic position of the Mariková Klippen (Middle Váh Valley, western Slovakia). *Acta Geol. Slov., 2, 1, 1 – 9.*

Plašienka, D., Soták, J., Jamrichová, M., Halásová, E., Pivko, D., Józsa, Š., Madzin, J. & Mikuš, V., 2012: Structure and evolution of the Pieniny Klippen Belt demonstrated along a section between Jarabina and Litmanová villages in Eastern Slovakia. *Miner. Slov., 44, 1, 17 – 38.*

Plašienka, D., Józsa, Š., Gedl, P. & Madzin, J., 2013: Fault contact of the Pieniny Klippen Belt with the Central Carpathian Paleogene Basin (Western Carpathians): new data from a unique temporary exposure in Ľutina village (Eastern Slovakia). *Geol. Carpath., 64, 2, 165 – 168.*

Plašienka, D., Michalík, J., Soták, J. & Aubrecht, R., 2017: Discussion of "Olistostromes of the Pieniny Klippen Belt, Northern Carpathians". *Geol. Mag., 154, 1, 187 – 192.*

Potfaj, M., Samuel, M., Raková, J. & Samuel, O., 1991: Geologická stavba Kubínskej hole (Orava). *Západ. Karpaty, Sér. Geol., 15, 25 – 66.* [English summary: Geologic structure of Kubínska hoľa Range (Orava)].

Rakús, M., 1997: Manín gorge. Excursion Guide. *Internat. Conference Alpine evolution of the Western Carpathians and related areas, Bratislava, Sept. 11 – 14, 1997, 6 – 11.*

Rakús, M. & Hók, J., 2005: Manínska a klapská jednotka – litostratigrafická náplň, tektonické zaradenie, paleogeografická pozícia a vzťah k váhiku. *Miner. Slov., 37, 1, 9 – 26.* (English summary: The Manín and Klape units: Lithostratigraphy, tectonic classification, paleogeographic position and relationship to Váhicum).

Rakús, M. & Marschalko, R., 1997: Position of the Manín, Drietoma and Klape units at the boundary of the Central and outer Carpathians. In: Plašienka, D., Hók, J., Vozár, J. & Elečko, M. (eds): Alpine evolution of the Western Carpathians and related areas. Internat. Conference, Introductory articles to the excursion. *Bratislava, GS SR, D. Štúr Publ., 79 – 97.*

Ratschbacher, L., Frisch, W., Linzer, H.-G., Sperner, B., Meschede, M., Decker, K., Nemčok, M., Nemčok, J. & Grygar, R., 1993: The Pieniny Klippen Belt in the Western Carpathians of northeastern Slovakia: structural evidence for transpression. *Tectonophysics, 226, 471 – 483.*

Reháková, D., Matyja, B. A., Wierzbowski, A., Schlögl, J., Krobicki, M. & Barski, M., 2011: Stratigraphy and microfacies of the Jurassic and lowermost Cretaceous of the Veliky Kamenets section (Pieniny Klippen Belt, Carpathians, Western Ukraine). *Volumina Jurassica, 9, 61 – 104.*

Roth, Z., 1963: Strukturbeziehungen des Sedimentationsgebietes der Flyschzone der Westkarpaten zum Karpatenvorland und den Zentralkarpaten. *Geol. Práce, Zpr., 28, 5 – 22.*

Roth, Z., 1964: Die Tektonik des Westabschnittes der Äußeren Karpaten in der CSSR. *Z. Dtsch. geol. Gesell., 116, 2, 312 – 341.*

Salaj, J., 1991: Biostratigrafická korelácia flyšových súvrství kriedy bradlovej a pribradlovej zóny stredného Považia a jej paleogeograficko-tektonický vývoj. *Miner. Slov., 23, 4, 295 – 113.* (English summary: Biostratigraphic correlation of Cretaceous flysch formations in the Klippen- and Peri-Klippen zones of the Middle Váh river valley and their paleogeographic-tectonic history).

Salaj, J., 1997: Survey of Upper Cretaceous and Paleogene biostratigraphy of the Klippen and Periklippen Belts in the middle Váh valley. In: Plašienka, D., Hók, J., Vozár, J. & Elečko, M. (eds): Alpine evolution of the Western Carpathians and related areas. Internat. Conference, Introductory articles to the excursion. *Bratislava, GS SR, D. Štúr Publ., 99 – 117.*

Scheibner, E., 1961: The tectonic style of the Klippen Belt and the idea about its origin. *Geol. Sbor., 12, 2, 153 – 158.*

Scheibner, E., 1963a: Relationship between material and tectonic style, and selective tectonics in the Klippen Belt of West Carpathians. *Geol. Práce, Zpr., 28, 59 – 68.*

Scheibner, E., 1963b: The possibility of paleogeographical reconstructions in the Klippen Belt on the basis of analysis of tectonic building. *Geol. Sbor., 14, 1, 29 – 35.*

Scheibner, E., 1968: The Klippen Belt of the Carpathians. In: Maheľ, M. & Buday, T. (eds.), 1968: Regional geology of Czechoslovakia. Part II – Western Carpathians. *Praha, Academia, 304 – 371.*

Scheibner, E., 1969: Some notes to the Pieniny lineament. *Acta geol. geogr. Univ. Comen., Geol., 18, 9 – 17.*

Schlögl, J., Rakús, M., Krobicki, M., Matyja, B. A., Wierzbowski, A., Aubrecht, R., Sitár, V. & Józsa, Š., 2004: Beňatina Klippe – lithostratigraphy, biostratigraphy, palaeontology of the Jurassic and Lower Cretaceous deposits (Pieniny Klippen Belt, Western Carpathians, Slovakia). *Slovak Geol. Mag., 10, 4, 241 – 262.*

Schlögl, J., Plašienka, D., Aubrecht, R., Michalík, J. & Potfaj, M., 2008: Composition, structure and evolution of the Pieniny Klippen Belt and adjacent zones in western Slovakia – Excursion Guide. In: Németh, Z. & Plašienka, D. (eds): SlovTec08. 6th Meeting of the Central European Tectonic Studies Group (CETeG) and 13th Meeting of the Czech Tectonic Studies Group (ČTS), Upohlav, Slovakia, 23 – 26 April 2008. Proceedings and Excursion Guide. *Bratislava, St. Geol. Inst. D. Stur, 203 – 235.*

Sikora, W., 1974: The Pieniny Klippen Belt (Polish Carpathians). In: Maheľ, M. (ed.): Tectonics of the Carpathian-Balkan regions. *Bratislava, Geol. Inst. D. Štúr, 177 – 180.*

Sikora, J. W., 1976: On lineaments found in the Carpathians. *Rocz. Pol. Tow. geol. (Ann. Soc. géol. Pol.), 46, 1 – 2, 3 – 37.*

Soták, J., 1992: Evolution of the Western Carpathian suture zone – principal geotectonic events. *Geol. Carpath., 43, 6, 355 – 362.*

Spišiak, J. & Sýkora, M., 2009: Geochémia a mineralógia bazaltov z Hanigovce – pročské vrstvy. In: Jurkovič, Ľ., Slaninka, I. & Ďurža, O. (eds): Geochémia 2009. *Konferencie – Sympóziá – Semináre. Bratislava, St. Geol. Inst. D. Štúr, 106 – 109* (in Slovak: Geochemistry and mineralogy of the Hanigovce basalts – the Proč beds).

Spišiak, J., Plašienka, D., Bučová, J., Mikuš, T. & Uher, P., 2011: Petrology and palaeotectonic setting of Cretaceous alkaline basaltic volcanism in the Pieniny Klippen Belt (Western Carpathians, Slovakia). *Geol. Quart., 55, 1, 27 – 48.*

Stegena, L., 1975: Plattentektonik, Tethys and das Pannonische Becken. In: Maheľ, M. (ed.): Tectonic problems of the Alpine system. *Bratislava, Veda, 87 – 108.*

Stráník, Z., 1965: Geologie magurského flyše Čerchovského pohoří a západní části Ondavské vrchoviny. *Sbor. geol. Vied, Západ. Karpaty, 3, 125 – 178.* (German summary: Zur Geologie des Magura-Flysches im Gebirge Čerchovské pohoří und Ondavská vrchovina).

Stille, H., 1953: Der geotektonische Werdegang der Karpaten. *Beihefte Geol. Jb., 8, 239 p.*

Stur, D., 1860: Bericht über die geologische Uebersichts-Aufnahme des Wassergebietes der Waag und Neutra. *Jb. K.-Kön. geol. Reichsanst., 11, 17 – 151.*

Suess, E., 1885: Das Antlitz der Erde, Band I. *Wien, Tempsky, 778 p.*

Szádecky-Kardoss, E., 1975: The belts of subduction in the Carpathian-Pannonian-Dinaric area. In: Maheľ, M. (ed.): Tectonic problems of the Alpine system. *Bratislava, Veda, 69 – 85.*

Šefara, J., Bielik, M. & Bezák, V., 1998: Interpretation of the West Carpathians lithosphere on the basis of geophysical data. In: Rakús, M. (ed.): Geodynamic development of the Western Carpathians. *Bratislava, GS SR, D. Štúr Publ., 273 – 280.*

Šimonová, V. & Plašienka, D., 2011: Kinematická a paleonapäťová analýza zlomov v butkovskom lome (manínska jednotka, Západné Karpaty). *Acta Geol. Slov., 3, 1, 21 – 31.*

[English summary: Fault kinematics and palaeostress analysis in the Butkov quarry (Manín Unit, Western Carpathians)].

Šimonová, V. & Plašienka, D., 2017: Stepwise clockwise rotation of the Cenozoic stress field in the Western Carpathians as revealed by kinematic analysis of minor faults in the Manín Unit (western Slovakia). *Geol. Quart., 61, 1, 252 – 265.*

Tomek, Č., 1993: Deep crustal structure beneath the central and inner West Carpathians. *Tectonophysics, 226, 417 – 431.*

Tomek, Č. & Hall, J., 1993: Subducted continental margin imaged in the Carpathians of Czechoslovakia. *Geology, 21, 535 – 538.*

Trümpy, R., 2006: Geologie de Iberger Klippen und ihrer Flysch-Unterlage. *Eclogae geol. Helv., 99, 1, 79 – 121.*

Uhlig, V., 1890: Ergebnisse geologischer Aufnahmen in den westgalizischen Karpathen. II. Der pieninische Klippenzug. *Jb. K.-Kön. geol. Reichsanst., 40, 3 – 4, 559 – 824.*

Uhlig, V., 1903: Bau und Bild der Karpathen. In: Diener, C., Hoernes, R., Suess, F. E. & Uhlig, V. (eds): Bau und Bild Österreichs. *Wien, Tempsky – Leipzig, Freytag, 649 – 911.*

Uhlig, V., 1904: Über die Klippen der Karpathen. Congrès Géologique International Compte Rendu de la IX. Session, Vienne 1903, Premier Fascicule. *Vienne, Imprimerie Hollinek Fréres, 427 – 453.*

Uhlig, V., 1907: Über die Tektonik der Karpathen. *Sitz.-Ber. K. Akad. Wiss., math.-naturwiss. Kl., 116, I, 871 – 982.*

Wierzbowski, A., Aubrecht, R., Krobicki, M., Matyja, B. A. & Schlögl, J., 2004: New data on Jurassic stratigraphy and palaeogeography of the Czertezik Succession, Pieniny Klippen Belt (Western Carpathians) of Poland and Slovakia. *Ann. Soc. geol. Pol., 74, 237 – 256.*

Karpatské bradlové pásmo a typy jeho bradiel – pokus o genetickú klasifikáciu

Bradlá a bradlová stavba spolu s pozíciou v orogéne sú najcharakteristickejšími znakmi pieninského bradlového pásma. Ako bradlá tu definujeme inklúzie rigidnejších jursko-spodnokriedových karbonátov (rádovo x až x 100 m), ostro oddelených od okolitých nekompetentných sedimentov bradlového „obalu“, ktorými sú spodnojurské a vrchnokriedové až paleogénne bridlice, slieňovce a pieskovce (štruktúry „*block-in-matrix*“). Typologickou klasifikáciou bradiel sa v minulosti zaoberali vo viacerých prácach najmä D. Andrusov a E. Scheibner (Andrusov a Scheibner, 1960, 1968; Scheibner, 1968; Andrusov, 1968, 1974). V princípe rozlíšili netektonické (napr. rify, olistolity, bloky v zosuvoch) a tektonické typy bradiel: švajčiarsky (príkrovové trosky), moravský (šupiny v čelách príkrovov) a pieninský typ (s viacerými podtypmi ako rudinský, vršatský, pieninský s. s.), ako aj bradlá typu Czerwonej skaly (diapírové štruktúry – „*raisins in cake*“ podľa Birkenmajera, 1959). Takáto klasifikácia by po morfoštruktúrnej stránke možno obstála aj dnes (s výnimkou diapírových štruktúr, ktorých existenciu nepotvrdzujeme), žiada sa však do nej viac zaviesť aj genetické aspekty.

V tejto práci sa navrhuje klasifikovať bradlá podľa troch základných kritérií: 1. spôsob separácie bradiel (genetický aspekt); 2. generálny uhol sklonu dominantnej foliácie bradiel (štruktúrny aspekt); 3. modifikácie spôsobené naloženými pripovrchovými procesmi, ako sú erózia, gravitačné pohyby alebo ľudské aktivity (morfologický faktor). Podľa genézy sa tak rozlišujú primárne separované bradlá (A1 tektonické bradlá a A2 sedimentárne olistolity) a sekundárne oddelené a modifikované bradlá (B1 erózne, B2 gravitačné a B3 antropogénne ovplyvnené). Ak je foliácia subhorizontálna (X), bradlá zvyčajne vytvárajú areálne (plošné) skupiny, ak je subvertikálna (Y), tak máme lineárne (radové) skupiny.

Kombináciou týchto aspektov sa dajú vyčleniť nasledujúce typy bradiel a ich skupín (obr. 5): A1XY – tektonické bloky a fragmenty „plávajúce“ v silne zbridličnatenom matrixe; A1X – plató a mozaikové skupiny; A1Y – najčastejšie vretenovité bloky a „dračie chrbty“; A2XY – olistolity a ich skupiny; B1XY – často len brachyklinály a „rebrá“ preparované eróziou; B1X – stolové a svedecké hory, „korytnačie chrbty“; B1Y – skalné veže a ihly (resp. mogoty) a „kozie chrbty“ (kvesty); B2XY – rôzne „odvalené“ a „stratené“ bradlá (bloky) a ich skupiny v zosuvoch; B3XY – bradlá, ktorých morfológia je modifikovaná lomovou ťažbou a inými antropogénnymi vplyvmi. Na základe vnútornej stavby možno rozlišovať aj jednoduché bradlá tvorené tektonicky neprerušeným litostratigrafickým sledom (často len jedným súvrstvím či členom) a zložené bradlá budované viacerými tektonickými šupinami s opakujúcim sa sledom. Navrhované kategórie však predstavujú len koncové členy bradlových foriem a v mnohých prípadoch sa v určitých bradlách kombinujú znaky dvoch alebo aj viacerých typov. Prakticky všetky primárne bradlá sú, pokiaľ sa objavia na zemskom povrchu, ovplyvňované sekundárnymi procesmi. Sekundárne procesy však môžu vytvoriť formy podobné bradlám aj z častí sukcesií, ktoré pôvodne nemali charakter primárnych bradiel. Účelom tejto klasifikácie je preto lepšie odlíšiť primárne, najmä tektonické bradlá od bradiel, na vzniku ktorých sa v podstatnej miere podieľali sekundárne procesy. Klasifikácia je ilustrovaná príkladmi z rôznych úsekov pieninského bradlového pásma.

Doručené / Received: 26. 4. 2018
Prijaté na publikovanie / Accepted: 5. 6. 2018

Mineralia Slovaca, Web ISSN 1338-3523, ISSN 0369-2086
50 (2018), 25 – 36, © Authors 2018. CC BY 4.0

Fold deformation of the Fatricum – a case study from the Banka section (Považský Inovec Mts., Slovakia)

ONDREJ PELECH[1], ŠTEFAN JÓZSA[2] and PAVOL FAJDEK[2]

[1]State Geological Institute of Dionýz Štúr, Mlynská dolina 1, SK-817 04 Bratislava, Slovakia;
ondrej.pelech@geology.sk
[2]Comenius University in Bratislava, Faculty of Natural Sciences, Department of Geology and Paleontology,
Mlynská dolina, Ilkovičova 6, SK-842 15 Bratislava, Slovakia

Abstract: Unique temporal exposure of Fatricum Zliechov sub-unit in the road cut near Banka (Piešťany district, Slovakia) allowed to document deformed sedimentary sequence ranging from Rhaetian to Albian. It was possible to identify the Fatra, Kopienec, Osnica and Párnica formations. Due to their lithology and better exposure, the latter two were characterized by a variety of fold and fault structures. Their strong deformation results in significant thickness reduction of several members of the sequence and suggests that most of sedimentary contacts are tectonized. West-vergent folds and reverse faults are classified to the Paleoalpine (Mid- to Late Cretaceous) deformation phase related to the thin-skinned emplacement of Fatric nappes. The east-vergent low-angle thrust faults and folds represent younger retro-vergent (probably Oligocene–Early Miocene) "back-thrusting" phase. Younger normal faults are a result of Miocene to Quaternary extensional events.

Key words: kinematics, thin-skinned tectonics, folding, back-thrusting, Fatricum, Zliechov sub-unit

Graphical abstract

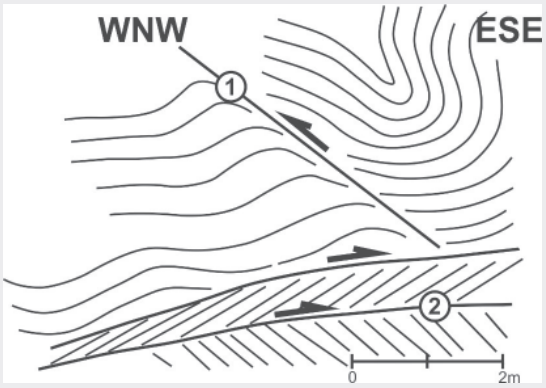

Highlights

- Observed sequence in the Fatric Zliechov sub-unit is composed of the Fatra, Kopienec, Osnica and Párnica formations.
- Thin-bedded limestones of the Osnica Formation are intensively deformed into number of mesoscale folds, including one complex fold - "digitation", probably related to non-coaxial shear, affecting the nappe body in the later stages of emplacement.
- Fatricum in the road cut was initially thrusted to the West (1) during Paleoalpine nappe emplacement. East-vergent back-thrusts (2) represent younger probably Oligocene–Early Miocene deformation phase.

Introduction

The Miocene horst block of the Považský Inovec Mts. (PI) is situated in the western part of the Western Carpathians (Slovakia) and surrounded by the embayments of the Pannonian Basin Miocene sediments (Fig. 1; Ivanička et al., 2007, 2011; Hók et al., 2016). Thanks to its characteristic horst and basin structure, this zone in the northern Internal Western Carpathians (*sensu* Vass et al., 1988 or Hók et al., 2014) is called the Core mountains belt. Each of Core mountains is built by subautochtonous Tatricum, as well as Fatric and Hronic cover nappes. The Fatricum (term defined by Andusov et al., 1973, cf. Plašienka et al., 1997a, 1997b), or formerly known as the Krížna nappe (Andrusov, 1935, 1938; Maheľ, 1983, 1986) represents originally 1–2 km thin, more or less imbricated thrust system (tectonic slices, duplexes and recumbent folds; Kováč, 2007), generally composed of Triassic to Early Cretaceous carbonates and minor siliciclastics. Internal structure is usually divided by lithofacial criteria into one or two lower-order thrust sheets, often called "partial nappes" (Maheľ, 1983; Plašienka et al., 1997b, Bezák et al., 2004). Structurally lower and spatially less abundant is the so-called Vysoká (Belá and Beckov) sub-unit, with shallow water Jurassic formations. The more widely distributed Zliechov sub-unit is forming structurally higher thrust-sheet characterized by the deep water Jurassic deposits. Deformation and emplacement of the Fatricum was studied by numerous authors from its root regions in the Veporic Veľký bok unit, through the regions where its nappe position is apparent (Jaroš, 1971; Plašienka, 1983, 1995, 2003; Prokešová, 1994; Plašienka & Prokešová, 1996; Kováč, 2007; Pečeňa & Vojtko, 2011; Sentpetery & Hók, 2012; Prokešová et al., 2012). The Fatricum is generally

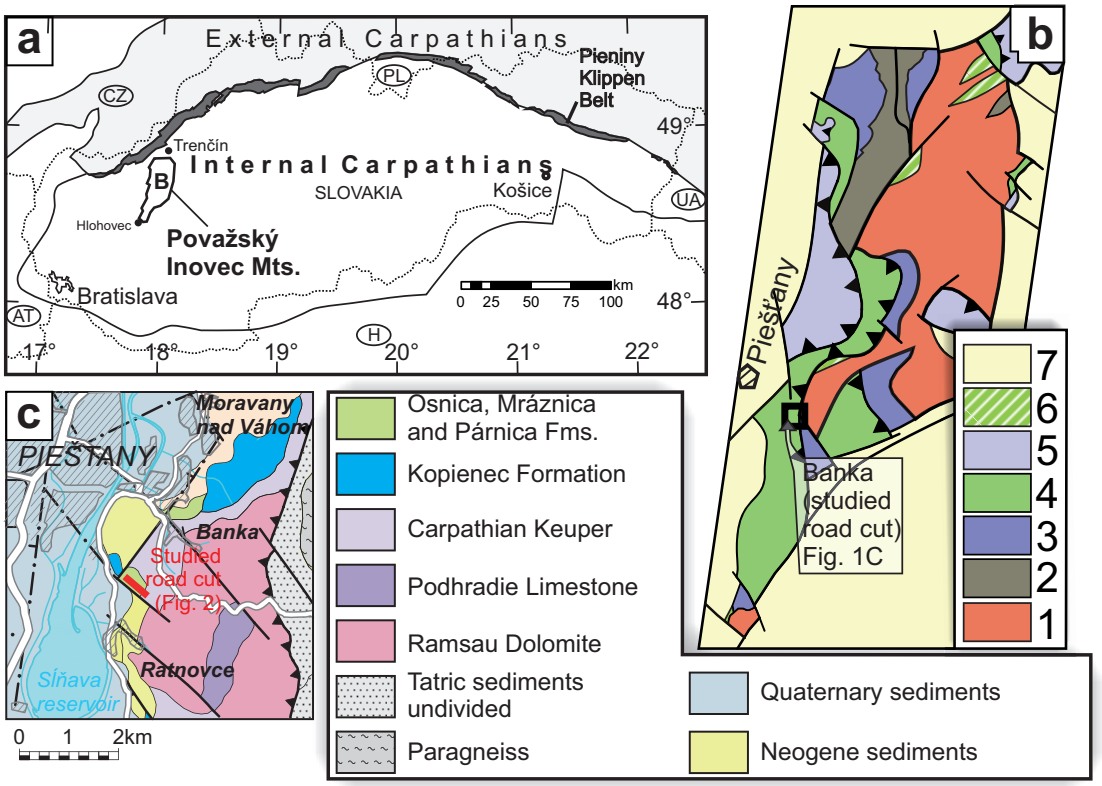

Fig. 1. Location of investigated territory. **a** – Location of the Považský Inovec Mts. in the Western Carpathians. **b** – Tectonic map of the Považský Inovec Mts. (modified from Bezák et al., 2011). 1 – Tatric crystalline basement, 2 – Tatric Upper Paleozoic volcanosedimentary Kálnica Group, 3 – Tatric Mesozoic rocks, 4 – Fatricum, 5 – Hronicum, 6 – Upper Cretaceous Horné Belice Group, 7 – Cenozoic sediments. c – Geological map of the area between Ratnovce and Moravany nad Váhom with marked location of the studied road cut (simplified from Elečko et al., 2008).

characterized by the north- to northwest-vergent Paleoalpine structures (Prokešová, 1994; Kováč & Bendík, 2002; Plašienka, 2003). The nappe deformation lasted from the Albian and the emplacement occurred during the Middle Turonian according to earlier assumptions (Plašienka, 1997; Plašienka, 1999; Prokešová et al., 2012). However, also younger - Middle Turonian–Santonian sediments are documented from below the sole of the Fatricum in the Považský Inovec Mts in the Striebornica section (Pelech et al., 2017). It suggests that the emplacement occurred after the Santonian, thus later than in the other Core mountains.

Fatricum rock sequences are known mostly from the central and western portion of the Považský Inovec Mts. (Ivanička et al., 2007; Ivanička et al., 2011). The Zliechov sub-unit is dominant in central block of the PI. The occurrences in the northern block are limited to the margins of the PI near Beckov and Patrovec, where they are formed by the Vysoká Unit (term Beckov Unit is used in PI; Pelech et al., 2012).

This paper presents observations of the Fatricum deformation from the Banka section in the Považský Inovec Mts. and compares it with situation in nearby Moravany nad Váhom.

Aims and methods

Main aim of this paper is to study structural characteristics, lithology and age of the sequence in the distinctive exposure of the Mesozoic carbonate rocks observed during the years 2013–2014 in temporary uncovered road cut south of the Banka village (Piešťany district, Western Slovakia). Additional structural data from the Fatric nappe of central and northern Považský Inovec Mts. are further discussed. Due to the need of verification of the stratigraphic assignment of the studied rocks, 16 samples were collected for the preparation of thin-sections, and 2 samples were collected for washing. The samples of marls were washed through sieves with 71µm and 125µm mesh size. Calpionellids and their stratigraphic age was determined according to Reháková & Michalík (1997).

Results

Stratigraphy

Approximately 180 m long section (Fig. 2) was temporarily exposed in artificial cut during earthworks on the new road south of the Banka village (N48.569821°,

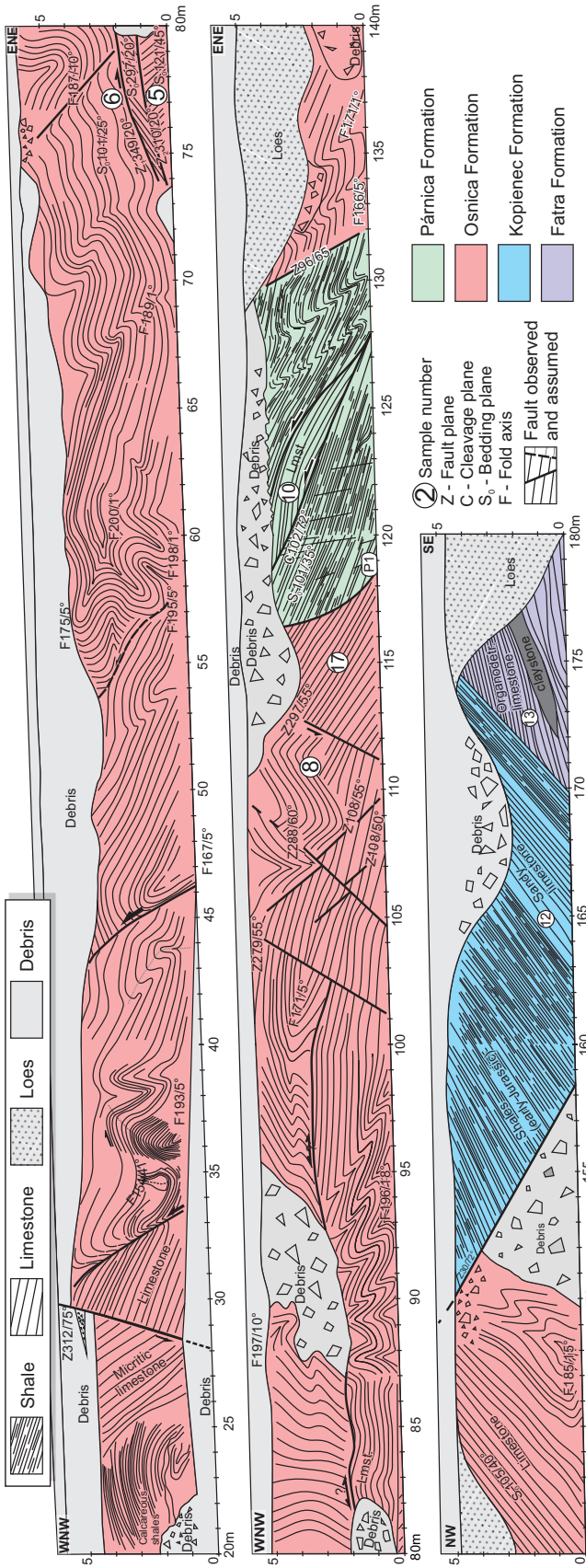

Fig. 2. Mesoscopic structures and lithology in the road cut near Banka (N48.569821°, E17.842179°).

E17.842179°). Studied section is oriented in WNW–ESE direction and exposes approx. 80 m thick (true thickness) sequence consisting of various lithostratigraphic members of the Fatric Zliechov sub-unit.

The oldest rocks assigned to the Rhaetian Fatra Formation (cf. Gaździcki et al., 1979; Tomašových, 2004) are present in the SE part of the section (168–180 m) and separated from the higher members by a normal fault. Grey limestones are characterized by the packed biomicrite to biosparite (packstone, grainstone to floatstone) with fragments of bivalves, gastropods, bryozoans and brachiopod shells, locally also micrite (calcimudstone) is present, samples 0 and 13, Fig. 3a, b).

Overlying sediments occurring south-east of the normal fault (150–168 m) are represented by the grey and reddish sandy limestones and grey shales. Limestones are characterized as a packed oolitic biomicrite to biosparite with hematite cement (oolitic grainstone). It contains chamosite ooids, clastic quartz of fine sand fraction and remains of bivalves, brachiopods and echinoderm fragments (sample 12, Fig. 3c, d). It probably represents Lower Jurassic Kopienec Formation (cf. Gaździcki et al., 1979). Other Middle and Late Jurassic formations are missing in this part of the section.

The higher portion of the sedimentary sequence (20–117 m) exposed to the north-west of the young normal fault consists of strongly deformed (folded and faulted) pelagic carbonates, represented by the pink and grey micritic limestones that probably belong to the Osnica Formation (Michalík et al., 1990 and 1993). The formation is characterized as altered biomicrite (mudstone to wackestone). Alteration is manifested by recrystallization of finer grained material of matrix, obliteration of finer bioclasts and higher abundance of authigenic pyrite, in the microscale and partly by the occurrence of pink and reddish weathering of the rocks and veins, filled by opaque minerals in the macroscale. Limestones contain occasional calpionellids *Calpionella elliptica* Cadisch and (from sample 17, Fig. 3d), *Remaniella duranddelgai* Pop (Fig. 3g), *Calpionellites oblonga* (Cadisch) (from sample 5) and *Calpionellites major* (Colom) (sample 6, Fig. 3f) indicating Middle Berriasian to Early Valanginian age.

Overlying grey clayey shales and grey limestones (117–132 m) are separated by faults. Limestones are partly recrystallized mudstones containing planktonic foraminifers *Globigerinelloides algerianus* Cushman & TenDam, which allow to biostratigraphically date the observed sediments into the Late Aptian Globigerinelloides algerianus Zone. Abundant sections of *Globigerinelloides ferreolensis* Moullade, *Hedbergella aptiana* Glaessner, *Hedbergella infracretacea* Glaessner were present (sample P1). In the sample above yielding only small globular chambered planktonic foraminifers, rare *Spiroplectinata annectens* (Parker & Jones) (Fig. 3i, sample 10) was present in the assemblage, suggesting a ?Late Aptian but mostly an Albian age (Tyszka & Thies, 2001). Based on the observed lithology, position in sedimentary sequence and stratigraphic age, the grey clayey shales and limestones are assigned to the Párnica Formation (cf. Hauer, 1872; Boorová & Filo, 2013).

Observed thickness of the Fatra, Kopienec and Párnica formations is significantly reduced due to strong deformation. Missing parts of sedimentary sequence, e.g. Jurassic spotted limestones of the Janovky Formation or radiolarites, are the result of repeated tectonic reduction during nappe emplacement, as well as later tectonic events. The older Triassic members are missing, as the studied section represents the sequence preserved above the Carpathian Keuper décollement (Prokešová et al., 2012).

The Mesozoic formations are covered by Quaternary sediments. They represent yellowish-grey silty loess of Würmian age (Ivanička et al., 2011). Overlying deposits are represented by deluvial loams and coarse-grained debris of pebble to cobble size. They are post-Würmian to Holocene age.

Structural geology

As it was stated before, the sedimentary sequence is strongly folded and faulted. Expressive fold deformation was followed by later faulting. Folding caused redistribution of the bedding planes into two groups with east and west oriented dip (Fig. 4a). The fold deformation was a result of flexural slip that is common in the well bedded sedimentary bodies. It is locally characterized by the striae and slickensides on the bedding planes. Overall 39 fold axes were recorded. Asymmetric mesoscale folds with dip of the axial plane to the east and dominant foreland-vergent tectonic transport (top to west or northwest) are prevailing (Fig. 5a–c). Good examples are seen in the segments between 55–75, 87–100 and 132–137 m (Fig. 2). The fold axes are generally trending N-S, with local undulations (Fig. 4b). Another west-vergent structure is represented by the thrust sheet of Párnica Formation located in the pink micritic limestones between 118–132 m. The shales and claystones of the Párnica Formation display prominent east-dipping cleavage which highlights the dominant direction of tectonic transport (Fig. 5b, d).

Complex overturned fold ("digitation") present between 55–65 m is similar to larger-order structures known from the Morcles nappe of the Western Alps, where it is interpreted as a result of simple shear deformation during later evolution of the nappe body (Ramsay et al., 1983). The same explanation could be applied to the observed structure in the road cut.

Fold axes perpendicular to dominant WNW-vergent folds, otherwise relatively common in the Považský

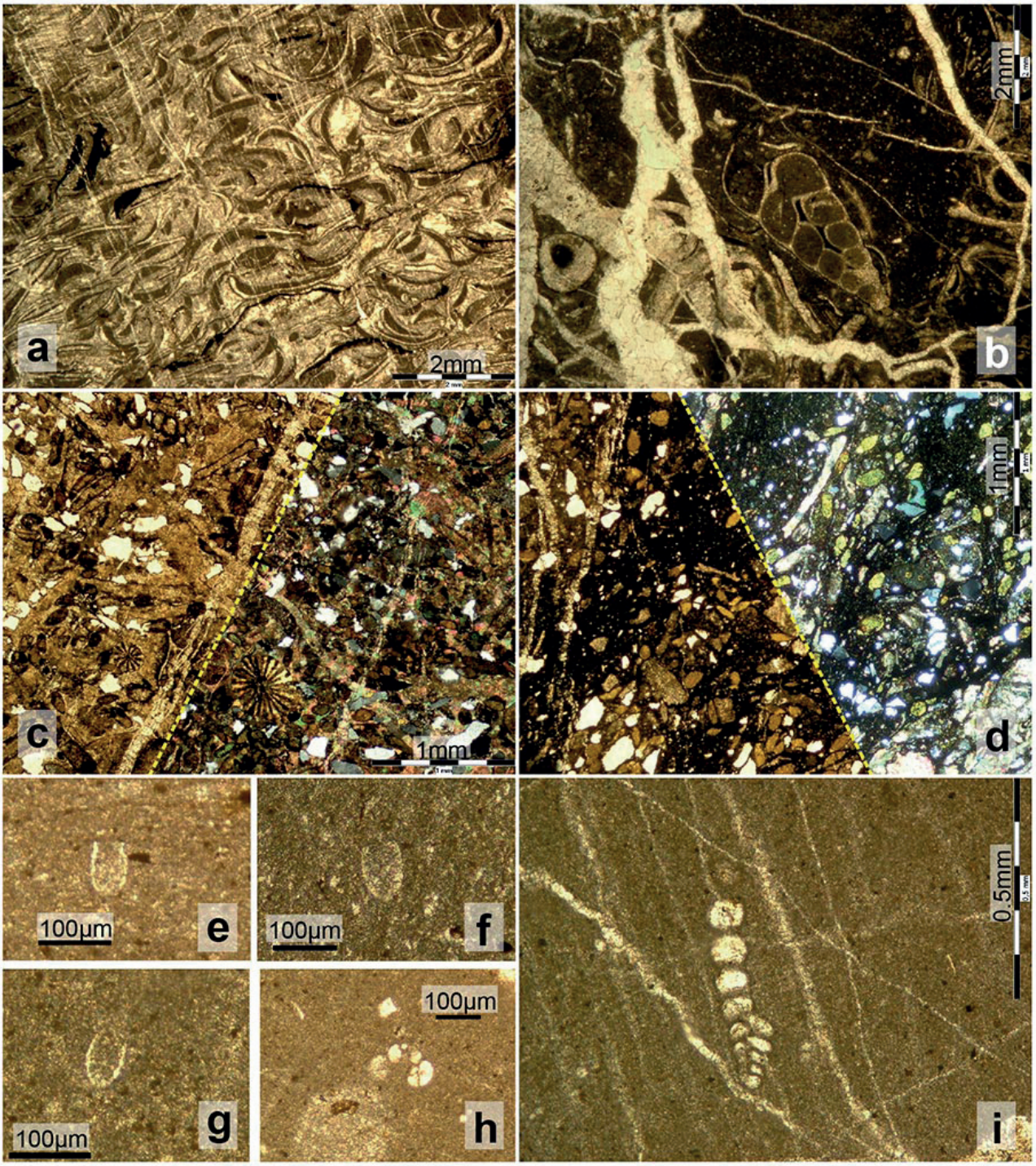

Fig. 3. a – Biosparite consisting of densely packed bivalvia fragments. Sample 13. Rhaetian Fatra Formation. **b** – Wackestone to floatstone with a gastropod shell, Sample 0. Rhaetian Fatra Formation. **c** – Sandy-crinoidal limestone, plane polarized light (left), crossed polarized light (right), Kopienec Formation. Sample 12. **d** – Sandy crinoidal limestone with chamositic Fe-ooids, plane polarized light (left), crossed polarized light (right), Kopienec Formation. Sample 12. **e** – *Calpionella elliptica* Cadisch (Sample 17). **f** – *Calpionellites major* (Colom, Sample 6). **g** – *Remaniella duranddelgai* Pop (Sample 5). **h** – Section of "hedbergellid" planktonic foraminifer (Sample 10). **I** – *Section of Spiroplectinata* annectens (Parker & Jones, Sample 10).

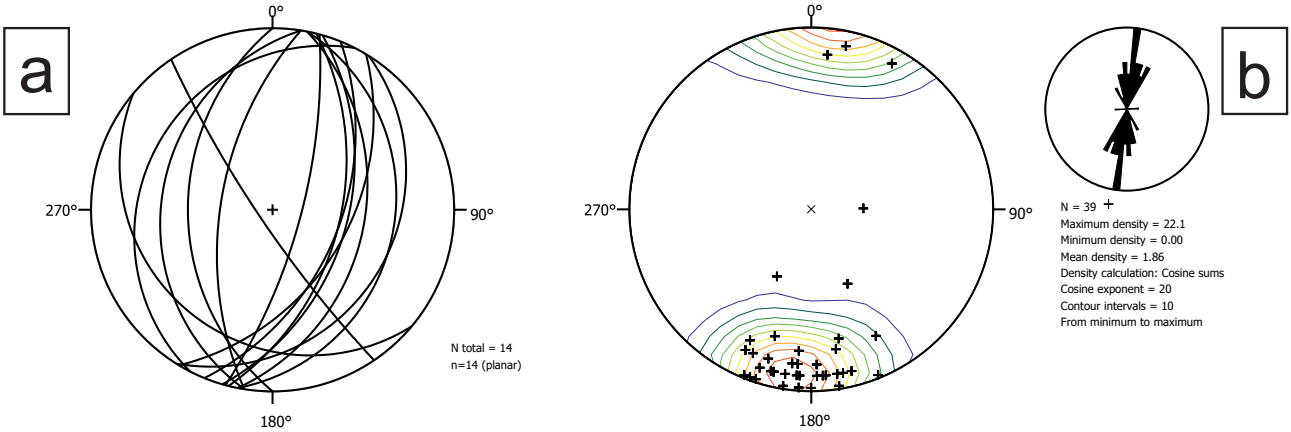

Fig. 4. Structural measurements in the Fatric sequence at the studied road cut near Banka. **a** - Orientation of bedding planes. **b** - Orientation of fold axes (+).

Inovec Mts. (cf. Plašienka & Marko, 1993; Pelech et al., 2016; Pelech & Hók, 2017) were present only in negligible extent.

The investigated Fatricum succession is, in addition to ordinary folds with the west-vergence, also deformed by back-thrusts and folds with east-vergence. The latter are less numerous than the west-vergent folds but more striking. They are mostly represented by passive, flexural folds which bend the original north-vergent and neutral folds (Fig. 2 - 36–38 m). However, some seemingly east-vergent folds are in fact only Z-folds of larger complex folds (Fig. 6b). Locally observed S-C' bands also indicate tectonic transport to the east. Back-thrusts modify the original structure and rarely separate rigid blocks with structural paragenesis of the northwestern vergence (Fig. 6a). Back-thrust structure between 75–80 m (possibly continuing up to 103 m) represents evidently a younger (thus "post-nappe") superimposed deformation phase. According to regional context, we can assume that the back-thrusting has occurred after the Santonian and before Middle Miocene.

Apart of the ductile structures several younger normal faults were observed in the road cut as well. It is worth mentioning that some of them apparently offset the Quaternary sediments (Fig. 6c).

Moravany nad Váhom

The second section in the Fatricum is documented in a road cut in the valley of Hraničný kanál Brook, west of the Moravany nad Váhom (48.587167° N, 17.867667° E). Grey and black calcareous shales and sandy limestones of the Kopienec Formation represent part of the Zliechov sub-unit. The observed sequence is generally monoclinally dipping to the west and southwest (Fig. 7a). The axial plane cleavage is dipping to the southeast, and the fold axes are oriented in southwest-northeast direction (Fig. 7b, 6d). Aforementioned indicators suggest top to northwest tectonic transport of the Fatricum at this locality.

Discussion

Tectonic transport direction of North Veporic Veľký bok Unit between Poniky and Liptovská Teplička (Plašienka, 1983, 1995) is top to NW-NNW, that is similar to supposed internal portions of the Fatricum in the northeastern (Rázdiel) part of the Tribeč Mts. (Hók et al., 1994). In the Sklené Teplice area, the sense of tectonic transport of the Northern Veporic sedimentary cover was to the west (Hók et al., 2013). In the area between Banská Bystrica, Korytnica and Ružomberok, the direction of the tectonic transport of the Fatricum was to the NW and NNW (Prokešová, 1994). Direction of the tectonic transport in the area of Donovaly was identified as top to NW (Kováč & Bendík, 2002). Observations from the northern slopes of the Nízke Tatry Mts. show top to NNW or N tectonic transport of the Fatricum (Plašienka, 2003). Tectonic transport of Belá sub-unit (equivalent of Vysoká sub-unit) in the Strážovské vrchy Mts. is to the WNW, while the Zliechov sub-unit was thrust to the NNW in this region (Pečeňa & Vojtko, 2011). Documented sense of tectonic transport of the Beckov sub-unit near Patrovec in the northeastern Považský Inovec Mts. is top to NNW (Pelech et al., 2012). Overall picture is summarized in Fig. 8.

While the recorded tectonic transport of Northern Veporicum and Fatricum is relatively uniform east of Banská Bystrica (Central Slovak Fault System *sensu* Kováč & Hók, 1993), thus top to NNW. More to the west, the deviations from the NNW direction of tectonic transport are more common. Diverse directions of movement are recorded as well in the Považský Inovec Mts. While the direction of the Beckov (Vysoká) sub-unit emplacement in the northern part of the mountain range (Patrovec) is to the NNW (Pelech et al., 2012), the directions of the Zliechov

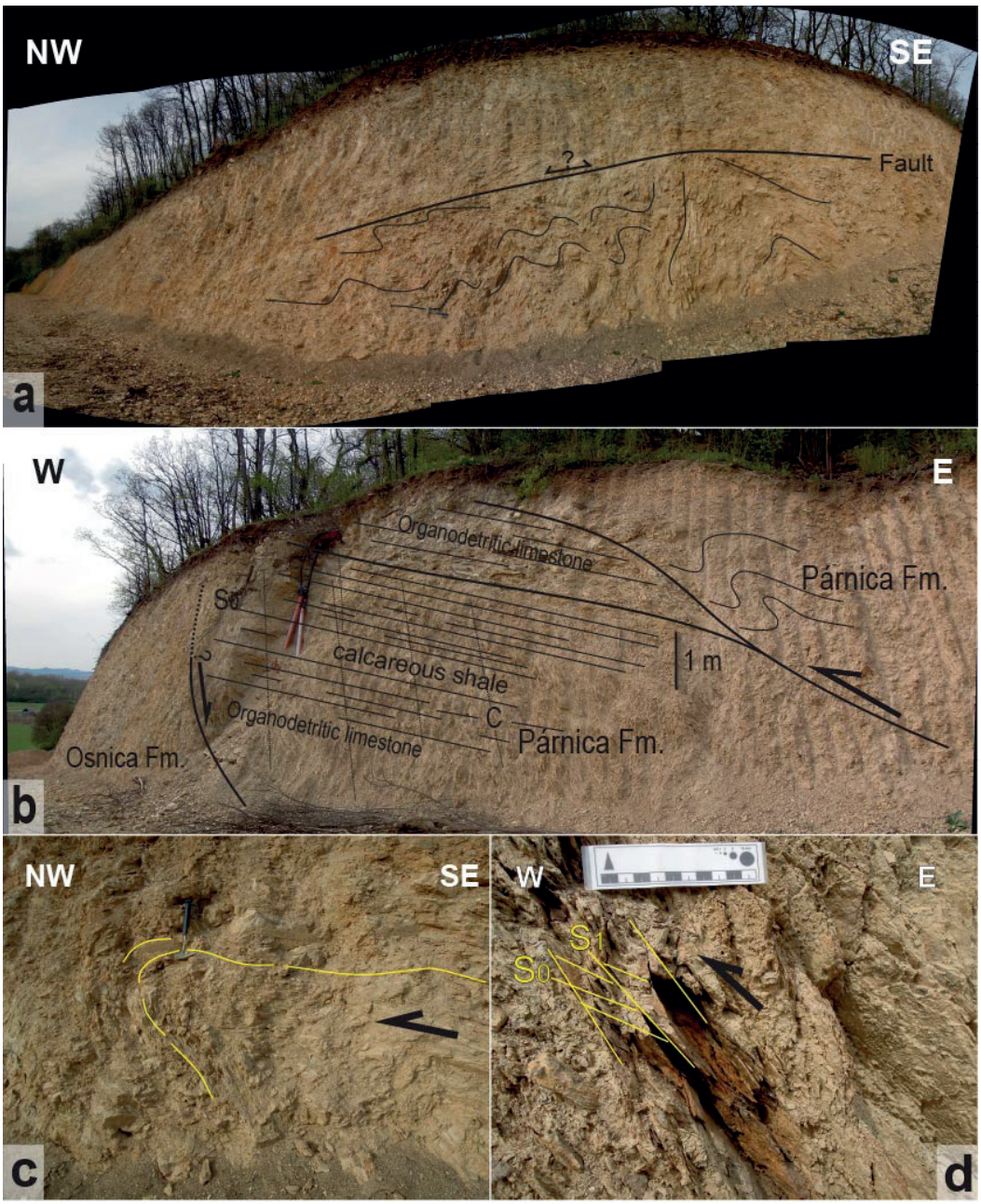

Fig. 5. a – Folded part of road cut section with low angle fault (?back-thrust; 85–100 m); **b** – Duplex in shales and organodetritic limestones of the Párnica Formation (road cut section between 117–130 m); **c** – Foreland-vergent inclined fold in limestones of the Osnica Fm. (54–55 m). **d** – Detail view on cleavage in the marly shales of the Párnica Fm. (from figure 5 b).

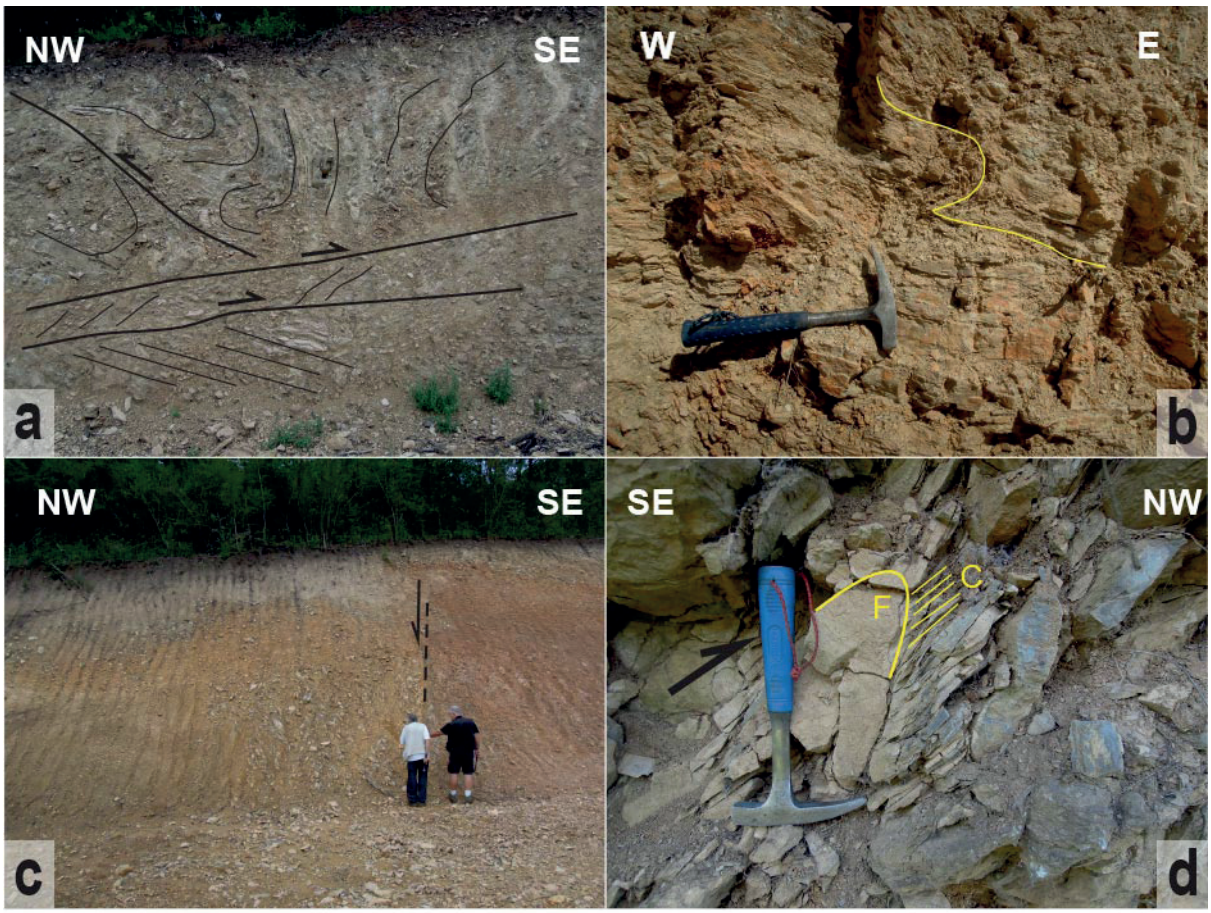

Fig. 6. a – Older foreland-vergent reverse fault above younger back-thrust with south-east vergence (75–80 m) in limestones of the Osnica Formation. **b** – Fold with apparent vergence to the hinterland, in fact representing parasitic – lower order Z-fold in the overturned limb of "digitation" (61–63 m). **c** – Quaternary normal fault offsetting folded Mesozoic sequence as well as Quaternary debris. **d** – North-west-vergent fold and axial plane cleavage in the sandy limestones of the Kopienec Formation near Moravany nad Váhom.

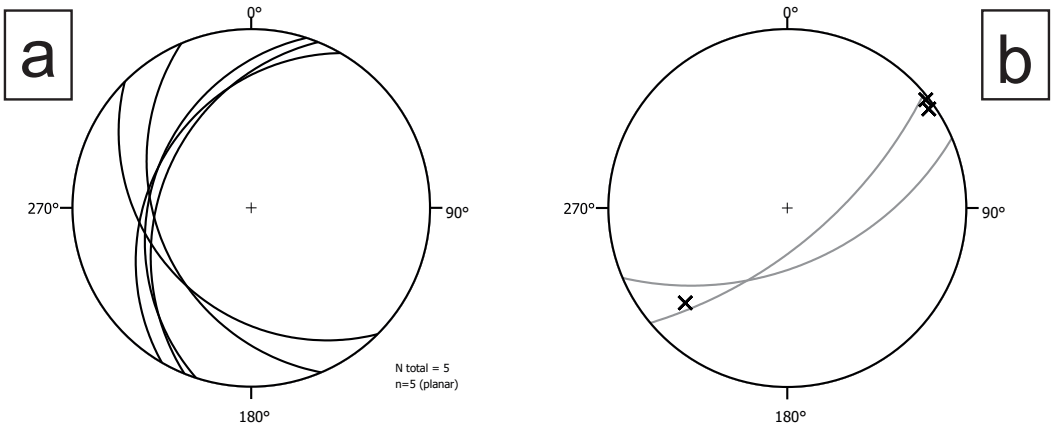

Fig. 7. Structural characteristics of the studied rocks at the locality near Moravany nad Váhom. **a** – Bedding planes. **b** – Cleavage (grey) and fold-axes (x).

sub-unit in the central part of the mountain range vary between NW (Moravany nad Váhom) and W (Banka). This difference suggests that structural discordance might exist between the Vysoká and Zliechov sub-units ("partial nappes"). Kováč (2007) explains similar phenomenon in the various thrust sheets of Fatricum in Demänová and Iľanovo valleys as a result of the existence of oblique thrust ramps. In PI, it can be alternatively a result of dextral movement on the Hrádok-Zlatníky shear zone (Pelech & Hók, 2017). Prevailing west (Fig. 4b) or northwest direction of tectonic transport, well manifested at the studied road cut near Banka, can be considered as a consequence of the Cenozoic counter-clockwise block rotation known from western segment of the Western Carpathians (Márton et al., 2013; Márton et al., 2015).

The studied road cut exhibits also several east-vergent structures. Similar structures with hinterland (generally south- or southeast) vergence are known from Northern Veporicum-Fatricum system. In the Northern Veporic area, they are usually interpreted as related to the final phase of convergence of the root area of the nappe (Plašienka, 1983, p. 224). Retro-vergent structures can form contemporary to the foreland-vergent thrusts (e.g. McClay & Whitehouse, 2004). However, the back-thrusts in the area of the Považský Inovec Mts. are not a result of such processes. Regional context suggests that they represent younger superimposed retro-vergent deformation that is observed along the entire western edge of the Western Carpathians (Marko et al., 2005; Pešková, 2011; Hók et al., 2016). They are usually interpreted as Oligocene–Early Miocene in age (Hók et al., 2016).

Conclusions

This contribution presents result of the structural analysis of the Fatric sequences in central part of the Považský Inovec Mts. It documents structural style and thin-skinned tectonics of the Fatric cover nappe in the well exposed road cut near the Banka village. The main conclusions can be summarized as follows:

1) The sedimentary sequence composed of the Fatra, Kopienec, Osnica and Párnica formations ranging from Rheatian to Albian is tectonically reduced and strongly deformed. In majority the "sedimentary" contacts are tectonized. This knowledge can have important implications for other areas as the Zliechov sub-unit represents one of the most common Mesozoic sequences, occurring at the surface in many regions of the Core mountains in Slovakia.
2) Forward-vergent thrusts and steep reverse faults together with west- and northwest-vergent folds of different shape and magnitude represent the main Paleoalpine structures of probably Early to Late Cretaceous age.
3) Back-thrusts of supposed Oligocene to Early Miocene age are documented. They are characterized by the ret-

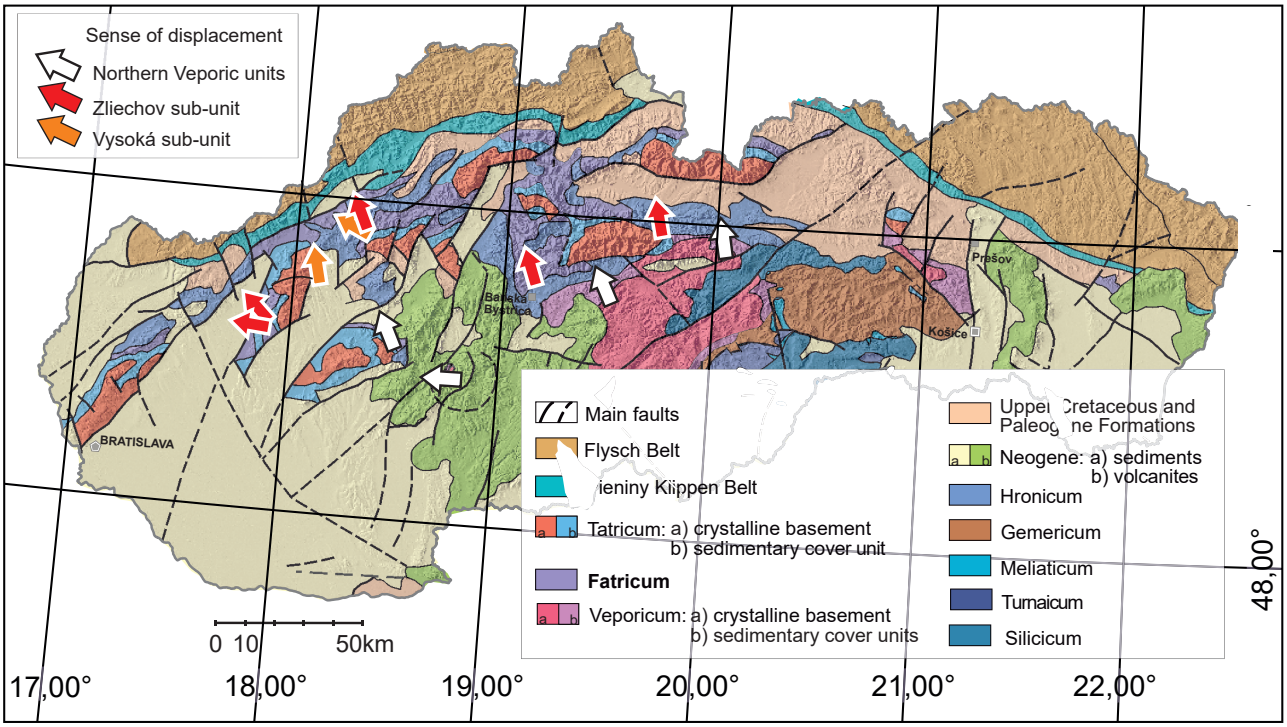

Fig. 8. Simplified tectonic map of Slovakia (modified from Biely et al., 1996) with marked sense of tectonic transport of the Fatricum (grey arrows) and Northern Veporicum nappes (white arrow) during Paleoalpine phase. Tectonic transport directions from Plašienka (1983, 2003), Hók et al. (1994, 2013), Prokešová (1994), Kováč & Bendík (2002) and Pečeňa & Vojtko (2011) and own data.

ro-vergent top to the east tectonic transport and superimposed on older foreland-vergent structures.

4) Cenozoic normal faults including several Quaternary faults represent the youngest deformation phase.

Acknowledgements

This research was carried out during the preparation of O. Pelech's dissertation and P. Fajdek's bachelor thesis. The authors are thankful to the VEGA Scientific Grant Agency (Project VEGA 2/0136/15) and to the Slovak Research and Development Agency (Projects APVV-14-0118 and APVV-0212-12) for their financial support. First author is thankful to Prof. D. Reháková for consultation during determination of Calpionellids, as well as to Profs. D. Plašienka a J. Michalík contributing by constructive comments to former manuscript. We also thank employees of the company Reality Gala Piešťany, for the possibility to access to the studied section.

References

Andrusov, D., 1935: Subtatranské příkrovy Západních Karpat. *Carpatica, Ř. B (Praha), I, 50.*

Andrusov, D., 1938: Geologie Slovenska. Sbor pro výzkum Slovenska a Podkarpatské Rusi. *Praha, Orbis, 111 p.*

Andrusov, D., Bystrický, J. & Fusán, O., 1973: Outline of the structure of the Western Carpathians. Guide book, X Congress CBGA. *Bratislava, Geol. Úst. D. Štúra, 44 p.*

Bezák, V., Broska, I., Elečko, M., Havrila, M., Ivanička, J., Janočko, J., Kaličiak, M., Konečný, V., Lexa, J., Mello, J., Plašienka, D., Polák, D., Potfaj, M. & Vass, D., 2004: Tectonic map of Slovak Republic. *Bratislava, Št. Geol. Úst. D. Štúra.*

Bezák, V., Biely, A., Elečko, M., Konečný, V., Mello, J., Polák, M. & Potfaj, M., 2011: A new synthesis of the geological structure of Slovakia – the general geological map at 1 : 200,000 scale. *Geol. Quart., 55, 1, 1 – 8.*

Biely, A., Bezák, V., Elečko, M., Kaličiak, M., Konečný, V., Lexa, J., Mello, J., Nemčok, J., Potfaj, M., Rakús, M., Vass, D., Vozár, J. & Vozárová, A., 1996: Geological map of Slovakia 1 : 500 000. *Bratislava, Geol. Surv. Slovak Republic.*

Boorová, D. & Filo, I., 2013: Štúdium párnického súvrstvia na stratotypovom profile Žaškov (krížňanský príkrov). *Miner. Slov., 45, 61 – 68.*

Elečko, M. (ed.), Polák, M., Fordinál, K., Bezák, V., Ivanička, J., Mello, J., Konečný, V., Šimon, L., Nagy, A., Potfaj, M., Maglay, J., Broska, I., Buček, S., Gross, P., Havrila, M., Hók, J., Kohút, M., Kováčik, M., Madarás, J., Olšavský, M., Pristaš, J., Salaj, J. & Vozárová, A., 2008: Prehľadná geologická mapa Slovenskej republiky 1 : 200 000. Mapový list 35 – Trnava (General Geological Map of the Slovak Republic 1 : 200 000, Map sheet 35 – Trnava). *Bratislava, Št. Geol. Úst. D. Štúra.*

Gaździcki, A., Michalík, J. & Sýkora, M., 1979: An Upper Triassic – Lower Jurassic sequence in the Krížna nappe (West Tatra mountains, West Carpathians, Czechoslovakia). *Západ. Karpaty, Sér. Geol., 5, 119 – 148.*

Hauer, F. R. von, 1872: Geologische Uebersichtskarte der österreichischen Monarchie. *Jb. K.-Kön. geol. Reichsanst., 22, 149 – 228.*

Hók, J., Ivanička, J. & Kováčik, M., 1994: Geologická stavba rázdielskej časti Tríbeča – nové poznatky a diskusia. *Miner. Slov., 26, 3, 192 – 196.*

Hók, J., Pelech, O. & Slobodová, Z., 2013: Kinematická analýza horninových komplexov veporika a hronika v oblasti sklenoteplického ostrova (stredoslovenské neovulkanity). *Acta Geol. Slov., 5, 2, 129 – 134.*

Hók, J., Šujan, M. & Šipka, F., 2014: Tektonické členenie Západných Karpát – prehľad názorov a nový prístup. *Acta Geol. Slov., 6, 2, 135 – 143.*

Hók, J., Kováč, M., Pelech, O., Pešková, I., Vojtko, R. & Králiková, S., 2016: The Alpine tectonic evolution of the Danube Basin and its northern periphery (southwestern Slovakia). *Geol. Carpath., 67, 5, 495 – 505.*

Ivanička, J., Havrila, M., Kohút, M. (eds.), Olšavský, M., Hók, J., Kováčik, M., Madarás, J., Polák, M., Rakús, M., Filo, I., Elečko, M., Fordinál, K., Maglay, J., Pristaš, J., Buček, S., Šimon, L., Kubeš, P., Scherer, S. & Zuberec, J., 2007: Geologická mapa Považského Inovca a jv. časti Trenčianskej kotliny, M = 1 : 50 000. *Bratislava, Št. Geol. Úst. D. Štúra.*

Ivanička, J., Kohút, M. (eds.), Olšavský, M., Havrila, M., Hók, J., Kováčik, M., Madarás, J., Polák, M., Rakús, M., Filo, I., Elečko, M., Fordinál, K., Maglay, J., Pristaš, J., Buček, S., Šimon, L., Kubeš, P., Scherer, S. & Zuberec, J., 2011: Vysvetlivky ku geologickej mape regiónu Považský Inovec a jv. časť Trenčianskej kotliny, M = 1 : 50 000. *Bratislava, Št. Geol. Úst. D. Štúra, 389 p.*

Jaroš, J., 1971: Tectonic styles of the homelands of superficial nappes. *Rozpr. Čs. Akad. Věd, Ř. mat. přír. Věd, 81, 6, 59.*

Kováč, P., 2007: The internal structure of Paleoalpine thrusts of the Western Carpathians: A case study from the Krížna thrust system. *Centr. Eur. Geol., 50, 1, 19 – 28.*

Kováč, P. & Hók, J., 1993: The Central Slovak Fault System – The field evidence of a strike slip. *Geol. Carpath., 44, 3, 155 – 159.*

Kováč, P. & Bendík, A., 2002: Štruktúrna analýza adnetských vápencov na lokalite Zvolen – Donovaly. *Miner. Slov., 34, 207 – 210.*

Maheľ, M., 1983: Krížna nappe, example of polyfacial and polystructural unit. *Miner. Slov., 15, 3, 193 – 216.*

Maheľ, M., 1986: Geológia Československých Karpát 1. Paleoalpínske jednotky. *Bratislava, Veda, Vyd. Slov. Akad. Vied, 510 p.*

Marko, F., Vojtko, R., Plašienka, D., Sliva, Ľ., Jablonský, J., Reichwalder, P. & Starek, D., 2005: A contribution to the tectonics of the Periklippen zone near Zázrivá (Western Carpathians). *Slovak Geol. Mag., 11, 1, 37 – 43.*

Márton, E., Grabowski, J., Plašienka, D., Túnyi, I., Krobicki, M., Haas, J. & Pethe, M., 2013: New paleomagnetic results from the Upper Cretaceous red marls of the Pieniny Klippen Belt, Western Carpathians: Evidence for general CCW rotation and implications for the origin of the structural arc formation. *Tectonophysics, 592, 1 – 13.*

Márton, E., Grabowski, J., Tokarski, A. K. & Túnyi, I., 2015: Palaeomagnetic results from the fold and thrust belt of the

Western Carpathians: An overview. In: Pueyo, E. L., Cifelli, F., Sussman, A. J. & Oliva-Urcia, B. (eds.): Palaeomagnetism in Fold and Thrust Belts: New Perspectives. *Geol. Soc. London, Spec. Publ., 425, 7 – 37.*

McClay, K. R. & Whitehouse, P. S., 2004: Analog modeling of doubly vergent thrust wedges. In: *McClay*, *K. R.* (ed.): *Thrust* tectonics and hydrocarbon systems. *Amer. Assoc. Petrol. Geol. Mem., 82, 184 – 206.*

Michalík, J., Vašíček, Z. & Borza, V., 1990: Aptychy, tintinidy a stratigrafia hraničných jursko-kriedových súvrství v profile Strážovce (zliechovská jednotka krížňanského príkrovu, Strážovské vrchy, Centrálne Západné Karpaty). *Knih. Zem. Plyn Nafta, 9a, 69 – 92.*

Michalík, J., Vašíček, Z. & Borza, V., 1993: Biostratigrafia a mikrofácie vrchnojurskej a spodnokriedovej panvovej sekvencie v krížňanskom príkrove fatrika (profil Zrázy pri Dolnej Porube, Strážovské vrchy). *Geol. Práce, Spr., 97, 105 – 112.*

Pečeňa, Ľ. & Vojtko, R., 2011: Nové poznatky o geologickej stavbe fatrickej jednotky v okolí Valaskej Belej (Strážovské vrchy, Západné Karpaty). *Miner. Slov., 43, 19 – 30.*

Pelech, O., Soták, J. & Hók, J., 2012: Geological setting of the Patrovec block in the Považský Inovec Mts. Western Carpathians. *Miner. Slov., 44, 3, 231 – 240.*

Pelech, O., Hók, J., Pešková, I. & Havrila, M., 2016: Structural position of the Upper Cretaceous sediments in the Považský Inovec Mts. (Western Carpathians). *Acta Geol. Slov., 8, 1, 43 – 58.*

Pelech, O. & Hók, J., 2017: Metodika mezoskopického štúdia strižných zón a jej aplikácia pri kinematickej analýze hrádocko-zlatníckej strižnej zóny v Považskom Inovci. *Geol. Práce, Spr., 130, 47 – 67.*

Pelech, O., Hók, J. & Józsa, Š., 2017: Turonian-Santonian sediments in the Tatricum of the Považský Inovec Mts. (Internal Western Carpathians, Slovakia). *Austrian J. Earth Sci., 110, 1, 19 – 33.*

Pešková, I., 2011: Tektonická interpretácia západného úseku kontaktnej zóny externíd a internid Západných Karpát. Dissertation thesis. Manuscript. *Bratislava, Archive of Department of geol. and paleont., 94 p.*

Plašienka, D., 1983: Kinematický obraz niektorých štruktúr severného veporika vo vzťahu k formovaniu krížňanského príkrovu. *Miner. Slov., 15, 3, 217 – 231.*

Plašienka, D., 1995: Cleavages and folds in changing tectonic regimes: The Veľký Bok Mesozoic cover unit of the Veporicum (Nízke Tatry Mts., Central Western Carpathians). *Slovak Geol. Mag., 2, 97 – 113.*

Plašienka, D., 1997: Cretaceous tectochronology of the Central Western Carpathians, Slovakia. *Geol. Carpath., 48, 2, 99 – 111.*

Plašienka, D., 1999: Tektochronológia a paleotektonický model jursko-kriedového vývoja centrálnych Západných Karpát. *Bratislava, Veda, Vyd. Slov. Akad. Vied, 125 p.*

Plašienka, D., 2003: Development of basement-involved fold and thrust structures exemplified by the Tatric-Fatric-Veporic nappe system of the Western Carpathians (Slovakia). *Geodin. Acta, 16, 21 – 38.*

Plašienka, D. & Marko, F., 1993: Geologická stavba strednej časti Považského Inovca. *Miner. Slov., 25, 11 – 25.*

Plašienka, D. & Prokešová, R., 1996: Towards an evolutionary tectonic model of the Krížna cover nappe (Western Carpathians, Slovakia). *Slovak Geol. Mag., 3 – 4, 279 – 286.*

Plašienka, D., Grecula, P., Putiš, M., Kováč, M. & Hovorka, D., 1997a: Evolution and structure of the Western Carpathians: An overview. In: Grecula, M., Hovorka, D. & Putiš, M.: Geological Evolution of the Western Carpathians. Bratislava, *Miner. Slov. – Monograph., 1 – 24.*

Plašienka, D., Havrila, M., Michalík, J., Putiš, M. & Reháková, D., 1997b: Nappe structure of the western part of the Central Carpathians. In: Plašienka, D., Hók, J., Vozár, J. & Elečko, M. (eds.): 100th anniversary Dimitrij Andrusov; Alpine evolution of the Western Carpathians and related areas. International conference; abstracts and introductory articles to the excursion. *Bratislava, GS SR, Dionýz Štúr Publishers, 139 – 161.*

Prokešová, R., 1994: Štruktúrna analýza krížňanského príkrovu v jeho prikoreňovej a superficiálnej pozícii. *Miner. Slov., 26, 347 – 354.*

Prokešová, R., Plašienka, D. & Milovský, R., 2012: Structural pattern and emplacement mechanisms of the Krížna cover nappe (Central Western Carpathians). *Geol. Carpath., 63, 1, 13 – 32.*

Ramsay, J. G., Casey, M. & Kligfield, R., 1983: Role of shear in development of the Helvetic fold-thrust belt of Switzerland. *Geology, 11, 439 – 442.*

Reháková, D. & Michalík, J., 1997: Evolution and distribution of calpionellids – the most characteristic constituents of Lower Cretaceous Tethyan microplankton. *Cret. Res., 18, 493 – 504.*

Sentpetery, M. & Hók, J., 2012: Geologická stavba tatrika a fatrika v oblasti medzi Belianskou a Vrátnou dolinou (Kriváňska Fatra). *Acta Geol. Slov., 4, 1, 65 – 74.*

Tomašových, A., 2004: Microfacies and depositional environment of an Upper Triassic intra-platform carbonate basin: The Fatric Unit of the West Carpathians (Slovakia). *Facies, 50, 77 – 105.*

Tyszka, J. & Thies, A., 2001: *Spiroplectinata*, key benthic foraminifer genus for palaeoceanographic reconstruction of the Albian Lower Saxony Basin. *Cret. Res., 174, 199 – 220.*

Vass, D., Began, A., Gross, P., Kahan, Š., Krystek, I. Köhler, E., Lexa, J., Nemčok, J., Ružička, M. & Vaškovský, I., 1988: Regionálne geologické členenie Západných Karpát a severných výbežkov Panónskej panvy na území ČSSR. Mapa 1 : 500 000. *Bratislava, Geol. Úst. D. Štúra.*

Vrásová deformácia fatrika – prípadová štúdia z profilu Banka (Považský Inovec, Slovensko)

Horninové sekvencie fatrika vystupujú v Považskom Inovci prevažne v strednej a západnej časti pohoria (Ivanička et al., 2007, obr. 1). V bojnianskom bloku horniny fatrika tvorí dominantne zliechovská jednotka. Výskyty v seleckom bloku sú plošne obmedzené na okraje pohoria okolo Beckova a Patrovca, kde ich buduje beckovská jednotka (Ivanička et al., 2011; Pelech et al., 2012). V hlohoveckom bloku sa prítomnosť fatrických komplexov nepotvrdila.

Skúmaný zárez novobudovanej cesty v južnej časti katastra obce Banka (obr. 2), ktorý je hlavným predmetom tohto článku, vznikol v priebehu rokov 2013 – 2014. Rozsiahle defilé v sedimentárnej sekvencii fatrika tvoria horniny triasového až spodnokriedového veku, z ktorých dominujú horniny osnického súvrstvia (obr. 3). Zárez cesty s odkrytými horninami fatrika je dlhý asi 180 m, má generálne južnú expozíciu a v.-z. priebeh. Nápadná vrásová deformácia hornín na lokalite je kombinovaná s mladším zlomovým porušením. Výrazná je tektonická redukcia viacerých členov, ako aj fakt, že väčšina sedimentárnych kontaktov je tektonizovaná. V dôsledku zvrásnenia na lokalite dominuje východný aj západný sklon vrstvovitosti (obr. 4). Vrásová deformácia je dôsledkom ohybového sklzu, častého vo vrstvovitých telesách, čo dokumentujú tektonické zrkadlá na zvrásnených medzivrstvových plochách. Prevládajú asymetrické mezovrásy so sklonom osovej roviny na východ a vergenciou na západ (obr. 5). Orientácia vrás je generálne v smere S – J, s lokálnymi undulácíami (obr. 4b). Priečne prevrásnenie bolo pozorované v zanedbateľnej miere. V bridliciach párnického súvrstvia sme pozorovali aj kliváž sklonenú na východ, ktorá zdôrazňuje dominantný smer tektonického transportu (obr. 5d). Západovergentné štruktúry zodpovedajú paleoalpínskej deformačnej fáze veku spodná („stredná“) až vrchná krieda.

Skúmaná fatrická sekvencia je okrem západovergentných vrás a násunov postihnutá aj spätnými násunmi a vrásami s východnou vergenciou. Markantné, no menej početné ako západovergentné, sú spätné, východovergentné vrásy. Predstavujú ich prevažne pasívne ohybové vrásy, ktoré buď ohýbajú pôvodné západovergentné vrásy, alebo vzpriamené vrásové osi pôvodne neutrálnych vrás (obr. 2, 35 – 37 m). Niektoré zdanlivo východovergentné vrásy sú v skutočnosti iba Z-vrásy väčších komplexných vrás (obr. 6b). Aj lokálne pozorované S/C′ pásy indikujú tektonický transport na východ. Spätné prešmyky modifikujú pôvodnú stavbu a nezriedka oddeľujú rigidné bloky so štruktúrnou paragenézou a západnou vergenciou (obr. 6a). Sukcesia štruktúr naznačuje, že spätné prešmyky sú mladšia naložená deformačná fáza, pravdepodobne oligocénneho až spodnomiecénneho veku. Zdokumentovaná je aj prítomnosť viacerých kenozoických zlomov vrátane kvartérnych.

Doručené / Received: 7. 2. 2018
Prijaté na publikovanie / Accepted: 5. 6. 2018

Mineralia Slovaca, Web ISSN 1338-3523, ISSN 0369-2086
50 (2018), 37 – 46, © Authors 2018. CC BY 4.0

The depth range and possible continuation of the Havranická jaskyňa cave system revealed by geological methods and electrical-resistivity tomography (ERT), the Malé Karpaty Mts., Slovakia

TAMÁS CSIBRI[1], ALEXANDER LAČNÝ[1,2], RENÉ PUTIŠKA[3], IVAN DOSTÁL[3] and DAVID KUŠNIRÁK[3]

[1]Comenius University, Faculty of Natural Sciences, Department of Geology and Paleontology, Ilkovičova 6, SK-842 15 Bratislava, Slovakia; tamas.csibri@gmail.com
[2]State Nature Conservancy of the Slovak Republic, Little Carpathians Protected Landscape Area, Štúrova 115, SK-900 01 Modra, Slovakia; lacny@fns.uniba.sk
[3]Comenius University, Faculty of Natural Sciences, Applied and Environmental Geophysics, Ilkovičova 6, SK-842 15 Bratislava, Slovakia; putiska@fns.uniba.sk; dostal@fns.uniba.sk; kusnirak@fns.uniba.sk

Abstract: Geological (sedimentology, structural geology) and geophysical (electrical-resistivity tomography; ERD) methods were carried out to investigate the possible continuation and depth range of the Havranická jaskyňa cave, situated in the Malé Karpaty Mts. (western part of Slovakia). The origin of the investigated cave is connected with the N–S trending fault, activated during the Pliocene–Quaternary. The cave system is developed in Gutenstein Fm., built dominantly of limestone. According to XRD analyses, the subjacent Gutenstein Fm. dolomite interferes with the cave system in the form of boudins, which modifies the development of the cave in its lower parts. However, the boudins do not affect the course of the cave system. Based on ERT measurement a 3D model of the cave was produced, being complemented by the cave's polygonal traction points. The primary geophysical measurements in 2010 contributed to discovery of new passages in the cave system, so the application of used methodology also in other caves world-wide would be meaningful.

Key words: geological and geophysical research, Havranická jaskyňa cave, the Malé Karpaty Mts., Western Carpathians

Graphical abstract

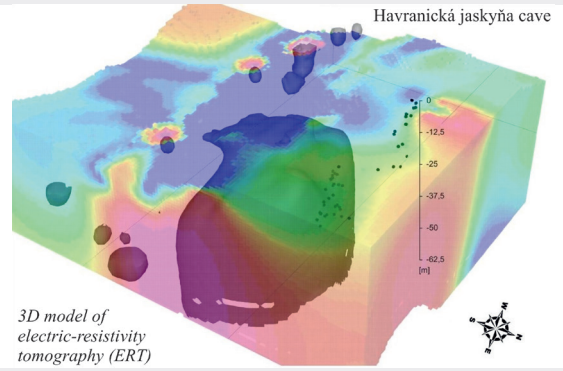

Highlights

- Multidisciplinary research of Havranická jaskyňa cave system in the Malé Karpaty Mts. indicates the prior origin of the cave on Miocene N-S trending fault, being re-activated and karstified in Plio-Quartenary period.
- New underground spaces indicated by electrical-resistivity tomography (ERT) were confirmed by speleological works

Introduction

More than 300 caves situated in several karst areas are registered in the Malé Karpaty Mts. The karst forms in the studied mountain range have a typical obscure development, so the comprehensive research involving several disciplines is needed to obtain more detail knowledge. The complex methodic approach requires the application of sedimentological (microfacial analyses of carbonatic rocks), structural-geological and geophysical (electrical-resistivity tomography; ERT) methods. Our research was focused on the Havranická jaskyňa cave, situated in the region of the Malé Karpaty Mts. - the Plavecký Karst Area (Šmída, 2010) in the western Slovakia.

The area around the Havrania skala elevation point is characteristic with complicated geological and tectonic setting, being observable on the surface and in the cave system. Since the cave originated due to the corrosive effect of the water, leaking through the fractures, it retained the general direction of the fault structures visible directly

in the cave and controlling the shape and direction of its passages. The development of fractures was affected by lithology. For example, preserved slicken slides found on faults in the dolomite, forming rheologically harder material relative to the limestone, have originated due to the relative displacements of the dolomite blocks.

Besides geological methods, the geophysical methods can be beneficial in the karst research - they allow to distinguish properties of the material, filling the voids, and when it is significantly different from the surrounding host rock, they indicate a material contrast (cf. Gibson et al., 2004; Dobečka & Upchurch, 2006; Monchales et al., 2008, as well as Putiška et al., 2012). In our case, we have used the ERT (electrical-resistivity tomography) method, producing the 3D model of the material discontinuities as an output.

Geological setting

The studied area is situated in the Malé Karpaty Mts., app. 1 km northwest of the village of Smolenice. The entrance to the Havranická jaskyňa cave is located only a few meters from the top of the Havrania skala elevation point (599 m a.s.l.), which is a part of the Havranica hill (717 m a.s.l.). This area includes the Považie nappe, being a part of the Hronic nappe system (Polák et al., 2012; Fig. 1). Within the karst regionalization, it is incorporated into the Plavecký Karst Area (Mitter, 1983).

The Havrania skala area is built of the Middle Triassic limestone of Gutenstein Fm., forming 50–100 meters thick bed. The lower part of this formation was correlated with the Annaberg limestone, occurring in the Eastern Alps. This type of limestone was described in the Malé Karpaty Mts. by Bystrický (1972, 1973). The Gutenstein dolomite (Polák et al., 2012), occurring under the limestone, partially interferes into the cave system. A slightly bland position of detrital limestone with a predominance of monotonous micrite (mudstone-wackestone) with rare organodetritic interbeds (foraminiferal-dasykladacea grainstone-packestone) is developed in the upper part of the grey Gutenstein Fm. limestone. The rare fragments of organisms, occurring in the biodetritic interbeds, represent ostracods, segments of crinoids, small gastropods, foraminifers and dasycladacea (Buček, 1988; Buček et al., 1991).

The limestone setting in the Havranica ridge is relatively simple, manifesting bedding with the dip of 60-80° to the north (Maheľ, 1986). Around the cave the bedding has a dip only of 36° to the north.

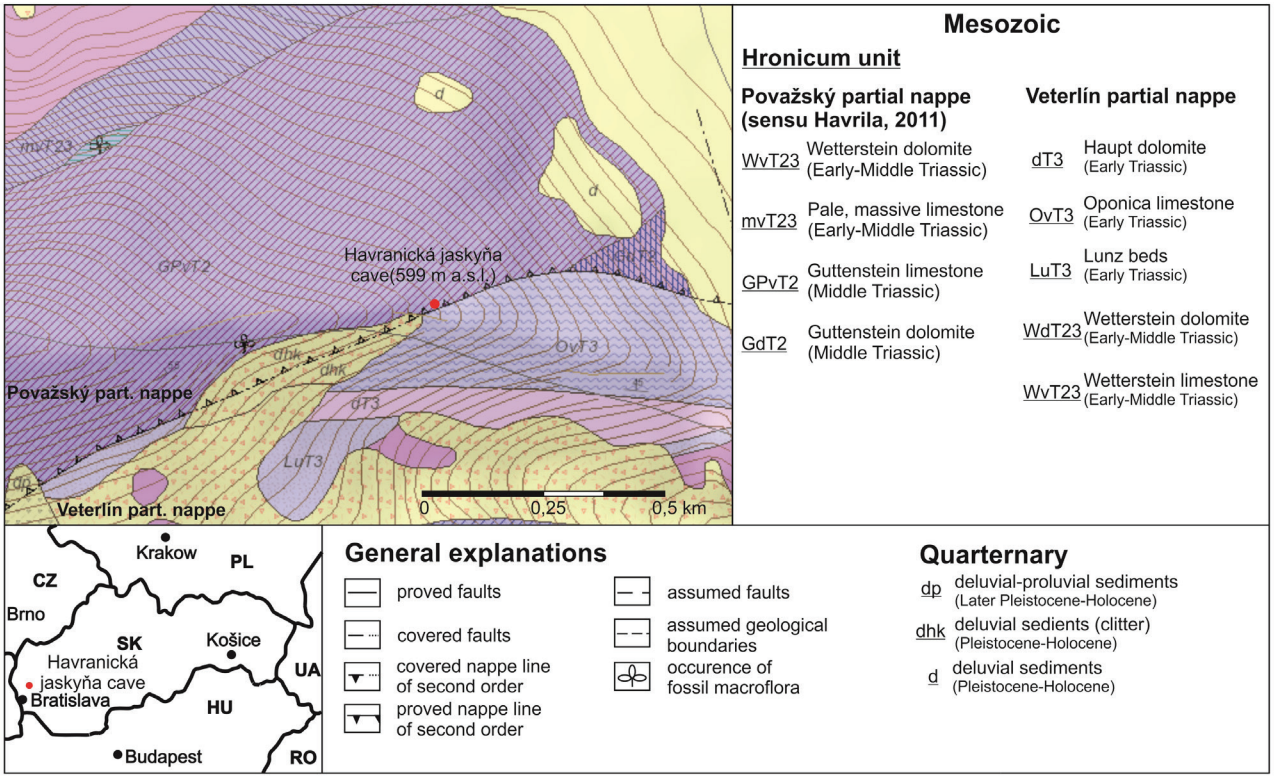

Fig. 1. Geological map of investigated area (taken with permission from the map-server of the State Geological Institute of Dionýz Štúr, Slovakia).

History of research

The Havranická jaskyňa cave is known from the time immemorial. The original entrance was probably destroyed during the World War II, when the Havrania skala hill was under fire. The re-discovery of the cave dates back to 18 September 2004 (Lačný, 2006). After the first mapping work, the cave length was less than 90 meters. However, during 12 years of work, speleologists discovered more than 80 meters of new space, and 14 meters of the depth range. The first exploration work started immediately after the re-discovery of the Zbojnická Chamber, representing the largest hall. As can be seen from the map (Fig. 2), the cave is located in a tectonic dislocation trending N-S. The cave system continues to the north as was confirmed by geophysical measurements in 2010 (Lačný et al., 2012). New exploration work was conducted on the basis of these measurements and new phase of discoveries began in 2013. Speleologists found 15 meters of new passages in the small hall called Michal's chamber. The next discovery came a year later when 30 meters of new passages were found. The current workplace is situated at a depth of -51 meters under the lower earlier discovered part known as the Objavná chamber.

Description of passages

Havranická jaskyňa cave (585 m a.s l.), length: 174.3 m; depth: -51 m

The genetic type of the cave is tectonic-corrosive, while in the lower part we can see passages that were modelled by the water. It is possible that the cave type changes with lithology and increasing depth. During the research, 5 limestone samples were subjected to XRD analysis and petrographic study applying the thin sections. Thin sections of three samples confirmed the presence of dolomite crystals, and the XRD analysis confirmed the occurrence of dolomite and partially dolomitized limestone. The entrance to the cave is situated only few meters from the apical parts of the Havrania skala elevation point (599 m a.s.l.). The first passage is represented by a narrow and steep chimney which leads to the first small chamber of dimensions 4 x 3 m. The atypical air current varies according to the season and wind intensity. Following creep passage is formed of limestone, and partially dolomitized limestone (Fig. 2a, b; sample s1 and s2). Subsequently the passage spreads to Zbojnícka Chamber, the largest hall in the cave (5 x 10 m, 5 m height). This hall was formed on a tectonic dislocation having azimuth 19° and dip 40° (19/40°). Its eastern side is formed of Fe-rich dolomite (Fig. 2, sample s3). From the Zbojnícka Chamber the passage leads to a small tunnel with the azimuth of 250°, reaching the Smoke Chamber (2 x 3 m), situated over it. Then the passage leads from the Smoke Chamber to the small hall (1.5x3 m), representing a vertical joint. The Michal's Chamber, comprised of dolomite with small Ca impurities (Fig. 2, samples s4, s5), is located to the east of the Smoke Chamber. The Objavná Chamber (4 x 7 m), formed on a continued discontinuity of N-S trend, leads to the current workplace at a depth of -51 m, situated below Michal's Chamber.

Jaskyňa v Havranej skale cave (574 m a.s.l.), length: 20 m

Jaskyňa v Havranej skale cave is situated in close vicinity to the Havranická jaskyňa cave, as the entrance to this small cave is located 15 meters southwest of the Havranická jaskyňa cave. It is formed on a remodeled discontinuity (105/76°), which is 0.5 to 1 meters wide and 2 to 6 meters high (Šmída, 2010). However, the connection of these caves should be considered as the vertical difference is only 10 meters, and a notable air draught occurs at the end of the Jaskyňa v Havranej skale cave.

Structural research

Both caves (Havranická jaskyňa cave and Jaskyňa v Havranej skale cave; Fig. 3) were formed on the same sub-vertical discontinuity trending N-S, which can also be seen on the surface at the cave entrance. Fractures of this trend are characteristic in the entire area around the cave. The beginning of the cave origin features another important system of discontinuities - the bedding with 36–76° dip northward (Fig. 4A, B). We have to note that the caves overlap each other in different depths. The N-S trending sub-vertical discontinuities dominate in the Plavecký Karst Area and can often be found in other karst areas of the Malé Karpaty Mts. The direction of cave passages has a connection with faults of N-S affinity, being accompanied with those of NW-SE trend, so they were formed on a paired system of discontinuities.

The discontinuities trending N-S have contributed to karstification process by allowing the penetration of atmospheric rainfalls through the carbonatic massif and dissolution of carbonate, as well as allowing subsequent water corrosive effects. The current compression is approximately of N-S direction (Kováč et al., 2002). The earlier tectonic research, based on tensometer measurements of relative movement of blocks in the Driny cave, located ca 10 km ENE of the Havranická jaskyňa cave in similar tectonic conditions (Briestenský et al., 2011), revealed the dextral displacements on the NW-SE trending discontinuities and sinistral displacements on NNE-SSW trending discontinuities. Authors deduce that the current stress field is represented by a compression of NNW-SSE direction, applying the pure shear model for the origin of N-S trending faults, where the NW-SE and NE-SW discontinuities

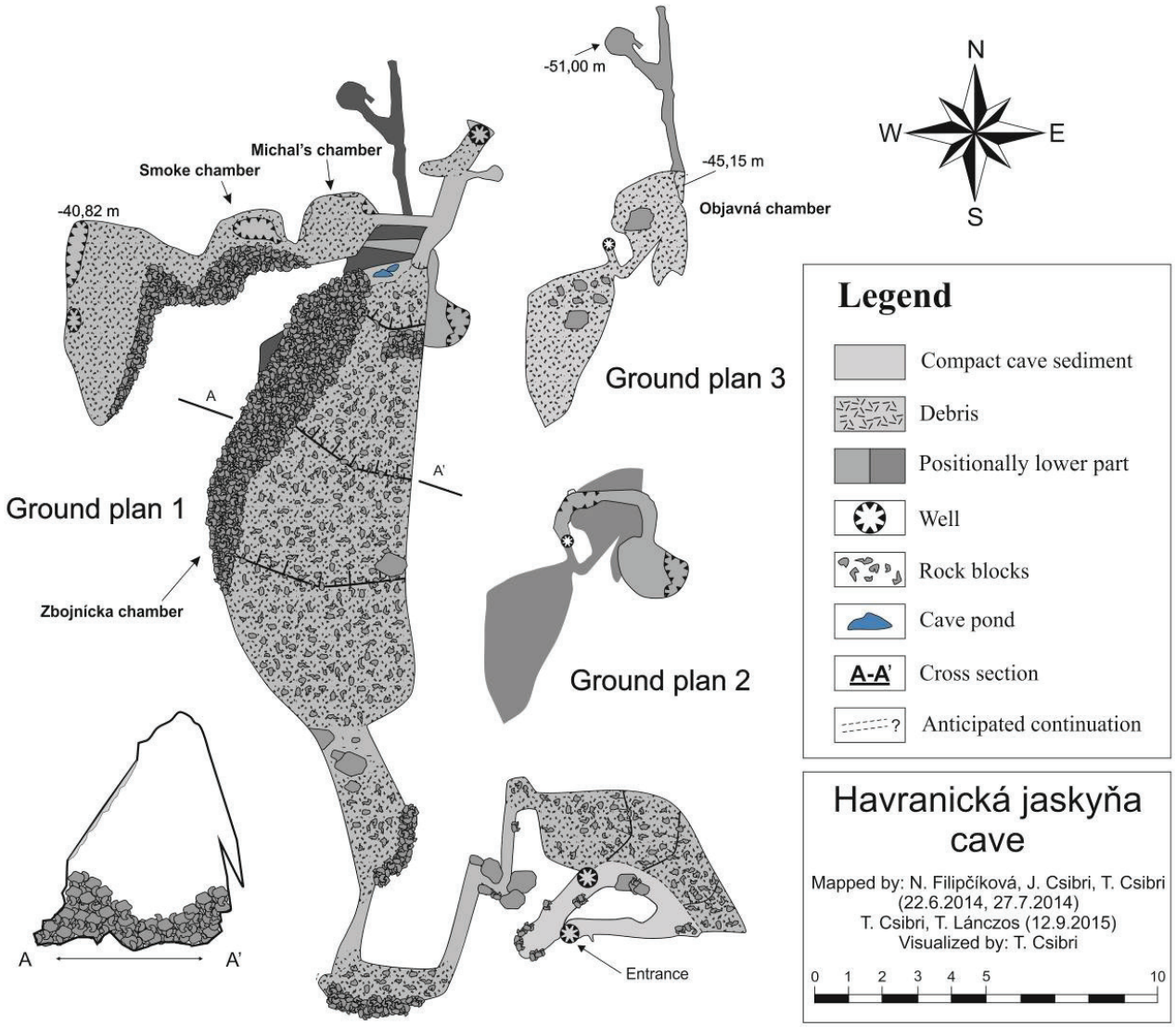

Fig. 2a. Ground plan of the Havranická jaskyňa cave.

represent the paired system of faults. These results correspond to mechanism of recent stress field in the region of the Malé Karpaty Mts. (cf. Kováč et al., 2002).

Applying the current compression field and the pure shear model, there should be reactivated also earlier existing N-S trending structures. Revealed shifts on geological discontinuities indicate that they represented the sinistral faults also in the past, forming paired system to the dextral faults of NW-SE trend. Later, during the middle Miocene compression of N-S direction they were reactivated as normal faults, being associated with opening of the Badenian deposition centre of the Vienna Basin (Marko & Jureňa, 1999).

Our research results confirmed that the Havranická jaskyňa cave was formed on a significant fault trending N-S. There is a presumption of later re-activation of this fault in the Plio-Quaternary period. The role of tectonic discontinuities of the earlier period at the cave formation can not be excluded, because similar structures of this affinity are registered in the Malé Karpaty Mts. from the middle Miocene. The uplift of the Malé Karpaty Mts. (except of the earlier Upper Cretaceous-Paleogene event) took place in the Upper Miocene, so the karstification should occur only after the Miocene time. Therefore we assume, that the main phase of karstification should be associated with a Plio-Quaternary period.

For comparison there is worth to mention the tectonic result of the research in the eastern part of the Western Carpathians (Németh in Gaál et al., 2017; cf. Fig. 10 ibid.), being focused on the caves developed in magnesite bodies along the contact zone of Veporic and Gemeric units). The

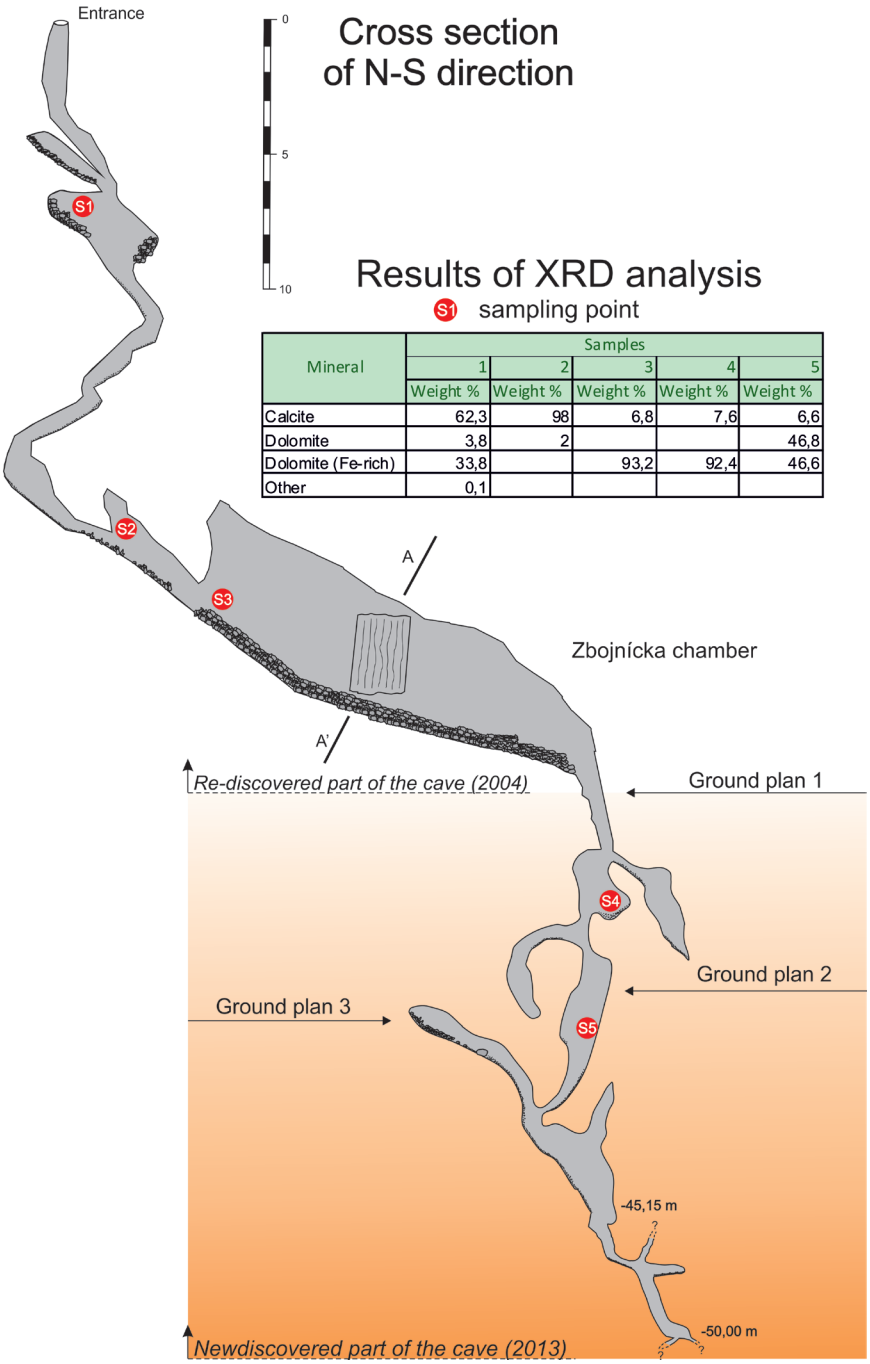

Mineral	Samples				
	1	2	3	4	5
	Weight %	Weight %	Weight %	Weight %	Weight %
Calcite	62,3	98	6,8	7,6	6,6
Dolomite	3,8	2			46,8
Dolomite (Fe-rich)	33,8		93,2	92,4	46,6
Other	0,1				

Fig. 2b. Cross section of Havranická jaskyňa cave.

research has revealed that the origin of a system of N-S trending faults is a consequence of the post-Upper Cretaceous subhorizontal displacements on conjugate NE-SW (sinistral shearing) and NW-SE (dextral shearing) trending faults and the generally N-S trending faults represent the synthetic faults related to both systems (l.c.). In the Malé Karpaty area, located in the western limb of the Western Carpathian arc, the sinistral shearing on NE-SW trending faults is much more dominant.

We can find calcified terra rossa in the discontinuities on the cave walls. Autochthonous clastics of carbonates, which are differently rounded (0.5 to 2.5 cm), occur in the terra rossa. Sharp-edged fragments are interpreted as products of tectonic processes. In a smaller amount we identified also well rounded pebbles, their roundness is related to their transport. Despite we have not found shapes created by erosion, their existence in the past cannot be excluded. They were probable erased by the corrosive effect of percolating water or the destruction of the walls, related to younger tectonic processes. As one example of such processes we interpret the origin of the Zbojnícka Hall. Below this hall, Šmída (2010) assumes that there was a larger corrosion hall, which after the neotectonic and gravitational movements has collapsed. The wedge-shape profile of the Zbojnická Hall (Fig. 5) represents a result of this event. The cave system continues northward, and the passages become more vertical (70-80°).

Geophysical research

Seven 2-dimensional, direct-current electrical-resistivity traverses were carried out. Electrical resistivity tomography (ERT) prospecting was performed using an ARES (GF Instruments) multi-electrode system with a set of 48 electrodes evenly spaced for every 5.5 m. A dipole-dipole array configuration was used with a geometrical factor of "$k = 2\pi\, n\,(n+1)\, a$", where "**a**" is the dipole length and "**n**" is the dipole separation. For surveys with this array, the "a" spacing is initially fixed at the smallest unit electrode spacing and the "n" factor is increased from 1 to 2 to 3.

In the first phase of the geophysical survey we re-measured three sections: the first profile (pf-1-09) was situated just behind the largest known chamber in the Havranická jaskyňa cave; the other two sections: pf-2-09 and pf-3 09 (Fig. 6) were outlined parallel to the first profile in the direction of the expected continuation of the cave system. An

Fig. 3. Position of the Havranická jaskyňa cave and Jaskyňa v Havranej skale cave in the Havrania skala massif (599 m a.s.l.). Orientation of figure corresponds with that in Fig. 2a, which re- presents the northern (black) part of Fig. 3.

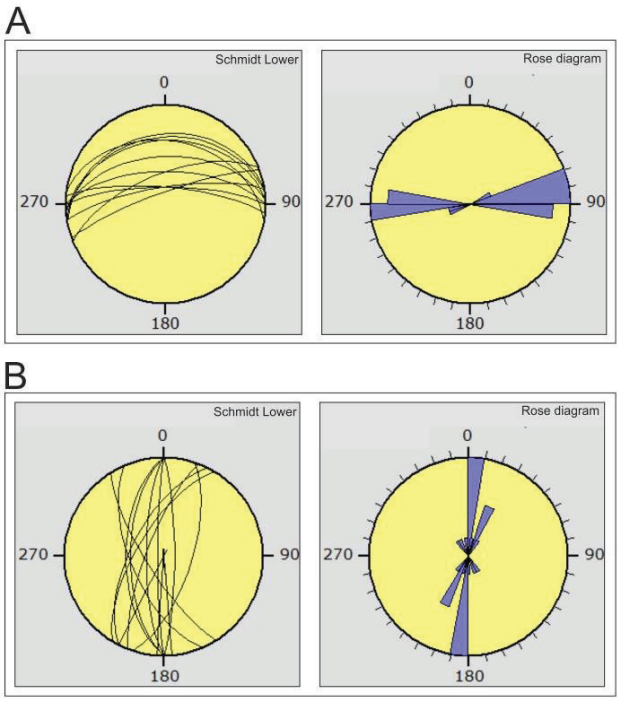

Fig. 4. Tectonograms: **A** – bedding in the Havranická jaskyňa cave and its surroundings. **B** – discontinuities measured in the Havranická jaskyňa cave, the Havrania skala hill and surrounding.

Fig. 5. The wedge-shape profile of the Zbojnická Chamber in the Havranická jaskyňa cave. Photo: A. Lačný.

inversion model of these profiles demonstrates considerably high resistivity anomalies – greater than 21 000 Ωm, which highlights the great cavities (caves). On the basis of these results, we added new ERT measurements. These new profiles were measured due to thickening and the dissemination of information on the locality. Four other sections were also measured on this site. The first profile (pf-0-10) was situated above the already known part of the Havranická jaskyňa cave. The second profile (pf-4-10) was situated 44 m from the pf-0-10 profile. The next two profiles: pf-5-10 and pf-6-10 (Fig. 6) were situated perpendicular to the previous profiles. Thus, we created a network of measurement points 44 m x 264 m with a density of 11 m x 5.5 m. Such density measurements allowed us to create a detailed 3D visualization of the results (Fig.7).

Geophysical results

The main purpose of the geophysical survey was to find the direction of the possible continuation of the cave system. According to the spatial distribution of resistivity values, a significant area with a high resistivity value is visible in the central part of the studied area (Fig. 7). In this area, we anticipate the occurrence of other karst formations. The system of fractures and smaller cavities in the rock environment increases the overall resistivity of

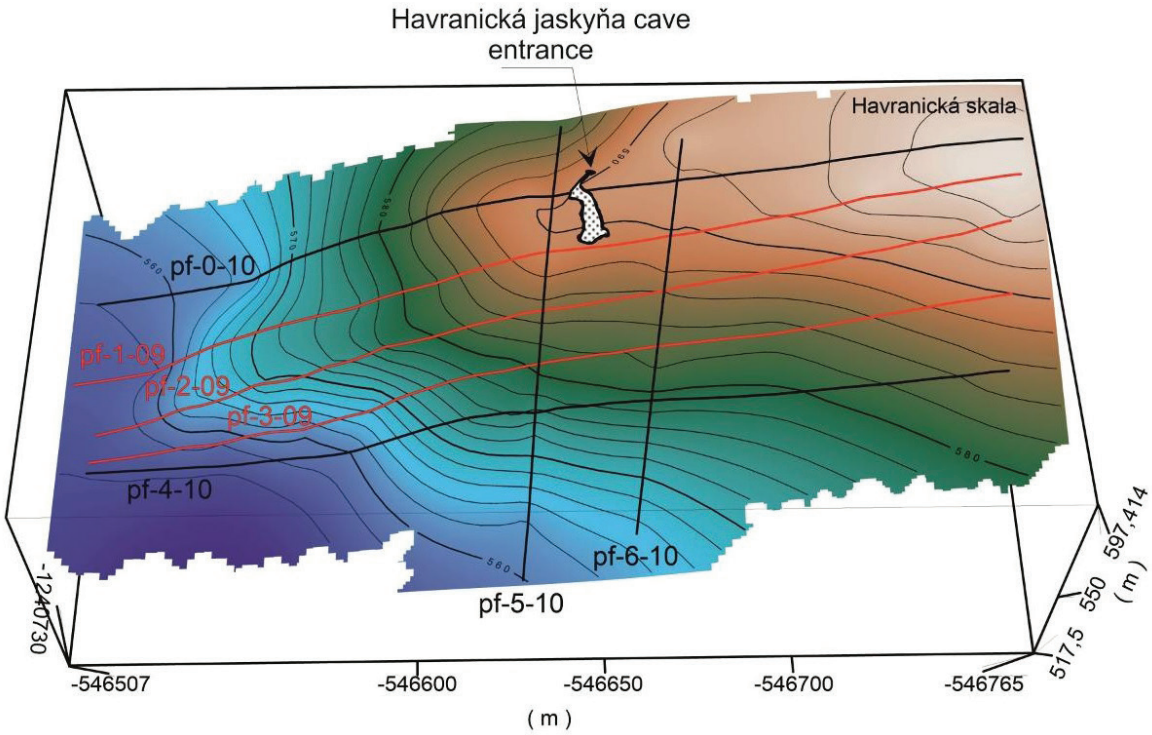

Fig. 6. Position of profiles around the Havranická jaskyňa cave (S-JTSK GPS coordinate system).

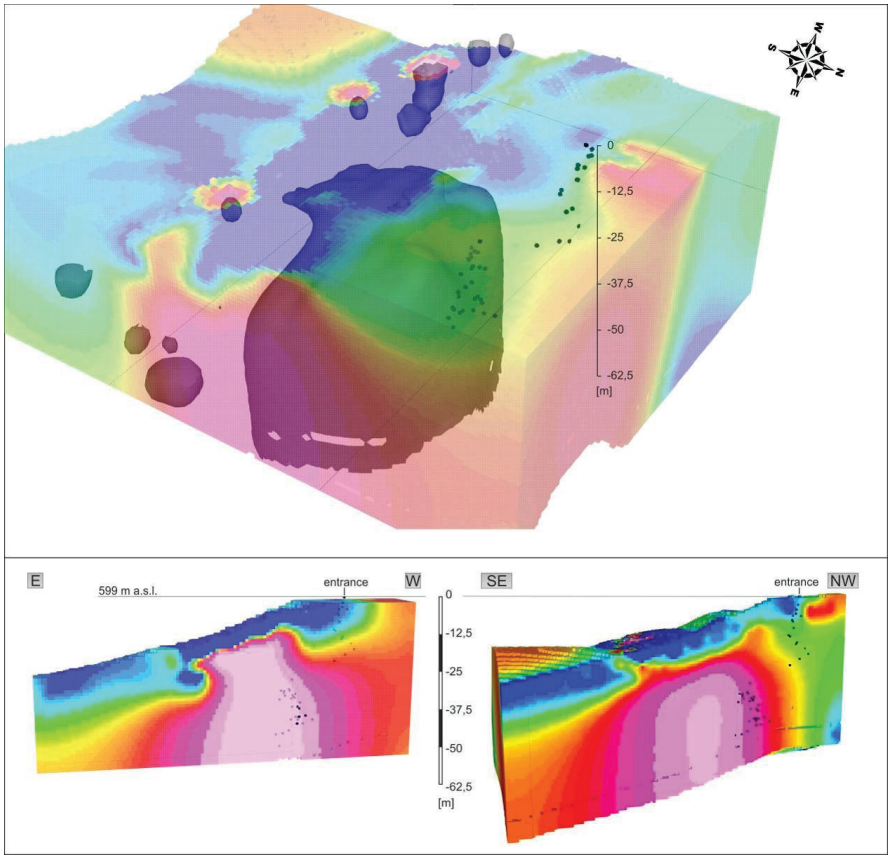

Fig. 7. The 3D models of ERT surveys with the polygonal traction points of the Havranická jaskyňa cave (A – isosurface's value – 12 000).

the environment. According to the results of ERT measurements and subsequent 3D visualization, the highly resistive anomalous region of the concentric shape is followed and its continuation can be traced downwards (in depth). Based on these findings, we continued to consider the continuation of the cave system only to depth. Subsequent speleological studies confirmed the prerequisites of the geophysical survey, and new cave areas were discovered up to a depth of -50 m (Fig. 2). The course of newly discovered spaces was geodetically oriented and confronted with the results of geophysical research. The correlation between the high resistivity area and the black dots has confirmed the original assumption that the cave system continues downwards (Fig. 7).

Conclusion

During the research of Havranická jaskyňa cave the geological (sedimentology, structural geology) and geophysical (electrical resistivity tomography – ERT) survey methods were combined to detect possible lateral and depth continuation of the cave system.

The Havranická jaskyňa cave was formed on a sub-vertical discontinuity trending N-S. At the beginning of the cave formation, the primary limestone bedding with the dip of 36–76° to the north has played an important role. The lithological research has revealed the dolomitized parts in the lower parts of the cave. These dolomite boudins interfered into the cave system and affected the karstification; however the course of the cave system remained unchanged, which was confirmed also by the geophysical measurements.

During the geophysical research, seven 2-dimensional, direct-current electrical-resistivity traverses were carried out. Overall, we re-measured seven profiles. The results show that a significant area with a high resistivity value is visible in the central part of the studied area. From the spatial distribution of the resistivity values, it is evident that the system of fractures and smaller cavities in the rock environment increases the overall resistivity of the environment. According to the results of ERT measurements and subsequent 3D visualization, the highly resistive anomalous region of the concentric shape is followed and its continuation can be traced downwards (in the depth). This model, which was geodetically referenced and completed by the measured points during the cave mapping, convincingly proves the presumptions of the geophysical survey.

Subsequent speleological and structural geological studies confirmed the continuation of the cave system, but only downward. Based on the results of the geophysical survey and new cave spaces were discovered down to a depth of -50 m. The results of the geophysical ERT measurement were confirmed by speleological work; however, speleologists are still working in the deepest parts of the cave – still finding new until unknown cave spaces.

Acknowledgement

This work was supported by the Slovak Research and Development Agency under contract No. APVV-16-0146. Authors express their thanks to Dr. Ľ. Gaál and Dr. I. Zeman for inspiring remarks and suggestions, which improved the manuscript.

References

Buček, S., 1988: Dasycladacea and biostratigraphy of Biela hora region (Malé Karpaty Mts.). PhD thesis. *Manuscript. Bratislava, archive Geol. Inst. SAV, 1 – 258.*

Buček, S., Jendrejáková, O. & Papšová, J., 1991: Contribution to biostratigraphy of Veterlín and Havranica units of the Biela hora region. *Geol. Práce, Spr., 92, 29 – 51.*

Briestenský, M., Stemberk, J., Michalík, J., Bella, P. & Rowberry, M., 2011: The use of a karstic cave systems in a study of active tectonics: fault movements recorded at Driny cave, Malé Karpaty Mts. (Slovakia). *J. Cave Karst Stud., 73, 2, 114 – 123.*

Bystrický, J., 1972: Faziesverteilung der mitt leren und oberen Trias in den Westkarpaten. *Mitt. Gessell. Geol.-u. Bergb.--Studenten Wien, 21, 1, 289 – 310.*

Bystrický, J., 1973: On the stratigraphy and tectonic appurtenance of limestones of the Varajská Deposit (Malé Karpaty Mts.). *Miner. Slov., 5, 1, 1 – 7.*

Gaál, Ľ., Németh, Z., Bella, P. & Koděra, P., 2017: Caves in magnesite – a rare phenomenon of karstification: The case study from Slovakia. *Miner. Slov., 49, 2, 157 – 168.*

Geological Map of the Slovak Republic 1 : 50 000. Bratislava, Štátny geologický ústav Dionýza Štúra [online]. Available on web: http://apl.geology.sk/gm50js. [Accessed 1th January 2013].

Gibson, P. J., Lyle, P. & George, D. M., 2004: Application of resistivity and magnetometry geophysical techniques for near-surface investigations in karstic terranes in Ireland. *J. Cave Karst Stud., 66, 2, 35 – 38.*

Kováč, M., Lexa, J., Konečný, V. & Šefara, J., 2002: Geodynamic evolution of the Carpatho-Pannonian region during the Neogene. *Geol. Carpath., 53, spec. iss., 1 – 2.*

Lačný, A., 2006: The secret of cave on Havrania skala hill (Havranické tajomstvo). *Bull. Slovak Speleol. Soc., 37, 4, 20 – 22.*

Lačný, A., Putiška, R., Dostál, I. & Kušnirák, D., 2012: Utilization of ERT method in research of caves in the Crow Rock (the Plavecký Karst). *Slov. Kras (Acta Carsol. Slov.), 50, 1, 41 – 60.*

Maheľ, M., 1986: Geological structure of Czechoslovakian Carpathians – Paleoalpine units 1. *Bratislava, Veda, 1 – 503.*

Marko, F., 2012: Cenozoic stress field and faulting at the northern margin of the Danube Basin (Western Carpathians, Slovakia). *Miner. Slov., 44, 3, 213 – 230.*

Marko, F. & Jureňa, V., 1999: Zlomová tektonika východného okraja viedenskej panvy a hrastu Malých Karpát. *Miner. Slov., 31, 1999, 513 – 524.*

Mitter, P., 1983: Geomorfologická rajonizácia krasu Malých Karpát. *Slov. Kras, 21, 3 – 34.*

Polák, M., Plašienka, D., Kohút, M., Putiš, M., Bezák, V., Filo, I., Olšavský, M., Havrila, M., Buček, S., Maglay, J., Elečko, M., Fordinál, K., Nagy, A., Hraško, L., Németh, Z., Ivanička, J. & Broska, I., 2012: Vysvetlivky ku geologickej mape regiónu Malých Karpát 1 : 50 000. Bratislava, Št. Geol. Úst. D. Štúra, 1 – 287.

Putiška, R., Nikolaj, M., Dostál, I. & Kušnirák, D., 2012: Determination of cavities using electrical resistivity tomography. *Contr. Geophys. Geodesy, 42, 2, 201 – 211.*

Šmída, B., 2010: Geomorphology and genesis of Plavecká Karst as a model area called the contact karst of the Western Carpathians with lower energy of creation of relief. PhD thesis. *Manuscript. Bratislava, archive Fac. Natur. Sci., Comen. Univ., pp. 221.*

Hĺbkový rozsah a možné pokračovanie jaskynného systému Havranickej jaskyne, zistené geologickými metódami a elektrickou odporovou tomografiou (ERT), Malé Karpaty

V krasových územiach pohoria Malé Karpaty sa nachádza viac ako 300 registrovaných jaskýň. Krasové formy tohto územia je potrebné študovať z viacerých hľadísk v spolupráci s viacerými vednými disciplínami. Tento komplexný metodický postup vyžaduje aplikovať sedimentologické (mikrofaciálna analýza karbonatických hornín), štruktúrnogeologické a geofyzikálne (elektricko-odporová tomografia – *electrical-resistivity tomography*; ERT) metódy. Uvedené metódy výskumu sme aplikovali na Havranickú jaskyňu, ktorá sa nachádza v Plaveckom krase v centrálnej časti pohoria Malé Karpaty.

Havranická jaskyňa je situovaná približne 1 km západne od obce Smolenice, pričom vchod sa nachádza iba pár metrov od kóty Havrania skala, ktorá je súčasťou vrchu Havranica (717 m n. m.). Jaskyňa bola známa od nepamäti, pričom počas druhej svetovej vojny bol pôvodný vchod zasypaný. Jaskyňu znovu objavila jaskyniarska skupina Speleoklub Trnava 18. 9. 2004 (Lačný, 2006). Jaskyňa bola prvotne dlhá približne 90 m. V roku 2010 tu boli vykonané geofyzikálne merania, ktoré potvrdili pokračovanie jaskynného systému. Na základe týchto meraní jaskyniari začali s výkopovými prácami. V roku 2013 došlo k novým objavom v jaskyni na základe geofyzikálnych modelov z roku 2010. Havranická jaskyňa má momentálne dĺžku 174,3 m s celkovou hĺbkou –51 m.

Študovaná jaskyňa je vytvorená prevažne v gutensteinských vápencoch hronika, resp. v jeho čiastkovom príkrove – považskom čiastkovom príkrove (Polák et al., 2012). Na základe mikrofaciálnej analýzy a röntgenovo-difrakčných analýz sa potvrdilo, že jaskynný systém tvoria vo vyšších častiach čiastočne dolomitizované vápence, pričom smerom do hĺbky dominujú dolomity s vysokým obsahom Fe. Najnovšie objavené časti jaskyne sú tvorené vápencami až dolomitickými vápencami (obr. 2b).

Zo štruktúrnogeologického hľadiska Havranická jaskyňa vznikla na subvertikálnej diskontinuite s.-j. smeru, ktorá je sledovateľná aj na povrchu pri samotnom vchode. Sklon vrstvovitosti varíruje medzi 36 – 76°, pričom sa lavice skláňajú na sever (obr. 4). Najaktuálnejšie výsledky z pohľadu recentnej tektoniky prináša práca Briestenského et al. (2011). Na základe svojich výsledkov sa domnievajú, že v súčasnosti na sz.-jv. štruktúrach dochádza k dextrálnym pohybom a na ssv.-jjz. poruchách k sinistrálnym pohybom. Autori dedukujú, že súčasné napätie je ssz.-jjv. kompresia. Vychádzajú z predstavy čistého strihu, kde sz.-jv. a sv.-jz. poruchy tvoria párový systém. To korešponduje s predstavou a mechanizmom recentného napätia v oblasti Malých Karpát (Kováč et al., 2002). V modeli čistého strihu by mali vznikať, resp. sa reaktivovať aj extenzné s.-j. štruktúry. Preto sa domnievame, že súčasná kompresia môže mať vplyv aj na staršie zlomové štruktúry s.-j. smeru. Z posunov na geologických rozhraniach vyplýva, že v minulosti fungovali aj ako sinistrálne smerné zlomy, ktoré so sz.-jv. dextrálnymi zlomami tvorili párový systém. Neskôr pri pôsobení strednomiocénneho kompresného napätia s.-j. smeru sa reaktivovali ako poklesy súvisiace s mechanizmom (*pull-apart*) otvárania bádenského depocentra sedimentácie Viedenskej panvy (Marko a Jureňa, 1999).

Výsledky štruktúrnogeologického výskumu potvrdili, že Havranická jaskyňa vznikla na významnej zlomovej poruche práve s.-j. smeru. Predpokladá sa neskoršia aktivácia v pliocénno-kvartérnom období. Nie je však vylúčené ani tektonické porušenie v skoršom období, keďže zlomy s touto afinitou registrujeme v oblasti Malých Karpát v strednom miocéne. Samotné vynorenie Malých Karpát (s výnimkou vrchnokriedovo-paleocénneho eventu) sa udialo vo vrchnom miocéne, preto krasovatenie mohlo nastať až po tejto fáze, najskôr v období pliocénu. Podľa našich predpokladov hlavnú fázu krasovatenia priraďujeme do pliocénno-kvartérneho obdobia s klímou odlišnou od súčasnej.

Počas geofyzikálnych meraní sa vyhotovilo 7 dvojdimenzionálnych profilov metódou ERT. Pri meraniach sa využil multielektródový systém ARES (GF Instruments). Celkovo sa použilo 48 elektród v intervale 5,5 m, pričom meranie prebehlo v konfigurácii dipól – dipól. Prvé profily boli vedené nad systémom Havranickej jaskyne (obr. 6),

neskôr boli doplnené ďalšie profily. Na základe 2D profilov sa vyhotovil 3D model jaskynného systému, doplnený bodmi polygónového ťahu, ktoré sa využívajú pri mapovaní podzemných priestorov (obr. 7). Jaskynný systém na obr. 7 preukazuje vysoký odpor v centrálnej časti študovanej jaskyne.

Nové priestory definované multidisciplinárnym výskumom Havranickej jaskyne potrvdili speleologické práce a nové objavy až do hĺbky –51 m. Speleologický výskum pokračuje na najhlbšom mieste jaskyne, kde jaskyniari neustále nachádzajú nové nepoznané miesta.

Doručené / Received: 21. 1. 2018
Prijaté na publikovanie / Accepted: 5. 6. 2018

Mineralia Slovaca, Web ISSN 1338-3523, ISSN 0369-2086
50 (2018), 47 – 54, © Author 2018. CC BY 4.0

Simple processing and retilting of the oriented lineations and its application in paleocurrent analysis

FRANTIŠEK TEŤÁK

State Geological Institute of Dionýz Štúr, Mlynská dolina 1, 817 04 Bratislava, frantisek.tetak@gmail.com

Abstract: Traditionally used graphic method of the lineations retilting according to horizontal axis in the projection net is relatively demanding. The paper proposes easily applicable method for the field processing of oriented lineations and their retilting to horizontal plane. Presented calculation is appropriate mainly for oriented lineations – vectors, but it can be used also for processing of not oriented lineations – the axes data. It is also adapted for reversed sedimentary beds. Method mitigates the possibility of errors at retilting determinations. The paper presents also a practical example of processing and retilting of oriented lineations in sediments of gravity flows in the flysch sequences of the Western Carpathians. Besides the paleocurrent analysis, presented method can be also used in structural geology.

Keywords: geological methods, sedimentology, structural geology, paleocurrent analysis, Western Carpathians

Graphical abstract

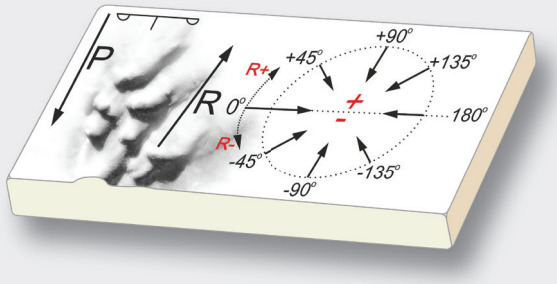

Highlights

- easily applicable method for retilting of oriented lineations to horizontal plane is beneficial in sedimentology for determining directions of paleocurrents: $\mathbf{L = P_n - R + 90°}$, $\mathbf{L = P_i - R - 90°}$
- practical use of retilting method in the quarry in Zábava Fm. (equiv. of Piwniczna Mb.) of Krynica Unit, the Magura Nappe, Outer Western Carpathians

Introduction

Oriented lineations – vector data are commonly processed in geology. The lineations can be represented by slicken side lineations and slicken fibres on a fault surface, fold axes, mineral stretching lineations or paleocurrent structures such as flute casts, groove and prod casts. The procedure for the collection and interpretation of lineation data from the horizontal planes is simple. It becomes more difficult if the strata have been tilted or even inverted. The direction of lineation has to be recorded as an angle between lineation and the strike of bedding – a pitch (rake resp.). The stereonet techniques are customary geological methods used to retilt bedding planes back to the primary depositional state (Melichar, 1991; Lisle & Leyshon, 2004; Fossen, 2010), but they are methodically difficult.

The manual processing of retilting in projection networks is recently used only scarcely. The recent available geological-structural software provides a module for rotation of structural elements. However, the data processing requires a good understanding of 3D geometry on the projection network, which may lead to errors.

Proposed field measuring of lineation data is similar to the method used for graphic processing in the projection network. New methodology provides a simplification of the processing of retilting the paleocurrents back to the depositional state. The significance of presented methodology is mainly in the case of greater number of measurements (tens to hundreds of measurements; e.g. Teťák, 2008). This methodology is best applicable at the paleocurrent analyses in sedimentological research, but can be useful also in the structural geology and other disciplines. As an example of application of this methodology we provide the processing of paleocurrent measurements of turbidity currents of the Outer Western Carpathians.

Geological settings

The need to simplify the retilting method arose at solving the paleogeographic problems of sedimentary sequences of the Western Carpathians. Collecting and evaluating of hundreds of paleocurrent measurements is crucial when tackling issues of geological evolution and setting of this area.

The evolution of the Magura sedimentary basin can be traced from the Albian to Early Miocene. Even the oldest sediments have a deep-sea character. The Magura sedimentation basin was gradually filled with dominating

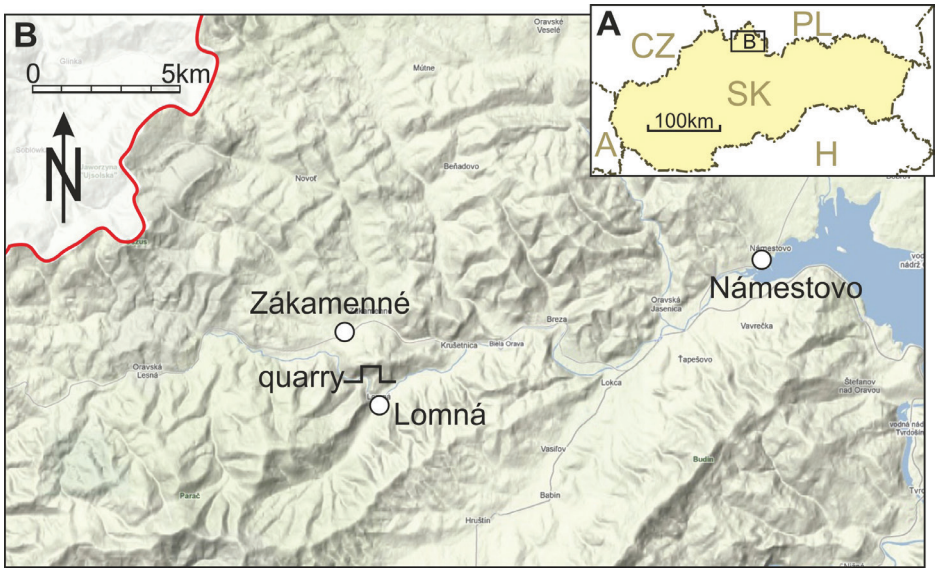

Fig. 1. Location of the Zábava Fm. profile (equiv. Piwniczna Mb.) in the quarry between Lomná and Zákamenné villages (northern Slovakia).

flysch sequences. They have formed in relation to position and morphology of the deposition fans in the basin, tectonic activity of the basin floor and source areas of the sedimentary material, as well as the sea level changes (Teťák et al., 2016).

As an example of the use of presented methodology we show the sedimentological profile through the Zábava Fm. of Krynica Unit in the quarry between the Lomná and Zákamenné villages (Fig. 1). The Krynica Unit represents the southernmost tectonic-lithofacial unit of the Magura Nappe. The bed succession reaches the thickness up to 5,000 m. The Zábava Fm. was defined by Potfaj et al. (1991). In the Polish territory it can be correlated with the Piwniczna Mb. or sandstones (Cieszkowski et al., 1998). It is characteristic by the alternation of 10–200 m thick interbeds of Magura-type sandstones and thin-bedded flysch lithofacies. The thickness of the formation is up to 3,000 m. The age of the The Zábava Fm. is Late Paleocene to Middle Eocene (Potfaj et al., 1991; Teťák, 2005, 2010; Teťák et al., 2016).

The beds of sandstones of Magura-type are prevailingly thick 40–150 (600) cm. The amalgamation of the beds is common. Mostly they are formed of the fine- to coarse-grained greywacke sandstone (up to the fine-grained para-conglomerates). They are characterized by the thick massive Bouma Ta interval (Bouma, 1962), or rather by the Lowe S3 interval (Lowe, 1982). The water escape structures are well visible after weathering. Only the highest laminated part of the bed (Bouma Tc interval) has sedimented by the traction from the finer-grained "tail" of the gravity flow. It is wavy laminated with plenty of muscovite and plant crumble. The clay galls of 3–30 cm dimensions sedimented usually in the higher part of the bed at the termination of sedimentation of the Lowe S3 interval immediately beneath, or in the mentioned wavy laminated interval (between Ta and Tb). In the case of stronger erosion, they sedimented also on the basis of the bed. A significant feature of the Magura-type sandstones is represented by the traces of the bottom erosion. Typical there are the groove and prod casts. Common there are also flute casts and load casts and locally also smaller erosion channels.

The thin bedded flysch lithofacies has 5–11 (max. 20) beds/m. The ratio of sandstones/claystones is 2/1 to 3/1. The sandstones are 2–25 (45) cm thick fine-grained and distinctly laminated with bioglyphs. They alter with harder claystones to siltstones.

Numerical method of retilting of oriented lineations

In the field, the lineations can be commonly observed on the bed plane, fault or other tectonic plane. If this plane is tilted or overturned and there is necessary to perform the paleocurrent analysis, the retilting of lineations into horizontal level represents a demanding procedure. Processing large dataset is therefore much time consuming. Despite, the methodically demanding stereonet technique, based on projection of lineation into the projection hemisphere (Melichar, 1991; Lisle & Leyshon, 2004; Fossen, 2010), can be alternated with simple calculation method.

On the plane with lineation there is necessary to measure two values – **P** and **R** (Fig. 2). First value represents the dip of the plane ***P***, measured in degrees. It is commonly measured at standard geological documentation. The second value, we need to measure (or eventually extrapolate), is ***R*** parameter (in degrees), representing the value of the angle between the lineation and the trend (azimuth) of the bed in the range of 0 to 180°. The value ***R*** is subtracted always from the left to the right. In the case of lineations – vectors directed from the top downward, ***R*** has a positive

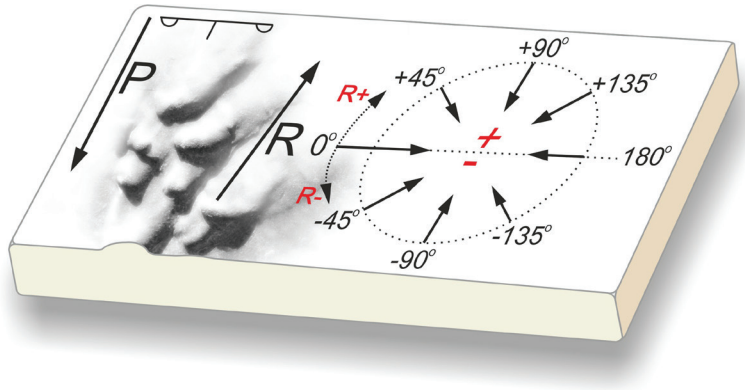

Fig. 2. A method of the ***R*** value counting on the bed plane. If the oriented lineation is directed from the top downward, ***R*** has a positive value. If it is directed upwards, ***R*** is negative. Explanation of abbreviations: ***P*** *– direction of the plane dip.* ***R*** *– the angle of the folded line to the direction of the bed.*

value. In the bottom-up direction, the **R** value is negative. The value ***R*** is from the left 0° and gradually to the right increases its value up to 180°. The paleocurrent directions are used to be displayed in the rosette diagrams at 5° or 10°, so we recommend to measure the ***P*** and ***R*** values at 5°.

The resulting direction of the line after tilting ***L*** is calculated according to the formula, where P_n represents the dip of the plane in normal position:

$$L = P_n - R + 90°$$

This relation is valid for the normal position of the bed (P_n). It is e.g. in the case of sedimentary rocks, where we distinguish the normal and inverse position of the beds.

For the inverted (reversed) position of the bed (P_i) we apply a slightly modified relationship:

$$L = P_i - R - 90°$$

The ***L*** value in degrees states were the oriented lineation – vector – is heading (e.g. where the paleocurrent was flowing). In the case, when the *L* will have negative value, there is necessary to recalculate it adding *360° (i.e. L + 360°)*. In the case when *L* value is *above 360°*, it is necessary to count out *360°* (i.e. *L – 360°*) to obtain the *L* value within the range of 0° to 360°.

For this calculation, it is not necessary to apply the methodically difficult stereonet techniques or to use special software. The use of commonly available Microsoft Excel spreadsheets has proven to be beneficial at greater amount of measurement.

Results

In geological research of the region of Biela Orava (Teťák et al., 2016) more than 1,000 paleocurrent measurements were done. The application of simple processing and retilting of the oriented lineations in such cases was very helpful. For this reason, we give a practical example of the use of this methodology on paleocurrents in the profile of Zábava Fm. of Krynica Unit belonging to Magura Nappe in the quarry between Lomná and Zákamenné settlements (northern Slovakia) (Figs. 1, 3 and 4).

Example of processing and retilting of paleocurrents

As an practical example of the processing of oriented lineations during the paleocurrent analysis we use the case of the sandstone bed of the Magura Nappe flysch sequence of the (Fig. 3). Intentionally we choose the more demanding case when the bed is in inverted position, the R value is negative and L value resulting from the calculation is over 360°.

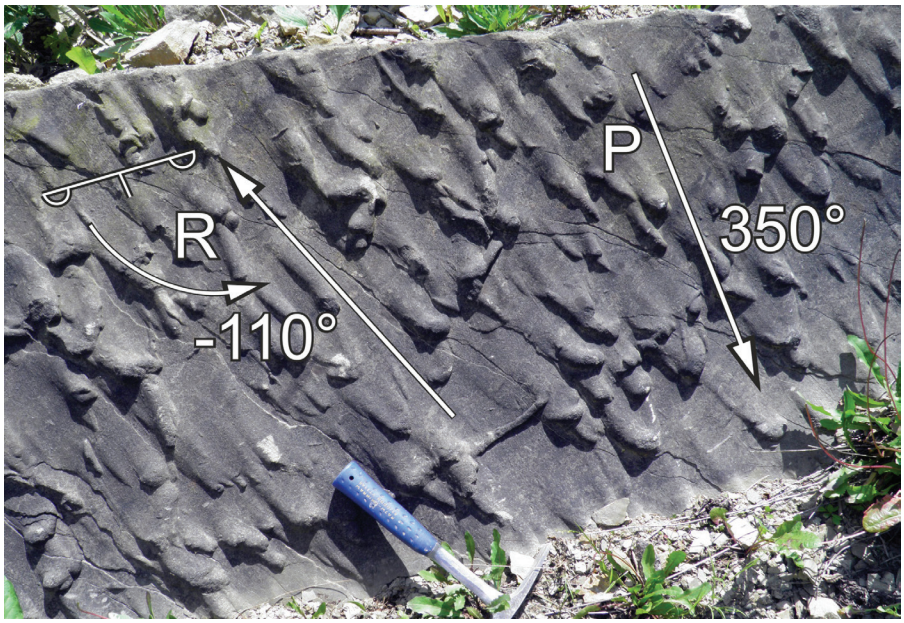

Fig. 3. An example of processing of paleocurrent measurements on the lower surface of the sandstone bed of the Zábava Fm. flysch sequence.

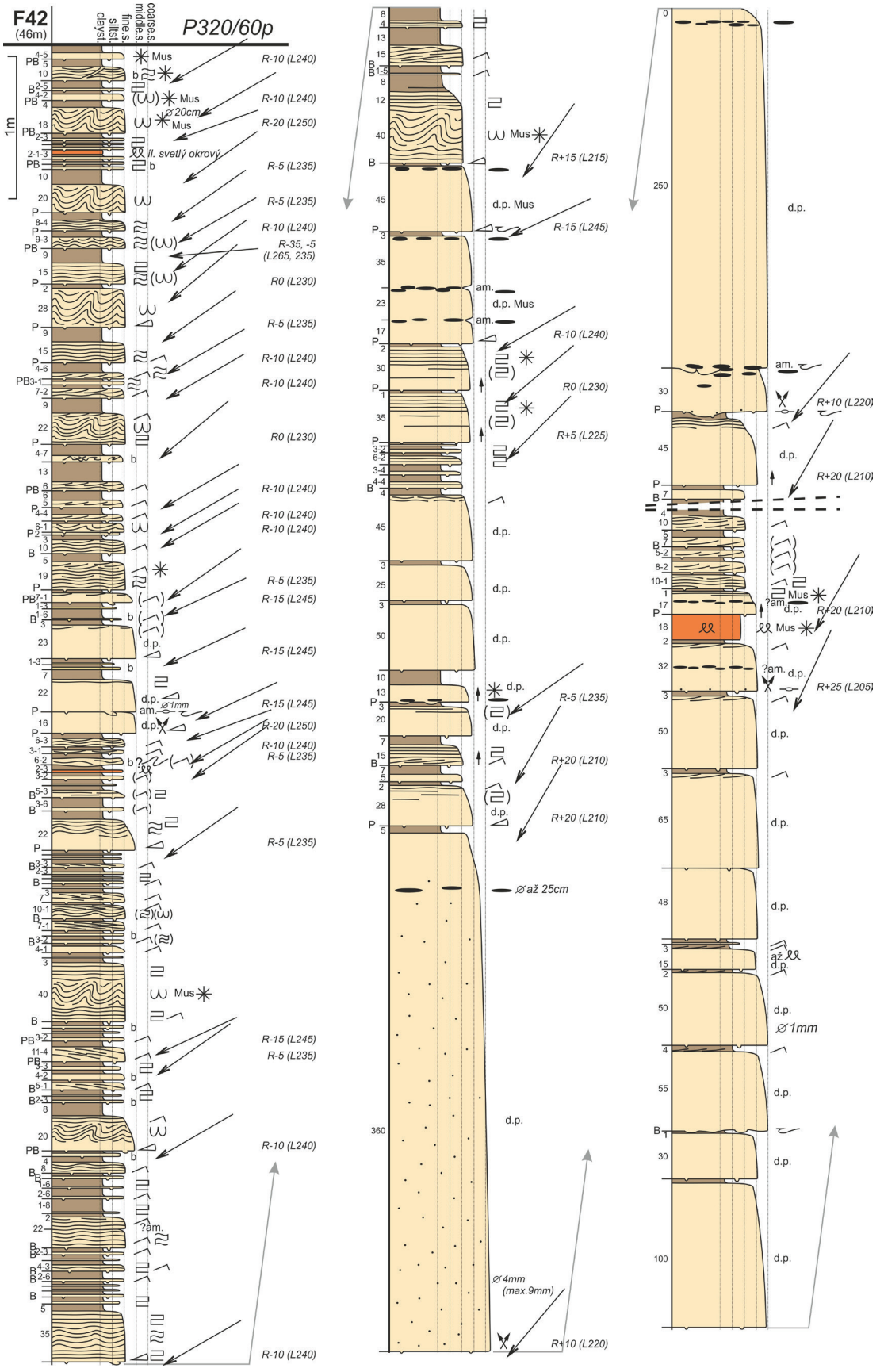
F42
(46m)
P320/60p
clayst.
siltst.
fine s.
middle s.
coarse s.
1m
il. svetlý okrový
Mus
d.p.
am.
?am.
Ø 1mm
Ø 20cm
Ø až 25cm
Ø 4mm
(max.9mm)
R-10 (L240)
R-20 (L250)
R-5 (L235)
R-35, -5
(L265, 235)
R0 (L230)
R-15 (L245)
R+15 (L215)
R-15 (L245)
R+5 (L225)
R+20 (L210)
R+10 (L220)
R+25 (L205)

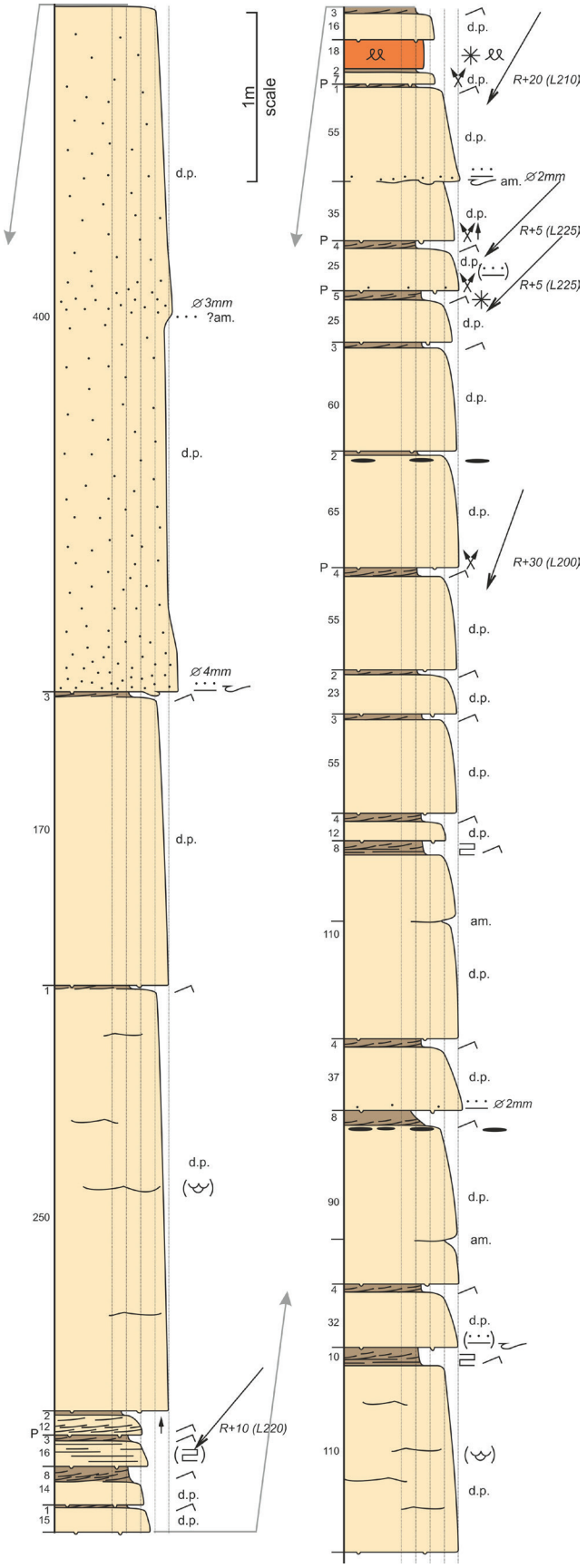

Explanation of the lithological profiles:

- plant detritus
- clay intraclasts
- Mus abundant muscovite
- cross bedding
- wavy lamination
- plane parallel lamination
- convoluted lamination
- water escape structures
- slide with preserved original structure
- slide with unpreserved original structure
- am. amalgamated beds
- ∅6mm grains or intraclasts diameter
- horizon (lens) of coarse grains
- gradation
- larger grains on the basal plane
- b bioturbated bed
- B bioglyphs
- P current marks
- load and flute casts
- flute casts
- groove and prod casts
- ( ) less distinctive feature is in brackets
- d.p. Magura-type greywacke sandstone
- R-15 (L245) current direction – measured *R* (retilted *L*)

Fig. 4. An example of the use of simple measurement and retilting of oriented lineations – vectors (paleocurrents) in profile of the Zábava Fm. (equivalent of the Piwniczna Mb.) of Krynica Unit in the Magura Nappe quarry between Lomná and Zákamenné villages (northern Slovakia). Beds occur here in inverted position with a dip 320° to NW.

The dip direction ***P*** of the bed in the case study (Fig. 3) is 350° (to the N). The angle between the paleocurrent direction and the bed direction is 110°. As it is oriented from the bottom upwards, its value is negative. R = -110°

The measured bed is in inverted position. (The value of the bed dip is not necessary to be known.) Therefore, for the calculation, we use the formula for beds in inverted position:

$$L = P_i - R - 90°$$

$$L = 350° - (-110°) - 90°$$

$$L = 370°$$

As the result is greater than 360°, we deduct 360°

$$L = 370° - 360°$$

$$L = 10°$$

The azimuth of paleocurrent direction after retilting the paleocurrent direction according to horizontal axis in the case study is 10° to the north.

Application of simple processing and tilting of the oriented lineations in paleocurrent analyses

In the 46 m long profile in the quarry at Lomná municipality we performed 46 paleocurrent measurements. Fig. 4, graphically visualizing the paleocurrent direction, provides also ***R*** values together with ***L*** values after their rotation of lineation into horizontal position. The bed direction in the quarry is 320° to NW. Beds are in inverted position. The bed dip 60° is not necessary to use during the retilting of paleocurrent lineations.

The sediments of the Zábava Fm. originated by the deposition of clastic material in the deep-see environment from the gravity flows in two deposition environments. The Magura sandstones facies sedimented in the middle to proximal part of the fan directly from its lobe. The thin-bedded flysch facies sedimented as the interchannel phase in the period, when the lobes of the fan laterally moved to a more distant location, or during the reduced material input (Teťák, 2010; Teťák et al., 2016). This reflects in a slightly different orientation of the paleocurrent directions of individual facies.

Discussion

The paleocurrent measurements in sedimentological analyses have experienced great development since the 1960s (Potter & Pettijohn, 1977). Their significance has increased with the recognition of the origin of paleocurrent traces, the mechanism and environment of gravity flows (e.g. Bouma, 1962; Lowe, 1982; Shanmugam, 2000). Each geologist has used or eventually developed for measuring lineations and their subsequent retilting his own procedure. Part of the geologists retilted the lineations already in the field with the aid of a geological compass. However, in the case of overturned or tilted beds, inaccuracies and errors may occur. The stereographic projection is more accurate but methodically more demanding (Melichar, 1991; Lisle & Leyshon, 2004; Fossen, 2010). For the first group of geologists the presented methodology offers a more accurate and reliable method and for the second group offers a simpler alternative.

Conclusion

The traditional graphical method of retilting lineations along a horizontal axis is methodically relatively demanding. Presented new methodology of lineations retilting allows to process hundreds of measurements with mitigation of errors. An advantage is that the ***P*** value (dip of bed) is regularly measured in outcrops of sedimentary rocks and there is enough to simply additionally measure (or estimate) the ***R*** value (an angle between the retilted lineation and the bed direction). Mathematically the calculation is very simple. It is suitable also for the beds in inverted position. It saves time and minimizes the possibility of mistakes. The methodology of retilting of oriented lineations was verified by a twenty-year use in sedimentary research of the flysch sequences of the Western Carpathians. It would be interesting to apply it also in other areas of geology.

Acknowledgement.

Author is thankful to Ministry of Environment of the Slovak Republic for funding large regional geological projects and contributing by this way to progress in geological knowledge of the Western Carpathians. Author appreciates the recommendations and assistance of F. Marko and Z. Németh, who increased the quality of primary manuscript.

References

Bouma, A. H., 1962: Sedimentology of some flysch deposits. *Amsterdam – New York, Elsevier, 168 p.*

Cieszkowski, M., Zuchiewicz, W. & Schnabel, W., 1998: Sedimentological and tectonic features of the Poprad sandstone Member, Eocene, Magure Nappe: Case study of the Klikuczowa quarry, Outer West Carpathians, Poland. *Bull. Pol. Acad. Sci. (Earth Sci.), 46, 1, 55 – 74.*

Fossen, H., 2010: Structural Geology. *New York, Cambridge University Press, 463 p.*

Lisle, R. & Leyshon, P., 2004: Stereographic projection techniques for geologists and civil engineers. *New York, Cambridge University Press, 112 p.*

Lowe, D. R., 1982: Sediment gravity flows: II. Depositional models with special reference to the deposits of high-density turbidity currents. *J. sed. Petrology, 52, 279 – 297.*

Melichar, R., 1991: Metody strukturní geologie. Orientační analýza. Methods of structural geology. Orientation analysis. *Masaryk University, Fac. Sci., 180 p.* [in Czech].

Potfaj, M., Samuel, M., Raková, J. & Samuel, O., 1991: Geologická stavba Kubínskej hole (Orava). *Západ. Karpaty, Sér. Geol., 15, 25 – 66* [in Slovak, English summary].

Potter, P. E. & Pettijohn, F., 1977: Paleocurrens and Basin Analysis. *Berlin – Heidelberg – New York, Springer-Verlag, 465*.

Shanmugam, G., 2000: 50 years of the turbidite paradigm (1950s – 1990s): deep-water processes and facies models – a critical perspective. *Mar. Petrol. Geol., 17, 285 – 342.*

Teťák, F., 2005: Geologická stavba pohoria Javorníky. Distribúcia klastického materiálu v západnej časti magurského bazénu (Javorníky, Orava). *Dissertation thesis. Manuscript. Bratislava, archive Fac. Natur. Sci. Comen. Univ., 62 p.* [in Slovak].

Teťák, F., 2008: Paleogene depositional systems and paleogeography of the submarine fans in the western part of the Magura Basin (Javorníky Mountains, Slovakia). *Geol. Carpath., 59, 4, 333 – 344*.

Teťák, F., 2010: The gravity flow dynamics of submarine fan sedimentation in the Magura Basin of the Western Carpathians (Magura Nappe, Slovakia). *Geol. Carpath., 61, 3, 201 – 209*.

Teťák, F. (ed.), Kováčik, M., Pešková, I., Nagy, A., Buček, S., Maglay, J., Vlačiky, M., Laurinc, D., Žecová, K., Zlinská, A., Liščák, P., Marcin, D., Žilka, A., Kucharič, Ľ., Gluch, A. & Baláž, P., 2016: Vysvetlivky ku geologickej mape regiónu Biela Orava v mierke 1 : 50 000. *Bratislava, MŽP SR – Št. Geol. Úst. D. Štúra, 217 p.* [in Slovak, English summary].

Jednoduché spracovanie a sklápanie usmernených lineácií a jeho aplikácia pri paleoprúdovej analýze

Potreba zjednodušenia merania a sklápania lineácií vznikla z dôvodu riešenia paleogeografických problémov sedimentárnych sekvencií. Zozbieranie a vyhodnotenie stoviek paleoprúdových meraní je rozhodujúce pri riešení otázok geologického vývoja a stavby.

Na vrstvovej ploche, zlome alebo inej geologickej ploche v teréne bežne pozorujeme lineácie. Ak je plocha sklonená alebo prevrátená, je potrebné na účely paleoprúdovej analýzy sklápať lineácie do horizontálnej roviny, čo je pomerne náročná procedúra. Spracovanie väčšieho množstva údajov je preto časovo náročné. Manuálne spracovanie a rotácia na projekčných sieťach sa už dnes využíva len zriedka. Mnohé dostupné štruktúrnogeologické softvéry poskytujú modul rotácie štruktúrnych prvkov. Spracovanie údajov si však vyžaduje od používateľa dobré porozumenie problematike geometrie zobrazovania 3D údajov na projekčnej sieti, čo môže viesť k omylom. Metodicky náročnú grafickú metódu založenú na premietaní lineácie do projekčnej stereografickej hemisféry (Melichar, 1991; Lisle a Leyshon, 2004; Fossen, 2010) môžeme nahradiť jednoduchou výpočtovou metódou. Nová metodika prináša zjednodušenie spracovania a sklápania lineácií späť do horizontálnej roviny. Význam metodiky je najmä pri väčšom počte meraní (napr. Teťák, 2008).

Terénne zameranie lineácií je podobné ako pri zaužívanom spôsobe pri grafickom spracovaní v projekčnej sieti. Pri pohľade na plochu s lineáciou je potrebné zmerať dve hodnoty: *P* a *R* merané v stupňoch (°) (obr. 2, 3). Prvou je smer sklonu plochy ***P***. Pri geologickej dokumentácii sa meria bežne. Druhou hodnotou, ktorú potrebujeme zmerať (prípadne odhadnúť), je hodnota ***R***. Je to uhol, ktorý zviera lineácia so smerom vrstvy v rozpätí od 0 do 180°. Hodnotu *R* odčítavame vždy zľava doprava. Pri usmernených lineáciách – vektoroch prebiehajúcich zhora nadol – má *R* kladnú hodnotu, zatiaľ čo pri smere zdola nahor je hodnota *R* záporná. Hodnota *R* je zľava 0° a postupne doprava až do 180°. Paleoprúdové smery sa zvyknú zobrazovať v ružicových diagramoch po 5 alebo 10°, preto odporúčame aj hodnoty *P* a *R* merať po 5°.

Výsledný smer línie po sklopení ***L***vypočítame podľa vzorca:

$$\mathbf{L = P_n - R + 90°.}$$

(*Vysvetlivky skratiek:* ***P*** *– smer sklonu plochy,* $\boldsymbol{P_n}$ *– smer sklonu vrstvy v normálnej pozícii,* $\boldsymbol{P_i}$ *– smer sklonu vrstvy v prevrátenej pozícii,* ***R*** *– uhol sklápanej línie k smeru vrstvy,* ***L*** *– výsledný smer línie po sklopení.*)

Uvedený vzťah platí pri normálnej pozícii vrstvy (P_n), napríklad v prípade sedimentárnych vrstiev, kde rozlišujeme normálnu a inverznú pozíciu vrstiev.

Pri inverznej (prevrátenej) pozícii vrstvy (P_i) platí mierne upravený vzťah:

$$\mathbf{L = P_i - R - 90°.}$$

Výsledná hodnota ***L*** je v stupňoch a udáva, kam usmernená lineácia – vektor – smeruje (napr. kam smeroval paleoprúd). V prípade, ak dostaneme hodnotu *L* zápornú, je potrebné pripočítať 360° (L + 360°). V prípade, ak je

hodnota *L* vyššia ako 360, je potrebné od nej odpočítať 360° (L – 360°) tak, aby bola hodnota *L* v rozmedzí 0 až 360°.

Na uvedený výpočet nie je potrebné ovládať metodicky náročné stereografické techniky alebo používať špeciálny softvér. Pri väčšom počte meraní sa osvedčilo použitie bežne dostupného tabuľkového programu Microsoft Excel. Metodika je aplikovateľná najmä v sedimentológii pri paleoprúdovej analýze, ale aj v štruktúrnej geológii a inde.

Ako príklad využitia metodiky ponúkame praktickú ukážku jednoduchého merania a sklápania usmernených lineácií (paleoprúdov) na profile zábavského súvrstvia krynickej jednotky magurského príkrovu v lome medzi obcami Lomná a Zákamenné (región Orava) (obr. 1, 3, 4). Magurský sedimentačný bazén sa od albu po starší miocén zapĺňal prevažne flyšovými hlbokomorskými sekvenciami. Formovali sa v závislosti od pozície a tvaru depozičných vejárov v bazéne, tektonickej aktivity dna bazénu a zdrojových oblastí prínosu sedimentárneho materiálu, ako aj zmien výšky morskej hladiny (Teťák, 2010). Krynická jednotka je najjužnejšia tektonicko-litofaciálna jednotka magurského príkrovu. Pre zábavské súvrstvie je typické striedanie 10 až 200 m hrubých horizontov drobových pieskovcov magurského typu a tenko vrstvenej flyšovej litofácie. Hrúbka súvrstvia je do 3 000 m. Vek zábavského súvrstvia (ekv. *Piwniczna Mb.* – Cieszkowski et al., 1998) je mladší paleocén až stredný eocén (Potfaj et al., 1991; Teťák, 2010; Teťák et al., 2016).

Paleoprúdové merania v sedimentologických analýzach zaznamenali veľký rozvoj od 60. rokov 20. storočia (Potter a Pettijohn, 1977). Ich význam vzrastal s poznávaním pôvodu paleoprúdových stôp, mechanizmu a prostredia vzniku gravitačných prúdov (napr. Bouma, 1962; Lowe, 1982; Shanmugam, 2000). Každý geológ mal na meranie lineácií a následné sklápanie do horizontálnej roviny zaužívaný postup, prípadne si vyvinul vlastný. Časť geológov sklápa lineácie už v teréne pomocou geologického kompasu. Pri prevrátených alebo strmšie sklonených vrstvách však môžu vznikať nepresnosti a chyby. Stereografická projekcia je presnejšia, ale metodicky náročná (Melichar, 1991; Lisle a Leyshon, 2004; Fossen, 2010). Prezentovaná metodika ponúka prvej skupine geológov presnejšiu a spoľahlivejšiu metódu a druhej skupine ponúka jednoduchšiu alternatívu. Výhodou je, že hodnota *P* (smer sklonu vrstvy) sa pri odkryvoch sedimentárnych hornín meria automaticky a k nej stačí jednoduchým spôsobom zmerať uhol sklápanej línie k smeru vrstvy (*R*). Výpočet je matematicky veľmi jednoduchý. Je vhodný aj pri vrstvách v inverznej pozícii, šetrí čas a minimalizuje možnosť omylu.

Doručené / Received: 9. 2. 2018
Prijaté na publikovanie / Accepted: 5. 6. 2018

Mineralia Slovaca, Web ISSN 1338-3523, ISSN 0369-2086
50 (2018), 55 – 99, © Authors 2018. CC BY 4.0

Variscan epidote-eclogite, blueschists and pumpellyite-actinolite facies Cpx/Sr-rich epidote-metagabbro blocks exhumed in Carboniferous, with Permian amphibolite facies overprint (Gemeric unit, Western Carpathians)

MARTIN RADVANEC and ZOLTÁN NÉMETH

State Geological Institute of Dionýz Štúr, Mlynská dolina 1, SK-817 04 Bratistava 11, Slovakia;
martin.radvanec@geology.sk

Abstract: The diopside, jadeite, aegirine-augite and Sr-rich epidote bearing metagabbro, exhumed in individual tectonic blocks in the Carboniferous subduction zone, was in the Western Carpathians revealed along the northern rim of Gemeric unit in localities of Dobšinský potok, Ostrá, Babiná, Šajby, as well as in the southern part of the Gemeric unit in the Zadné Porče locality.

The primary gabbro age was dated only in the Zadné Porče locality (ca. 461 Ma). This age was recorded by the zircon, which originated by the replacement of baddeleyite during the magmatic stage, where the "hot magma" was transported by the mantle plume up to the cooler upper mantle. This magmatic process pre-dated the Paleo-Tethyan oceanic riftogenesis in the Paleo-Gemeric zone of the future Western Carpathians in the Devonian.

The primary gabbro was cryptocrystalline (diopside and bytownite were not completely crystallized in the upper mantle) and was in Carboniferous (Mississippian; 348 Ma) transported by the mantle flow to the slab of subducted lower crust. It is a reason why the REE and trace elements normalized patterns characterize the gabbro formation in the lower crust. Here in the depth of ca 70 km at ca 1100 °C the gabbro obtained a solidus coarse-grained texture, being characteristic with its unique mineral composition of Ca/Na/Sr-rich feldspar (decomposed to Sr-rich epidote; SrO content reaches up to 14 wt.%), diopside, bytownite, K feldspar, anortoclase, anthophyllite, kearsutite, Mg chromite-chromite and decomposed pseudobrookite/armalcolite.

The Zircon regeneration at ca. 307 Ma records the exhumation in subduction channel, where the gabbro blocks underwent hydratation and metamorphism in several successive steps, passing from the epidote-eclogite facies through the blueschist and finaly the pumpellyite-actinolite facies. Here the exhumation of individual blocks has stopped. This high pressure metamorphic and exhumation evolution, revealed in all investigated localities, is designated as **M1a**. In the Ostrá locality, besides the ductile deformation and the origin of mylonites, the exhumation of the metagabbro was accompanied also with the origin of tectonic breccia, consisting of metagabbro fragments within the fine-grained matrix of the same mineral composition. In localities of Šajby and Dobšinský potok, the exhumed metagabbro manifests ductile mylonitic / ultramylonitic fabric.

In Permian – 261 Ma, the partially exhumed **M1a** metagabbro blocks were re-metamorphosed from the pumpellyite-actinolite facies to the amphibolite (Babiná, Ostrá), or epidote-amphibolite facies (Dobšinský potok, Ostrá-breccia, Šajby, Zadné Porče), and subsequent retrograde greenschist facies. This Permian metamorphism, being a product of the overheating above a hot line, accompanied also with the origin of S-type anatectic granites from different protoliths, is designated as **M1b**. In localities Dobšinský potok, Šajby and Zadné Porče, the Permian **M1b** metamorphism strongly overprints older Carboniferous metamorphic-microstructural evolution of **M1a**, from which only remnant mineral assemblage was preserved. The evidence of polymetamorphism during the exhumation of the metagabbro, having Ordovician magmatic protolith, have contributed to better understanding of the Variscan evolution of the Western Carpathians. The recent positioning of the metagabbro tectonic blocks on the surface was finalized by the Alpine orogenic processes.

Key words: Cpx/Sr-epidote metagabbro, subduction, lower crust, P-T-t path, Gemeric unit, Western Carpathians

Graphical abstract

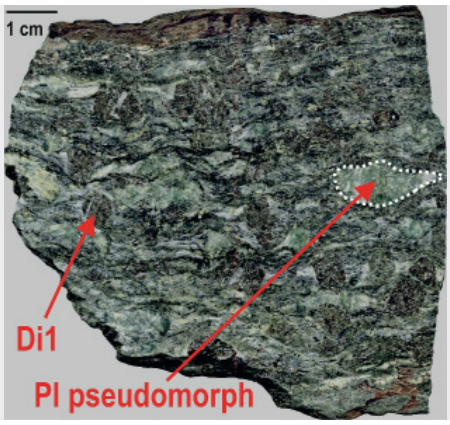

Highlights

- The cryptocrystallic Ordovician gabbro (485–458 Ma; zircon ages) was transported by the mantle flow to upper mantle and then through the slab of subducted lower crust in Carboniferous (348 Ma). Here the solidificated gabbro obtained coarse-grained texture and unique mineral composition of Ca/Na/Sr-rich feldspar (decomposed to Sr-rich epidote; SrO up to 14 wt.%), diopside, bytownite, K feldspar, anortoclase, anthophyllite, kearsutite, Mg chromite, baddeleyite and decomposed pseudobrookite/armalcolite. The whole-rock trace elemets spider shows the lower crust origin of the gabbro.
- Variscan Cpx/SrEp metagabbro exhumation (307 Ma, M1a HP mineral assemblages; VD1a def. stage) from the epidote-eclogite, blueschist, pumpellyite-actinolite facies towards the surface by the reversal (roll-back) transport in the Carboniferous subduction zone was followed by Permian (M1b; VD1b, VD2) overprint in amphibolite or epidote-amphibolite facies (261 Ma).

Introduction

The Gemeric tectonic unit represents an Alpine basement nappe of the Western Carpathians, being north-vergently thrust over the Veporic unit during the Paleo-Alpine collision (Plašienka et al., 1997; Grecula et al., 2009). Concerning the Variscan evolution, according to Grecula (1982), altogether seven nappes have originated in the Paleo-Gemeric complex (Fig. 1a). The Variscan tectonic and metamorphic events in the Paleo-Gemeric complex were recorded by its Paleozoic sedimentary and magmatic complexes, as well as several genetic types of mineralization. The recent tectonic setting of the Gemeric unit is affected also by the subhorizontal displacements along the Alpine shear zones (Grecula et al., 2009).

Extended field works, related to exploration and survey of mineral deposits, have confirmed the lithostratigraphic division of the Early Paleozoic rocks (sensu Grecula, 1982). This represented a starting point for defining the sequence of sedimentary, magmatic and tectonic events, as well as related general interpretation of paleotectonic evolution of the recent Gemeric unit (Grecula, 1982; Grecula et al., 1995).

The geotectonic model of continual Ordovician-Jurassic evolution, produced by Grecula & Radvanec (2005), as well as Radvanec & Grecula (2016), took into account also previous works by Grecula (1982), Radvanec (1998), Grecula et al. (1995), Kobulský et al. (2001), as well as Németh (2002).

The Paleozoic evolution of the pre-rift stage was bound to an active (Gondwana) continental margin in Cambrian to Ordovician times (Putiš et al., 2009; Radvanec & Grecula, 2016). The first phases of evolution represent the megacycles of the Ordovician and mainly Silurian ages, forming the anoxic (organic matter-rich) sedimentary basin fill with lydite and bimodal (basalt and keratophyre) volcanism of inferred Devonian age (Grecula, 1982; Grecula et al., 1995; Radvanec & Grecula, 2016). This Early Paleozoic evolution of Gemeric complex is connected with opening of a riftogeneous basin and related formation of the complete ophiolite suite (basalt, Cpx-bearing gabbro and peridotite), including formation of the plagiogranite in Devonian (Grecula, 1982; Grecula et al., 1995; Radvanec et al., 2017). The effusive basalts and keratophyres were accompanied with stratiform and disseminated Fe>>Cu>Pb>Zn+Ba±Mo-Sn, resp. Fe>Cu-Pb-Zn-Ag-As sulphide mineralization (Grecula et al., 1995). In the ophiolite suite the massive effusions, extrusions and formation of plagiogranite have provided Devonian ages of ca 410–380 and 374 Ma respectively. However in the rift the last evidence for the formation of **Variscan** Cpx gabbro is of Early Carboniferous age of ca 342 Ma (Putiš et al., 2009; Radvanec et al., 2017). The rifting in the mid-oceanic ridge with the ocean-floor metamorphism **M0** of low pressure amphibolite facies has contributed to the origin of oceanic-type crust (Radvanec et al., 2017).

The Early Paleozoic complexes, including **M0** metaophiolite suite, were deformed and tectonically segmented during the Variscan orogeny in the Late Carboniferous. A part of metaophiolite blocks was obducted on Lower Paleozoic sequences (Grecula et al., 2009, Radvanec & Grecula, 2016). The compression related metamorphism

Fig. 1. **a** – The positions of studied Cpx/Sr-rich epidote bearing metagabbro blocks (red circles), exhumed from the lower crust, in the Ostrá, Babiná, Šajby, Dobšinský potok and Zadné Porče localities of the Gemeric unit. The common sign of these gabbro blocks is the Sr-bearing epidote, though their ductile deformation and multiple metamorphic recrystallization tends to obscure their gabbro petrographic affiliation (mylonites, compacted tectonic breccia). The course of Variscan nappes is according to Grecula et al. (2009). Distribution of violet areas represents the rock chemical composition of 21 elements that are normalized to the lower crust composition. The violet areas in part **a** were distinguished by the linear data correlation with lower crust composition on the base of 75 % accordance. These distributions areas of the lower crust are related to the metamorphic facies. **b –** position of Gemeric unit within the Western Carpathians and a detail map (**d**) of western part of Rakovec zone within the Gemeric unit with the Cpx/SrEp metagabbro occurrences (item **1** in **d**), **c –** Projection of Variscan planar and linear mezoscopic structures into the lower hemisphere of the tectonograms (Schmidt projection). **d** – Detail map with the occurrences of studied Cpx/SrEp metagabbro occurrences in the zone Ostrá - Babiná - Šajby. Geological map by Grecula et al. (2009) slightly modified by Németh (in Németh & Radvanec, 2013) and supplemented by new structural data: **Early Paleozoic of the Gemeric unit** (Ordovician to Devonian) **- Hnilec Formation: 1 – Cpx/SrEp metagabbro**; 2 – coarse-grained basalt (dolerite); 3 – basalt locally with thin intercalations of ultrabasic rocks, basalt metapyroclastics, green and violet phyllites, 4 – basalt metapyroclastics, locally with intercalations of green and violet phyllites, greenish and pinkish silicites and carbonates, 5 – basalt metapyroclastics, locally with fine-grained amphibolites, intercalations of keratophyre metapyroclastics and phyllites. **Smolník Formation:** 6 – dark-green, green and yellow-green chl.-ser. phyllites with intercalations of violet hematite phyllites and basic, locally keratophyre metapyroclastics, 7 – crystalline to porphyroblastic violet-green chl.-ser. phyllites, 8 – crystalline to eyed green chl.-ms. phyllites, locally violet with intercalations of silicites, basalt and keratophyre rocks locally in amphibolite facies, 9 – metamorphosed variegated volcanic complex. **Betliar Formation:** 10 – black and grey gr.-ser. phyllites (alternation of light and dark lamina and bodies) with intercalations of metapsammites, 11 – alternation of coarse-laminated recrystallized to eyed grey to black gr.-bt. metapelites and metapsammites. **e** – The metagabbro mylonite in locality Šajby manifests a pervasive Variscan ductile mylonitic foliation. As manifested also by tectonograms (**c**), the combination of WSW-ENE a ESE-WNW trending lineations and secondary foliation planes generally dipping to NWN-N, locally also to NNE, indicates the transpression kinematics in this phase of exhumation. The outcrop is penetrated by insignificant Alpine cleavage trending to NNW. **f-g** – hand-samples of metagabbro mylonite, showing recrystallization fabric from the magmatic phase due to overprints by succession of tectonometamorphic events **M1a** and **M1b**.

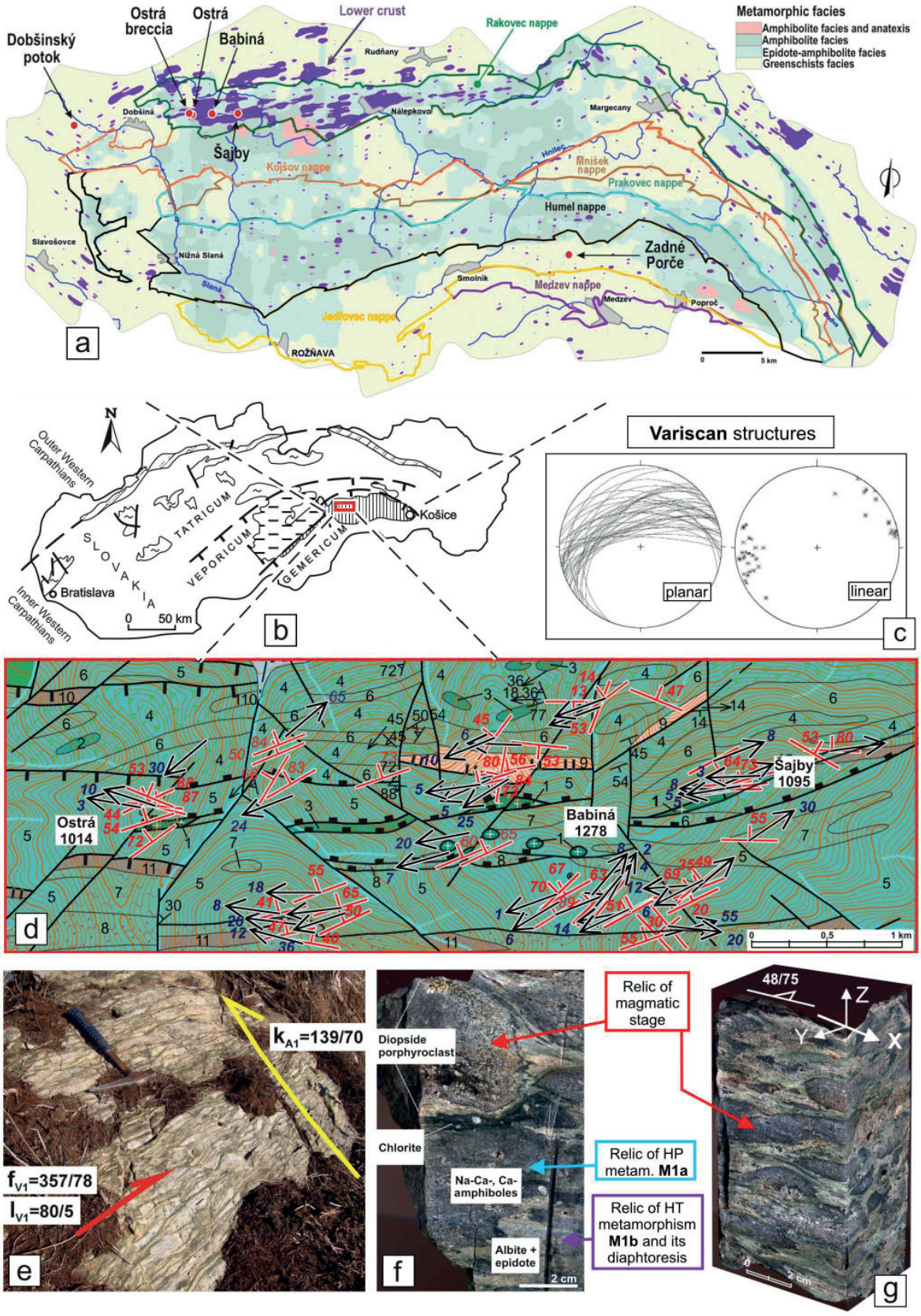
Metamorphic facies
Amphibolite facies and anatexis
Amphibolite facies
Epidote-amphibolite facies
Greenschists facies
Dobšinský potok
Ostrá breccia
Ostrá
Babiná
Lower crust
Rakovec nappe
Rudňany
Dobšiná
Nálepkovo
Margecany
Šajby
Kojšov nappe
Hnilec
Mníšek nappe
Prakovec nappe
Humel nappe
Slavošovce
Nižná Slaná
Slaná
Zadné Porče
Smolník
Meďzev nappe
Meďzev
Poproč
Jedľovec nappe
ROŽŇAVA
a
Outer Western Carpathians
Inner Western Carpathians
SLOVAKIA
TATRICUM
VEPORICUM
GEMERICUM
Košice
Bratislava
50 km
b
Variscan structures
planar
linear
c
Ostrá 1014
Babiná 1278
Šajby 1095
d
k_{A1}=139/70
f_{V1}=357/78
l_{V1}=80/5
e
Diopside porphyroclast
Chlorite
Na-Ca-, Ca-amphiboles
Albite + epidote
2 cm
f
Relic of magmatic stage
Relic of HP metam. M1a
Relic of HT metamorphism M1b and its diaphtoresis
48/75
Z
Y
X
2 cm
g

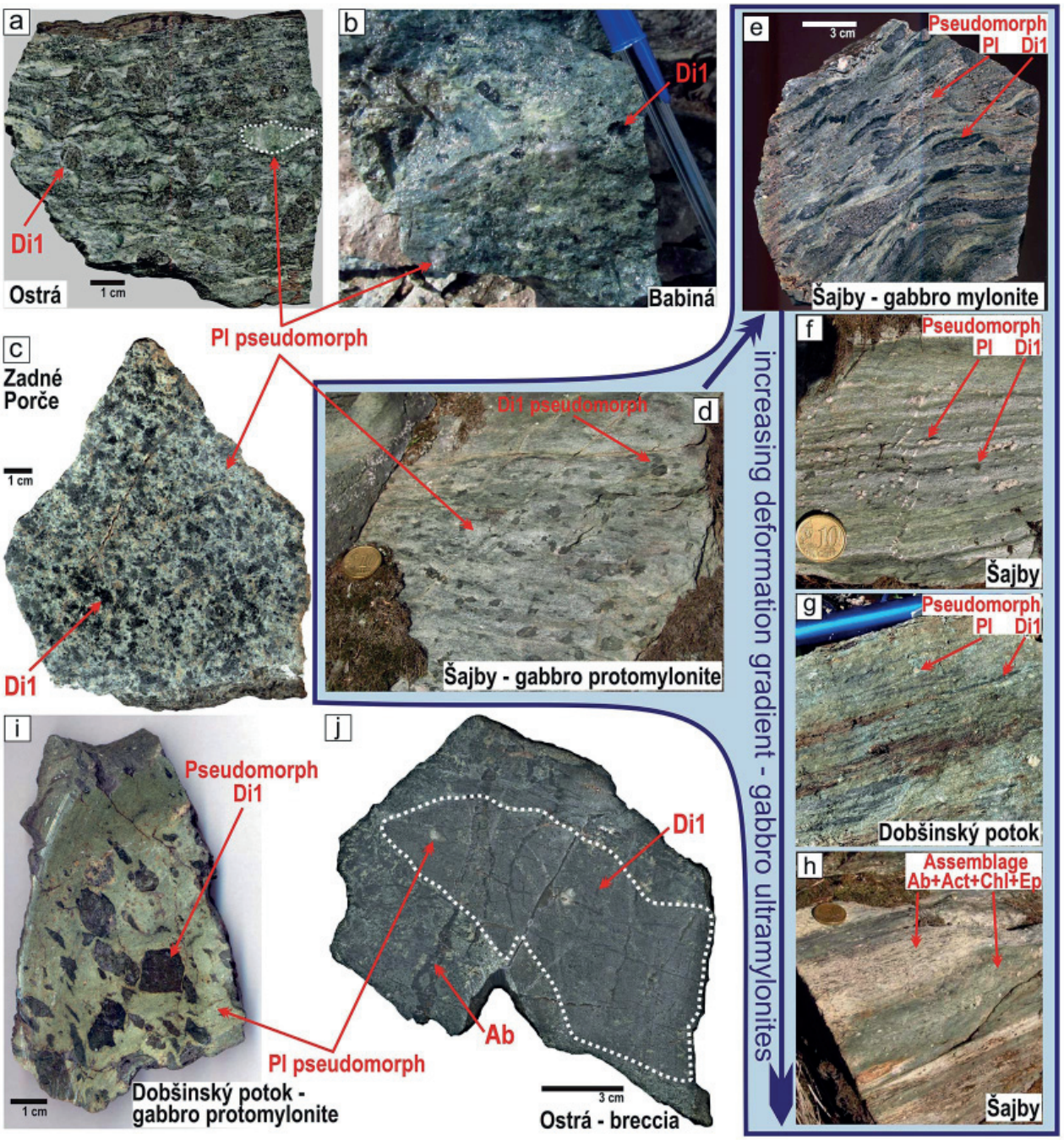

Fig. 2. Hand-samples of studied Cpx/SrEp metagabbros occurring in localities Ostrá, Babiná, Šajby, Dobšinský potok and Zadné Porče. The space of magmatic diopside-1 (Di1) reaches up to 1 cm. **a-c –** the coarse-grained texture of metagabbro. The central figure and column located right shows the microstructural development from the protomylonite (Šajby **– c**, Dobšinský potok – **h**) through the mylonite (Šajby **- d**) to ultramylonite (Dobšinský potok **- f**, Šajby **– e, g**). In the locality of Ostrá also the tectonic breccia (**i**) of the final stage of **M1a** was revealed, being subsequently compacted by increased temperature in **M1b** of epidote-actinolite facies. Pl-pseudomorph – space of former magmatic feldspar/plagioclase contains mixture of albite, Sr-rich epidote group, clinozoisite and epidote. The space of Pl-pseudomorph has the same size like Di1. Di1-pseudomorph – mixture of amphiboles, albite, calcite and chlorite. Ab – albite fills cracks in tectonic breccia in the Ostrá locality.

Mla has occurred in the pumpellyite-actinolite facies. However the rest of the Paleozoic complexes underwent an obduction directly. This Late Carboniferous orogenic process transported most of the Early Paleozoic basin-fill rock sequences over the northern continental plate and formed seven Variscan nappes in the Gemeric complex (Fig. 1; Grecula, 1982; Grecula et al., 2009 and 2011). The compression related to the onset of subduction slab and exhumation caused the Late Carboniferous metamorphism **M1a** in the pumpellyite-actinolite facies. It was accompanied by further Gondwana and Armorica plate convergence and by the formation of mélange-related conglomerates (Radvanec & Grecula, 2016).

In Permian, the culminated melting in the subducted slab produced the calc-alkaline volcanism of andesite and rhyolite, located along the northern boundary zone of Gemeric with Veporic units. Permian high thermal gradient along the hot line initiated the new regional metamorphism **Mlb** in amphibolite or epitote-amphibolite facies (Radvanec et al., 2017) and produced anatectic melt and related formation and emplacement of S-type granite during the late Variscan evolution (Radvanec et al., 2009; Radvanec & Grecula, 2016). This increased thermal gradient metamorphosed again the Early Paleozoic complexes, including the tectonic blocks of metaophiolite suite, which were previously metamorphosed in **M0** and **M1a** overprints (Radvanec et al., 2017). The **Mlb** metamorphic facies are coinciding with the origin of the Sn-W-Mo-B-Li-F-As±Bi-Sb mineralization and Fe-Mn-Mg carbonate and sulphide veins and stratabound (metasomatic) mineralization, located in the exocontact of S-type granite (Radvanec et al., 2004). The deciphering of the metamorphic events **M0**, **M1a** and **M1b** and compressional and extensional Variscan tectonic processes completes arguments for the existence of Variscan nappe and overthrust setting of the Gemeric unit (Fig. 1a; Grecula, 1982; Grecula et al., 2009 and 2011; Németh, 2002).

In addition to the tectonic blocks of metaophiolite suite, the pre-rift stage was bound to the Gondwana continental margin in Cambrian/Ordovician times in the future Gemeric zone (Radvanec & Grecula, 2016). The Ordovician evolution was dated by the zircon ages in the range of 482–458 Ma, obtained from tectonic blocks of volcanic rocks of rhyolite and dacite composition, as well as clinopyroxene/Sr-rich epidote (Cpx/SrEp) metagabbro (Putiš et al., 2009; Grecula et al., 2009 and 2011). These tectonic blocks of rhyolite, and Cpx/SrEp metagabbro from the pre-rift stage were tectonically mixed with blocks of metaophiolite suite and other metasediments in the Variscan nappe and imbricated setting of the present Gemeric unit (Grecula et al., 2009 and 2011). Especially the Cpx/SrEp metagabbro, being formed in the Ordovician, has polymetamorphic evolution comparable to that of the metaophiolite suite (Hovorka et al., 1988; Faryad & Bernhardt, 1996; Ivan in Grecula et al., 1997; Radvanec, 1999).

This study is based on mineralogical, petrological, geochemical, structural, microtectonic and geochronological data, allowing to explain and compare the evolution, exhumation and geological setting of individual Cpx/SrEp metagabbro blocks with a polymetamorphic evolution of Variscan orogenesis in Gemeric unit (Radvanec et al., 2017). The Cpx/SrEp metagabbro differs from the metagabbro of the gneiss-amphibolite complex (metaophiolite suite) by its genesis and composition. The Cpx/SrEp metagabbro blocks were found in the Rakovec nappe and studied in the Ostrá, Babiná and Šajby localities, as well as in the south located Jedľovec nappe in localities of Lastovičí vrch and Zadné Porče. In metasediments of Upper Carboniferous (Dobšiná Group) the Dobšinský potok locality is located. (Fig. 1a). The tectonic bodies of Cpx/SrEp metagabbro contain the identical magmatic diopside (large up to 2.5 cm) and identical successive polymetamorphic evolution with the formation of minerals like Sr-rich epidote, Na-rich clinopyroxene, including jadeite, albite, pumpellyite, as well as other corresponding minerals. The Cpx/SrEp metagabbro has the lower crust geochemical characteristics in all mentioned localities (Fig. 4, cf. with Fig. 5). There must be emphasized that the same Cpx/SrEp metagabbro is present in the northern and southern zones of Lower Paleozoic sequences of Gemeric unit, i.e. in the Rakovec and Gelnica groups according to the former division of Gemeric unit sensu Bajaník et al. (1984). Previous research of corresponding rocks was done or treated by Bajaník (1975, 1976); Faryad & Bernhard (1996); Hovorka et al. (1988); Ivan (1996, 1997); Radvanec (1999); Ivan & Hovorka (2000) and Putiš et al. (2009).

Methodology

We have taken following samples of Cpx/SrEp metagabro, applying the Slovak names of individual localities: **Babiná** (hill; GPS **48° 49` 53.2``N; 20° 27` 27.7``E**), **Ostrá** (hill; GPS **48° 49` 57.1`` N; 20° 25` 29.9`` E**), **Ostrá** (breccia; GPS **48° 50` 0.7``N, 20° 25` 33.7``E**), Šajby (mountain range; GPS **48° 50` 7.6``N; 20° 28` 41.5``E**), **Dobšinský potok** (slopes of the forest road above brook; GPS **48° 48` 43.3``N; 20° 18` 8.8``E**) and **Zadné Porče** (GPS **48° 43` 48.6``N; 20° 49` 36.2``E**). The research consisted of the mineralogical-petrological and microtectonic methods, aiming to reveal the sequence of individual mineral assemblages in the Cpx/SrEp metagabbro in relation to the sequence of tectonometamorphic events in the Gemeric unit. The separated zircons of the Ostrá and Zadné Porče samples were dated by the SHRIMP U-Pb method in laboratories in St. Petersburg (Russia) and in Beijing (China; Putiš, personal communication). The Cpx/SrEp metagabbro samples were studied petrographically and polished thin sections underwent the EMPA analyses in the State Geological Institute of Dionýz Štúr (SGIDŠ) in Bratislava by the EDS and WDS quantitative chemical

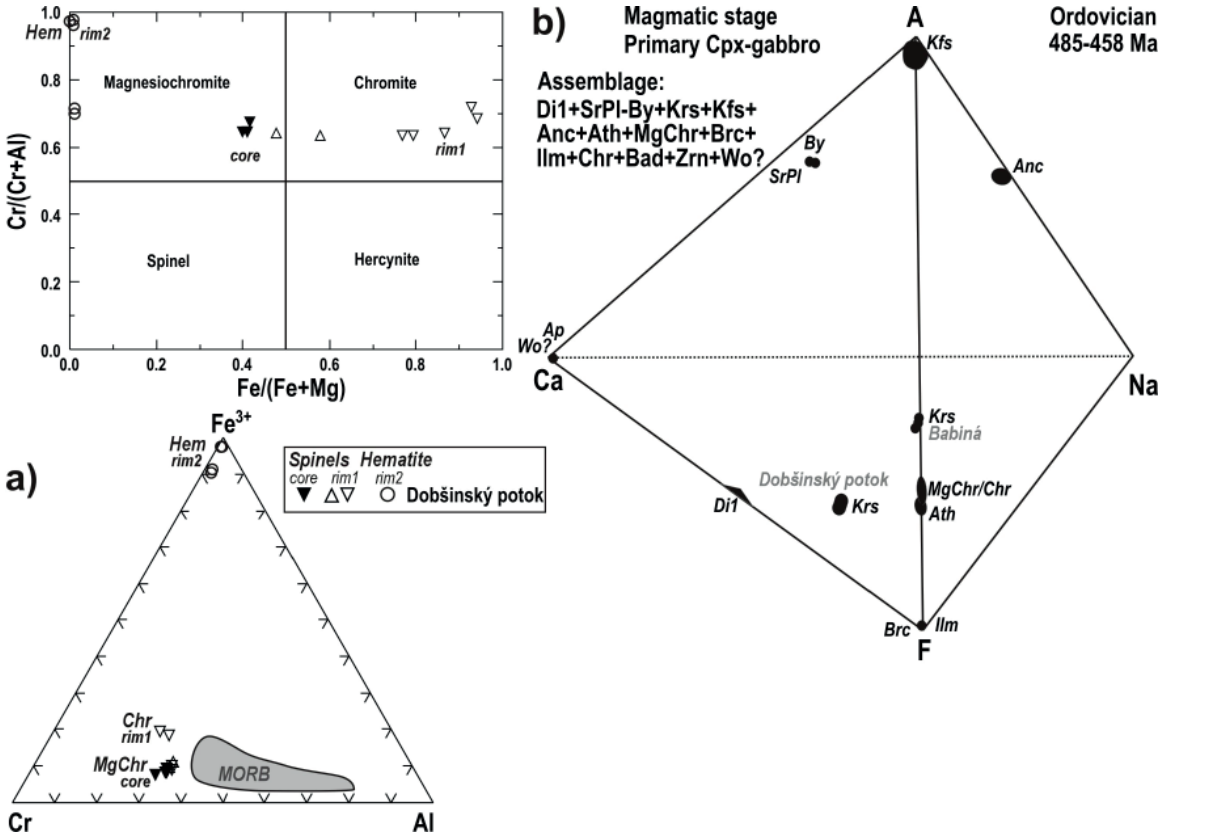

Fig. 3. **a –** Chemical classification of zoned spinels and relationship between the core and inner rim 1 in diagrams. All spinel grains are partly replaced by hematite to form new outer rim 2. **b –** CaFNaA diagrams showing the plotting positions of the minerals of primary gabbro. The minerals of former gabbro were revealed in all studied localities. Assumed mineral in solidus is wollastonite Wo. Di1 – diopside 1; SrPl – Sr-rich feldspar; By – bytownite; Kfs – K feldspar; Anc – anorthoclase; Ant – antophylite; Krs – kearsutite; Brc – pseudobrookite/armalcolite; Ilm – ilmenite; Ap – apatite; Bad - baddeleyite; MgChr – Mg-rich chromite, Chr – chromite; Hem – hematite; Zrn – zircon.

analyses, applying the natural standards. Analyses were evaluated by the Kevex program with ZAF correction. Mineral assemblages and individual minerals were studied in the back-scattered electrons. Chemical zonality of minerals was studied also by mapping the element contents (Na, Ca, Al and Fe) in Kα.

The whole-rock analyses were done in accredited Geoanalytical Laboratories of the SGIDŠ, Spišská Nová Ves, Slovakia, applying the ICPMS, ARS-ICP and RFS methods (Table 1).

The mineral analyses were recalculated for chemical formulas. Analyses of amphiboles were recalculated on chemical formulas by the procedure 15NK, 13CNK, 15-K, Fe^{2+}, AV(2, 4) according to Leake (1997). Pyroxene analyses were recalculated with the distribution of the analytical error for all cations (Morimoto, 1988). Representative mineral analyses are in Tables 2–4 recalculated by the procedure of Hawthorn et al. (2012), Rieder et al. (1998) and Grew et al. (2013). The P-T conditions of the metagabbro multiple metamorphic overprint were derived from metamorphic reactions calculated from the data on mineral activities in a given crystallization system by Berman (1987) and Spear (1995).

Tectonic and microtectonic research in studied localities consisted of measuring of azimuth and dip of planar and linear structures in the outcrop scale and taking oriented samples. From each representative oriented sample there were prepared two thin sections, representing the cuts in XZ and YZ planes. In the some cases, where lineations were not very clear, deciphering the kinematics (sense of shearing) in both perpendicular thin sections allowed the reconstruction of the real spatial parameters of the sense of shearing (exhumation). In accord with our previous researches and papers (e.g. Radvanec et al., 2007), the deformation stages were designated correspondingly with metamorphic stages – **VD1a** acting during the late Carboniferous metamorphism **M1a** and **VD1b** – deformation during Permian **M1b** metamorphic stage.

Petrography

As described above, the studied clinopyroxene and Sr-rich epidote metagabbros (in the next text shortened

to metagabbro/s) occur in localities Ostrá, Babiná, Šajby, Dobšinský potok and Zadné Porče. The metagabbro has hypidiomorphic coarse granular texture with a grain-size of about 1–3 cm and bluish-green colour. Metagabbro contains brown-green idiomorphic to hypidiomorphic diopside 1 in amount of 20–40 vol.% of the rock and the same volume is represented also by pseudomorphoses after former magmatic feldspar/plagioclase, having the porphyroblast shape (Fig. 2). Grains of primary magmatic diopside 1 are usually large up to 1 cm, but sometimes reach up to 3 cm. In localities Ostrá, Babiná and Zadné Porče the diopside 1 grains are fragmented and individual parts are rotated in amphibole-epidote-chlorite matrix with albite and titanite. The cracks in diopside 1 are filled with chlorite, biotite, actinolite, albite, grossular-andradite, pumpellyite, glaucophane-winchite and pargasite. Around the diopside 1 the disintegration textures are macroscopically visible, as well as the light rims and fine-grained rock matrix. The amphiboles, prevailingly pargasite, actinolite, as well as biotite, titanite and chlorite crystallized along the margins of diopside 1, forming asymmetric structures including the mylonite tails. Their study in oriented thin-sections allowed to determine the kinematics during the gabbro tectonometamorphic evolution.

The gabbro has primarily crystallized into a solidus state as a holocrystallic rock with generally equal dimensions of the main rock-forming euhedral crystals – diopside 1 and feldspar/plagioclase (Fig. 2a). The primary shape preferred orientation of these main minerals can be attributed to magmatic flow closely before the rock solidification. Fig. 2a shows the rock closest to this state, though we interpret that the gabbro protomylonite in this figure shows also the effect of deformation at the onset of gabbro exhumation. The next "solid state" rock deformation (cf. Passchier & Trouw, 2005) - mylonitization during the exhumation at the metagabbro further metamorphic evolution led to recrystallization of primary gabbro minerals depending on their rheological behaviour at differerent P-T conditions in successive metamorphic events (epidote-eclogite facies up to pumpellyite-actinolite facies). As known from the research of other authors (cf. Tsuchiyama, 1985a, b; Lang & Gilotti, 2001; Kanagawa et al, 2008; Raphanel et al., 2010; Zhou & He, 2015), the diopside 1 represented at these conditions rheologically harder phase than other present minerals, leading in the case of diopside 1 to origin of its shape preferred orientation (e.g. Fig. 2e). Rheologically softer feldspar/plagioclase in these metamorphic conditions totally recrystallized to mixture of prevailing epidote group minerals, forming the matrix around deformed diopside. By this way the rock obtained a new fabric resembling the porphyric structure (Fig. 2c, d, h).

The former magmatic feldspar/plagioclase had the same size as the diopside 1 and the present area of porphyroclast is filled with the mixture of albite, Sr-rich epidote, epidote 1 and epidote 2. Sometimes grossulars occur as inclusions or relics in epidote 1. This mineral assemblage shows decomposition of former Sr-rich feldspars to their pseudomorphs during the metamorphic events (Fig. 2).

The primary magmatic texture of the metagabbro is well recognizable in localities Ostrá, Babiná and Zadné Porče (Fig. 2a, b, c). In locality Ostrá also a tectonic breccia of the metagabbro was revealed in the outcrop (Fig. 2j). In the tectonic breccia the relics of the magmatic diopside 1 have the size of few mm and the former diopside 1 was mechanically destructed by the displacement and rotation within the metamorphic matrix minerals. By this way the rock represents the tectonic breccia with numerous oval fragments rotated during exuhumation.

The mylonite of metagabbro in the Šajby locality (Fig. 2d, e, f, h) shows pseudomorphs after diopside 1, as well as after the former magmatic feldspar/plagioclase. The ductile deformation during the mylonitization has modified the shape of magmatic diopside 1 and feldspar/plagioclase forming their porphyroclasts (Fig. 2). In the locality Dobšinský potok (Fig. 2i, g) the pseudomorph of diopside 1 reaches the size up to 1 cm and former diopside 1 is completely replaced by the mixture of actinolite 1 and 2, chlorite and calcite. The primary magmatic feldspar/plagioclase decomposed to the mixture of albite, Sr-rich epidote and two generations of epidote, identically as it occurs in other localities (Fig. 2).

Magmatic minerals and Sr-rich epidote in the metagabbro

The metagabbro contains a common magmatic mineral assemblage of diopside 1, bytownite, K-feldspar, anorthoclase, spinels, apatite, kearsutite, anthophyllite, ilmenite, baddeleyite, zircon, mottramite, creaseyite, chrysocola and pseudomorh of pseudobrookite/armalcolite. Except the occurrence of bytownite, the Sr-rich feldspar must have been formed in primary gabbro, because in the frame of former magmatic phases the Sr-rich feldspar decomposed to Sr-rich epidote and albite (Fig 2). Grains of pseudobrookite/armalcolite decomposed to the mix of ilmenite, rutile and hematite (Fig. 9a and 29b). Spinels are zoned. The magnesiochromite forms the core of grains and chromite their rim 1, however the zoned spinels are replaced by hematite to form the outer rim 2. The chemical classification of spinels shows their formation apart from a MORB (Fig. 3a, Table 3).

The ACFN diagram showing the plotting positions of the magmatic minerals in the former gabbro that were found in studied localities (Fig. 3b). Besides the same magmatic mineral assemblage, the identical Sr-rich epidote was found in all above listed localities. Each thin section shows high relief of Sr-rich epidote, which is green and always forms a core of clinozoisite/epidote porphyro-

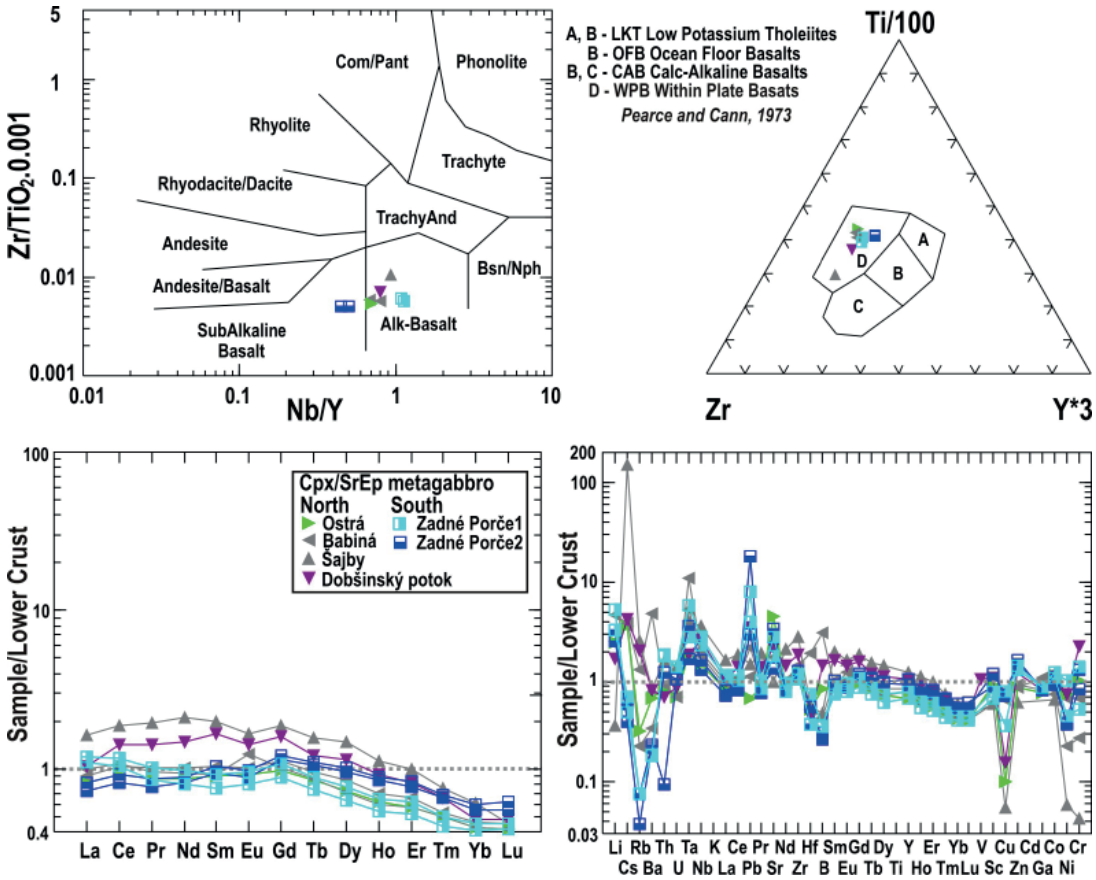

Fig. 4. Chemical classification according to whole-rock analyses of Cpx/SrEp metagabbros and their normalization to the lower crust contents according to the data by Sun & McDonough (1989), as well as Pearce & Cann (1973), using equivalent of volcanic rocks for the gabbro chemical classification. North – localities of Cpx/SrEp metagabbro in the northern zone of Gemeric unit - in the Rakovec nappe. South – localities of Cpx//SrEp metagabbro in the southern zone of Gemeric unit - the Jedľovec nappe (Grecula et al., 2009). Zadné Porče 1 – locality near the Lastovičí vrch hill. Zadné Porče 2 – locality Zadné Porče.

blasts. The magmatic mineral assemblage with the common occurrence of Sr-rich epidote exclusively characterizes the tectonic blocks of metagabbro as the identical rock in all studying localities in Gemeric unit (Figs. 1 and 2).

Chemical analyses of metagabbro

The whole-rock analyses of Cpx/SrEp metagabbro chemical composition in localities Ostrá, Babiná, Šajby, Dobšinský potok and Zadné Porče have revealed that the geotectonic background of its origin and crystallization corresponds in all localities (Table 1). According to the chemical classification of the rocks in diagram Nb/Y vs. Zr/TiO_2 (Winchester & Floyd, 1977), normalized on REE contents and trace elements in diagrams the former subalkaline/alkaline gabbro was formed in the lower crust. The contents of Rb, Ba, Hf, Cu, Ni and Cr are depleded and contents of Ta, Nb, Pb and Sr are enriched in normalization to the lower crust, which is shown in spider trace elements diagram (Fig. 4). For comparison, the trace elements analyses are normalized to contents of chondrite and primitive mantle respectively (Fig. 5). That comparison of patterns confirms well the lower crust origin of the former gabbro. The long-lasting crystallization of the low crust alkaline melt caused the origin of diopside 1 and correspondingly large plagioclase/feldspar porphyroblasts, reaching dimensions up to 2–3 cm (Fig. 2). The chemical classification in the triangle diagram Zr-Y-Ti (according to Pearce & Cann, 1973) has revealed the within plate origin of the metagabbro in all localities (within plate basalts/gabbros, WPB; Fig. 4). The within plate origin of the gabbro suggests a geotectonic setting before the rift stage, i.e. the formation of the gabbro before the time when an "active rift" has existed and the basalt lava has reached and spilled on the see floor, or formed pillows, and by this way it contributed to the formation of future ophiolite suite within the Gemeric unit. The active rift ophiolite suite of this zone was previously studied by Bajaník (1975, 1976), Hovorka et al. (1988), Faryad & Bernhardt (1996), Ivan (1997), Grecula et al. (2009), Radvanec & Grecula (2016) and Radvanec et al. (2017). The active rift rocks of the ophiolite suite in the Gemeric unit provided ages ranging from Devo-

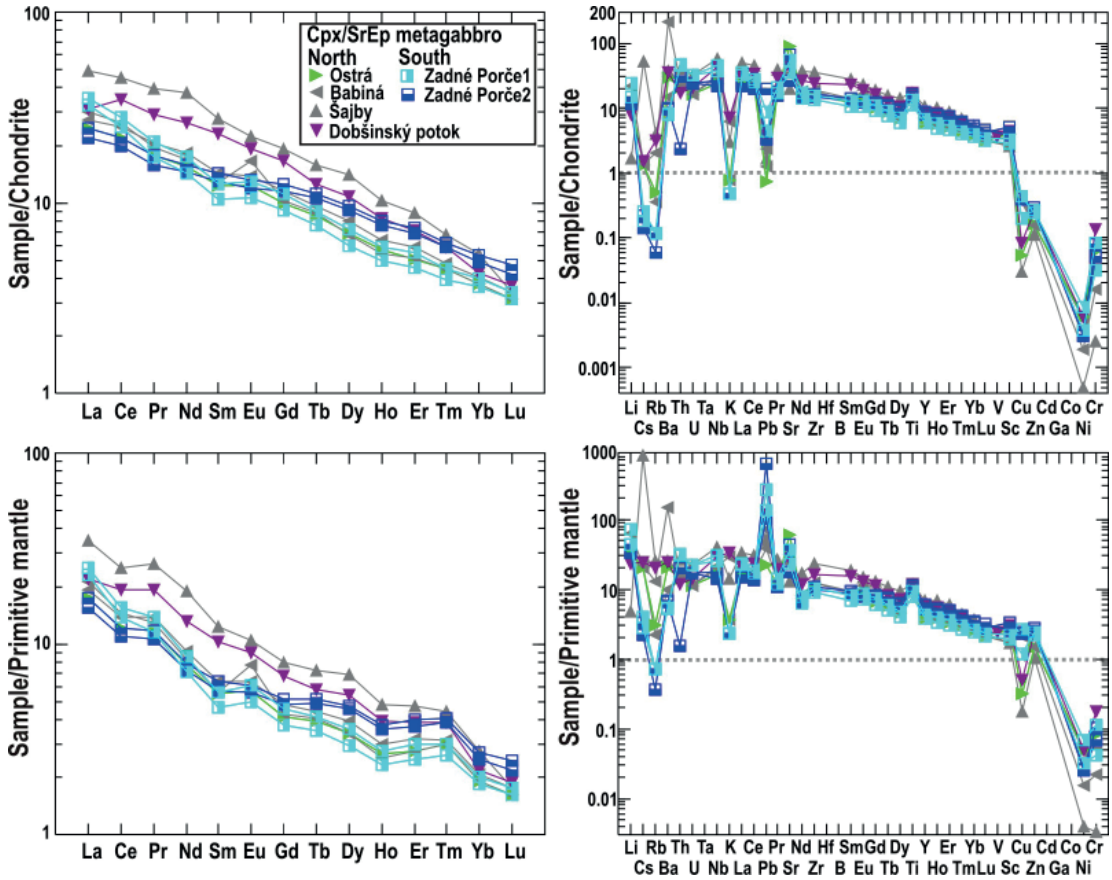

Fig. 5. Chemical classification according to whole-rock analyses and their normalization to the primitive mantle and chondrite contents according to the procedure by Sun & McDonough (1989).

nian to Lower Carboniferous (Putiš et al., 2009). Basalt and gabbro of that suite are polymetamophosed and show andesite/basalt, ocean floor basalt (OFB) and midle ocean ridge basalt whole-rock chemical classification (Radvanec et al., 2017, see Introduction).

Zircon ages

Zircon is present in Cpx/SrEp metagabbros in all investigated localities. In locality of Zadné Porče the magmatic baddeleyite is replaced by zircon or zircon occurs in the metagabbro matrix individually (Fig. 11b and 29c). Concordant zircon age was obtained by the SHRIMP method at ca. 461 Ma from the Zlaté Porče locality (Putiš, personal communication). This Ordovician age represents the magmatic age of the gabbro.

Different younger zircon generations, originating in the metagabbro after Ordovician, has in Ostrá locality the prismatic shape and were found in the form of inclusions in the mixture of ilmenite, hematite, rutile and titanite, or in the metagabbro matrix. In the Ostrá locality the separated zircons from the mixture of oxides and metagabbro matrix are correspondingly large, zonal and prismatic. One zircon grain spot ages are ranging 351–343 Ma and have determined the age of older **M1a** gabbro metamorpism in the Lower Carboniferous (Mississippian). Second similarly large and prismatic zircon grain is younger and has crystallized separately from the older Lower Carboniferous zircon. The centre of younger zircon has the age of 313 and the average age of 307 Ma (Upper Carboniferous), but margin of this grain has grown in Permian – 261 Ma. The younger zircon generation has determined the age of a new and younger Permian metamorphism **M1b**. According to the same prismatic shape of the zircon, both generations of the different age have crystallized at the temperature of at least 600 °C, which indirectly determines the same temperature peak of both metamorphic overprints **M1a** and **M1b** of the metagabbro in Variscan orogenesis. The metamorphogenic zircons **M1a** and **M1b** were dated by the SHRIMP method and obtained ages were concordant (Putiš et al., 2009).

Mineralogy
Na/Ca clinopyroxenes

The magmatic clinopyroxenes occur in the form of euhedral and subhedral crystals with sizes up to 2.5 cm (Figs. 2, 6a-b, 7a-b, 8a and 11). They have a homogeneous

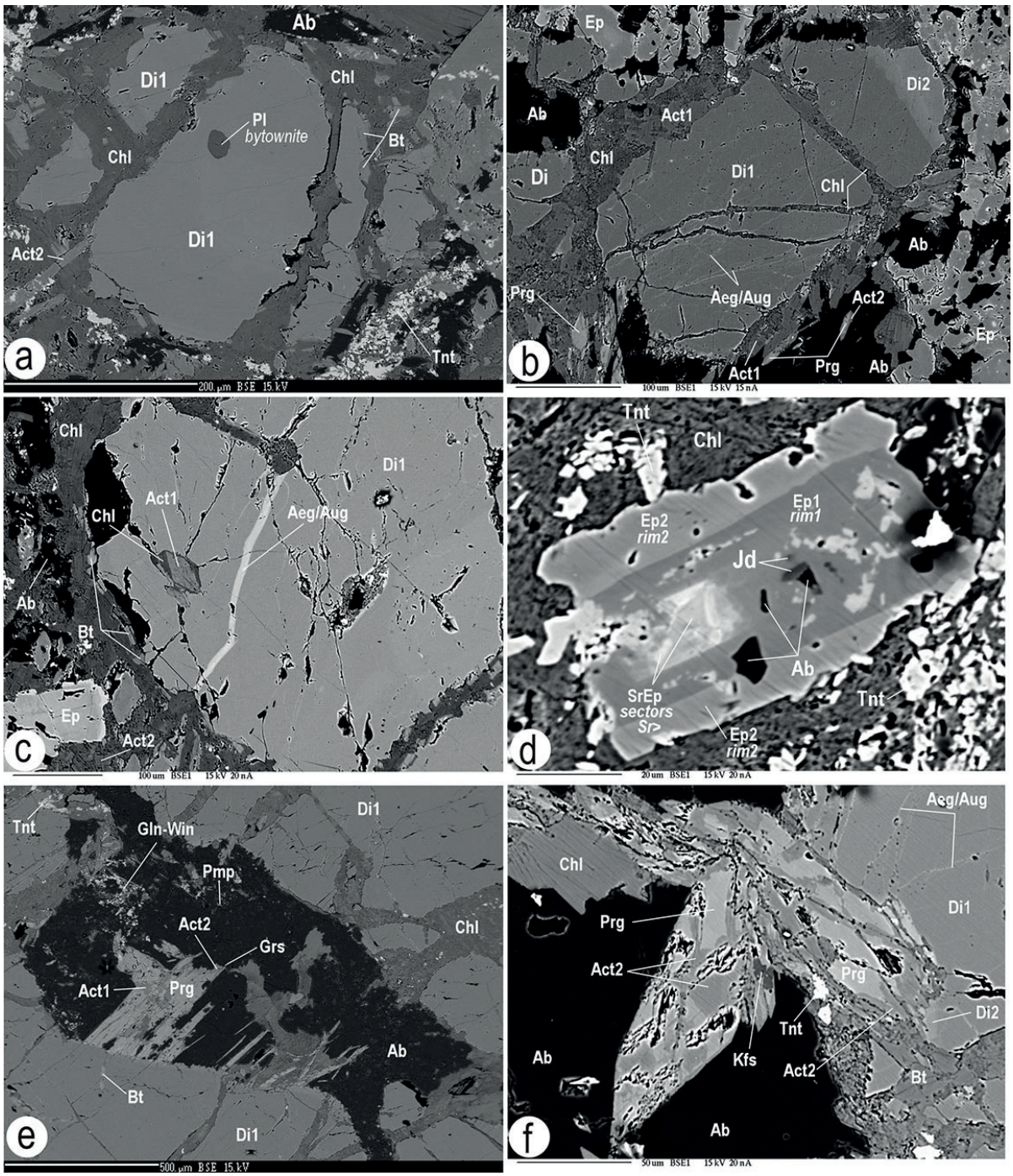

Fig. 6. Mineral assemblages of Cpx/SrEp metagabbro in the Babiná locality. **a** – Di1 – primary magmatic dioside 1; Pl – plagioclase, bytownite; **b-c** – Metasomatic lamellas of Aeg/Aug – aegirine/augite in Di1; Di2 – diopside 2 forms the rim of primary magmatic Di1; Ab – albite; Tnt – titanite; Chl – chlorite; Act1, 2 – actinolite 1 and new actinolite 2; Bt – biotite; **d** – SrEp – sectors of Sr-rich epidote (Sr>) forms the core of epidotes porphyroblasts. Rim 1 – epidote 1. Rim 2 – new epidote 2; Jd – jadeite and Ab inclusions occur only in the rim 1 of Ep1. Ep2 – new epidote 2 forms the rim 2 in porphyroblast of epidotes; **e** – Inside Di1 the place of former Pl is filed by Ab, Pmp – pumpellyite, Gln-Win – glaucophane-winchite, Act1 and Chl – chlorite. Younger assemblage there shows the replacement of Prg – pargasite and Act1 by Act2. Grs – grossular and Tnt – titanite occur in Ab., Bt – biotite in crack of Di1; **f** – In the matrix the Prg – pargasite is replaced by Act2 and minerals Chl-Bt-Ab usually occur on the rim of Di1. In Di1 lamellas of Aeg/Aug are presented and Di2 replaced Di1 on its rim. Kfs – K-feldspar relict in Prg/Act2 is presented. Backscattered electron images.

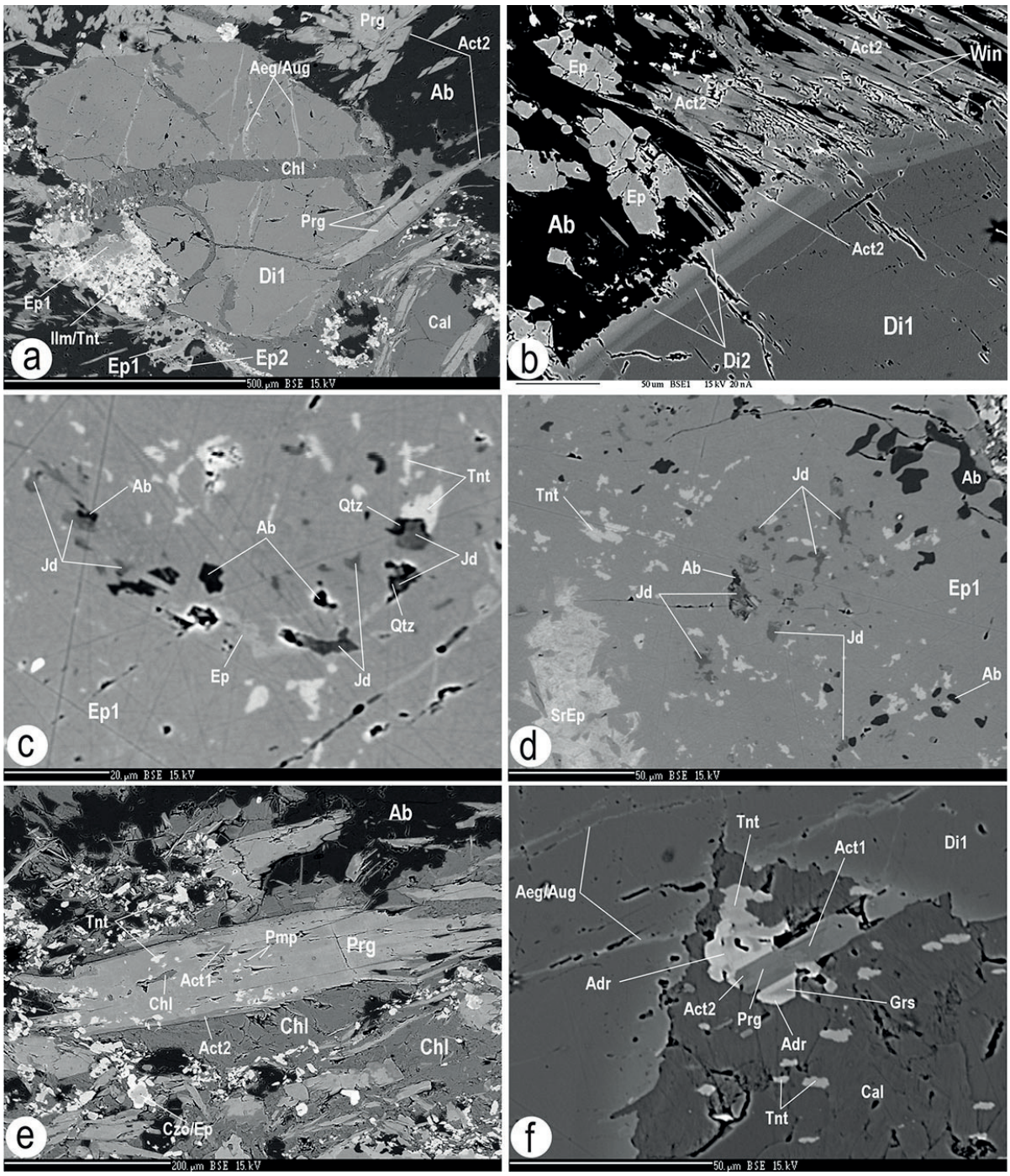

Fig. 7. Mineral assemblages of Cpx/SrEp metagabbro in the Ostrá hill locality. **a** – Metasomatic lamellas of Aeg/Aug – aegirine/augite in Di1 – primary magmatic diopside 1. Matrix assemblage is composed by albite (Ab), pargasite (Prg), epidote (Ep1), epidote 2 (Ep2) and calcite (Cal). The Ilm/Tnt – ilmenite is replaced by titanite and Prg by Act2. **b** – Di1 is replaced by diopside 2 (Di2) and then by the actinolite 2 (Act2). The matrix amphiboles are composed of winchite (Win) in the core and Act2 in the rim. **c-d** – jadeite (Jd) and decomposition of Jd to albite (Ab) was formed due to the reaction of Jd + quartz (Qtz) = Ab. Jd inclusions occur as relicts only in epidote 1 (Ep1). Ep1 replaced the former SrEp and forms the rim1 in SrEp-Ep1-Ep2 porphyroblast; **e** – Pmp – pumpellyite, Chl – chlorite and Act1 relics found in host Prg. Prg is partly replaced by Act2 in the contact with matrix; **f** – Inside Di1 with lamellas Aeg/Aug the former Pl is decomposed to Grs – grossular, Adr – andradite and Cal – calcite. This mineral assemblage is accompanied by the series of Act1-Prg-Act2 and Tnt. Backscattered electron images.

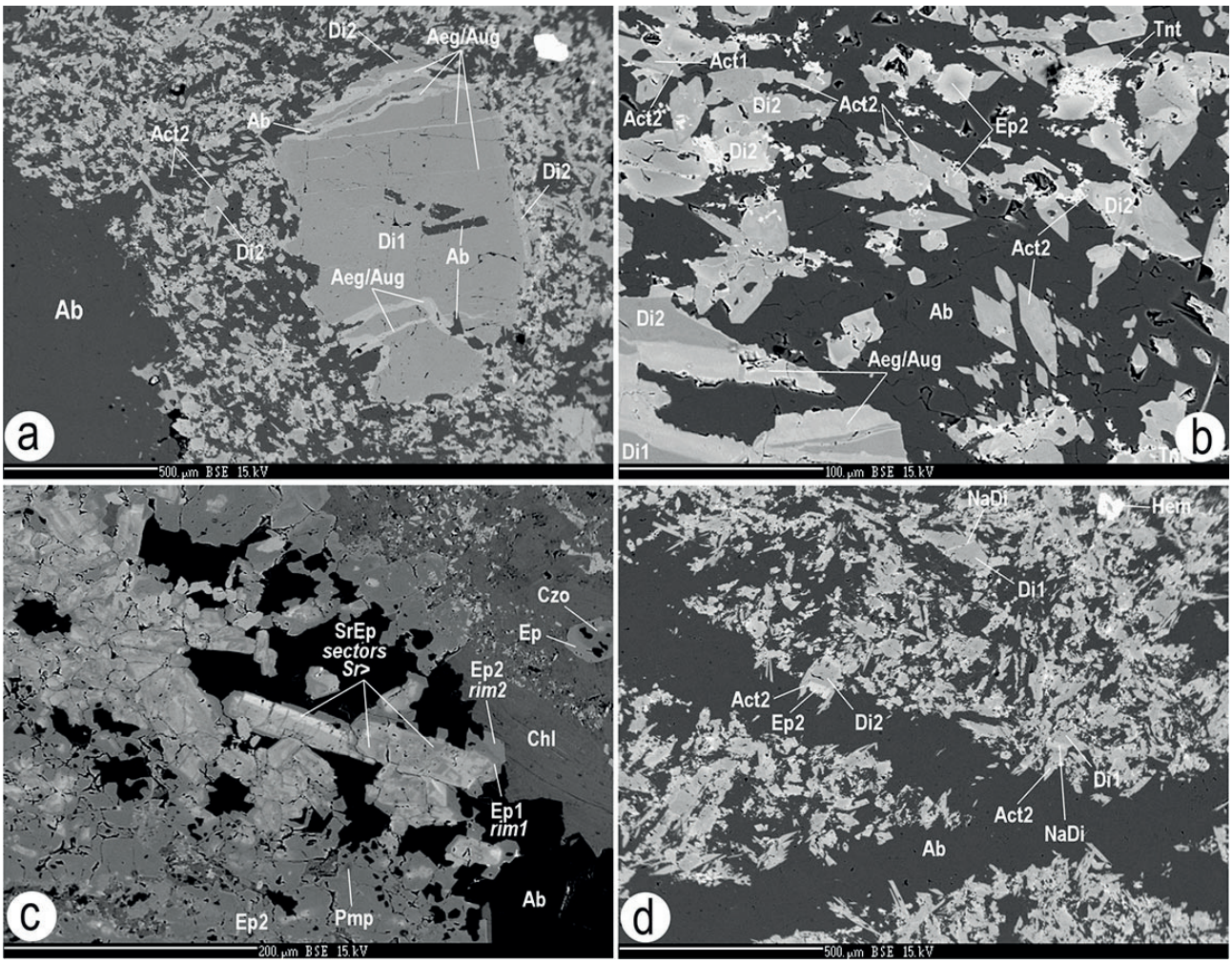

Fig. 8. Mineral assemblages of Cpx/SrEp metagabbro in the tectonic breccia in the Ostrá locality. **a-b** – Relationship of primary magmatic diopside 1 – Di1 with the fine-grained mixture of albite – Ab, diopside 2 – Di2 and actinolite 2 – Act2 related to Permian metamorphic event **M1b** in the fragment of tectonic breccia. Metasomatic lamellas of Aeg/Aug – aegirine/augite and albite (Ab) in Di1; **c** – Sr-rich epidote SrEp replaced by epidote 1 to form rim 1 and by epidote Ep2 on the outer rim 2 of the epidotes porphyroblast. Relict of actinolite 1– Act1 is rimed by Act2. **d** – Cement of the tectonic breccia consisting of Act2 + Di2 + Ep2 formed during Permian metamorphic event of **M1b**. Locally the relics of Di1 with metasomatic Na-rich diopside – NaDi are presented in the cement and Pmp – pumpellyite found in Ep2. Assemblage NaDi, Act1 and Pmp relates to the older Carboniferous HP metamorphic event of **M1a**; Tnt – titanite; Hem – hematite. Backscattered electron images.

core composition of $En_{33-49}Fs_{9-17}Wo_{42-50}Jd_{0.4-2.2}Ae_{0.4-2.2}$, Mg# of 72–89 [Mg# = Mg/(Mg+Fe*)], TiO_2 = 0–1.24 wt.% and Al_2O_3 = 0–4.52 wt.% in the Babiná, Ostrá and Zadné Porče localities. In the breccia (Ostrá locality) the homogeneous magmatic core of Cpx has a composition of $En_{23-24}Fs_{27-28}Wo_{49-50}Jd_{0.1-5.3}Ae_{0-5.4}$, Mg# of 48–53, TiO_2 = 0–0.2 wt.% and Al_2O_3 = 0.07–0.3 wt.%. According to the classification of Morimoto (1989), the magmatic core of Cpx is formed by diopsides 1 and/or hedenbergite 1 respectively (Fig. 12, Table 3).

In the Babiná and Ostrá localities, the anhedral jadeites of $WEF_{5-19}Jd_{53.0-87.2}Ae_{0-32.9}$ were found only in the clinozoisite-epidote 1. The jadeite occurs as inclusions and/or relics with quartz and albite. Sizes of that inclusions reach up to 20 µm (Figs. 6d, 7c-d and 12, Table 3). However, the Na/Ca Cpx of $WEF_{35.6-91.6}Jd_{0.7-15.1}Ae_{0-52.2}$ as metasomatic lamellas were formed strictly in the diopside 1. These Na-rich diopside and aegirine-augite lamellas were frequently found in the Babiná and Ostrá localities, as well as in the breccia of Ostrá locality (Figs. 6b-c, 6f, 7a, 7f, 8a and 12, Table 3).

In the Babiná, Ostrá, Ostrá (breccia) and Zadné Porče localities, the 40-50 vol.% of the the magmatic diopside 1 crystals show a rim zoning pattern with the rim composition of new diopside/augite 2 with $En_{31-48}Fs_{9-26}Wo_{40-50}Jd_{0-3.5}Ae_{0.2-3.6}$, Mg# of 57-87, TiO_2 = 0.85–4.27 wt% and Al_2O_3 = 2.49–5.98 wt% (Figs. 6b, 6f, 7b, 8a, 11a and 12,). The diopside/augite 2 occurs in the cement of breccia re-

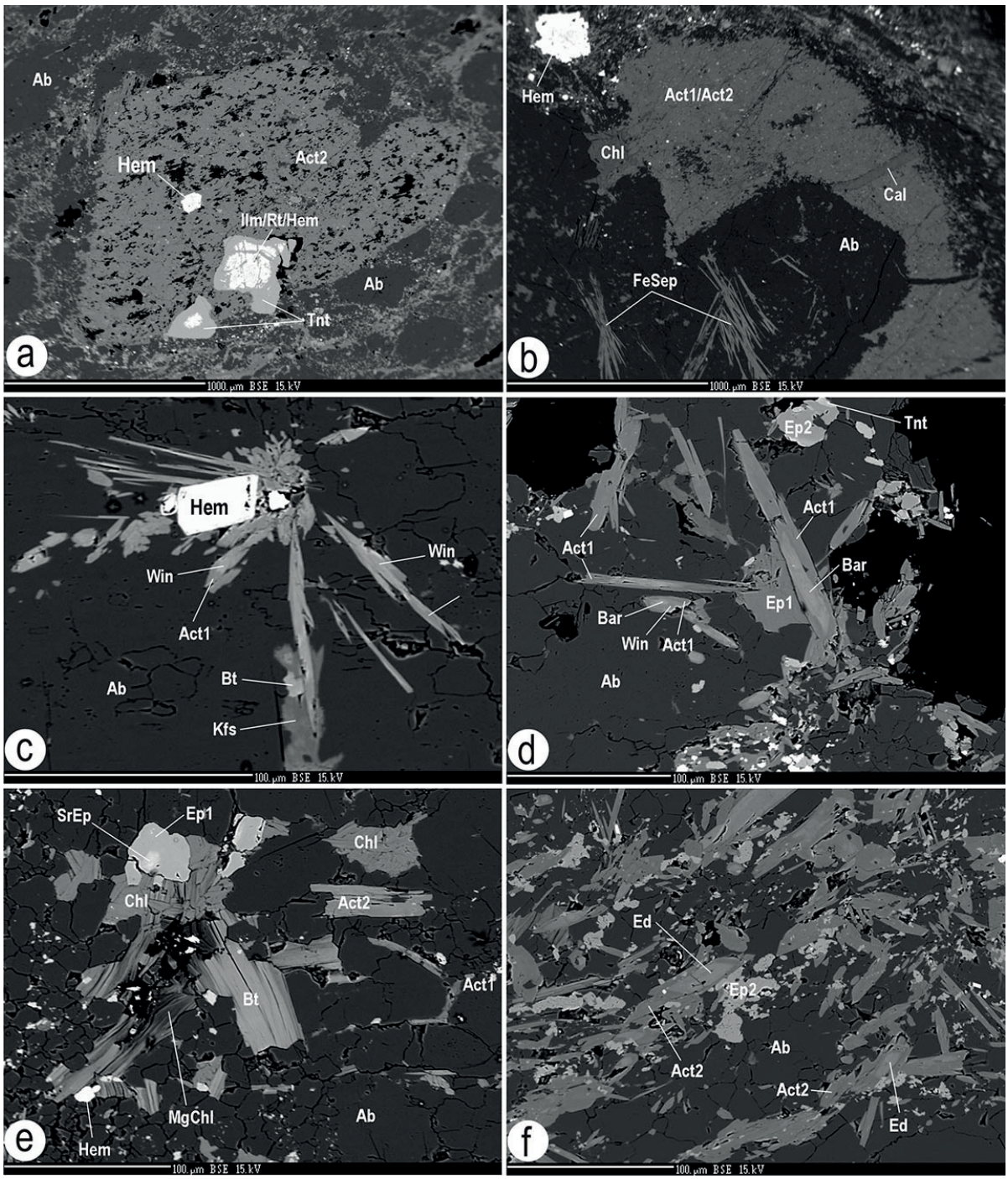

Fig. 9. Mineral assemblages of mylonitic Cpx/SrEp metagabbro in the Šajby locality. **a-b** – Pseudomorph of primary magmatic diopside 1 replaced by actinolite 2 – Act2 and calcite – Cal or by the mixture of Act1/Act2 and Cal respectively. MnIlm – Mn-rich ilmenite decomposed to Rt – rutile, Hem – hematite and to Tnt – titanite. **c-f –** Mineral assemblages in the matrix and relationship between the older blueschist facies minerals - Bar – barroisite, Win – winchite, Act1– actinolite 1, Ab – albite, and MgChl – Mg-rich chlorite of the Carboniferous **M1a** metamorphism and those formed in the **M1b** Permian epidote-amphibolite facies - Ed – edenite, Ep2 – epidote, Act2, Bt – biotite; Chl – chlorite and FeSep – Fe-rich sepiolite; **e –** SrEp – Sr-rich epidote is replaced by Ep1 – epidote 1 in **M1a**. Backscattered electron images.

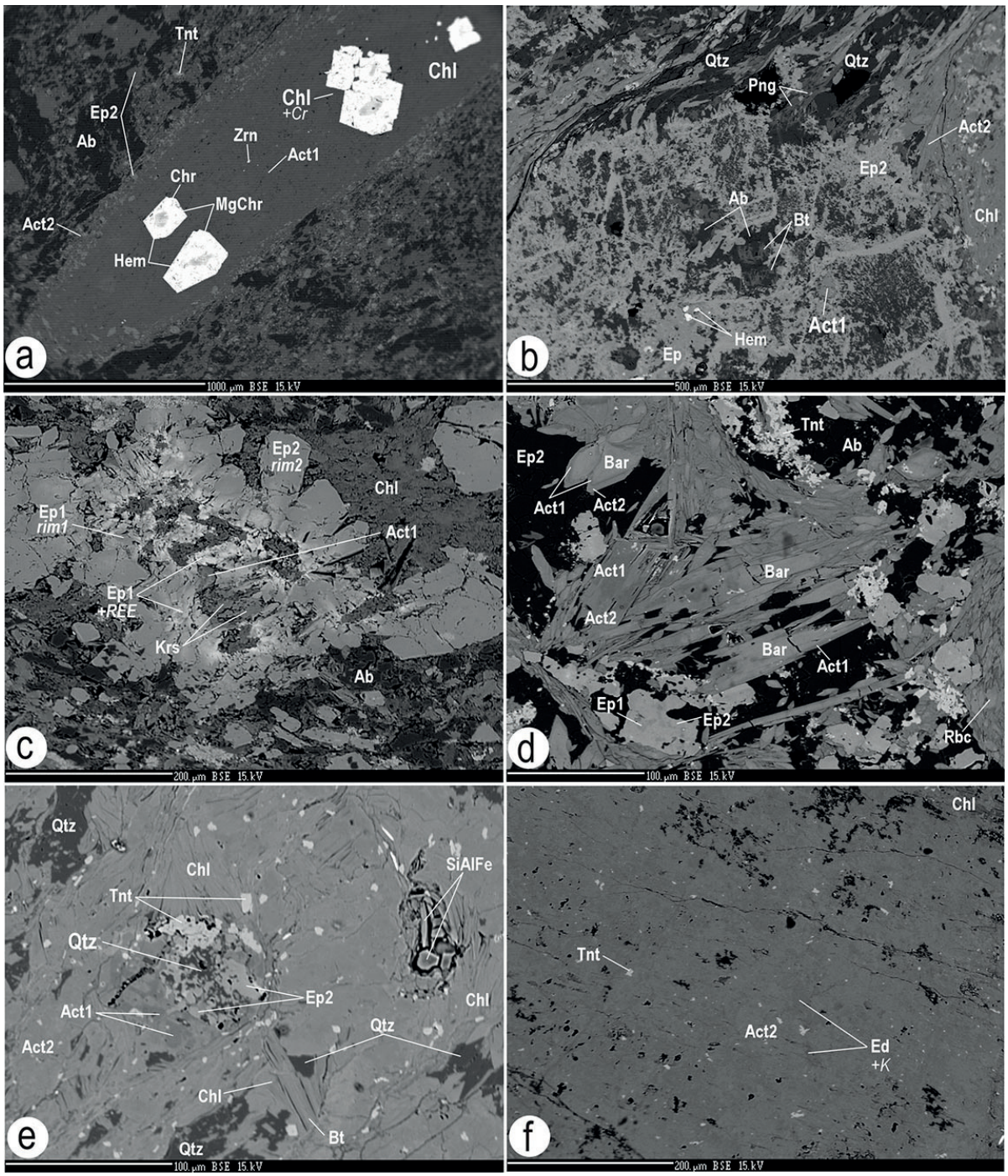

Fig. 10. Mineral assemblages of mylonitic Cpx/SrEp metagabbro and pseudomorph of primary magmatic diopside 1 in the Dobšinský potok locality. **a-b** – Primary magmatic spinel is zonal. The core is magnesiochromite – MgChr and and chromite (rim1) – Chr is rimming the core within the pseudomorph of primary magmatic diopside 1 - Di1. The former Di1 is replaced by assemblage of actinolite 1 - Act1, + chlorite Chl + quartz - Qtz in M1a metamorphism and their relationship to new minerals of younger M1b metamorphism. Metamorphic event M1b is represented by the assemblage of epidote 2 – Ep2 + actinolite 2 -Act2 + biotite – Bt + phengite – Png and chromites are replaced by hematite (rim2) – Hem and by Cr-rich chlorite – CrChl; **c** – Primary magnatic kearsutite – Krs is replaced by actinolite1 – Act1 and by REE-bearing epidote1 – Ep1+REE; **d** – In the matrix the mineral assemblage of M1a shows the relationship between Bar – barroisite and Rbc – riebeckite that are replaced by Act1, Ab – albite; Tnt – titanite. **e** – Act1 of M1a is replaced by Act2 of M1b, SiAlFe – pseudomorph after SiAlFe mineral (hydrated). **f** – K-rich edenite is replaced by Act2. Backscattered electron images.

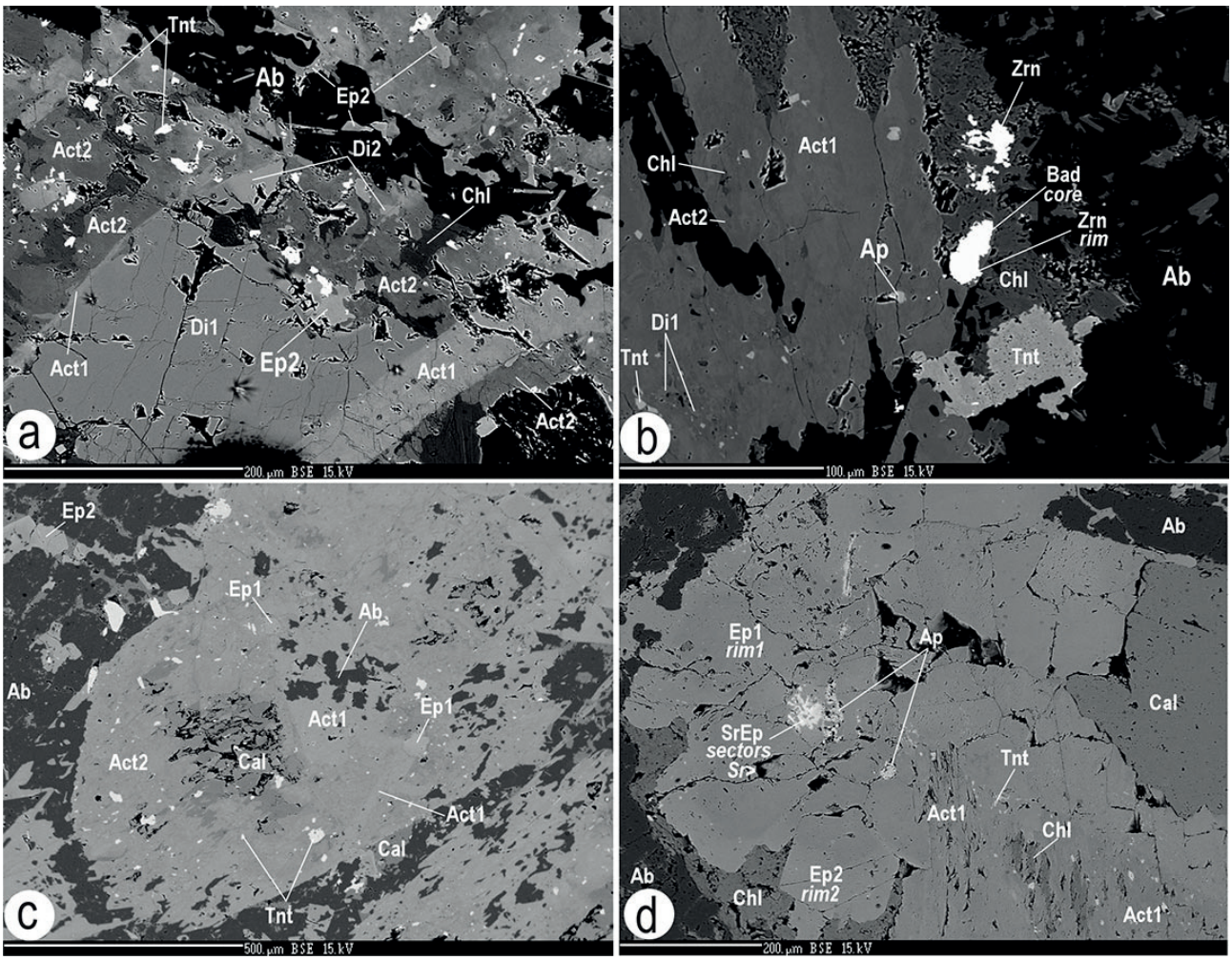

Fig. 11. Mineral assemblages of Cpx/SrEp metagabbro in the Zadné Porče locality. **a –** Primary magmatic diopside 1 **–** Di1 is replaced by actinolite 1 **–** Act1 + chlorite **–** Chl. The relationship to matrix minerals of **M1b** event is represented by a new assemblage of Act2 + Ep2 + Di2. **b –** Baddeleyite – Bad (core) is replaced by zircon – Zrn (rim) of the magmatic origin and their relationship to metamorphic minerals in matrix. Di1- dioside 1; Ap – apatite; Ab – albite; Chl – chlorite; Act 2 – actinolite 2; Tnt – titanite; **c –** Pseudomorph of Di1 represents metamorphic assemblage of Act1/Act2 + Ep1 + Ab + Tnt + Cal. **d –** Sr-rich epidote is replaced by the Ep1 and by the new epidote Ep2 on the other rim of epidote porphyroblast. Backscattered electron images.

spectively (Figs. 8a-b, 8d). The replacement of the diopside 1 by the diopside/augite 2 is a separate and younger process in comparison to the formation of aegirine-augite, whichoccurs as the metasomatic lamellas only in diopside 1. The lamellas of aegirine-augite contain Na, however the new diopside/augite 2 is free of Na (Fig. 12). The Na-rich lamellas were formed during the older HP/LT metamorphic event of **M1a**, however the Na-free diopside/augite 2 has replaced the former diopside 1 during new HT/medium P metamorphic event of **M1b** in the epidote-amphibolite and/or amphibolite facies respectively.

In localities Šajby (mylonite) and Dobšinský potok the pseudomorphs after former magmatic diopside 1 were found (Fig. 2d-i). In these localities the diopside 1 was fully replaced to mixture of two generations of actinolite, chlorite and calcite, while the actinolite 2 from younger metamorphism **M1b** prevails above actinolite 1 from older metamorphism **M1a** (Figs. 9a-b, 10a-b and 10e).

Feldspars

In the metagabbro the feldspars were found in two modes of occurrence. The pseudomorph on porphyroblasts of former magmatic plagioclase is the main occurrence in all localities amounting about 50 vol.% of the former gabbro. These pseudomorphs reach the equal size as those of diopside 1 (Fig. 2). In the diopside 1, the inclusions of magmatic bytownite are rarely found. The bytownite has an average of $An_{86-87}Ab_{13-14}Or_{0.2}$ and the content of SrO reaches to 0.12 wt.% without a zoning (Fig. 6a and 13). In addition, the very rare presence of oligoclase ($An_{19}Ab_{80.5}Or_{0.5}$) was found in diopside 1 as well, however

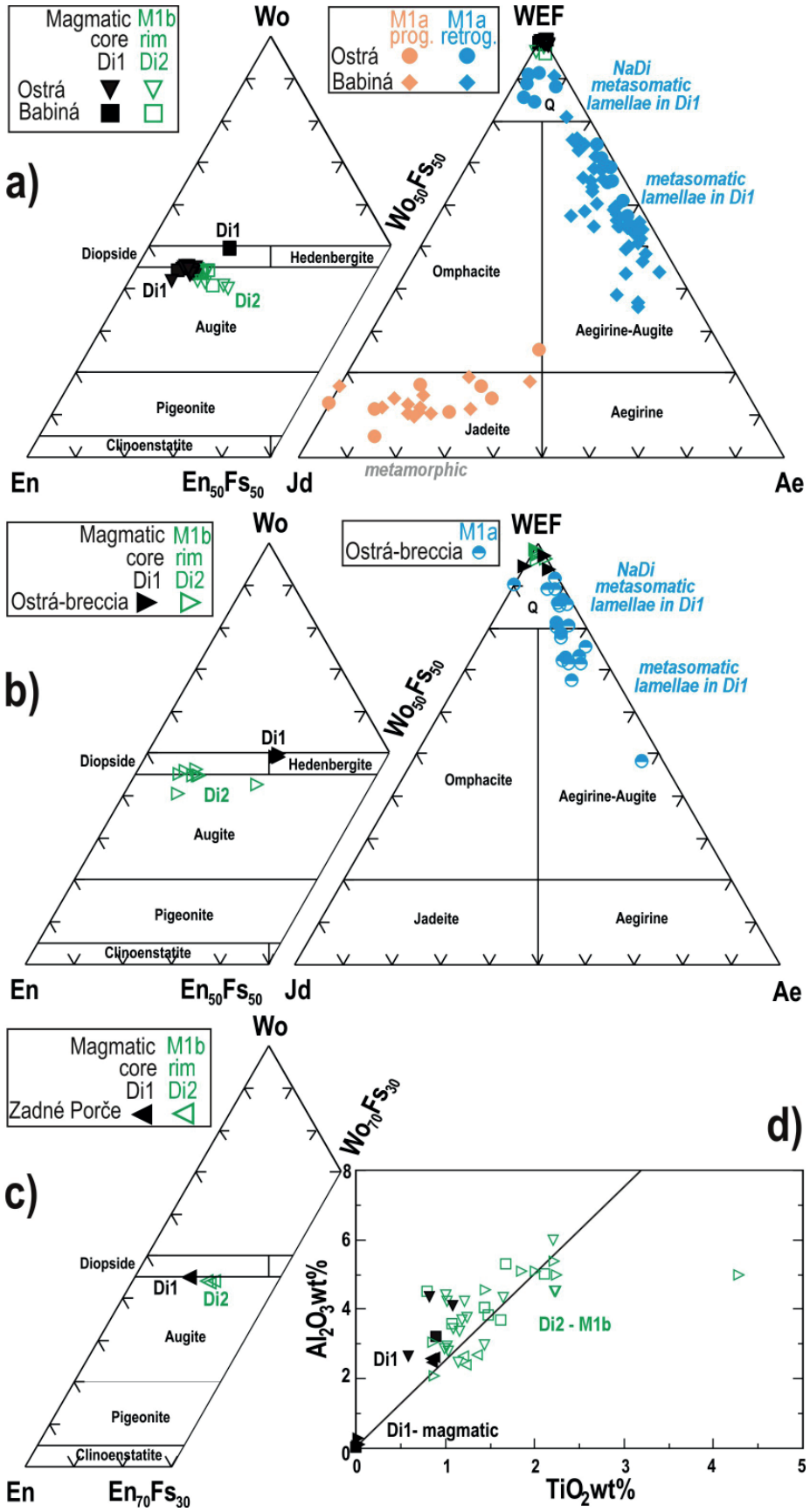

Fig. 12. a-c – Compositional ranges of magmatic diopside Di1, jadeite/aegirine-augite metamorphic HP event of **M1a** (Carboniferous) and diopside Di2 from the new metamorphic event **M1b** (Permian) found in Cpx/SrEp metagabbro in localities Ostrá, Babiná, Ostrá – tectonic breccia and Zadné Porče (sensu Morimoto et al., 1988); **d** – Relationship of magmatic dioside 1 and diopside 2 formed during amphibolite, resp. epidote-amphibolite facies of **M1b** in diagram TiO_2 vs. Al_2O_3.

bytownite is considered to be the prevalent plagioclase of the former magmatic gabbro.

The second mode represents the occurrence of K feldspars, rarely found as an irregular and corroded grains of $An_{0-4}Ab_{0-6}Or_{90-100}$ in the Sr-rich epidote and in the clinozoisite-epidote 1 respectively. However, the K feldspar and anorthoclase of $Ab_{67-75}Or_{25-33}$ are found in the matrix as well. The size of K feldspars ranges from few µm to 30 µm and are regarded to be relics, which were formed during the magmatic/subsolidic stage of the gabbro (Figs. 6f and 13).

Except for the finding of bytownite in diopside 1, the area of porphyroblasts on the former plagioclase is filled by the mix of albite $An_{0-8}Ab_{92-100}Or_{0-1}$ and by the zoned porphyroblasts of epidote group, where the core always forms the Sr-rich epidote. The inner rim is formed by clinozoisite/epidote 1 and the outer rim of porphyroblasts are formed by new generation of epidote 2 (Figs. 2, 14 and 15). In the clinozoisite/epidote 1 inclusions of grossular, jadeite, quartz, albite, pumpellyite and pseudomorph of pumpellyite were commonly found (Figs. 6d, 7c-d and 14a). The main assemblage of Sr-rich epidote, clinozoisite/epidote 1, grossular and albite represents a decomposition minerals that were formed on the primary magmatic Ca/Na/Sr-rich feldspar. This assemblage supplies the pseudomorph on the area of former Ca/Na/Sr-rich feldspar in all studied localities. (Figs. 2, 14 and 15).

Sr-rich epidote – clinozoisite/epidote 1 and epidote2 porphyroblasts

The BSE figures and X-ray mapping show the sector zoning of Sr-rich epidote always in the core of epidote porphyroblasts. The core of Sr-rich epidote X_{Fe}^{3+} = 0.23-0.41 is successively replaced by the clinozoisite/epidote 1 X_{Fe}^{3+} = 0.12-0.23 in the inner rim 1 and finally by the new epidote 2 X_{Fe}^{3+} = 0.24-0.36 in the outer rim 2 (Figs 6d, 7d, 8c, 10c, 11d and 14-16, Table 2). In the clinozoisite/epidote 1, inclusions of grossular, jadeite, quartz, titanite, chlorite and albite were found (Figs. 6d, 7c-d and 14). In addition, the core of Sr-rich epidote and the inner rim 1 of clinozoisite/epidote 1 were partly replaced by pumpellyite. However the outer rim 2 of new epidote 2 is free of pumpellyite (Figs 6d, 7d, 8c, 10c, 11d and 14-15). The new metamorphic event that formed the epidote 2 reversible replaced the pumpellyite by the epidote/clinozoisite that is enclosed in rim 1. In this case the inner rim1 of epidote/clinozoisite 1 shows pseudomorphs after pumpellyite. Especially in the inner rim 1, the former pumpellyite occurs only sporadically, however in the core of Sr-rich epidote the occurrence of pumpellyite is common (Fig. 14).

In sectors of Sr-rich epidote, the content of Sr ranges from 0.1 to 0.7 apfu and the contents of REE-sum range from 0 to 0.22 (Figs 15-16). The negative linear correlation of Ca content versus Sr shows two different substitutions. One is for the REE(+) bearing sectors and the next is for the REE(-) free sectors. They were found in the Sr-rich epidotes (Fig. 16a-c). The Sr-rich epidote has originated with albite and both coexisted minerals fill the pseudomorph area up to the decomposition of former Ca/Na/Sr-rich feldspar (Fig. 15a). In the literature the occurrence of Sr-rich epidote have been reported in the metagreywacke-quartzofeldspathic schist (Grapes & Watanabe 1984), in the meta-eclogite and metasomatized eclogite (Brastad, 1985) and in the ultra-high pressure (UHP) metamorphic rocks (Nagasaki & Enami, 1998). The Sr-rich zoisite and epidote are regarded as the most important Sr reservoirs under HP and UHP conditions where Ca/Sr-rich plagioclase and titanite are unstable (Nagasaki & Enami, 1998; Zellmer et al., 1999). In the Babiná and Ostrá localities of Gemeric unit the decomposition of Sr-rich plagioclase to Sr-rich epidote and albite under similar HP conditions was firstly described by Radvanec (1999 and 2000). The magmatic mineral assemblage with the common occurrence of Sr-rich epidote exclusively characterizes the tectonic blocks of the metagabbro as the identical rock in all studying localities (Figs 1–2).

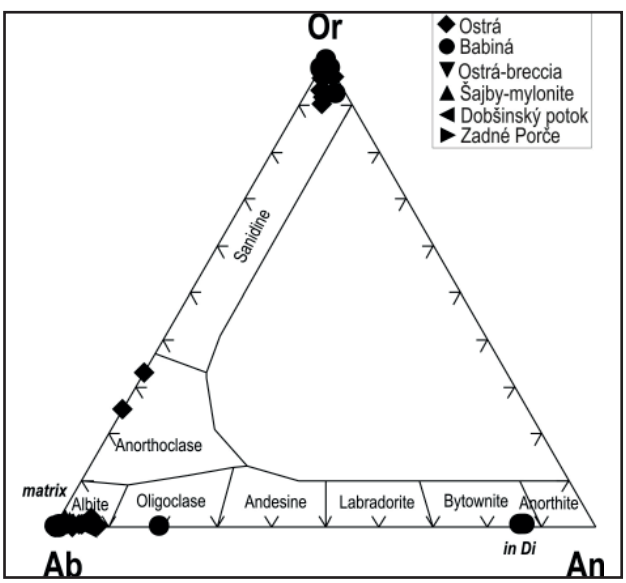

Fig. 13. Chemical classification of feldspars present in Cpx/SrEp metagabbro of investigated localities in triangle diagram Ab-An-Or.

Amphiboles

The rare, tiny and oval anthophyllite inclusions from the group of Fe-Mg-Mn amphiboles were found in the diopside 1 in the Babiná locality. Besides anthophyllite in localities Babiná and Dobšinský potok we have found also the kearsutite (Figs 17a, d, Table 3). In locality of Dobšinský potok the kearsutite is replaced by the epidote 1 (Fig. 10c). It is probable that the anthophyllite and ke-

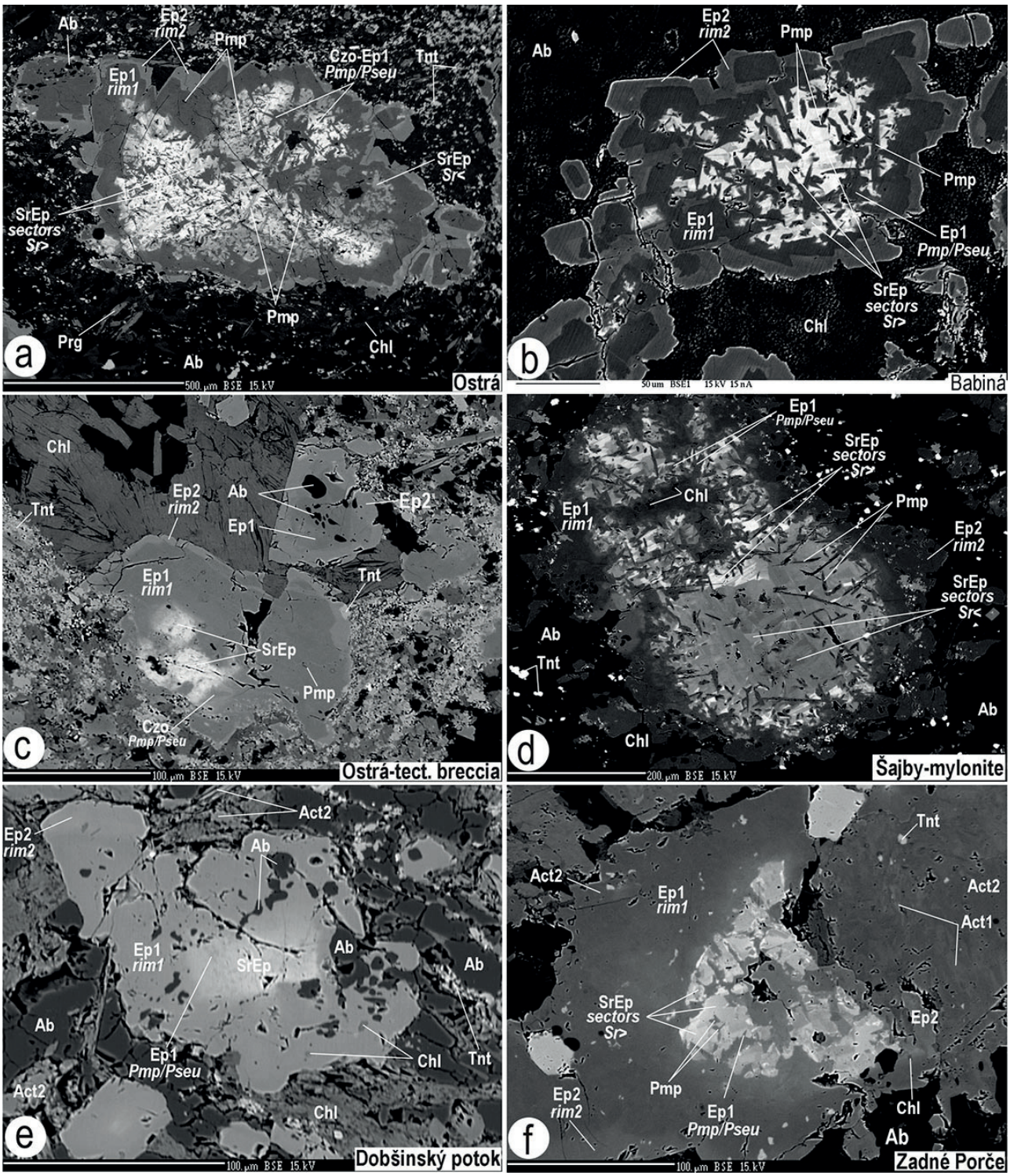

Fig. 14. Porphyroclasts/porphyroblasts of epidote group are gradually formed by the sectors in core of Sr-rich epidote – SrEp; Sr> – sectors with high contents of Sr; Sr< – sectors with lower contents of Sr. The core-rim transition is formed by clinozoisite-epidote 1 – Czo-Ep1 and finally the outer rim 1 is formed by new epidote 2 – Ep2 in the rim 2. The Sr-rich epidote and the younger clinozoisite/epidote 1 are always replaced by the pumpellyite – Pmp, however the new epidote 2 is free of Pmp. The pumpellyite is partly replaced by Ep2 to show pseudomorph – Pmp/Pseu. The formation of Sr-rich epidote and its successive replacement identifies and characterizes the polymetamorphic evolution of the gabbro in all studied localities and considers metagabbro as a unique rock in Gemeric unit. That zonal and successive formation of epidote group minerals were formed during two metamorphic events **M1a** and **M1b**. Ab – albite, Chl – chlorite, Tnt – titanite, Act1, 2 – actinolite-1 and 2. Pmp/Pseu – pseudomorph of pumpellyite. Backscattered electron images.

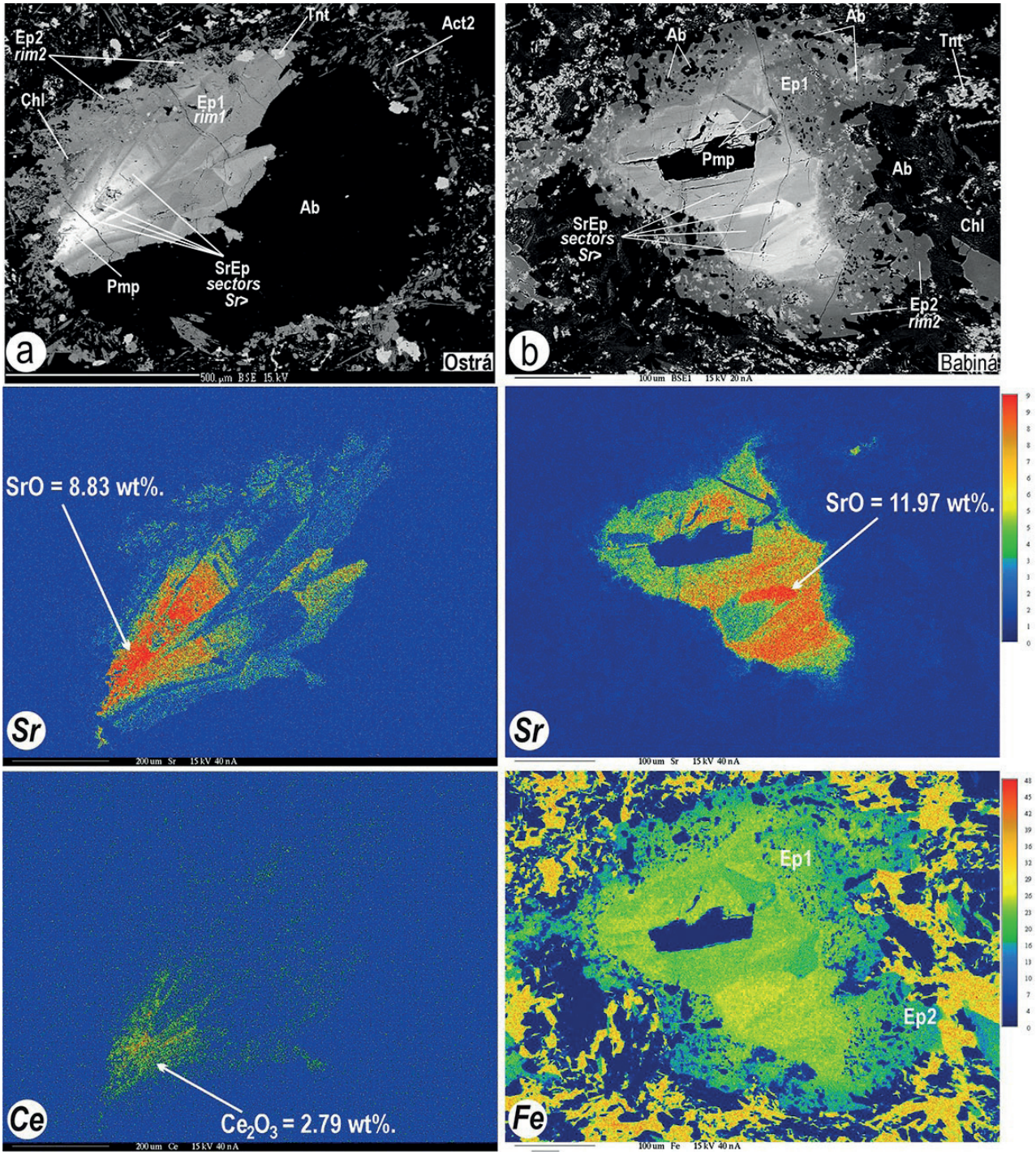

Fig. 15. X-ray mapping of Sr, Ce and Fe contents in porphyroblasts of epidote group from the Ostrá **(a)** and Babiná **(b)** localities. **a –** Decomposition of former magmatic Sr-rich feldspar to Ab – albite and to sectors of SrEp – Sr-rich epidote, following by the unbalanced model reaction Sr/Ca/NaPl + H_2O = SrEp + Ab. Positions of pumpellyite (Pmp) in SrEp and epidote 1 (Ep1)-rim 1, epidote 2 (Ep2)-rim 2, chlorite (Chl) and actinolite 2 (Act2), Backscattered electron images; **b –** Relations of Ab, sectors of SrEp, Pmp, Ep1-rim 1, Ep2-rim 2, titanite (Tnt) and Chl, Backscattered electron images; **Sr –** contents show a sector zoning of Sr-rich epidote in the core of epidote porphyroblasts. **Ce –** higher content shows area of REE-rich parts only in the sector of SrEp. **Fe –** content shows successive formation from the core of SrEp to younger rim1 of Ep1and to rim2 of Ep2 respectively in the zonal structure of epidote porphyroblast.

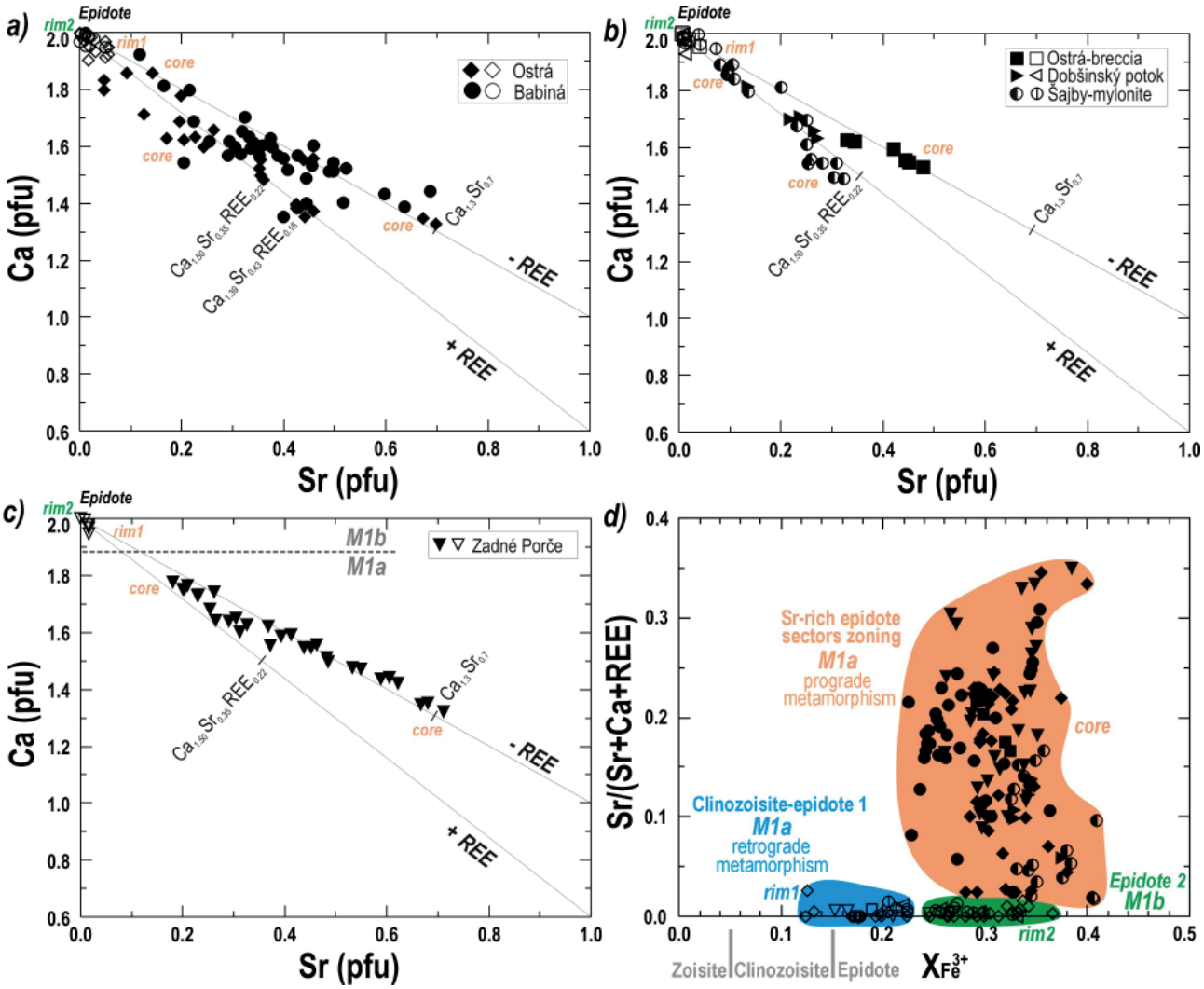

Fig. 16. a – c – Relation of Ca (pfu) vs. Sr in chemical formulas of epidotes due to their successive formation from the core towards new epidotes in outer rim1 and rim2 in all studied metagabbro localities. Line + REE characterizes the substitution in Sr-rich epidote with the REE content. Line – REE characterizes a substitution in Sr-rich epidote without the REE content. **d** – Relation of X_{Fe}^{3+}vs. Sr/(Sr+Ca+REE) in chemical formulas. Core – ratios in sectors of Sr-rich epidote that formed in metamorphic event **M1a** (Carboniferous age); Rim 1 – ratios of in clinosoisite-epidote1 that formed a retrograde metamorphic event in **M1a**; Rim 2 – ratios in epidote2 that formed in new metamorphic event **M1b** (Permian age).

arsutite have crystallized at the end of magmatic or subsolidic stage of the gabbro crystallization together with diopside 1, feldspars and spinel (Fig. 3b). Small amount of Ca + Na, which replaces Fe and Mg in anthophyllite has a value up to 0.34 apfu (Fig. 17a, Table 3). In the solid solution this value is at upper boundary of possible limit of the replacement between the Fe-Mg and Ca amphiboles (Deer et al., 1992). The kearsutite is typical species of high P-T (1000–1100 °C) and low-H_2O melt (3-5.5 and ΔNNO conditions being the alkaline igneous product (Ridolfi & Renzulli, 2012).

In all localities we have found two different generations of metamorphogenic and zonal amphiboles in the metagabbro matrix. Chemical composition of metamorphogenic amphiboles, expressed by the formula $Al^{VI}+Fe^{3+}+2Ti$ vs. Ca/(Ca+Na) – M4 forms two substitution trends according to succession of their formation. The older substitution represents Na/Ca amphiboles, which originated in older HP metamorphism **M1a**. In the timely separated and younger metamorphism **M1b** there originated Ca amphiboles (Fig. 17).

The oldest metamorphogenic amphiboles in the metagabbro in the Babiná, Ostrá, Šajby and Dobšinský potok localities are represented by glaucophane, riebeckite, barroisite and winchite. In the Babiná locality, the glaucophane and winchite were found in the diopside 1 crack together with albite and pumpellyite. Winchite is often enclosed in the centre of the zonal amphibole, which

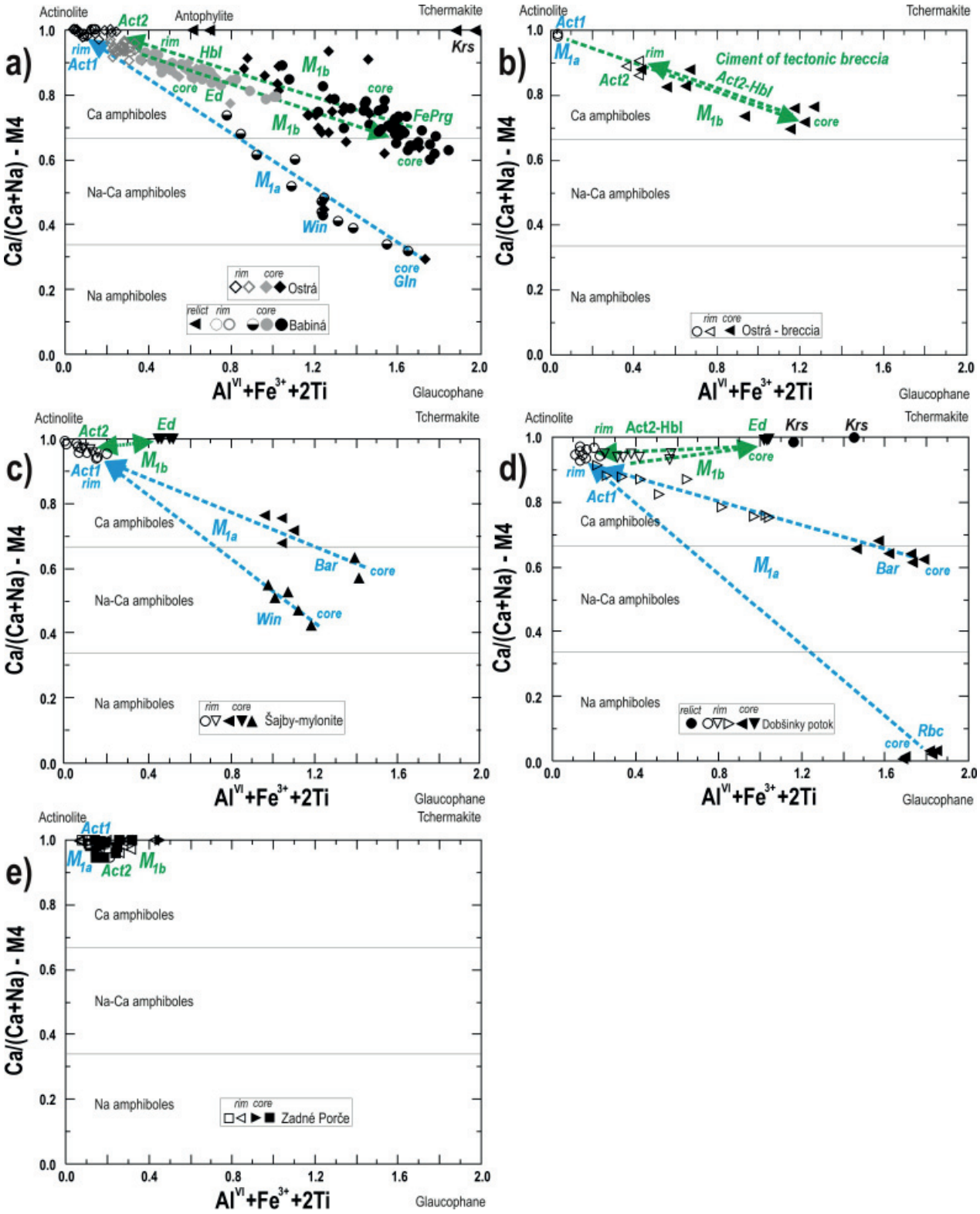

Fig. 17. Chemical classification of amphibole generations in the diagram $Al^{VI}+Fe^{3+}+2Ti$ vs. Ca/(Ca+Na) – M4 in Cpx/SrEp metagabbro in investigated localities. **M1a** – older HP-LT metamorphism (Carboniferous). **M1b** – younger metamorphism in amphibolite, resp. epidote-amphibolite facies (Permian). Core – the middle of the zonal amphibole grain. Rim – margin of the zonal grain. Hbl – hornblende; Ed – edenite; Act1,2 – actinolite 1,2; Win – winchite; Gln – glaucophane, Rbc – riebeckite; Bar – baroisite; FePrg – Fe-rich pargasite; Krs – kearsutite.

rim is formed by actinolite 1 (Fig. 6e). Similarly, in the Ostrá locality the glaucophane and winchite were found enclosed in actinolite 1. In the matrix, the winchite forms cores consisting of fibroidal amphiboles, which had grown at the margin by actinolite 1 (Fig. 7b). In The mylonites of the Šajby and Dobšinský potok localities contain zonal Na/Ca amphiboles, having the core formed of riebeckite, barroisite or winchite and their margins contain rim of actinolite 1 (Figs 9c-d, 10 d and 17c-d). In all these localities the Na/Ca amphiboles contain rims of actinolite 1 and together they represent the retrograde HP metamorphism **M1a** (Fig 17, Table 4).

Younger metamorphic and often timely separated process **M1b** replaced the amphiboles of previous HP metamorphism. The Fe-rich pargasite of this new metamorphism, being present in the metagabbro of Babiná and Ostrá, has crystallized around relics of older actinolite 1 and pumpellyite, which originated together at the end of retrograde HP metamorphism in pumpellyite-actinolite facies **M1a** (Fig. 6e-f, 7e).

Second younger substitution trend **M1b** is formed by actinolite1-edenite-Fe-rich pargasite and Fe-rich pargasite-hornblende in the core of grains and actinolite 2, which crystallized on their margin (Fig. 17a). In the frame of the end members of amphiboles, as well as according to the chemical classification, the Fe-rich pargasite belongs to substitution area of actinolite 1-hornblende-edenite-Fe-rich pargasite-tschermakite (Fig. 17a). Fe-rich pargasite on the rim is always replaced by new actinolite 2 (Figs. 6e-f, 7a, 7e and 17a). Fe-rich pargasite has variegated Na_2O content from 2.54 to 5.79 wt.% (Table 4). According to chemical classification, Fe-rich pargasite belongs to the group of Ca amphiboles (Leake, 1978, 1997; Deer et al., 1992). Analyses with high content of Na_2O (above 4.5 wt.%) place the Fe-rich pargasite on the boundary of Na-Ca amphiboles (Fig. 17a). In Fe-rich pargasite the main Al-Si bound in the chemical formula $ABC(Al_1^{VI})Al_2^{IV}$-Si_6 represents pargasite (Table 4). From this structure of chemical formula the Fe-rich pargasite was found also in until published analyses $ABC(Al_1^{VI})Al_{2\text{-}1.5}^{IV}Si_{6\text{-}6.5}$ (Hovorka et al., 1988) or $ABC(Al_{1.1\text{-}0.53}^{VI})Al_{1.9\text{-}1.5}^{IV}Si_{6.1\text{-}6.5}$ (Faryad & Bernhardt, 1996). Analyses in these works belong to chemically bound Fe-rich pargasite, not taramite, which has differing structure of chemical formula $ABC(AI_2^{VI})$ $AI_2^{IV}Si_6$ in comparison with pargasite $ABC(Al_1^{VI})Al_2^{IV}Si_6$ (Deer et al., 1992; Leake, 1997; Zhang et al., 1995; Radvanec 1999 and 2000).

In the metagabbro mylonite in the localities Šajby and Dobšinský potok the edenite from **M1b** substitution row of Ca amphiboles is on the margins replaced by actinolite 2 (Figs. 9f, 10f and 17d). In the tectonic breccia of metagabbro in the Ostrá locality the actinolite 2 prevails in the metamorphism **M1b**, which in the matrix replaces the diopside 2, or actinolite 2 was found on the margins of the grains around hornblende-actinolite (Figs. 8 and 17b). In the metagabbro from the Zadné Porče locality we have found the mixture of actinolite 1 and actinolite 2 (Figs. 11 and 17e).

During the younger metamorphism **M1b** in all investigated localities there crystallized zonal Ca amphiboles with the core formed of actinolite 1, edenite, hornblende or Fe-rich pargasite, having their margins always replaced by actinolite 2 in the retrograde metamorphism in the amphibolite and/or epidote amphibolite facies (Fig. 17).

Pumpellyite

In the metagabbro of all localities the pumpellyite replaces the Sr-rich epidote and clinozoisite-epidote1. In these minerals the pumpellyite has idiomorphic shape, forming heels and containing Mg (Figs. 8c, 14, 15a-b, Table 2). Pseudomorphs after pumpellyite are common and originated by the retrograde metamorphism of pumpellyite to epidote in P-T conditions of amphibolite or epidote-amphibolite facies during the younger metamorphism **M1b** (Figs. 14 and 15). Chemical composition of this epidote after pumpellyite is close to clinozoisite-epidote1 or the same as epidote 2. Relics after pumpellyite together with actinolite 1 were found enclosed in the Fe-rich pargasite. In albite the pumpellyite was found together with HP amphiboles (Figs. 6e a 7e). We have found Fe-rich pumpellyite with variegated composition of Fe^{2+} (Fig. 18, Table 2) in the matrix, though do not containing Mg. It is enclosed together with actinolite 1 and in thin section the Fe pumpellyite differs from the epidote by striae. Fe-rich pumpellyite is relatively older than pumpellyite from the alterations in Sr-rich epidote and clinozoisite-epidote 1. Both pumpellyite forms originated in retrograde HP metamorphism in the pumpellyite-actinolite facies of older metamorphism **M1a**.

Grossular and andradite

In the metagabbro from the localities Ostrá and Babiná, the Ca garnet occurs in small irregular grains – relics large up to 0.05 mm, together with the plagioclase relict. The grossular relic encloses albite in diopside 1 (obr. 6e). The zonal Ca garnet was found in diopside 1. It has originated during metamorphism from the decomposition of former magmatic Ca plagioclase (bytownite), being in diopside 1 enclosed. Aggregates or zonal grains of Ca garnets are formed in the core by grossular and at the margin it is replaced by andradite, while the younger andradite forms also individual aggregates together with titanite and calcite in the matrix. Grossular is older than andradite (Figs. 7f, 19). In the metagabbro matrix we have found the homogeneous grossular, being enclosed in clinozoisite-epidotite 1 or in clinozoisite-epidotite 1, where were found its

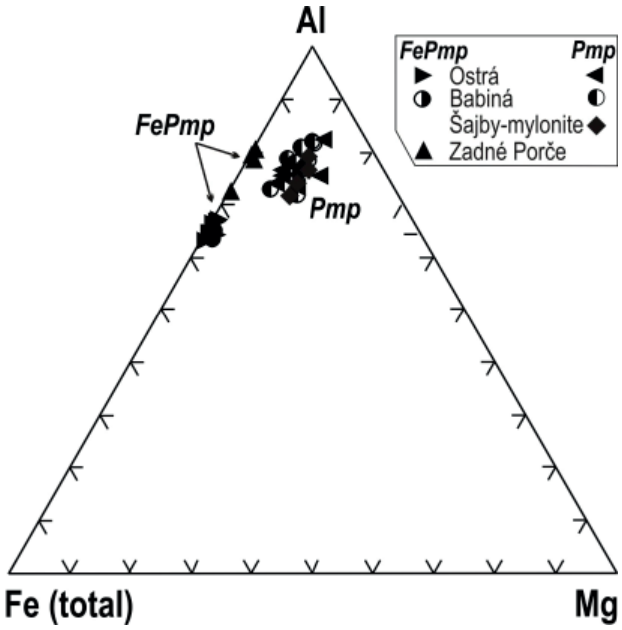

Fig. 18. Chemical classification of Fe-rich pumpellyite and pumpellyite (FePmp and Pmp) in triangle Fe-Mg-Al diagram.

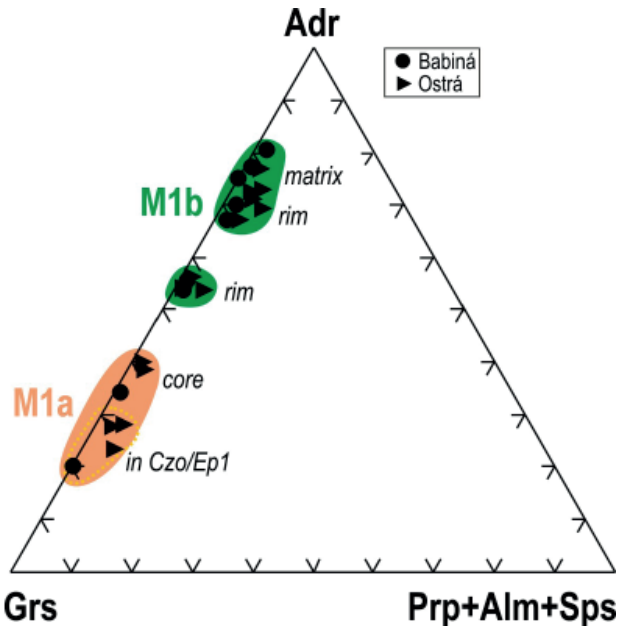

Fig. 19. Chemical classification of Ca garnets in Cpx/SrEp metagabbro from localities Babiná and Ostrá.

relics (Fig. 29). Andradite was not found in clinozoisite-epidotite 1.

According to chemical classification, the Ca garnets have variegated composition from grossular to andradite (Gross = 17.4–79.5 mol.%, And = 20.3–80.4 %, Alm = 0-5 %, Prp = 0-2.6 %, Spes = 0.1–3.1 %, Uvar = 0–1.5 %). The whole Fe content in Ca garnets is bound in the form of Fe^{3+} and in Ca garnet there is substitution instead of Al. Rare andradite with the content up to 30 mol.% of uvarovite $(Ca_{3,04}Mg_{0.03})_{3,07}(Cr_{0,50}Ti_{0,02}Fe^{3+}_{1,31}Al_{0.10})_{1,93}Si_3O_{12}$ indicates its origin from the chronite by metamorphic reaction in the amphibolite facies **M1b**. Homogeneous grossular originated together with Sr-rich epidote at the beginning of **M1a** metamorphism in P-T conditions of the decomposition of magmatic Ca plagioclase (bytownite) and Na/Ca/Sr feldspar (Fig. 29a). Andradite originated during the younger metamorphic event **M1b**. It is replacing the former grossular or occurs in cracks in the matrix also alone in the assemblage with chlorite- epidote 2 and biotite.

Fe phlogopite-eastonite (biotite)

In investigated localities Babiná, Ostrá, Ostrá (brekcia) and Šajby (mylonite) the dark mica occurs in the form close to Fe phlogopite-eastonite = biotite (Fig. 20). In the metagabbro of the Ostrá and Babiná localities with chlorite it fills the cracks in diopside 1 or occurs in diopside 1 cracks individually and separately of aegirine-augite (Figs. 6a and 6e). In the matrix the biotite was found with K feldspar, albite, pargasite and actinolite 2 and in chemically similar form also at the margin of epidote 2 together with chlorite, phengite, K feldspar and albite (Figs. 6c, 6f, 9c and 9e). The origin of biotie was carried out in metamorphic event **M1b**.

White micas

In the Ostrá locality the Al-rich celadonite (Si = 3.74–3.78 apfu; Table 3) forms mixture with K feldspar and jadeite (Fig. 21). This assemblage is enclosed in the clinozoisite-epidote 1 and Al-rich celadonite has originated from K feldspar during the HP metamorphism **M1a**. In the matrix and besides clinozoisite-epidote 1 in locality

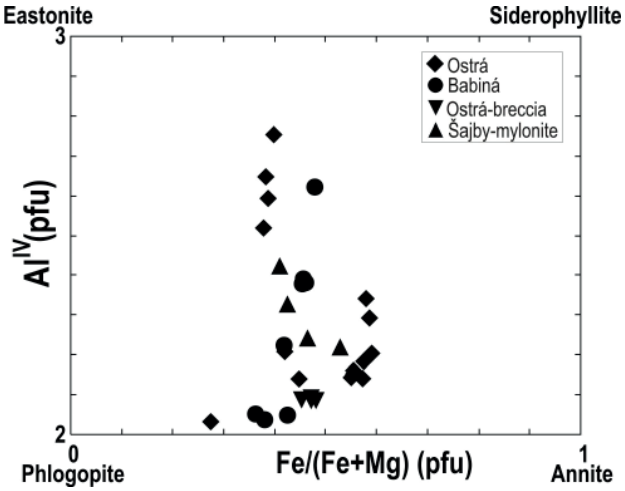

Fig. 20. Chemical classification of Fe phlogopite-eastonite = biotite in Cpx/SrEp metagabbro from investigated localities.

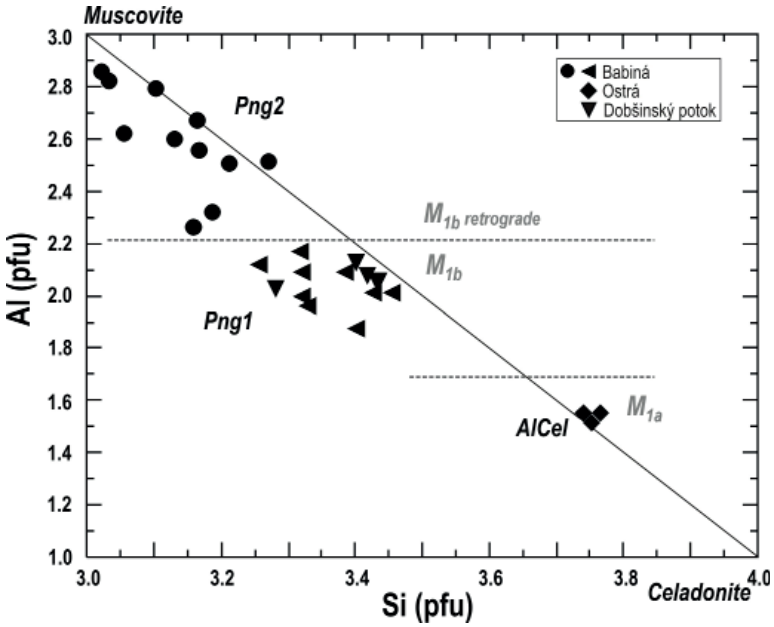

Fig. 21. Chemical classification of phengites (Png 1, Png 2) and Al-rich celadonite (AlCel) in polymetamorphosed Cpx/SrEp metagabbro. **M1a** – metamorphism (Carboniferous age); **M1b** – prograde and retrograde metamorphism (Permian age).

Babiná and the mylonite of Dobšinský potok locality the phengite 1 (Si = 3.26-3.46) occurs with K feldspar, forming the crystalline mixture and in the Babiná locality it rims K feldspar. The ratio Mg/(Mg+Fe) of phengite 1 from these localities ranges from 0.59 to 0.69. According to accompanying mineral assemblage chlorite and biotite, the phengite 1 was formed by reaction with K feldspar in younger metamorphic event **M1b**. Phengite 2 (Si = 3.02-3.21) also has formed in younger, retrogradne metamorphism **M1b** at lower pressure as phengite 1. Phengite 2 is enclosed in epidote 2, or it occurs in the rock matrix together with chlorite (Fig. 21).

Chlorite

Chlorite in all three investigated localities belongs to the group of the most frequently occurring minerals in the metagabbro. In the metagabbro matrix it has crystallized with pumpellyite, albite, actinolite 1, calcite and incompletely it replaces the diopside 1 in mylonite of the Šajby and Dobšinský potok localities, as well as the group of epidote a amphiboles. According to chemical classification of Si and Fe^{2+} + Fe^{3+} contents in chemical formula, in the diopside 1 cracks there crystallized brunsvigite with the ratio Mg/(Mg+Fe) = 0.46. In the matrix there occurs prevailingly the ripidolite with the ratio 0.5-0.6 and in the assemblage with biotite, epidote 2 and calcite there occurs the ripidolite – pycnochlorite with the ratio 0.6-0.7. Chlorite has originated during both metamorphisms **M1a** and **M1b**.

Further minerals

In localities Babiná and Šajby (mylonite) the Fe-rich sepiolite with the ratio Mg/(Fe^{2+}+Mg) = 0.3 in the assemblage with chlorite, albite, amphiboles and calcite occurs. Fe-rich sepiolite formed within the metamorphic event **M1a** in the pumpellyite-actinolite facies (Fig. 9b). Chemically pure calcite originated at the end of **M1a** metamorphism, as well as with chlorite, Fe sepiolite. In **M1b** metamorphism the calcite often replaces all epidote group minerals, fills cracks in the rock, where it occurs in assemblage with actinolite 2, as well as in the matrix with chlorite.

Large grains of pseudobrookite/armalcolite were during metamorphism **M1a** unstable and were replaced to mixture of ilmenite, rutile and hematite. This mixture is replaced by younger titanite, which originated in **M1b** metamorphism (Fig. 7a, 9a and 29b).

Ilmenite is a common mineral in the metagabbro. Smaller grains of ilmenite are at the margins always replaced to titanite, or the ilmenite is completely replaced to titanite. Titanite belongs to common minerals of the metagabbro in all localities. In the diopside 1 the inclusions of bravoite and argentite were rarely found. In the Zadné Porče locality the badelleyite is replaced by zircon (Fig. 11b and 29c). Pyrrhotine ($Fe_{0.98}S$) occurs only rarely in the matrix of metagabbro.

Polymetamorphic mineral assemblages in the CaFNaA projection and the exhumation P-T-t path of the metagabbro

In investigated localities the mineral assemblages A and B characterize the changes or stages of gradual metamorphism of the metagabbro from the solidus/subsolidus stages through the epidote eclogite facies, blueschist facies and pumpellyite-actinolite facies during the older metamorphism **M1a**. The changes in mineral assemblage in the stage C were performed in younger and timely separated metamorphism **M1b** in the amphibolite and epidote-amphibolite facies (Figs. 22–26). CaFNaA diagrams show the plotting positions of the typical minerals of Cpx/SrEp metagabbros according to Spear (1995). The construction of P-T-t path of the metagabbro exhumation is based on gradual changes of metamorphogenic mineral assemblages (A, B and C) and their stability at various P-T conditions of metamorphic events **M1a** and **M1b** (Fig. 28).

The results of the zircons dating show that the mineral assemblages have originated in the metagabbro for a long time from Ordovician to Permian. The mineral assemblag-

es were gradually formed first in the mantle of magmatic stage (Ordovician). Than the solidus assemblage is dated by the Mississippian age, when the gabbro was solidified in the subducted lower crust and obtained the coarse-grained texture (Figs. 2a, 2b and 4). Afterwards at P-T conditions of the A stage of the **M1a** metamorphism the gabbro was in the epidote-eclogite facies. Subsequently the metagabbro was exhumed in the subduction channel in B stage, firstly in the retrograde metamorphism **M1a** in blueschist facies and followingly in P-T conditions of the pumpellyite-actinolite facies. At the changed P-T conditions or during the reached exhumation from epidote-eclogite facies to blueschist facies around 600 ° C there originated new prismatic zircon dated to Upper Carboniferous (Pennsylvanian). The exhumed metagabbro blocks were mainly in the brittle regime deformed in blueschist and pumpellyite-actinolite facies conditions **M1a**. In locality Ostrá there originated a tectonic breccia from exhumed metagabbro and in the Šajby and Dobšinský potok localities there originated a metagabbro mylonite (Fig. 2). Exhumation of the metagabro from the epidote-eclogite facies through the blueschist facies into the P-T conditions of pumpellyite-actinolite facies represents older metamorphic-tectonic cycle **M1a** of the Variscan orogeny, dated by the zircon from the Lower (348 Ma) to Upper Carboniferous (307 Ma) (Figs. 22–27).

All tectonic blocks of metagabbro from **M1a** in investigated localities were again metamorphosed in the Permian, where in the metagabbro originated new zircon, having the age of 261 Ma. New Permian metamorphism of the Variscan orogenesis **M1b** contributed with the overheating in the amphibolite and epidote-amphibolite facies due to the effects of the hot line, causing the ductile deformation of the rocks. In the metapelite the overheating in P-T conditions of the amphibolite facies reached 650 °C and caused the anatectic melting and the origin of S-types of granites (Radvanec et al., 2007, 2010; Németh et al., 2016). In the metagabbro of the Ostrá and Babiná localities the mineral assemblage with the pargasite amphibole originated in amphibolite facies of **M1b** stage (Figs. 22 and 27). In further localities of the metagabbro the **M1b** metamorphism reached conditions of the epidote-amphibolite facies (Fig. 23–27). In the Gemeric unit the **M1b** metamorphism distinctly overwrites the products of older metamorphic event **M1a**. The areal distribution of revealed metamorphic facies in the Gemeric unit is visualized in Fig. 1.

Magmatic stage of the gabbro – a reconstruction

The initial and former metamorphic gabbro is evidenced by the magmatic Ordovician zircon ages 485-458 Ma (Putiš, personal communication, Putiš et al., 2009). In this initial stage and next solidification, the gabbro obtained coarse-grained texture (Fig 2a and 2b). The magmatic stage has formed magmatic phenocrysts of feldspars (bytownite-Sr/Ca/Na-rich feldspar-oligoclase-K feldspar--anorthoclase), diopside 1, anthophyllite, kearsutite, Mg chromite-chromite and decomposed pseudobrookite/armalcolite (Fig. 3). During the early magmatic stage, the baddeleyite is replaced by the zircon (Figs. 11b and 29c). According to thermodynamic data of Holland & Powel

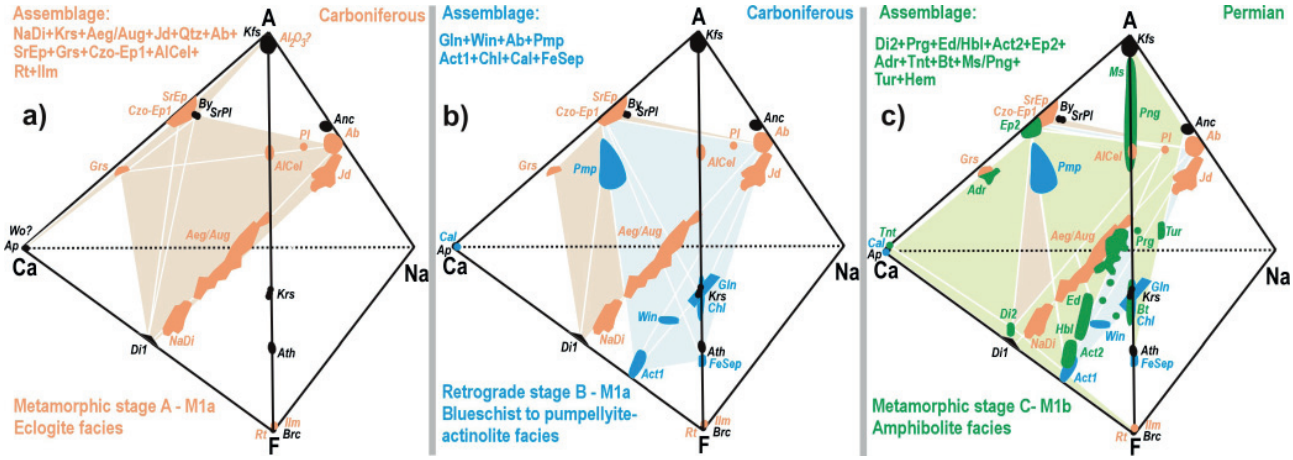

Fig. 22. a-c – CaFNaA diagrams showing the plotting positions of the minerals of primary gabbro (black) and the subsequent metamorphic mineral assemblages of Cpx/SrEp metagabbro were formed by stages from A to C in localities Babiná and Ostrá. Di1, 2 – diopside 1, 2; SrPl – Sr-rich feldspar; By – bytownite; Kfs – K feldspar; Anc – anorthoclase; Ant – anthophyllite Krs – kearsutite; Brc – pseudobrookite/armalcolite; Ilm – ilmenite; Ap – apatite; NaDi – Na-rich diopside; Aeg/Aug – aegirine/augite; Jd – jadeite; Ab – albite; Pl – plagioclase; SrEp – Sr-rich epidote; Czo-Ep1 – clinozoisite-epidote 1; Rt – rutile; Grs – grossular; Pmp – pumpellyite; Act1-2 – actinolite 1, 2; Win – winchite; Gln – glaucophane; Chl – chlorite; Tnt – titanite; Cal – calcite; Hbl – hornblende; Ed – edenite; Prg – pargasite; Tur – tourmaline; Hem – hematite; Bt – biotite; FeSep – Fe-rich sepiolite; Png – phengite; Ms – muscovite; Ep2 – epidote 2; Grs-Adr – grossular-andradite rim of grossular. The metamorphic evets from A to C represent exhumation of the former lower crust gabbro toward the surface in Carboniferous (**M1a**) and Permian (**M1b**) periods of the Variscan orogeny.

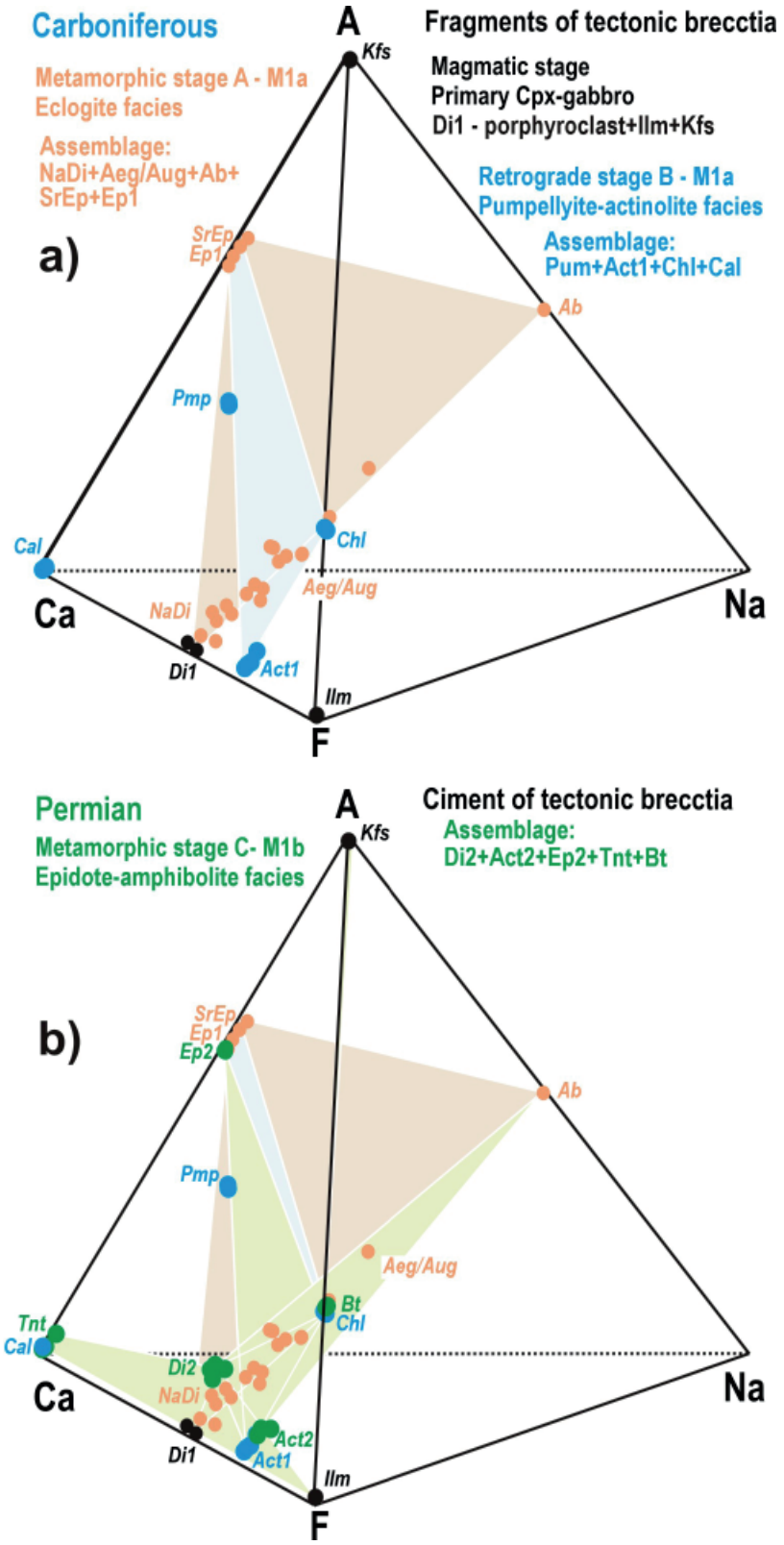

Fig. 23. CaFNaA diagrams showing the plotting positions of the minerals in tectonic breccia on the Ostrá hill. **a –** Mineral assemblages of subsequent metamorphic events A and B formed the Cpx/SrEp metagabbro of Carboniferous age in **M1a**. **b –** New and dominant metamorphic event – stage C of **M1b** replaced the former mineral assemblages of **M1a** and finalizes the formation of tectonic breccia during the rock exhumation in this locality. Abbreviations of minerals are explained in Fig. 22.

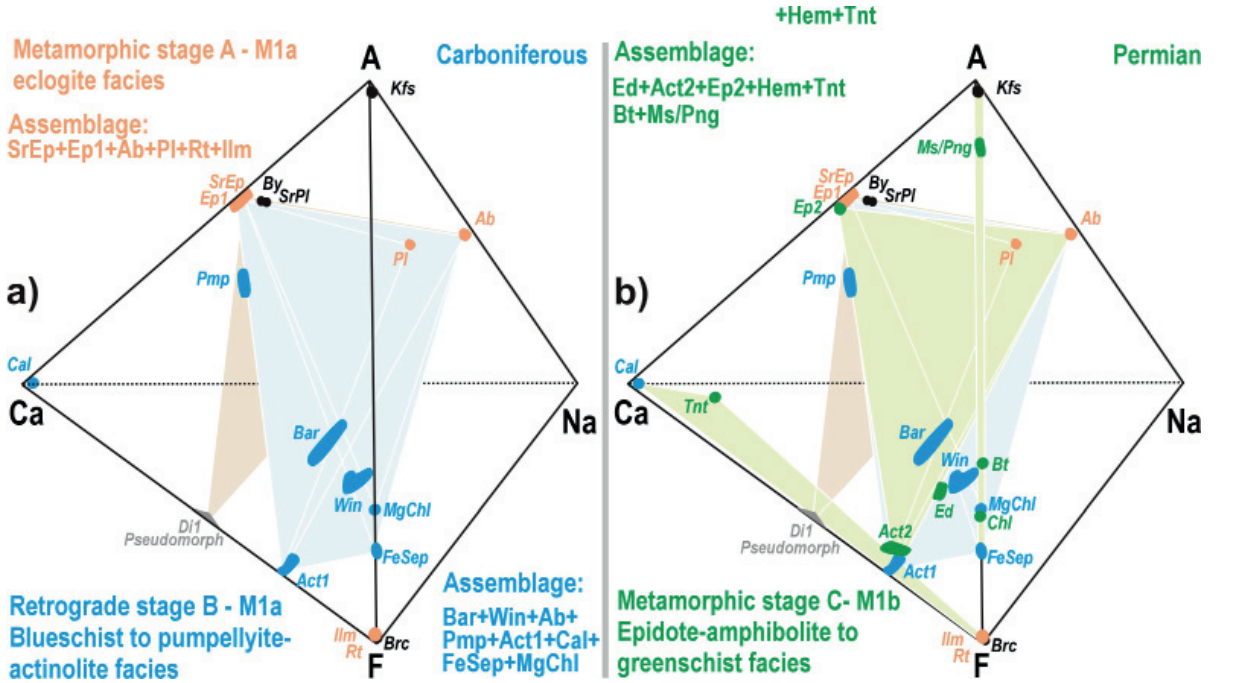

Fig. 24. CaFNaA diagrams showing the plotting positions of the minerals in the mylonite of Cpx/SrEp metagabbro on the Šajby mountain range. **a –** Mineral assemblages of subsequent metamorphic events A and B formed the Cpx/SrEp metagabbro of Carboniferous age in **M1a** event. **b –** New metamorphism – stage C of **M1b** event replaced the former mineral assemblages of **M1a** event and finalizes the formation of mylonite during the rock exhumation in this locality. Bar – barroisite. Others abbreviations of minerals are explained in Fig. 22.

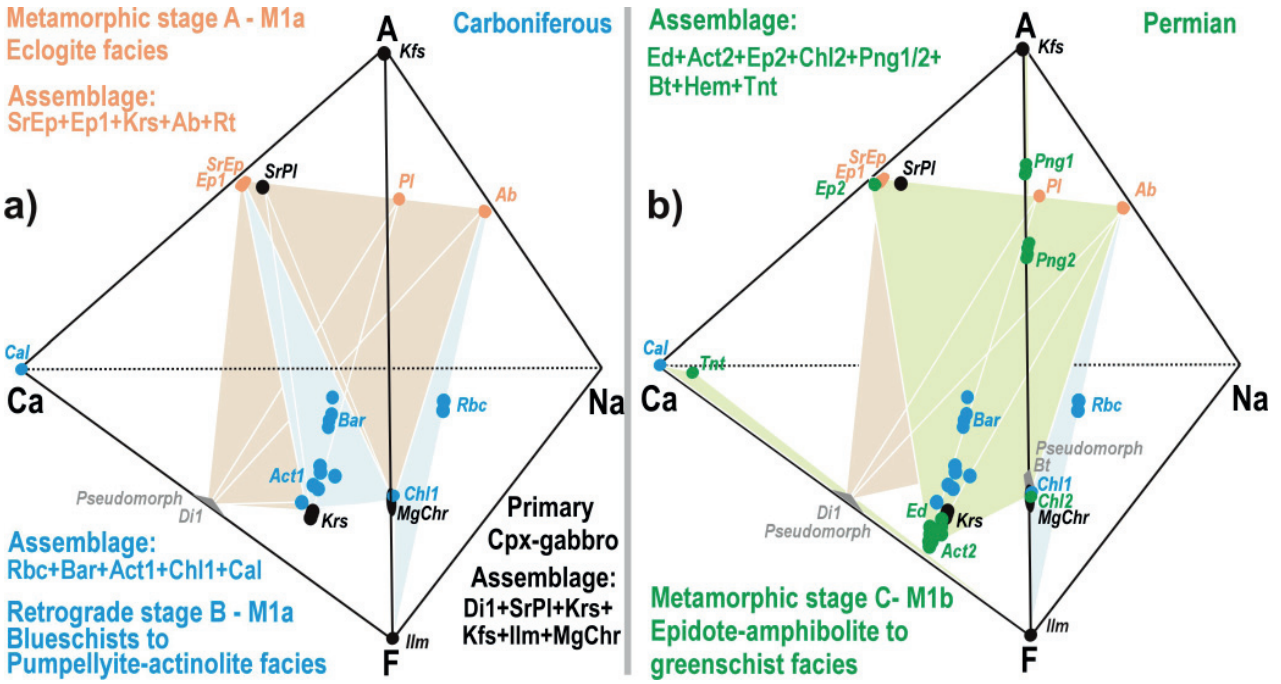

Fig. 25. CaFNaA diagrams showing the plotting positions of the minerals in the mylonite of the Cpx/SrEp metagabbro from the Dobšinský potok locality. **a –** Mineral assemblages of subsequent metamorphic events A and B formed the Cpx/SrEp metagabro of Carboniferous age in **M1a** event. **b –** New and dominant metamorphism – stage C of **M1b** event overprinted the former magmatic minerals and assemblages of **M1a** event. The M1a finalises the formation of Cpx/SrEp metagabbro during the rock exhumation in this locality. Bar - baroisite; Rbc - riebeckite. Others abbreviations of minerals are explained in Fig. 22.

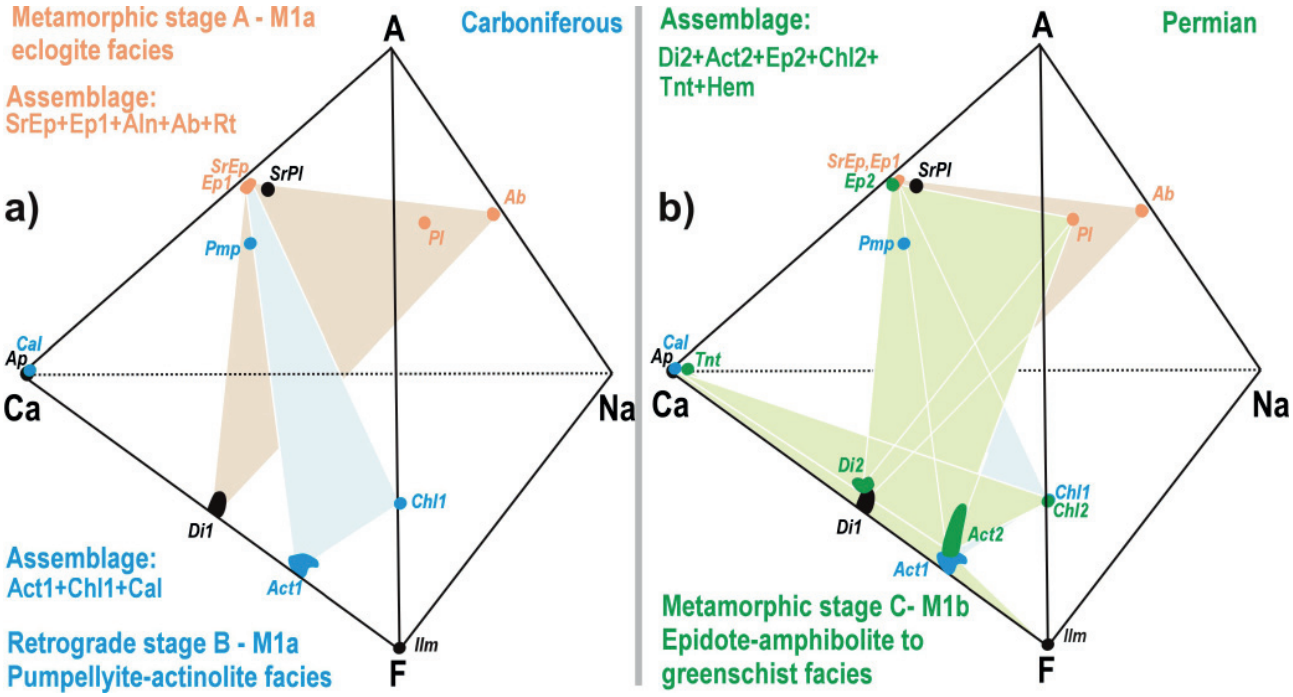

Fig. 26. CaFNaA diagrams showing the plotting positions of the minerals in the Cpx/SrEp metagabbro from the Zadné Porče locality. **a –** Mineral assemblages of subsequent metamorphism in stages A and B of Carboniferous age in **M1a** event. **b –** New metamorphism – stage C of Permian **M1b** event replaced the former mineral assemblages of **M1a** and finalises the formation and exhumation of Cpx/SrEp metagabbro in this locality. Abbreviations of minerals are explained in Fig. 22.

(1998) and Curtis & Sowman (1953), the P-T formation of zircon is determined by the reaction of badelleyite + quartz = zircon. The temperature of that replacement ranges from 1320 to 2000 °C and the presuure is below 10 kbar for that reaction (Fig. 28). The formation of zircon shows a fractionation of "hot magma" that is depending on the presence of the silica phases (quatz, cristobalite, SiO_2-lq) in the Si-saturated magma in the mantle. In this "hot magmatic" stage the fraction crystallization in the mantle ceased the formation of Sr/Ca/Na-rich feldspar that had a high content of the remnant Sr and REE. The existence of Sr/Ca/Na-rich feldspar formation was derived indirrectly from Sr-rich epidote, which has high contents of Sr and REE (Figs. 14–16). Petrological and structural data about Sr-rich feldspars are experimentally derived from crystallization of Sr/Ca-rich gel at the temperature 1350–1500 °C. Obtained data for synthetic Sr-rich feldspar on join of $CaAl_2Si_2O_8$ – $SrAl_2Si_2O_8$ as a model show a probable ordering in the natural Sr-rich feldspar that was possible formed at the temperature about 1350 °C, according to the inferred experimental data of Sr/Ca-rich gel (Tribaudino et al., 1995). Although the entry of Sr into natural plagioclase is of limited extent, the substitution of Ca by Sr to produce a synthetic analogue, $SrAl_2Si_2O_8$ was demonstrated by Bruno & Gazzoni (1968), who showed that a solid solution exists between anorthite and Sr feldspar. Single-crystals of stoichiometric $SrAl_2Si_2O_8$ were produced by Grundy & Ito (1974) from melts with an Al/Si ratio of unity, though in melts with Al/Si < 1, the resultant Sr feldspars had partially vacant alkali cation sites (e.g. $Sr_{0.84}Na_{0.03}\square_{0.13}Al_{1.69}Si_{2.29}O_8$). Mineralogical data about natural Sr-rich feldspars are absenting in the literature. Taking into account the chemical classification, normalized content of REE, immobile elements (IE), anortite component, Sr content in Ca plagioclase and the Sr content in epidote we reached a conclusion that former Sr/Ca/Na-rich feldspar and bytownite in the gabbro crystallized as porphyric phases from the alkaline magma, emplaced in the lower crust at high temperature 1350–1500 °C (Figs. 4 and 28). According to decomposition of these porphyroblasts of feldspar to mixture of Sr-rich epidote, clinozoisite/epidote 1, grossular and albite, it was confirmed that also in natural conditions the former magmatic feldspar had a composition of $(SrCaNa)(AlSi)_4O_8$. The metamorphic assemblage of Sr-rich epidote, clinozoisite/epidote 1, grossular and albite represents a decomposition minerals that were formed on the primary magmatic Sr/Ca/Na-rich feldspar. This assemblage supplies the pseudomorph on the area of former Sr/Ca/Na-rich feldspar in all studied localities (Figs. 2, 14 and 15).

The formation of former gabbro inicialy related to differentiation of the "hot magma" (T >1350–1600 °C) that was transported by a mantle plume up to the "cooler" upper mantle. Than this cryptocrystallized gabbro was transported by the upper mantle flow to the subducted lower crust in Carboniferous (Mississippian) age. Here in the subducted

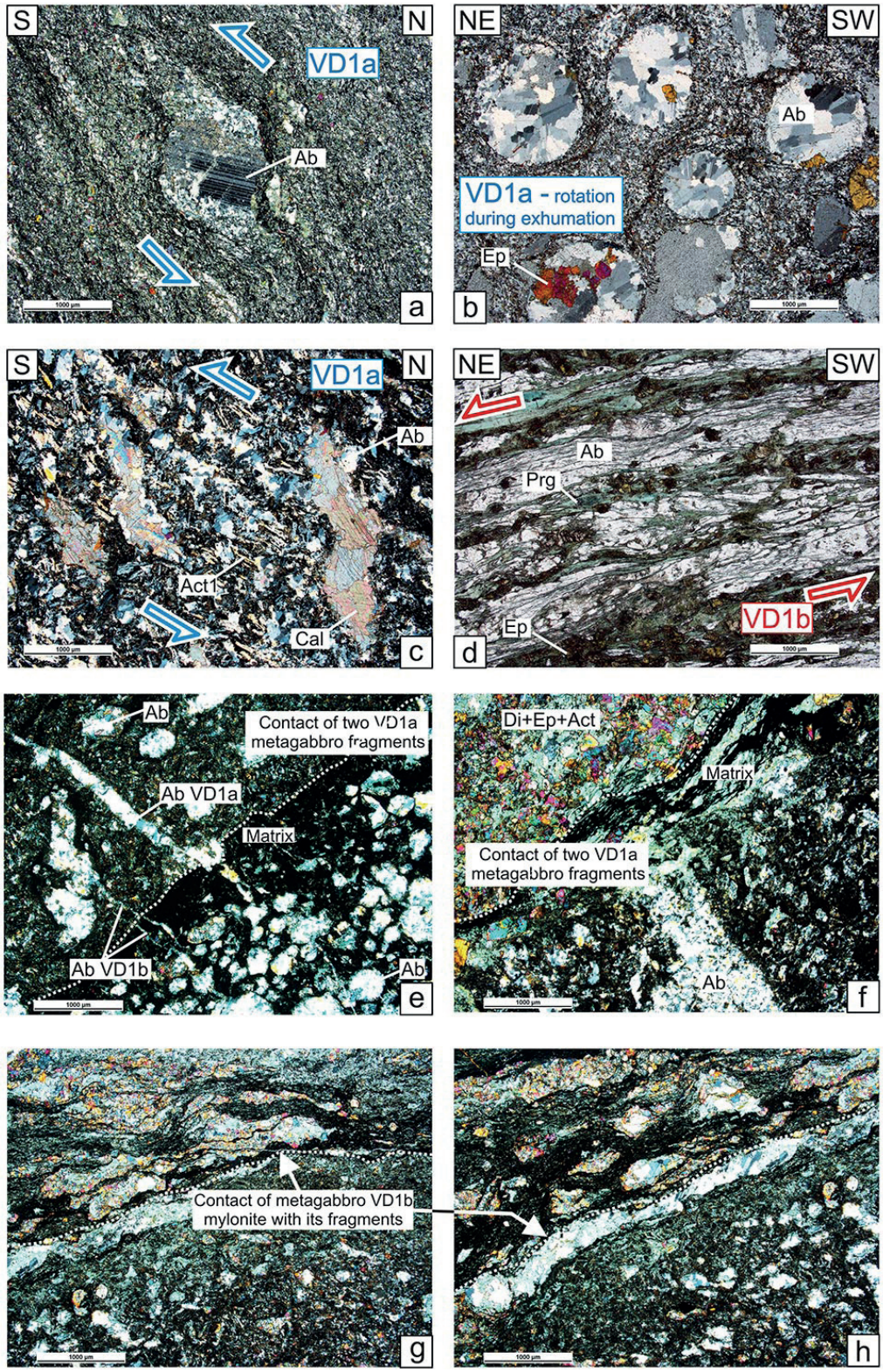

Fig. 27. Kinematics of **VD1a** (**M1a**) exhumation revealed in oriented thin sections in the Šajby locality. The sense of shearing (exhumation) is indicated by arrows. Each picture has indicated the real spatial orientation. In the case of rotated porphyroclasts (Ab + Ep) in 27b, they represent the pseudomorphs – the products of decomposition of former magmatic Sr/Ca/Na-rich feldspar to albite and Sr-rich epidote. It is evidenced in Fig. 15, where the X-ray mapping revealed the increased contents of Sr in the epidote, primarily occurring in the gabro Sr/Ca/Na-rich feldspar.

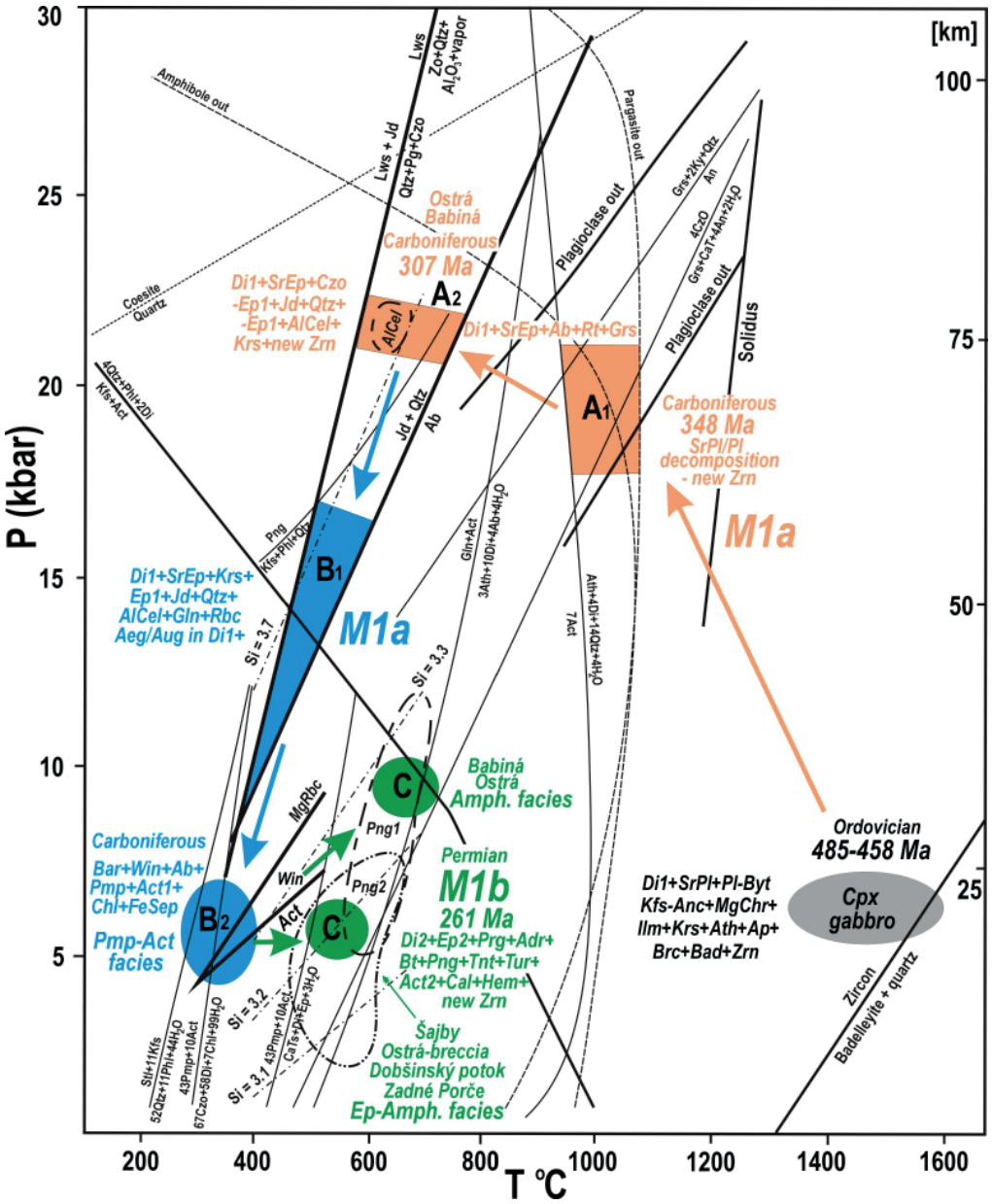

Fig. 28. P-T-t path of polymetamorphic events and mineral assemblages of Cpx/SrEp metagabbro exhumed from the mantle, encompassing the Ordovician stage and Lower Carboniferous solidus stage in the lower crust. $\mathbf{A_1}$ – eclogitization of the gabbro in prograde metamorphism **M1a** and origin of grossular (Grs) + Sr-rich epidote + clinozoisite-epidote 1(Czo-Ep1) + albite (Ab) from the former magmatic bytownite (Byt) and Sr/Ca/Na-rich feldspar (SrPl) in the field of plagioclase instability. **A2** – pressure peak of the **M1a** metamorphism and crystallization of Al-rich celadonite, jadeite (Jd) and quartz (Qtz) from albite (Ab) in the epidote-eclogite facies. **B1** – retrograde metamorphism **M1a** in blueschist facies and mineral assemblage glaucophane (Gln), riebeckite (Rbc) and aegirine-augite (Aeg/Aug) in diopside 1 (Di1). **B1** – retrograde metamorphism **M1a** in pumpellyite-actinolite facies and mineral assemblage barroisite (Bar), winchite (Win), pumpellyite (Pmp), actinolite 1 (Act1), chlorite (Chl), Fe-rich sepiolite (FeSep). **M1a** – Carboniferous metamorphic event. C – New Permian metamorphism **M1b** in amphibolite facies, localities Babiná and Ostrá, as well as in epidote-amphibolite facies in localities Šajby, Ostrá (breccia), Dobšinský potok (mylonite) and Zadné Porče with mineral assemblage: diopside 2 (Di2), epidote 2 (Ep2), pargasite (Prg), andradite (Adr), biotite (Bt) phengite 1 and 2 (Png1 and Png2), tourmaline (Tur), actinolite (Act2), titanite (Tnt), calcite (Cal) and hematite (Hem). The boundary zircone is according to Holland & Povell (1998). Line of the phengite geobarometer Si = 3.1–3.7 is according to Massone & Schreyer (1987). The boundary plagioclase - out, amphibole - out is according to Cloos (1993). The boundary pargasite – out is according to Niida & Green (1999). The boundary solidus and plagioclase out is according to Ringwood (1975). Metamorphic reactions were calculated from the databases of Berman (1987). The field of Act-Pmp facies and the stability boundaries of MgRbc, Win and Act are according to Banno (1998). Further abbreviations:: K feldspar – Kfs, anorthoclase – Anc, chromite – MgChr, apatite – Ap, kearsutite – Krs, anthophyllite – Ath, clinopyroxene – CaT, kyanite – Ky, Mg riebeckite – MgRbk, pseudobrookite/armalcolite – Brc, baddeleyite – Bad, zircon – Zrc, rutile – Rt, ilmenite – Ilm.

lower crust the gabbro obtained the coarse-grained texture of the solidus at about 1000 °C and 70 km (Fig. 28). The whole-rock trace element spider shows the lower crust conditions at the gabbro formation (Figs. 3–5 and Table 1). However the mineral composition of the former gabbro shows an upper mantle radius in CaFNaA diagram (Fig. 3).

During the next exhumation of the gabbro in the subduction zone, the magmatic diopside 1 represented the stable phase persisting all that stages of exhumation, however the coexisting magmatic feldspar/plagioclase were completely decomposed to the epidote group, grossular and albite. The gabbro exhumation is well evidenced by the individual grains of diopside 1 that preserved and show older high-temperature ductile deformation of **VD1a** – **M1a**, as well as two younger lower temperature overprints during the **M1a** and **M1b** respectively. The ductile deformation of diopside 1 is evidenced by the infiltration of Na-rich fluid phase to form the metasomatic aegirine-augite lamellas in the host diopside 1 (Figs. 6b-c, 6f, 7a, 7f and 8a). The beginning of the lower temperature deformation in diopside 1 is evidenced by filling of the cracks by chlorite of **M1a** in blueschist/pumpellyte-actinolite facies. The next formation of **M1b** formed the individual biotite in cracks of diobside 1 (Fig. 6e) and this deformation was followed by filling of the cracks by chlorite and by biotite in the retrograde amphibolite/epidote-amphibolite facies (Figs. 6 and 7). The stability of diopside 1 and the decomposition of feldspar/plagioclase to the successive mineral assembla- ges are demonstrated by the BSE figures and in CaFNaA diagrams. That all in comparison to microstructural evidences well confirms the anticlockwise P-T-t path for the exhumation of metagabbro in **M1a** events (Fig. 28). If the P-T of **M1a** would be in the clockwise path, the magmatic diopside 1 would be completely decomposed to calcite and actinolite or chlorite in the pumpellyite–actinolite facies at the beginning of **M1a**. In such case the idiomorphic shape or a pseudomorph of diopside 1 would not be identified in the studied metagabbro.

A – stage of prograde high-pressure metamorphism M1a in epidote-eclogite facies

From the prograde high-pressure metamorphism **M1a** in epidote-eclogite facies in the studied metagabbro localities there was preserved the mineral assemblage diopside1, kearsutite, antophylite, Sr-rich epidote, rutile, ilmenite, grossular, clinozoisite-zoisite 1, Al-rich celadonite, jadeite, quartz, albite and zircon (Figs. 22-28). Gabbro was in the P-T conditions of solidus/subsolidus transported in the upper mantle to lower temperature and higher pressure conditions of **A1** and **A2** stages in the epidote-eclogite facies (Fig. 28). At this displacement of the gabbro into the epidote-eclogite facies the diopside 1, kearsutite and antophylite represented the stable phases, though the former gabbro was in this facies hydrated. The former magmatic feldspars (Sr/Ca/Na-rich feldspar, bytownite) after hydratation were decomposed according to the model reactions 1-7 (Windom & Boettcher, 1976; Holland, 1980; Berman, 1987; Koziol & Newton, 1988). The decompositon of pseudobrookite/armalcolite to rutile, ilmenite and hematite took place at the same P-T conditions as the decomposition of Sr/Ca/Na-rich feldspar – around 18–22 kbar and 1000–600 °C between **A1** and **A2** stages (reaction 1 and 2; Fig. 28). Despite, according to Green in Veblen and Ribbe, (1982) the ilmenite was at the transport of the metagabro instable even at the boundary of solidus – at 15–30 kbar and 1000–1100 °C (Fig. 29b). At the P-T conditions of the **A1** and **A2** stages in the epidote-eclogite facies of metamorphism **M1a** there originated the mineral mixture of Sr-rich epidote, clinozoisite-epidote 1, grossular, jadeite, quartz, Al-rich celadonite, rutile, ilmenite and albite in the places of former magmatic porphyroblasts of Sr/Ca/Na-rich feldspar and bytownite. Former grains of pseudobrookite/armalcolite at the P-T conditions of **A1** and **A2** stages in the epidote eclogite facies have decomposed by the similar way (Fig. 28). The hydratation of Al_2SiO_5 solid phase to Al-rich celadonite took place at P-T conditions of **A2** stage in the stability fied of jadeite + quartz, at the stability of zoizite/clinozoisite and the stability field of phengite (Si=3.7), but besides the stability field of lawsonite.

$$\underset{\text{Sr/Ca/Na-rich feldspar}}{\{(NaCa)(AlSi)_4O_8 - SrAl_2Si_2O_8\}} + \underset{\text{bytownite}}{(NaCa)(AlSi)_4O_8} +$$

$$\underset{\text{ilmenite}}{FeTiO_3} + H_2O \rightarrow \underset{\text{Sr-rich epidote}}{CaSrFe^{3+}Al_2Si_3O_{12}(OH)} + \underset{\text{albite}}{NaAlSi_3O_8} +$$

$$\underset{\text{rutile}}{TiO_2} + Al_2SiO_5 \qquad (1)$$

$$\underset{\text{pseudobrookite/armalcolite}}{FeTi_2O_5} \rightarrow \underset{\text{rutile}}{TiO_2} + \underset{\text{ilmenite}}{FeTiO_3} \qquad (2)$$

$$2\text{wollastonite} + \text{Ca plagioclase} = \text{grossular} + \text{quartz} \qquad (3)$$

$$\text{Ca plagioclase} = \text{grossular} + \text{kyanite} + \text{quartz} \qquad (4)$$

$$4\text{Ca plagioclase} + H_2O = 2\text{zoisite} + \text{kyanite} + \text{quartz} \qquad (5)$$

$$\text{Grossular} + \text{clinopyroxene (CaTs)} + 4\text{Ca plagioclase} + 2H_2O = 4\text{epidote group} \qquad (6)$$

$$\text{Albite} \rightarrow \text{jadeite} + \text{quartz} \qquad (7)$$

The reactions 1 and 2 are derived from the occurrence of metamorphogenic assemblage Sr-rich epidote, ilmenite, albite, rutile and the finding of magmatic bytownite

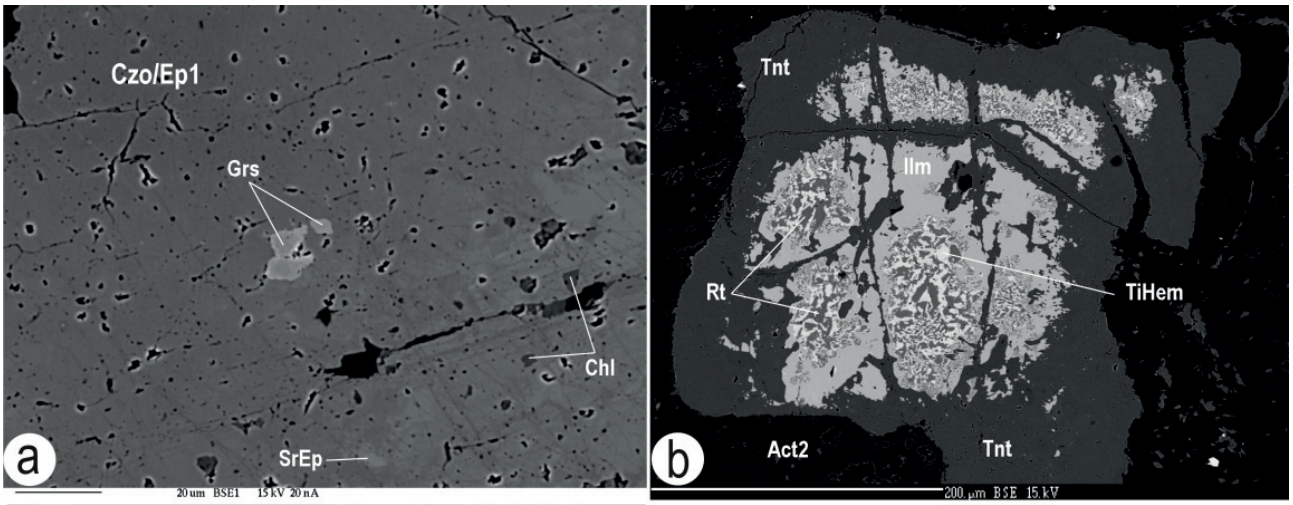

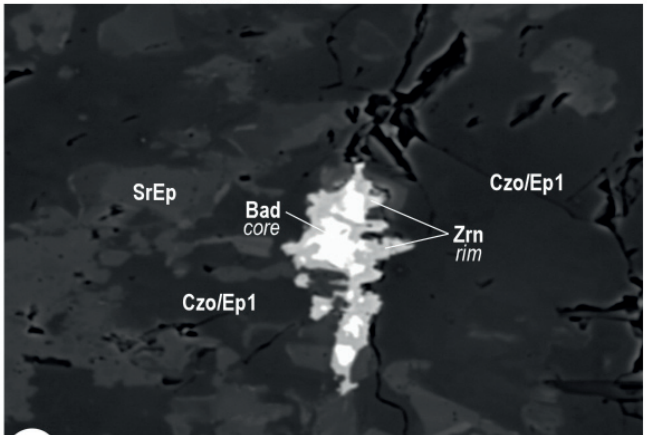

Fig. 29. a – Relic grossular (Grs) enclosed in clinozoisite/epidote1 (Czo/Ep1) in Cpx/SrEp metagabbro in locality Ostrá. Sr--rich epidote (SrEp); chlorite (Chl). **b –** decomposition of pseudobrookite/armalcolite to mixture of rutile (Rt) + ilmenite (Ilm) + Ti-rich hematite (TiHem) in metamorphism **M1a** and subsequent change of this mixture to titanite (Tnt) in new **M1b** overpring in the Šajby locality. **c** – Baddeleyite (Bad) is replaced by zircon (Zrn) in the magmatic stage of the gabbro. The replacent was revealed in the Sr-rich epidote (SrEp) – clinozoisite/epidote 1 (Czo/Ep1) matrix in the locality of Zadné Porče.

in the gabbro. From this assemblage, regarding the found pseudomorphs after Sr/Ca/Na-rich feldspar and pseudobrookite/armalcolite in the reactions there was derived the formula for Sr/Ca/Na-rich feldspar and the formula for pseudobrookite/armalcolite (Figs. 15 and 27a-b). The P-T conditions of these reactions are estimated in the P-T fields of the stability of known reactions 3-6. Their courses are visualized and referred in Fig. 28.

The corroded grossular, originating according to reactions (3) and (4) was preserved in the shape of fine clusters and relics together with jadeite and quartz in the clinozoisite-epidote 1 (Fig. 7c and 29a). The main quantity of grossular in the metagabbro was derived from reaction (3). There was accepted the assumption that the former gabbro at the boundary of subsolidus contained besides Ca and Sr feldspars also wollastonite (Fig. 29). The formation of anortite and wollastonite from the reaction of grossular and quartz was studied by Windom & Boettcher (1976): The reaction (3) was investigated at 1100 °C, using plagioclase of intermediate composition to determine a shift of the equilibrium pressure as a function of the composition at P-T conditions representative of the Earth`s lower crust and upper mantle. Using model reaction (3), in our case, the bytownite Xan = 88 mol.% occurs at 15.5 kbar and oligoclase Xan = 20 mol% shows the upper limit of about 19 kbar for the decomposition of plagioclase in gabbro. The 15.5-19 kbar and 1100 °C represent a possible P-T conditions for the formation of grossular and quartz in the solidus of gabbro that was eclogized between stages **A1** and **A2** in **M1a** metamorphic event (Fig. 28).

B – Stage of retrograde HP metamorphism M1a and exhumation of metagabbro in the blueschist and pumpellyite-actinolite facies

The metagabbro exhumation from the epidote-eclogite facies to stage **B1** of blueschist facies took place in the retrograde metamorphic path **M1a** in the field of stability of jadeite, quartz, glaucophane, zoisite/clinozoisite and besides the stability field of lawsonite (Fig. 28). The lamellas of Na-rich diopside and aegirine-augite originated in the diopside 1 (Figs. 6b-c, 6f, 7a, 7f, 8a, 12 and 28). According to projection in CaFNaA diagrams, these lamellas originated by the reaction diopside 1 + albite + Sr-rich epidote/clinozoisite-epidote 1 sensu Spear (1995) in conditions of epidote-eclogite facies (Fig. 22a). Indivi-

dual lamellas have irregular shape and variegated chemical composition from Na-rich diopside to aegirine-augite (Figs. 12 and 22). Lamellas originated gradually at the boundary of ductile and brittle deformation of individual mineral phases at ca 600 °C and ratio 20–15 kbar during the metagabbro exhumation in P-T conditions from **A2** to **B1** (Fig. 28). At this exhumation the glaucophane and riebeckite originated in the matrix (Figs. 6e, 10d and 17). The assemblage of Sr-rich epidote, grossular, clinosoisite-epidote 1, jadeite, quartz, diopside 1, anthophyllite keasrutite and Al-rich celadonite from the previous epidote-eclogite facies were in the blueschist facies of **B1** stages (Fig. 28). In the stage **B1** the jadeite forms inclusions of dimensions up to 50 µm together with quartz. They were found also around Sr-rich epidotes and in clinozoite-epidote 1 (Figs. 7c).

The metagabbro exhumation in the retrograde metamorphism **M1a** in **B1** stage of blueschist facies continued by the decrease of pressure and temperature into the metamorphic stage **B2** of pumpellyite-actinolite facies (Fig. 28). During this stage of metagabbro exhumation the jadeite and quartz changed to albite according to retrograde reaction (7). Albite forms in clinozoisite-epidote 1 oval grains, occurring together with non-reacted ones (Figs. 6d and 7c-d). The oval albite in clinozoisite-epidote 1 occurs frequently. This albite represents pseudomorphs after jadeite + quartz, originating in the albite stability field at the decrease of the pressure below 13 kbar and temperature below 500 °C (Fig. 28). At the end of HP metamorphism at P-T around 7 kbar and 450 °C there originated barroisite and winchite in exhumed metagabbro. Barroisite and winchite were found in the matrix and cracks in diopside 1, winchite has grown on glaucophane (Fig 6e). The margins of barroisite and winchite are replaced with cooexisting actinolite 1, being partly replaced to chlorite (Figs. 9c-d, 10d and 17).

In the stage **B2** of **M1a** metamorphism the metagabbro underwent the pumpellyite-actinolite facies overprint at 7–5 kbar and 320–390 °C (Fig. 28). In all investigated metagabbro localities at this conditions the Sr-rich epidote and clinozoisite-epidote 1 were partially replaced to Fe and Mg pumpellyite (Figs. 14–15). Pumpellyite originated by the hydratation of epidote according to following reaction (Deer et al., 1992):

$$\underset{\text{epidote group}}{4Ca_2Fe^{3+}_{0.68}Al_{2.34}Si_{3.10}O_{12}(OH)} + 5H_2O \rightarrow$$

$$\underset{\text{pumpellyite}}{2Ca_4\,Fe^{2+}Fe^{3+}Al_4Si_6O_{21}(OH)_7} + 0.5O_2$$

The blueschist to pumpellyite facies transition is characterized by the change of assemblage clinozoisite/epidote 1 + chlorite to pumpellyite + actinolite 1 (Figs. 22-26). Besides pumpellyite and actinolite 1 into this metamorphic assemblage belong also chlorite, Fe sepiolite and calcite (Fig 9b). The emplacement of tectonic blocks of exhumed metagabbro in conditions of pumpellyite-actinolite facies into sediments of Upper Carboniferous accretion prism was estimanted to time around 300 Ma. P-T conditions of pumpellyite-actinolite facies correspond to the depth of 20 km (Deer, 1995).

Concerning exhumation kinematics observable in the microscale, the asymmetric microstructures (rotated porphyroclasts, secondary foliation, synthetic and antithetic microshears) in a series of oriented thin-sections manifested the sense of shearing (exhumation) from top-to-the-WSW through top-to-the-S to top-to-the-ESE, which generally confirms the south-vergent exhumation kinematics (Fig. 27). The breccia in the Ostrá locality represents the final stage of exhumation in shallower levels, because represents the evidence of the colder post-mylonitization cataclastic flow of **M1a** (**VD1a**). The secondary compaction of the breccia is attributed to metamorphic recrystallization in **M1b**.

C – Stage of new prograde metamorphism M1b of the metagabro in amphibolite and/or epidote-amphibolite facies

Exhumed tectonic blocks of metagabbro, being during Carboniferous **M1a** event gradually metamorphosed in the eclogite-epidote facies up to the pumpellyite-actinolite facies, were in Permian again recrystallized during new Variscan **M1b** metamorphic overprint. This new metamorphism changed metagabbro in all investigated localities within the temperature range 500–650 °C and pressure 5–10 kbar. In localities Babiná and Ostrá it was in conditions of amfibolite facies, in further localities in epidote-amphibolite facies (Fig. 28). The intensity of new metamorphism **M1b** distinctly changed the mineral assemblages of older metamorphism **M1a**. In amphibolite facies revealed in localities Babiná and Ostrá there originated the assemblage diopside 2, pargasite, edenite-hornblende, epidote 2, andradite, titanite, biotite, phengite 1 and 2, actinolite 2, tourmaline and hematite (Fig. 22c). In the epidote-amphibolite facies in localities Ostrá (breccia), Šajby, Dobšinský potok and Zadné Porče originated the assemblage diopside 2, epidote 2, edenite, actinolite 2, titanite, phengite 1 and 2, biotite, chlorite and hematite (Figs. 23b, 24b, 25b and 26b). Besides pargasite and andradite, which originated in amfibolite facies in localities Babiná and Ostrá, the mineral assemblaged of both facies are the same (Fig. 28). Magmatic K-feldspar reacted in P-T conditions of amphibolite as well as epidote-amphibolite facies with chlotite and in metagabbro there originated the biotite, phengite 1 and phengite 2 (according to reaction

chlorite + K-feldspar = biotite + phengite/muscovite; Fleet 2003). Biotite fills the cracks in diopside 1 individually and separately from older lamellas of aegirine-augite or biotite fills cracks in diopside 1 together with chlorite (Figs. 6a, 6e-f). Biotite in the matrix occurs in assemblage with chlorite, albite, phengite 1, quartz and actinolite 2 (Figs. 9e and 10b). In all localities during metamorphism **M1b** there originated titanite. It occurs individually or at the margin of the mixture of rutile + ilmenite + hematite (Figs. 6-11 and 29b). In amphibolite as well as epidote amphibolite facies titanite originated from the reaction: rutile/ilmenite + calcite + quartz = titanite + CO_2 (Spear, 1995).

Geotectonic model of the origin, exhumation and polymetamorphic overprint of the Cpx/SrEp gabbro

In Gemeric unit the coarse-grained Cpx/SrEp gabbro (gabbro in the following text) was revealed in individual tectonic blocks in several localities (Fig. 1). Cpx/SrEp gabbro was polymetamorphosed, cataclastic (breccia) and mylonititic. The former mineral composition of the gabbro is bearing signs of well crystallized alkaline magma (Figs. 2, 3, 4 and 28). The gabbro crystallization took place during long interval without the origin of more significant amount of amphibolites in Ordovician at 1350–1600 °C and followingly at the boundary of solidus and amphibolite stability around 1200 °C (Fig. 28). Sufficient time for crystallization of silicates allowed the formation of coarse-grained fabric of the gabbro with porphyroblasts of feldspars and idiomorphic shape of diopside 1. Feldspar porphyroblasts and magmatic diopside 1 have the same grain-size up to 2 cm (Fig. 2).

In the Lower Carboniferous before 348 Ma at the boundary of the solidus, the former crypto-crystalline Ordovician gabbro started to interact with the mantle a subducted material beneath the lower crust and the continental plate. At the solidus boundary, the convection flow/displacement of the mantle transported and sinked gabbro to the edge of hanging continental plate towards the contact of subducted lower crust material with the mantle. The fragment of the gabbro was pulled by this flow into the mantle up to P-T conditions of instability of bytownite and Sr/Ca/Na-rich feldspar at temperature around 1000 °C in the depth ca 70 km. It is also near the solidus existence boundary (Fig. 28). In this stage **A1** the gabbro was hydrated and the interaction of gabbro and fluid deliberated from the subduction zone caused the decomposition of bytownite and Sr/Ca/Na-rich feldspar to clinozoisite/epidote 1, Sr-rich epidote and grossular in epidote eclogite facies. Here reacted also earlier crystallized pseudobrookite/armalcolite and the deliberated amount of Fe^{3+} from the pseudobrookite/armalcolite have passes to the metamorphogene silicate in the form of direct substitution Fe^{3+} = X_{Al} in epidote group and partially also in the grossular (Figs. 16 and 19). The bytownite and Sr-rich feldspar decomposition in the epidote eclogite facies was dated by the zircon to Lower Carboniferous (Figs. 28 and 30). Hydrated and metamorphosed gabbro changed its specific weight and in the mantle environment it moved into the area of the contact of subducted and exhumed material beneath the hanging wall of subduction zone. In this area the temperature was lowered to 660–700 °C and the metagabbro was in the depth of ca 75 km metamorphosed in the stage **A2**. The decrease of the temperature in the zone beneath the hanging wall caused the upward pulling of the light material with a high amount of water (Fig. 30). This stage of metamorphism – **A2** – in the epidote eclogite facies was determined as Upper Carboniferous - 307 Ma - by the zircon dating. After the crystallization of the jadeite, quartz, clinozoisite/epidote 1, Sr-rich epidote, grossular, Al-celadonite i.e. in the pressure peak of the **A2** metamorphism, the metagabbro exhumed towards the surface isothermally, but the pressure during exhumation sharply lowered. Metagabbro was exhumed through the blueschist up to P-T conditions of pumpellyite-actinolite facies. In the Ostrá locality during the metagabbro exhumation there originated the tectonic breccia. Metagabbro and its tectonic breccia were in the conditions of brittle deformation exhumed to the depth around 25 km at 300 °C (Fig. 28). The ductile deformation overprint revealed most strikingly in localities Šajby and Dobšinský potok is represented by the pervasive mylonitization, causing the origin of numerous porphyroclasts prevailingly of plagioclase/feldspar and diopside 1 pseudomorphs in the fine-grained matrix (Fig. 2a, b, e), and in advanced stage leading to origin of banded ultramylonites (Fig. 2f, g h). The dip of mylonitic foliation is to N-NNW and moderately inclined stretching lineation of prevailing E-W and ENE-WSW trend indicate at the beginning the transpressional trend of exhumation (Fig. 27). The younger brittle deformation regine, revealed only locally in the Ostrá (breccia) locality, is manifested by the origin of numerous metagabbro fragments within the rock, where most of them are rounded, indicating the rotation kinematics during the exhumation (Fig. 2j). It means that the metagabbro exhumed in the cold type of subduction at the temperature gradient around 6 °C/km (Cloos, 1993). The exhumation of the metagabbro was caused by the reverse movement or reverse, exhumation scrolling of subducted rocks synchronously Variscan subduction. The reverse movement of the mantle in the area of subduction plate is explained by the model by Ernst & Liou (1995). At the beginning of exhumation from the P-T conditions of epidote eclogite facies the metagabro recrystallized in blueschist facies of the stage **B1**. In localities Ostrá, Babiná, Šajby and Dobšinský potok there originated the aegirine-augite, riebeckite, glaucophane and jadeite was

replaced to albite. During the exhumation the metagabbro was constantly in the interaction with the colder fluid deliberated from the subducted material. At the end of exhumation the metagabbro reached the P-T conditions of the isotherm 350 °C, which course in the subduction zone was calculated by Trouw et al. (1998). It represents the conditions of the pumpellyite-actinolite facies (Banno, 1998), which finally overprinted the exhumed metagabbro in Upper Carboniferous around 300 Ma in the stage **B2**. In this period the tectonically separated fragments of metagabbro exhumed into Lower Paleozoic metasedimets.

In the period from Upper Carboniferous (300 Ma) to Permian the tectonic blocks of metagabbro were a part of displacements of exhumed Lower Paleozoic rocks in the accretion prism. In Permian (261 Ma) the blocks of metagabbro were again metamorphosed in amphibolite and epidote amphibolite facies of the metamorphism **M1b**, when on the northern and southern hot line of Paleo-Gemeric unit, parallel with the axis of collision orogen, the anatectic melting and the origin of S-type granite took part (Radvanec et al., 2007; 2010). In the depth around 15–18 km, resp. 30 km and close to hot line there crystallized new mineral assemblages, which in all localities dominantly changed and overprinted mineral assemblages of previous metamorphism **M1a** (Fig. 28).

Conclusion

The presented Ordovician coarse-grained gabbro (485–458 Ma; zircon ages), has a unique mineral composition of Ca/Na/Sr-rich feldspar (decomposed to Sr-rich epidote; SrO content reaches up to 14 wt.%), diopside, bytownite, K feldspar, anortoclase, anthophyllite, kearsutite, spinel, baddeleyite and decomposed pseudobrookite/armalcolite. It was solidified in Ordovician to Lower Carboniferous and transported by the mantle plume (T = 1350–1600 °C) than by upper mantle to subducted lower crust. The gabbro originated before the active Silurian-Devonian divergence caused the onset of rifting and the origin of the rift zone and subsequent oceanic crust. Hence, when the active Carboniferous subduction process has started, the gabbro was located above the asthenosphere in the lower continental crust away of the rift zone and gradually forming oceanic crust.

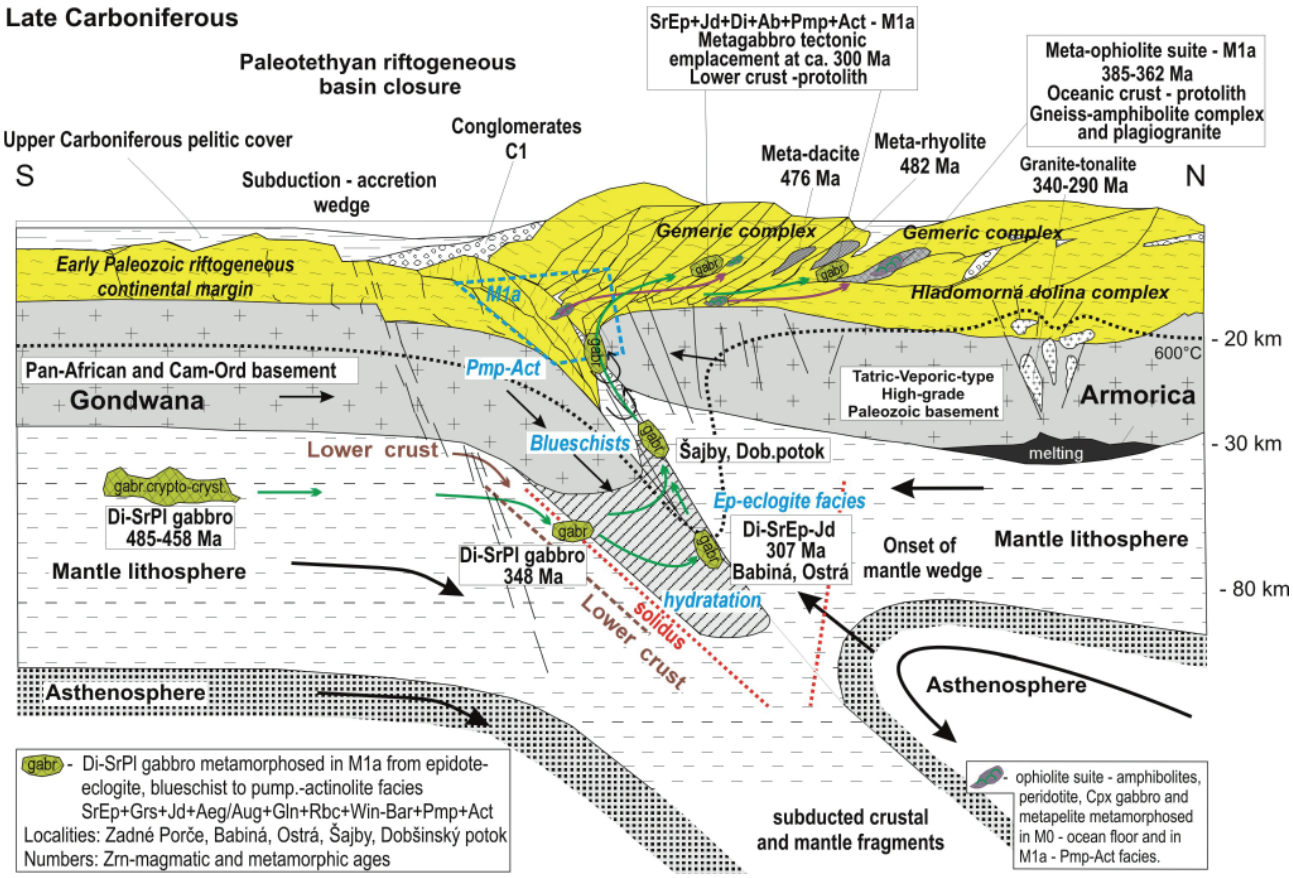

Fig. 30. Model of the origin of Cpx/SrEp metagabbro in the mantle, solidus, lower crust and its eclogitization and exhumation in the initial stage of Carboniferous subduction. Model updates the former geotectonic model of the evolution of Paleo-Gemeric unit in the Carboniferous (Grecula & Radvanec, 2005; Grecula et al., 2011; Radvanec & Grecula, 2016), being completed also with the age of rocks (Putiš et al., 2009).

The gabbro solidification in the subducted lower crust is the reason, why the chemical classifications of the whole-rock analyses characterize the solidus stage of the gabbro to be of the lower crust origin and not of the mantle origin in all studied localities. However the minerals composition of the gabbro shows an upper mantle radius in CaFNaA diagram.

During the Carboniferous exhumation (348–307 Ma; new generation of zircons), the lower crust gabbro blocks were hydrated and metamorphosed in several successive steps: from the epidote-eclogite facies through the blueschist and finaly the pumpellyite-actinolite facies. Here the exhumation of individual blocks has stopped. This high pressure metamorphic and exhumation evolution (**M1a; VD1a**), was revealed in all investigated localities. In the Ostrá locality, the exhumation of the metagabbro was besides mylonites accompanied also with the origin of tectonic breccia, consisting of metagabbro fragments within the fine-grained matrix of the same mineral composition, while, in localities Šajby and Dobšinský potok, the exhumed metagabbro manifests ductile mylonitic/ultramylonitic fabric.

During the next exhumation of gabbro from the lower crust and/or polymetamorphic events, the magmatic diopside 1 was generaly stable phase persisting all stages of exumation, however the coexisting magmatic feldspars were completely decomposed to the epidote group, grossular and albite. This occurrence in the relation to the successive mineral assemblages shoving in BSE figures, CaFNaA diagrams and that all in comparison to microstructural evidences well confirm the anticlolockwise P-T-t path for the exhumation of metagabbro in **M1a** evolution. If the P-T-t of **M1a** would be in the clockwise path, the magmatic diopside 1 would be completely decomposed to calcite and actinolite or chlorite in the pumpellyite-actinolite facies at the beginning of **M1a**. In such case the idiomorphic shape or a pseudomorph of diopside 1 would not be identified in the studied metagabbro.

In Permian – at ca. 261 Ma, partly exhumed **M1a** metagabbro blocks were metamorphosed again in the amphibolite (Babiná, Ostrá), or epidote-amphibolite facies (Dobšinský potok, Ostrá-breccia, Šajby, Zadné Porče), and subsequent retrograde greenschist facies. This Permian metamorphism (**M1b).** VD1b, VD2 was a product of the overheating above an increased heat flow zone or a hot line.

Acknowledgment

The presented data and results were obtained during several decades lasting research on regional, tectonic and metallogenetic projects funded by the Ministry of Environment of the Slovak Republic. Authors greatly appreciate also fruitful discussions and recommentations by Profs. Marián Putiš and Ján Spišiak, which increased the quality of primary manuscript.

References

Bajaník, Š., 1975: Pillow lavas of the Rakovec Group in the Spišsko-gemerské rudohorie Mts. *Geol. Zbor. Geol. carpath., 26, 341 – 348.*

Bajaník, Š., 1976: To petrogenesis of Devonian volcanic rocks of the Spišsko-gemerské rudohorie Mts. *Západ. Karpaty, Sér. Mineral. Petrogr. Geochém. Lož., 2, 75 – 94.*

Bajaník, Š., Ivanička, J., Mello, J., Pristaš, J., Reichwalder, P., Snopko, L., Vozár, J. & Vozárová, A., 1984: Geologická mapa Slovenského rudohoria – východná časť 1 : 50 000. *Bratislava, Geol. Úst. D. Štúra.*

Banno, S., 1998: Pumpellyite-actinolite facies of the Sanbagawa metamorphism. *J. metamorphic Geol., 16, 117 – 128.*

Berman, R. G., 1987: Geocalc. Software of the University of Brithish Columbia. *Vancouver, Canada VGT2B4.*

Brastad, K., 1985: Sr metasomatism and partition of Sr between the mineral phases of a meta-eclogite from Bjórkedalen, west Norway. *Tscliermaks minerál, petrogr. Min. TMPM, 34, 87 – 103.*

Bruno, E. & Gazzoni, G., 1968: Feldspati sintetici della serie $Ca(Al_2Si_2O_8)$-$Sr(Al_2Si_2O_8)$. *Atti Accad. Sci. Torino Cl. Sci. fis. mat. nat., 102, 81 – 93.*

Cloos, M., 1993: Lithospheric buoyancy and collisional orogenesis: subduction of oceanic plateaus, continental margins, island arcs, spreding ridges, and seamonts. *Geol. Soc. Amer. Bull. 105, 715 – 737.*

Curtis, C. E. & Sowman, H. G., (1953): Investigation of the thermal dissociation, reassociation, and synthesis of zircon. *J. Amer. ceram. Soc., 36, 6, 190 – 198.*

Deer, W. A., Howie, R. A. & Zussman, J., 1992: An Introduction to the Rock-Forming Minerals. Sec. ed. *Longman Scientific Technical, 1 – 696.*

Faryad, S. W. & Bernhardt, H. J., 1996: Taramite-bearing metabasites from Rakovec (Gemeric Unit, the Western Carpathians). *Geol. Carpath., 47, 349 – 357.*

Grapes, R. & Watanabe, T., 1984: Al-Fe^+ and Ca-Sr^+ epidotes in metagreywacke- quartzofeldspathic schist, Southern Alps, New Zealand. *Amer. Mineralogist, 69, 490 – 498.*

Grecula, P., 1982: Gemerikum – segment riftogénneho bazénu Paleotetýdy. *Miner. Slov. – Monogr. Bratislava, Alfa, 1 – 263.*

Grecula, P. (ed.), Abonyi, A., Abonyiová, M., Antaš, M., Bartalský, B., Bartalský, J., Dianiška, I., Drnzík, E., Ďuďa, R., Gargulák, M., Gazdačko, Ľ., Hudáček, J., Kobulský, J., Lörinz, L., Macko, J., Návesňák, D., Németh, Z., Novotný, L., Radvanec, M., Rojkovič, I., Rozložník, L., Rozložník, O., Varček, C. & Zlocha, J., 1995: Ložiská nerastných surovín Slovenského rudohoria. Zv. 1. *Bratislava, Geocomplex, 1 – 829.*

Grecula, P. & Radvanec, M., 2005: Geotectonic model of Gemericum. *Miner. Slov., 37, 193 – 198.*

Grecula, P. (ed.), Kobulský, J., Gazdačko, Ľ., Németh, Z., Hraško, Ľ., Novotný, L. & Maglay, J., 2009: Geologická mapa Spišsko-gemerského rudohoria. 1 : 50 000. *Bratislava, Št. Geol. Úst. D. Štúra.*

Grew, E. S., Locock, A. J., Mills, S. J., Galuskina, I. O., Galuskin, E. V. A. & Halenius, U., 2013: Nomenclature

of the garnet super group. IMA report. *Amer. Mineralogist, 98,785 – 811.*

Grundy, H. D. & Ito, J., 1973: The refinement of the crystals structure of a synthetic nonstechiometric Sr feldspar. *Amer. Mineralogist, 59, 1 319 – 1 326.*

Hawthorne, F. C., Oberti, R., Harlow, G. E., Maresch, W. V., Martin, R. F., Schumacher, J. C. & Welch, M. D., 2012: IMA report, nomenclature of the amphibole supergroup. *Amer. Mineralogist, 97, 2 031 – 2 048.*

Holland, T. J. B., 1980: The reacton albite = jadeite + quartz determined experimentaly in range 600-1200 ºC. *Amer. Mineralogist, 65, 129 – 134.*

Holland, T. J. B. & Powell, R., 1998: An internally consistent thermodynamic data set for phases of petrological interest. *J. Metamorph. Geol., 16, 309 – 343*.

Hovorka, D., Ivan., P., Jilemnická, I. & Spišiak, J., 1988: Petrology and geochemistry of metabasalts from Rakovec (Paleozoic of Gemeric unit, Inner Western Carpathians). *Geol. Zbor. Geol. carpath., 39, 395 – 425.*

Hovorka, D. & Spišiak, J., 1998: Mesozoic Meliata ocean dismembered ophiolites. In: Rakús, M. (ed.): Geodynamic development of the Western Carpathians. *Bratislava, GS SR, D. Štúr Publishers, 81 – 88.*

Ivan, P., 1996: Problems of geodynamic evolution and geological structure of the Paleozoic Gemeric unit (Inner Western Carpathians) as inferred by magmatic rocks study. *Slovak Geol. Mag, 3 – 4/96, 239 – 244.*

Ivan, P., 1997: Rakovec and Zlatník Formations: two different relics of the pre-Alpine back-arc basin crust in the Inner Western Carpathians. In: Grecula, P., Hovorka, D. & Putiš, M. (eds.): Geological evolution of the Western Carpathians. *Bratislava, Miner. Slov. – Monogr., 281 – 288.*

Ivan, P. & Hovorka, D., 2000: Metabazity na vrchu Babiná a Ostrá (Rakovecká skupina): Metabazity so znakmi nízkostupňovej subdukčnej metamorfózy alebo ultravysokotlakovo eklogitizované gabrá? Diskusia. *Miner. Slov., 32, 2, 141 – 145.*

Kanagawa, K., Shimano, H. & Hiroi, Y., 2008: Mylonitic deformation of gabbro in the lower crust: A case study from the Pankenushi gabbro in the Hidaka metamorphic belt of central Hokkaido, Japan. *J. struct. Geol., 30, 1 150 – 1 166.*

Kobulský, J., Gazdačko, Ľ., Grecula, P., Hojnoš, M., Kandrík, M., Kováčik, M., Németh, Z., Pramuka, S., Radvanec, M., Szalayiová, V. & Tréger, M., 2001: Atlas geomáp Spišsko-gemerského rudohoria. Záver. správa. *Manuskript. Bratislava, archive St. Geol. Inst. D. Štúr.*

Koziol, A. M. & Newton, R. C., 1988: Redetermination of the anorthite breakdown reaction and improvement of the plagioclase-garnet-Al_2SiO_5-quartz geobarometer. *Amer. Mineralogist, 73, 216 – 223.*

Lang, H. M. & Gilotti, J. A., 2001: Plagioclase replacement textures in partially eclogitised gabbros from the Sanddal mafic-ultramafic complex, Greenland Caledonides. *J. metamorphic Geol., 19, 497 – 517.*

Leake, B. E., 1978: Nomenclature of amphiboles. *Amer. Mineralogist, 68, 1 023 – 1 052.*

Leake, B. E., 1997: Nomenclatures of amphiboles: Report of the Sub-committee on Amphiboles of the International Mineralogical Association, Commission on New Minerals and Mineral Names. *Amer. Mineralogist, 82, 1 019 – 1 037.*

Massone, H. J. & Schreyer, W., 1987: Phengite geobarometry based on the limiting assemblage with K-feldspar, phlogopite and quartz. *Contr. Mineral. Petrology, 96, 212 – 223.*

Morimoto, N., 1988: Nomenclature of Pyroxenes. *Mineral. Petrol., 39, 55 – 76.*

Nagasaki, A. & Enami, M., 1998: Sr-bearing zoisite and epidote in ultra-high pressure (UHP) metamorphic rock from the Su--Lu province, eastern China: An important Sr reservoir under UHP conditions. *Amer. Mineralogist, 83, 240 – 247.*

Niida, K. & Green, D. H., 1999. Stability and chemical composition of pargasitic amphibole in MORB pyrolite under upper mantle condition. *Contr. Mineral. PetrolOgy, 135, 18 – 40.*

Németh, Z., 2002: Variscan suture zone in Gemericum: Contribution to reconstruction of geodynamic evolution and metallogenetic events of Inner Western Carpathians. *Slovak Geol. Mag., 8, 3 – 4, 247 – 257.*

Pearce, J. A. & Cann, J. R., 1973: Tectonic setting of basic volcanic rocks determined using trace element analyses. *Earth planet. Sci. Lett., 19, 290 – 300.*

Passchier, C. W. & Trouw, R. A. J., 2005: Microtectonics. Berlin – Heidelberg, Springer-Verlag, 1 – 366.

Plašienka, D., Grecula, P., Putiš, M., Kováč, M. & Hovorka, D., 1997: Evolution and structure of the Western Carpathians: An overview. In: Grecula, P., Hovorka, D. & Putiš, M. (eds.): Geological evolution of the Western Carpathians. *Bratislava, Miner. Slov. – Monogr., 1 – 24i.*

Putiš, M., Ivan, P., Kohút, M., Spišiak, J., Siman, P., Radvanec, M., Uher, P., Sergeev, S., Larionov, A., Méres, Š., Demko, R. & Ondrejka, M., 2009: Meta-igneous rocks of the West-Carpathian basement, Slovakia: Indicators of Early Paleozoic extension and shortening events. *Bull. soc. géol. France, 180, 6, 461 – 471.*

Radvanec, M., 1998: Vysokotlaková metamorfóza vrchnokarbónskeho konglomerátu z lokality Rudňany-Svinský hrb na severe gemerika. *Miner. Slov., 30, 95 – 108.*

Radvanec, M., 1999: Eklogitizované klinopyroxenické gabro s retrográdnou metamorfózou v pumpellyitovo-aktinolitovej fácii na vrchu Babiná a Ostrá (gemerikum). *Miner. Slov., 31, 467 – 484.*

Radvanec, M., Konečný, P., Németh, Z. & Grecula, P., 2007: P-T-t dráha a lokálne anatektické tavenie metapelitu s prímesou psamitického kremeňa vo variskej metamorfóze gemerika. *Miner. Slov., 39, 1 – 44.*

Radvanec, M., Németh, Z. & Bajtoš, P., 2010: Magnesite and talc in Slovakia: Genetic and geoenvironmental models. *Bratislava, St. Geol. Inst. D. Štúr, 1 – 130.*

Radvanec, M. & Grecula, P., 2016: Geotectonic and metallogenetic evolution of Gemericum (Inner Western Carpathians) from Ordovician to Jurassic. *Miner. Slov., 48, 2, 105 – 118.*

Radvanec, M., Németh, Z., Kráľ, J. & Pramuka, S., 2017: Variscan dismembered metaophiolite suite fragments of Paleo-Tethys in Gemeric unit, Western Carpathians. *Miner. Slov., 49, 1, 1 – 48.*

Raphanel, J., Dimanov, A., Nazarova, L. A., Nazarov, L. A. & Artemova, A. I., 2010: High temperature rheology of synthetic two-phase gabbroic aggregates: Microstructural heterogeneities and local deformation mechanism. *J. Mining Sci., 46, 5, 495 – 502.*

Rieder, M., Cavazzini, G. Dyakonov, Yu. S., Frank-Kamenetskii, V. A., Gottardi, G., Guggenheim, S., Koval', P. V., Müller, G., Neiva, A. M. R., Radoslovich, E. W., Robert, J.-L., Sassi, F. P., Takeda, H., Weiss, Z. & Wones, D. R., 1998: Nomenclature of the micas. *Canad. Mineralogist, 36, 905 – 912.*

Ridolfi, F. & Renzulli, A., 2012: Calcic amphiboles in calc-alkaline and alkaline magnas: thermobarometric and chemometric empirical equations valid up to 1,130 ºC and 2.2 GPa. *Contr. Mineral. Petrology, 163, 877 – 895.*

Ringwood, A. E., 1975: Composition and Petrology of the Earth's Mantle. *New York, McGraw Hill.*

Spear, F. S., 1995: Metamorphic Phase Equilibria and Pressure-Temperature-Time Paths. Monogr. *Mineral. Soc. America.*

Sun, S. S. & McDonough, W. F., 1989: Chemical and isotopic systematics of oceanic basalts; implications for mantle composition and processes. *In: Saunders, A. D. & Norry, M. J. (Eds.): Magmatism in the ocean basins. London, Geol. Soc. London, 42, 313 – 345.*

Tsuchiyama, A., 1985a: Dissolution kinetics of plagioclase in the melt of the system diopside-albite-anorthite, and origin of dusty plagioclase in andesites. *Contr. Mineral. Petrology, 89, 1 – 16.*

Tsuchiyama, A., 1985b: Partial melting kinetics of plagioclase-diopside pairs. *Contr. Mineral. Petrology, 91, 12 – 23.*

Trouw, R. A. J., Simóes, L. S. A. & Valladares, C. S., 1998: Metamorphic evolution of a subduction complex, South Shetland Islands, Antarctica. *J. metamorphic Geol., 16, 475 – 490.*

Tribaudino, M., Benna, P. & Bruno, E., 1995: I1-I2/c phase transition in alkaline-earth feldspars: Evidence from TEM observations of Sr-rich feldspars along the $SrAl_2Si_2O_8$-$CaAl_2Si_2O_8$ join. *Amer. Mineralogist, 80, 907 – 915.*

Veblen, D. R. & Ribbe, P. H., 1982: Amphiboles: Petrology and Experimental Phase Relations. *Rev. min., 9B, Mineral. Soc. Amer., 299.*

Windom, K. E. & Boettcher, A. L., 1976: The efect of reduced activity of anorthite on the reaction grossular + quartz = anorthite + wollastonite: a model for plagioclase in the Earth's lower crust and upper mantle. *Amer. Mineralogist, 61, 889 – 896.*

Winchester, J. A. & Floyd, P. A., 1977: Geochemical discrimination of different malpa8 series and their differentiation products using immobile elements. *Chem. Geol., 20, 325 – 343.*

Zellmer, G. F., Blake, S., Vance, D., Hawkesworth, Ch. & Turner, S., 1999: Plagioclase residence times at two island arc volcanoes (Kameni Islands, Santorini, and Soufriere, St. Vincent) determined by Sr diffusion systematics. *Contr. Mineral. Petrology, 136, 345 – 357.*

Zhang, Ru-Yuan., Hirajima, T., Banno, S., Cong, B. & Liou, J. G., 1995: Petrology of ultrahigh-pressure rocks from the southern Su-Lu región, eastern China. *J. metamorphic Geol., 13, 659 – 675.*

Zhou, Y. & He, Ch., 2015: Microstructures and deformation mechanisms of experimentally deformed gabbro. *Earth Sci., 28, 2, 119 – 127.*

Variská metamorfóza exhumovaných blokov metagabra bohatého na Cpx a Sr epidot v karbónskej epidotovo-eklogitovej fácii, fácii modrých bridlíc a pumpellyitovo-aktinolitovej fácii s permským prepracovaním v amfibolitovej fácii (gemerikum, Západné Karpaty)

Diopsid, jadeit, egirín-augit a epidot bohatý na Sr predstavujú asociáciu indexových minerálov Cpx/SrEp metagabra, ktoré bolo v karbóne v podobe samostatných tektonických blokov exhumované zo subdukčnej zóny. V súčasnosti sa tieto bloky zistili na severnom okraji gemerika na lokalitách Dobšinský potok, Ostrá, Babiná, Šajby, ale aj na juhu gemerika na lokalite Zadné Porče (obr. 1). Tieto tektonické bloky rovnakého Cpx/SrEp metagabra sa zistili v dobšinskej skupine (vrchný karbón) a v rakoveckom a jedľoveckom príkrove v zmysle tektonického členenia Greculu et al. (2009), resp. v rakoveckej aj gelnickej skupine v zmysle členenia Bajaníka et al. (1984).

Skúmané Cpx/SrEp metagabro je na všetkých lokalitách hrubo zrnité, s rovnakou veľkosťou pôvodného magmatického diopsidu a živcových porfyroblastov (do 3 cm; obr. 2). Toto gabro bolo zložené zo živca bohatého na Ca, Na a Sr, ktorý sa v metamorfóze rozpadol na zmes epidotu bohatého na Sr s obsahom SrO do 14 hmot. %. Gabro pôvodne obsahovalo aj bytownit, K-živec, anortoklas, antofylit, kearsutit, Mg-chromit/chromit, baddeleyit, pseudobrookit/armalcolit a pravdepodobne aj wollastonit (obr. 3, tab. 2).

Pseudobrookit/armalcolit sa v metamorfóze rozpadol na zmes ilment, rutil a hematit (obr. 29b). Podľa datovania zirkónu má pôvodné gabro ordovický predmetamorfný vek 485 – 458 mil. rokov. Tento vek sa zistil na lokalite Zadné Porče v zirkóne, ktorý vznikol premenou baddeleyitu v magmatickom štádiu (obr. 29c), keď „horúca magma" (1 350 – 1 600 °C – vznik zirkónu z baddeleyitu) z plášťového chochola prenikla do chladnejšieho vrchného plášťa (s teplotou okolo 1 100 °C) a vo vrchnom plášti čiastočne kryštalizovala. Tento ordovický magmatický proces predchádzal aktívnu divergenciu vrchnej kôry v silúre a devóne, keď v paleogemeriku vznikla riftová zóna s úplnou

ofiolitovou suitou hornín na morskom dne (Grecula, 1982; Grecula et al., 1995; Radvanec et al., 2017).

Medzi ordovikom a spodným karbónom bolo kryptokryštalické gabro v konvekčnom toku vrchného plášťa transportované k subdukčnej platni. V spodnom karbóne (348 mil. rokov) gabro na hranici solida v hĺbke okolo 70 km a pri teplote 1 100 °C a tiež v subdukovanej spodnej kôre kryštalizovalo. Tento vek zaznamenala nová generácia zirkónu na lokalite Ostrá (Putiš et al., 2009). Tu gabro získalo hrubo zrnitú textúru a celohorninové geochemické charakteristiky jeho kryštalizácie v spodnej kôre (obr. 2, 4 a 5). Následne bolo gabro vtiahnuté a transportované do subdukčnej zóny. V nej hydratovalo a pôvodné magmatické živce sa v podmienkach epidotovo-eklogitovej fácie stali nestabilnými. Na mieste magmatických živcových porfyroblastov vznikla zmes epidotu bohatého na Sr, grosuláru a albitu (obr. 14 – 16 a 19). Magmatický diopsid ostal stabilný. Cpx/SrEp metagabro v subdukčnej zóne exhumovalo z podmienok epidotovo-eklogitovej fácie vo vrchnom karbóne (307 mil. rokov). Zaznamenala to nová generácia prizmatického zirkónu na lokalite Ostrá (Putiš et al., 2009). Následne bolo Cpx/SrEp metagabro exhumované vo vrchných častiach subdukčnej zóny transportom typu „*roll-back*“ a zároveň aj postupne retrográdne metamorfované v podmienkach fácie modrých bridlíc až do pumpellyitovo-aktinolitovej fácie (obr. 6 – 14, 17 a 22 – 26). Táto variská **M1a** vysokotlaková metamorfóza vo vrchnom karbóne sa spája s postupnou mylonitizáciou Cpx/SrEp metagabra až do štádia ultramylonitizácie na lokalitách Šajby a Dobšinský potok (deformačné štádium **VD1a;** obr. 2d – h, 9, 10 a 27 a – c), ale aj so vznikom tektonickej brekcie na lokalite Ostrá (obr. 2j, 8 a 27e – h).

Jednotlivé bloky metagabra boli po exhumačnej metamorfóze v pumpellyitovo-aktinolitovej fácii znovu metamorfované v podmienkach epidotovo-amfibolitovej fácie a amfibolitovej fácie (**M1b;** obr. 6 – 14, 17 a 22 – 26). Túto novú permskú metamorfózu na horúcej línii zaznamenal nový okraj prizmatického zirkónu s vekom 261 mil. rokov (Putiš et al., 2009 a osobná inf.). Deformačné zmeny v Cpx/SrEp metagabre počas tejto novej variskej metamorfnej udalosti zaznamenali duktilné deformačné štádiá **VD1b** a **VD2** (obr. 27d).

Vznik gabra v ordoviku, jeho exhumácia v karbónskej subdukčnej zóne vrchného karbónu a následná permská metamorfóza sú zobrazené v P-T-t dráhe na obr. 28. Postupnosť vzniku minerálnych asociácií v CaFNaA projekcii je zobrazená na obr. 22 – 26. Geotektonické pozadie pohybu a exhumácie Cpx/SrEp metagabra v karbóne znázorňuje obr. 30.

Doručené / Received: 10. 5. 2018
Prijaté na publikovanie / Accepted: 5. 6. 2018

Supplement - Tables

Table 1. The whole rock analyses of Cpx/Sr epidote metagabbro.

Rock	Metagabbro	Metagabbro	Metagabbro	Metagabbro-mylonite	Metagabbro	Metagabbro	Metagabbro	Metagabbro	Metagabbro
Locality	Babiná 1	Babiná 2	Ostrá	Šajby	Dobšinský	Zadné Porče 1	Zadné Porče 1	Zadné Porče 2	Zadné Porče 2
Place	Babiná hill 1	Babiná hill 2	Ostrá hill	Šajby hill	potok	Lastovičí hill 1	Lastovičí hill 2	Piverský potok 1	Piverský potok 2
SiO_2 (wt.%)	45.20	46.50	46.60	56.10	48.70	50.60	51.30	46.50	48.70
TiO_2	1.74	1.77	1.59	1.85	1.89	1.77	1.62	1.23	1.50
Al_2O_3	17.00	21.70	15.30	14.81	14.00	15.50	13.40	16.90	15.50
Fe_2O_3	9.44	8.33	9.19	10.79	11.90	11.00	10.60	10.10	10.20
MnO	0.13	0.11	0.13	0.11	0.21	0.14	0.15	0.20	0.23
MgO	6.52	3.84	6.36	2.83	7.20	6.51	7.46	8.60	7.16
CaO	11.50	9.65	12.40	4.34	9.25	6.50	8.82	10.30	10.20
Na_2O	3.40	4.00	3.90	7.22	2.50	4.80	3.80	2.60	3.50
K_2O	0.08	0.64	0.08	0.31	0.73	0.05	0.05	0.05	0.05
P_2O_5	0.21	0.20	0.18	0.35	0.27	0.17	0.17	0.16	0.22
LOI	4.62	3.04	4.02	1.09	2.96	2.77	2.26	3.10	2.59
Total (wt.%)	99.84	99.78	99.75	99.80	99.61	99.81	99.63	99.74	99.85
Ba (mg/kg)	51	734	102	129	123	33	35	28	27
Rb	1.20	7	1.70	13.79	11	0.20	0.40	0.40	0.40
Sr	574	405	1040	233	504	310	775	412	659
Cs	0.36	0.39	0.36	14.86	0.43	0.04	0.06	0.05	0.07
Li	28	52	27	4	19	36	28	59	36
Ga	15	20	14	15	15	16	15	16	16
Ta	3.16	6.57	1.15	2.39	1.11	2.19	1.01	1.71	3.50
Nb	11	12	9	22	16	10	8	14	17
Hf	1.10	4.10	1.10	1.18	0.94	1.20	0.80	1.60	0.80
Zr	103	101	85	195	133	91	83	75	85
Y	16	15	13	23.39	20	20	18	13	15
Th	1	1	0.90	1.69	0.74	1.30	0.10	1.90	2
U	0.20	0.20	0.20	0.39	0.25	0.30	0.30	0.40	0.40
Cr	162	65	244	10	529	202	314	334	125
Ni	92	31	100	8	101	50	53	139	62
Co	43	26	41	23	39.9	36	33	43	39
Sc	30	22	34	22	39	33	44	25	29
Cu	68	60	9	5	14	66	67	33	73
Pb	4.50	8.70	2.70	6	14.10	12.20	73.30	15.90	32.30
Zn	77	72	74	51	119	125	138	122	110
B	3.70	26	7	4	12	2.20	2.60	3	2.90
Be	0.04	0.70	0.50	0.60	1.20	0.90	0.80	1.10	0.80
La	10	11	9	17.95	11.4	9	8	12	13
Ce	24	25	21	43.58	33	21	19	24	27
Pr	2.83	2.68	2.43	5.43	3.97	2.41	2.17	2.38	2.85
Nd	13	11.90	11.10	26.81	18.70	11.20	10.30	10.20	12.30
Sm	3.31	2.92	2.86	6.37	5.32	3.31	2.97	2.41	2.90
Eu	1.20	1.45	1.07	1.95	1.68	1.14	1.04	0.93	1.13
Gd	3.53	3.16	3.06	5.88	5.04	3.81	3.55	2.79	3.39
Tb	0.56	0.51	0.50	0.92	0.72	0.65	0.62	0.44	0.52
Dy	3.04	2.59	2.62	5.33	4.12	3.63	3.48	2.26	2.75
Ho	0.54	0.46	0.48	0.87	0.71	0.68	0.65	0.42	0.50
Er	1.46	1.27	1.26	2.19	1.79	1.84	1.71	1.14	1.36
Tm	0.17	0.16	0.16	0.24	0.21	0.22	0.21	0.14	0.16
Yb	1.01	0.93	0.93	1.34	1.06	1.32	1.21	0.90	0.99
Lu	0.13	0.12	0.12	0.13	0.14	0.18	0.16	0.12	0.13
Total (mg/kg)	1350.04	1733.81	1864.2	904.28	1801.53	1108.92	1745.44	1399.19	1405.15

Table 2.
Representative EMPA analyses of Fe-rich pumpellyite (FePmp), Pmp - pumpellyite (Pmp), grossular (Grs), andradite (Adr) and baddeleyite (Bad) from Cpx/SrEp metagabbro.

Mineral	FePmp	FePmp	Pmp	Pmp	Pmp	Pmp	Pmp	FePmp	Grs	Adr	**Mineral**	Bad
Place	matrix	matrix	in SrEp	in SrEp	in SrEp	in SrEp	in SrEp	in SrEp	in Czo/Ep1	core	**Place**	in Zrn
Locality	Babiná	Ostrá	Babiná	Ostrá	Babiná	Ostrá	Šajby mylonite	Zadné Porče	Ostrá	Babiná	**Locality**	Zadné Porče
Nappe	Rakovec	Rakovec	Rakovec	Rakovec	Rakovec	Rakovec	Rakovec	Jedľovec	Rakovec	Rakovec	**Nappe**	Jedľovec
Event	M1a-ret.	M1a-ret.	M1a-ret.	M1a-ret.	M1a-ret.	M1a-ret.	M1a-ret.	M1a-ret.	M1a	M1b	**Event**	Magma
SiO_2	37.36	38.19	36.81	37.82	37.11	37.82	37.09	37.02	37.46	36.75	**ZrO_2**	96.35
TiO_2	0.00	0.10	0.00	0.00	0.00	0.00	0.00	0.04	1.25	0.62	**TiO_2**	0.39
Al_2O_3	22.52	23.90	25.10	23.17	26.24	26.45	23.11	22.55	15.34	9.83	**SrO**	0.14
Cr_2O_3	0.00	0.00	0.00	0.00	0.00	0.00	0.00	0.00	0.46	0.00	**FeO**	0.79
Fe_2O_3	0.00	0.00	0.00	0.00	0.00	0.00	0.00	0.00	9.12	17.63	**CaO**	0.06
FeO	11.87	9.96	5.64	7.51	3.93	4.03	8.94	11.67	0.45	0.00	**Yb_2O_3**	0.14
MnO	0.00	0.00	0.00	0.00	0.00	0.00	0.00	0.15	1.25	1.10	**Tb_2O_3**	0.09
MgO	0.15	0.50	2.64	2.98	2.49	2.29	1.75	0.04	0.03	0.34	**Er_2O_3**	0.29
CaO	22.30	21.29	22.84	23.09	22.45	22.50	22.47	21.72	34.25	32.86	**Nb_2O_3**	0.41
Na_2O	0.00	0.30	0.73	0.56	0.92	1.05	0.40	0.00	0.09	0.01	**HfO_2**	1.85
K_2O	0.13	0.16	0.11	0.13	0.14	0.13	0.07	0.01	0.00	0.00	**P_2O_5**	0.07
Total	94.33	94.40	93.87	95.26	93.28	94.27	93.83	93.20	99.69	99.14	**Total**	100.58
Si	3.066	3.084	2.944	3.010	2.957	2.977	2.999	3.001	2.937	2.959	**Zr**	0.970
Al	2.176	2.273	2.364	2.171	2.462	2.452	2.200	2.152	1.416	0.932	**Ti**	0.006
Ti	0.000	0.006	0.000	0.000	0.000	0.000	0.002	0.002	0.074	0.038	**Sr**	0.002
Fe^{3+}	0.000	0.000	0.102	0.099	0.075	0.092	0.000	0.203	0.538	1.068	**Fe**	0.014
Cr	0.000	0.000	0.000	0.000	0.000	0.000	0.000	0.000	0.028	0.000	**Ca**	0.001
Mg	0.018	0.060	0.315	0.354	0.296	0.269	0.211	0.005	0.004	0.041	**Yb**	0.001
Fe^{2+}	0.815	0.673	0.275	0.401	0.187	0.173	0.604	0.655	0.029	0.051	**Tb**	0.001
Mn	0.000	0.000	0.000	0.000	0.000	0.000	0.000	0.010	0.083	0.075	**Er**	0.002
Na	0.000	0.047	0.113	0.086	0.142	0.160	0.063	0.000	2.877	0.000	**Nb**	0.010
Ca	1.961	1.842	1.957	1.969	1.916	1.898	1.946	1.886	0.014	2.834	**Hf**	0.011
K	0.014	0.016	0.011	0.013	0.014	0.013	0.007	0.001	0.000	0.000	**P**	0.001
Cations	8.050	8.001	8.081	8.103	8.049	8.034	8.031	7.915	8.000	7.998	**Cations**	1.019
OH	1.800	1.800	1.800	1.800	1.800	1.800	1.800	1.800				

Table 2. Continuation.
Representative EMPA analyses of Sr-rich epidotes (SrEp) from Cpx/SrEp metagabbro.

Mineral	SrEp	SrEp	SrEp	SrEp	SrEp	SrEp	SrEp	SrEp	SrEp	SrEp	SrEp	SrEp	SrEp	SrEp
Place	core	core	core	core	core	core	core	core	core	core	core	core	core	core
Locality	Babiná	Ostrá	Babiná	Ostrá	Ostrá breccia	Ostrá	Šajby mylonite	Dobšinský potok	Babiná	Šajby mylonite	Šajby mylonite	Ostrá	Babiná	Šajby mylonite
Nappe	Rakovec	Rakovec	Rakovec	Rakovec	Rakovec	Rakovec	Rakovec	Dobš. Group	Rakovec	Rakovec	Rakovec	Rakovec	Rakovec	Rakovec
Event	M1a-prog.	M1a-prog.	M1a-prog.	M1a-prog.	M1a-prog.	M1a-prog.	M1a-prog.	M1a-prog.	M1a-prog.	M1a-prog.	M1a-prog.	M1a-prog.	M1a-prog.	M1a-prog.
SiO_2	35.20	34.79	35.69	35.65	35.20	34.49	35.08	35.81	35.25	35.90	36.97	36.75	36.00	36.82
TiO_2	0.00	0.05	0.14	0.16	0.10	0.03	0.10	0.02	0.08	0.16	0.03	0.02	0.24	0.16
Al_2O_3	19.57	18.70	20.39	20.40	20.46	20.79	19.48	20.91	21.24	17.59	19.80	18.93	20.29	20.21
Fe_2O_3	14.76	16.14	14.30	13.42	13.27	13.32	15.20	16.68	13.74	19.11	16.47	18.16	16.44	16.66
Y_2O_3	0.01	0.00	0.00	0.32	0.30	0.00	0.00	0.00	0.00	0.00	0.00	0.09	0.00	0.00
La_2O_3	0.08	0.00	0.00	1.07	0.98	2.20	1.07	0.00	1.10	0.16	0.17	0.62	0.32	0.00
Ce_2O_3	0.00	0.00	0.00	1.32	1.06	2.22	2.48	0.00	1.98	0.35	0.36	0.81	0.65	0.03
Pr_2O_3	0.00	0.00	0.00	0.30	0.25	0.48	0.50	0.00	0.38	0.08	0.16	0.06	0.20	0.08
Nd_2O_3	0.00	0.00	0.00	0.47	0.45	0.51	1.39	0.00	0.89	0.18	0.24	0.32	0.37	0.04
Sm_2O_3	0.00	0.00	0.00	0.00	0.10	0.15	0.31	0.00	0.19	0.00	0.00	0.00	0.21	0.00
Gd_2O_3	0.00	0.00	0.00	0.42	0.30	0.00	0.35	0.00	0.00	0.00	0.00	0.00	0.00	0.00
Dy_2O_3	0.00	0.00	0.00	0.00	0.00	0.00	0.00	0.00	0.00	0.00	0.00	0.00	0.00	0.00
MnO	0.00	0.08	0.02	0.12	0.00	0.06	0.05	0.18	0.00	0.03	0.07	0.06	0.09	0.08
MgO	0.00	0.04	0.01	0.00	0.03	0.08	0.00	0.00	0.05	0.00	0.00	0.00	0.00	0.00
CaO	15.07	14.32	16.82	15.22	16.68	16.27	16.38	19.27	18.14	20.26	21.62	21.17	21.84	22.84
SrO	13.27	13.95	10.13	8.96	8.99	7.12	6.08	4.96	4.65	4.07	2.18	1.91	1.13	0.84
Na_2O	0.00	0.07	0.01	0.00	0.13	0.00	0.00	0.03	0.00	0.01	0.03	0.00	0.00	0.00
K_2O	0.00	0.00	0.01	0.00	0.02	0.00	0.00	0.00	0.00	0.00	0.00	0.00	0.00	0.00
F	0.00	0.00	0.00	0.00	0.00	0.00	0.00	0.00	0.00	0.00	0.00	0.05	0.00	0.00
Cl	0.00	0.00	0.00	0.00	0.01	0.00	0.00	0.00	0.00	0.00	0.00	0.00	0.00	0.00
Total	97.95	98.14	97.52	97.83	98.35	97.72	98.47	97.85	97.69	97.91	98.11	98.95	97.78	97.76
Si	3.023	3.008	3.020	3.041	2.995	2.961	2.997	2.961	2.970	3.007	3.028	3.014	2.963	2.998
Al	1.979	1.904	2.032	2.049	2.050	2.102	1.960	2.036	2.107	1.735	1.910	1.828	1.967	1.938
Ti	0.000	0.003	0.009	0.010	0.006	0.002	0.006	0.001	0.005	0.010	0.002	0.001	0.015	0.010
Fe^{3+}	0.953	1.049	0.910	0.860	0.849	0.860	0.976	1.037	0.870	1.203	1.014	1.120	1.017	1.020
Cr	0.000	0.000	0.000	0.000	0.000	0.000	0.000	0.000	0.000	0.000	0.000	0.000	0.000	0.000
Y	0.000	0.000	0.000	0.015	0.014	0.000	0.000	0.000	0.000	0.000	0.000	0.004	0.000	0.000
La	0.003	0.000	0.000	0.034	0.031	0.070	0.034	0.000	0.034	0.005	0.005	0.019	0.010	0.000
Ce	0.000	0.000	0.000	0.041	0.033	0.070	0.077	0.000	0.061	0.011	0.011	0.024	0.020	0.001
Pr	0.000	0.000	0.000	0.009	0.008	0.015	0.016	0.000	0.012	0.002	0.005	0.002	0.006	0.002
Nd	0.000	0.000	0.000	0.014	0.014	0.016	0.042	0.000	0.027	0.005	0.007	0.009	0.011	0.001
Sm	0.000	0.000	0.000	0.000	0.003	0.004	0.009	0.000	0.006	0.000	0.000	0.000	0.006	0.000
Gd	0.000	0.000	0.000	0.012	0.008	0.000	0.010	0.000	0.000	0.000	0.000	0.000	0.000	0.000
Dy	0.000	0.000	0.000	0.000	0.000	0.000	0.000	0.000	0.000	0.000	0.000	0.000	0.000	0.000
Mn	0.000	0.006	0.001	0.009	0.000	0.004	0.004	0.013	0.000	0.002	0.005	0.004	0.006	0.006
Mg	0.000	0.005	0.001	0.000	0.004	0.010	0.000	0.000	0.006	0.000	0.000	0.000	0.000	0.000
Ca	1.387	1.327	1.525	1.391	1.521	1.497	1.499	1.707	1.637	1.818	1.897	1.860	1.926	1.992
Sr	0.661	0.699	0.497	0.443	0.444	0.354	0.301	0.238	0.227	0.198	0.104	0.091	0.054	0.040
Na	0.000	0.012	0.002	0.000	0.021	0.000	0.000	0.005	0.000	0.002	0.005	0.000	0.000	0.000
K	0.000	0.000	0.001	0.000	0.002	0.000	0.000	0.000	0.000	0.000	0.000	0.000	0.000	0.000
Cations	8.006	8.013	7.998	7.942	8.020	7.985	7.982	7.998	7.995	8.003	8.000	7.985	8.018	8.009

Table 2. Continuation.
Representative EMPA analyses of Sr-rich epidote (SrEp), clinozoisite (Czo) and epidote (Ep1, Ep2) from Cpx/SrEp metagabbro.

Mineral	SrEp	SrEp	SrEp	SrEp	SrEp	SrEp	SrEp	SrEp	Czo1	Ep1	Ep2	Ep2	Ep2	Ep2
Place	core	core	core	core	core	core	core	core	rim1	rim1	rim2	rim2	rim2	rim2
Locality	Zadné Porče	Zadné Porče	Zadné Porče	Zadné Porče	Zadné Porče	Zadné Porče	Zadné Porče	Zadné Porče	All localities	All localities	All localities	All localities	All localities	All localities
Nappe	Jedľovec	Jedľovec	Jedľovec	Jedľovec	Jedľovec	Jedľovec	Jedľovec	Jedľovec						
Event	M1a-prog.	M1a-prog.	M1a-prog.	M1a-prog.	M1a-prog.	M1a-prog.	M1a-prog.	M1a-prog.	M1a-ret.	M1a-ret.	M1b	M1b	M1b	M1b
SiO_2	34.51	35.28	35.79	35.34	36.56	35.93	37.48	37.71	38.17	37.79	37.51	37.36	38.02	36.82
TiO_2	0.05	0.07	0.02	0.04	0.04	0.12	0.01	0.01	0.00	0.02	0.00	0.05	0.08	0.16
Al_2O_3	17.64	19.24	19.49	19.76	20.00	21.68	21.77	23.18	28.05	25.11	21.31	23.41	23.17	20.21
Fe_2O_3	17.26	16.14	15.99	15.45	16.45	14.04	14.35	13.29	8.69	10.42	13.78	13.07	12.91	16.66
Y_2O_3	0.00	0.00	0.00	0.00	0.00	0.00	0.00	0.00	0.00	0.00	0.00	0.00	0.00	0.00
La_2O_3	0.00	0.00	0.00	0.45	0.00	0.17	0.00	0.00	0.00	0.00	0.00	0.00	0.00	0.00
Ce_2O_3	0.00	0.00	0.00	0.94	0.00	0.43	0.00	0.00	0.00	0.00	0.00	0.01	0.00	0.00
Pr_2O_3	0.00	0.00	0.00	0.21	0.00	0.15	0.00	0.00	0.00	0.00	0.00	0.01	0.00	0.03
Nd_2O_3	0.00	0.00	0.00	0.28	0.00	0.10	0.00	0.00	0.00	0.00	0.00	0.10	0.00	0.08
Sm_2O_3	0.00	0.00	0.00	0.00	0.00	0.00	0.00	0.00	0.00	0.00	0.00	0.00	0.00	0.04
Gd_2O_3	0.00	0.00	0.00	0.00	0.00	0.00	0.00	0.00	0.00	0.00	0.00	0.00	0.00	0.00
Dy_2O_3	0.00	0.00	0.00	0.00	0.00	0.00	0.00	0.00	0.00	0.00	0.00	0.00	0.00	0.00
MnO	0.05	0.01	0.03	0.07	0.01	0.11	0.22	0.22	0.00	0.15	0.00	0.21	0.09	0.08
MgO	0.00	0.00	0.00	0.00	0.00	0.00	0.00	0.00	0.10	0.01	0.00	0.00	0.00	0.00
CaO	14.09	16.11	17.17	17.21	19.63	20.10	20.42	22.94	23.77	23.72	24.79	23.53	23.40	22.84
SrO	13.98	11.03	9.33	7.53	5.39	4.37	3.71	0.21	0.00	0.00	0.00	0.16	0.01	0.84
Na_2O	0.07	0.17	0.00	0.04	0.07	0.10	0.05	0.00	0.00	0.00	0.00	0.00	0.01	0.00
K_2O	0.00	0.01	0.00	0.00	0.00	0.00	0.00	0.00	0.09	0.00	0.00	0.00	0.00	0.00
F	0.00	0.00	0.00	0.00	0.00	0.00	0.00	0.00	0.00	0.00	0.00	0.00	0.00	0.00
Cl	0.02	0.00	0.00	0.00	0.00	0.00	0.00	0.00	0.00	0.00	0.00	0.00	0.00	0.00
Total	97.67	98.06	97.82	97.32	98.15	97.30	98.01	97.56	98.87	97.22	97.39	97.91	97.69	97.76
Si	3.015	3.005	3.024	3.004	3.020	2.975	3.044	3.016	2.955	3.002	3.029	2.984	3.030	2.998
Al	1.815	1.930	1.939	1.978	1.945	2.114	2.082	2.183	2.558	2.349	2.026	2.202	2.174	1.938
Ti	0.003	0.004	0.001	0.003	0.002	0.007	0.001	0.001	0.000	0.001	0.000	0.003	0.005	0.010
Fe^{3+}	1.134	1.034	1.016	0.987	1.021	0.874	0.876	0.799	0.506	0.622	0.836	0.785	0.773	1.020
Cr	0.000	0.000	0.000	0.000	0.000	0.000	0.000	0.000	0.000	0.000	0.000	0.000	0.000	0.000
Y	0.000	0.000	0.000	0.000	0.000	0.000	0.000	0.000	0.000	0.000	0.000	0.000	0.000	0.000
La	0.000	0.000	0.000	0.014	0.000	0.005	0.000	0.000	0.000	0.000	0.000	0.000	0.000	0.000
Ce	0.000	0.000	0.000	0.029	0.000	0.013	0.000	0.000	0.000	0.000	0.000	0.000	0.000	0.001
Pr	0.000	0.000	0.000	0.006	0.000	0.005	0.000	0.000	0.000	0.000	0.000	0.003	0.000	0.002
Nd	0.000	0.000	0.000	0.008	0.000	0.003	0.000	0.000	0.000	0.000	0.000	0.000	0.000	0.001
Sm	0.000	0.000	0.000	0.000	0.000	0.000	0.000	0.000	0.000	0.000	0.000	0.000	0.000	0.000
Gd	0.000	0.000	0.000	0.000	0.000	0.000	0.000	0.000	0.000	0.000	0.000	0.000	0.000	0.000
Dy	0.000	0.000	0.000	0.000	0.000	0.000	0.000	0.000	0.000	0.000	0.000	0.000	0.000	0.000
Mn	0.004	0.001	0.002	0.005	0.001	0.008	0.015	0.015	0.000	0.010	0.000	0.014	0.006	0.006
Mg	0.000	0.000	0.000	0.000	0.000	0.000	0.000	0.000	0.012	0.001	0.000	0.000	0.000	0.000
Ca	1.319	1.470	1.554	1.567	1.737	1.783	1.777	1.966	1.972	2.019	2.145	2.014	1.998	1.992
Sr	0.708	0.545	0.457	0.371	0.258	0.210	0.175	0.010	0.000	0.000	0.000	0.007	0.000	0.040
Na	0.012	0.028	0.000	0.007	0.011	0.016	0.008	0.000	0.014	0.000	0.000	0.000	0.000	0.000
K	0.000	0.001	0.000	0.000	0.000	0.000	0.000	0.000	0.000	0.000	0.000	0.000	0.000	0.000
Cations	8.010	8.018	7.993	7.987	7.995	8.016	7.978	7.990	8.017	8.004	8.036	8.012	7.986	8.009

Table 3.
Representative EMPA analyses of jadeite (Jd), aegirine-augite (Aeg-Aug), Na-rich diopside (NaDi), diopside (Di1, Di2), Al-rich celadonite (AlCel), phengite (Png1, Png2), biotite (Bt) and spinels – Mg-rich chromite (MgChr) and chromite (Chr) from Cpx/Sr epidote metagabbro.

Mineral	Jd	Jd	Jd	Jd	Aeg-Aug	Aeg-Aug	Aeg-Aug	Aeg-Aug	Aeg-Aug	Aeg-Aug	NaDi	NaDi	Aeg-Aug	Aeg-Aug	Aeg-Aug	NaDi	NaDi
Place	inclusion in Czo-Ep1	inclusion in Czo-Ep1	inclusion in Czo-Ep1	inclusion in Czo-Ep1	lamella in Di1	lamella in Di1	lamella in Di1	lamella in Di1	lamella in Di1	lamella in Di1	lamella in Di1	lamella in Di1	lamella in Di1	lamella in Di1	lamella in Di1	lamella in Di1	lamella in Di1
Locality	Ostrá	Ostrá	Babiná	Babiná	Ostrá	Ostrá	Ostrá	Babiná	Babiná	Babiná	Ostrá	Babiná	Ostrá breccia	Ostrá breccia	Ostrá breccia	Ostrá breccia	Ostrá breccia
Nappe	Rakovec	Rakovec	Rakovec	Rakovec	Rakovec	Rakovec	Rakovec	Rakovec	Rakovec	Rakovec	Rakovec	Rakovec	Rakovec	Rakovec	Rakovec	Rakovec	Rakovec
Event	M1a-ret.	M1a-ret.	M1a-ret.	M1a-ret.	M1a-ret.	M1a-ret.	M1a-ret.	M1a-ret.	M1a-ret.	M1a-ret.	M1a-ret.	M1a-ret.	M1a-ret.	M1a-ret.	M1a-ret.	M1a-ret.	M1a-ret.
SiO_2	57.57	57.88	57.05	58.64	53.19	54.27	52.98	52.59	52.85	53.02	54.22	54.17	52.72	52.91	52.80	53.08	54.24
TiO_2	0.05	0.22	0.13	0.15	0.07	0.12	0.01	0.03	0.01	0.01	0.01	0.03	0.04	0.05	0.32	0.02	0.06
Al_2O_3	16.79	17.26	19.75	19.72	2.79	3.22	1.33	0.97	0.57	0.44	0.44	2.11	1.65	1.82	1.85	1.16	2.45
FeO	9.60	9.85	5.82	5.88	19.74	12.37	15.79	19.76	15.75	14.67	10.53	9.09	19.73	16.13	12.11	12.80	16.20
Cr_2O_3	0.00	0.01	0.00	0.00	0.06	0.28	0.05	0.08	0.04	0.03	0.00	0.04	0.00	0.04	0.12	0.01	0.00
MnO	0.00	0.00	0.00	0.05	0.24	0.28	0.26	0.32	0.58	0.54	0.40	0.28	0.34	0.28	0.25	0.29	0.27
NiO	0.00	0.00	0.00	0.00	0.01	0.00	0.00	0.00	0.00	0.00	0.00	0.00	0.00	0.01	0.00	0.01	0.01
MgO	0.66	0.39	0.88	0.44	4.23	8.43	8.12	5.62	7.95	8.77	11.75	11.17	5.75	7.06	10.66	9.10	12.60
CaO	1.73	0.92	1.66	1.00	9.01	14.04	18.14	13.36	16.37	17.70	22.92	21.24	12.42	14.75	19.10	20.55	11.70
Na_2O	13.43	13.22	13.98	14.41	8.84	5.95	3.33	6.08	4.68	3.92	1.28	1.98	7.02	5.53	3.37	2.54	1.27
K_2O	0.02	0.01	0.00	0.00	0.00	0.01	0.01	0.00	0.00	0.00	0.01	0.04	0.01	0.00	0.00	0.00	0.13
Total	99.85	99.76	99.27	100.29	98.18	98.97	100.02	98.81	98.80	99.10	101.56	100.15	99.68	98.58	100.58	99.56	98.93

Mineral	Di1	Di1	Di1	Di1	Di2	Di2	Di1	Di2	AlCel	Png1	Png2	Bt
Place	core	core	core	core	rim	rim	rim matrix	rim	in Czo/Ep1	matrix	matrix	matrix
Locality			Ostrá breccia	Zadné Porče	Ostrá	Babiná	Ostrá breccia	Zadné Porče	Ostrá	Ostrá	Babiná	Ostrá
Nappe			Rakovec	Jedľovec	Rakovec	Rakovec	Rakovec	Jedľovec	Rakovec	Rakovec	Rakovec	Rakovec
Event	magmatic	magmatic	magmatic	magmatic	M1b	M1b	M1b	M1b	M1a	M1b	M1b	M1b
SiO_2	52.53	51.83	51.65	52.06	48.75	49.04	47.91	50.56	55.38	49.00	45.37	37.89
TiO_2	0.58	0.89	0.00	0.86	2.23	2.11	2.17	1.36	0.00	0.11	0.00	0.98
Al_2O_3	2.65	3.24	0.07	2.52	5.43	5.03	5.88	2.71	19.53	26.22	36.43	13.78
FeO	5.43	6.04	14.88	7.01	6.96	9.04	8.76	10.02	4.40	5.05	0.65	22.61
Cr_2O_3	0.49	0.26	0.00	0.10	0.42	0.05	0.13	0.01	0.00	0.00	0.00	0.30
MnO	0.17	0.11	1.59	0.18	0.15	0.23	0.12	0.24	0.00	0.00	0.00	0.20
NiO	0.00	0	0.00	0.01	0.07	0.00	0.00	0.01	0.00	0.00	0.00	0.00
MgO	17.38	16	7.89	15.14	14.04	13.73	13.79	13.52	4.15	4.12	1.13	10.18
CaO	20.53	21.8	23.72	21.64	21.68	20.95	20.99	21.12	0.00	0.00	0.00	0.09
Na_2O	0.45	0.21	0.38	0.38	0.30	0.34	0.30	0.28	0.63	0.00	0.27	0.02
K_2O	0.00	0	0.00	0.00	0.01	0.01	0.02	0.00	11.20	11.68	11.72	9.71
Total	100.21	100.38	100.18	99.90	100.05	100.53	100.06	99.83	95.29	96.18	95.57	95.76

Mineral	MgChr	MgChr	Chr
Place	inDi1 core	inDi1 core-rim	inDi1 rim1
Locality	Dobšinský potok	Dobšinský potok	Dobšinský potok
Nappe	Dobš. Group	Dobš. Group	Dobš. Group
Event	magmatic	magmatic	magmatic
TiO_2	1.38	1.34	0.96
Al_2O_3	16.73	16.55	13.03
Cr_2O_3	45.22	43.89	37.63
FeO	16.45	18.20	26.11
Fe_2O_3	6.60	7.73	13.61
MnO	0.30	0.76	2.14
MgO	13.24	11.23	0.67
ZnO	0.06	0.14	6.00
NiO	0.16	0.14	0.02
V_2O_3	0.24	0.23	0.00
Total	100.37	100.21	100.17

Table 4.
Representative EMPA analyses of amphiboles from Cpx/Sr epidote metagabbro. Anthophyllite (Ath), kearsutite (Krs), glaucophane (Gln), winchite (Win), actinolite (Act1, Act2), hornblende (Hbl), Fe-rich pargasite (FePrg), barroisite (Bar), riebeckite (Rbc) and edenite (Ed).

Mineral	Ath	Krs	Gln	Win	FeWin	Win	Win	Act1	Act1	Hbl	FePrg	FePrg	FePrg	FePrg	FePrg	FePrg	FePrg	Ed	Act-Hbl2	Act2	Act2
Place	in Di1	in Di1	core in Act1	core in Act1	core in Act1	core in Act1	core in Act1	rim of Act1	rim of Act1	core in Act2	crack in Di1	in Ab matrix	core matrix	core matrix	core matrix	crack in Di1	crack in Di1	rim of FePrg	rim of FePrg	rim of FePrg	rim of Act1
Locality	Babiná	Babiná	Babiná	Babiná	Ostrá	Babiná	Babiná	Babiná	Ostrá	Babiná	Babiná	Ostrá	Babiná	Babiná	Ostrá	Babiná	Ostrá	Babiná	Ostrá	Babiná	Ostrá
Nappe	Rakovec	Rakovec	Rakovec	Rakovec	Rakovec	Rakovec	Rakovec	Rakovec	Rakovec	Rakovec	Rakovec	Rakovec	Rakovec	Rakovec	Rakovec	Rakovec	Rakovec	Rakovec	Rakovec	Rakovec	Rakovec
Event	magmatic	magmatic	M1a	M1a	M1a	M1a	M1a	M1a	M1a	M1b	M1b	M1b	M1b	M1b	M1b	M1b	M1b	M1b	M1b	M1b	M1b
SiO_2	50.60	40.26	54.78	54.50	52.61	55.45	54.31	56.56	55.21	44.44	41.7	42.26	42.65	39.96	40.48	40.61	41.28	47.3	50.21	54.43	53.08
TiO_2	0.00	6.99	0.00	0.00	0.00	0.00	0.00	0.00	0.00	0.16	0.28	0.08	0.13	0.34	0.16	0.27	0.40	0.26	0.00	0.05	0.00
Al_2O_3	10.01	12.02	10.78	1.56	1.04	1.47	1.15	1.00	1.22	9.87	13.74	12.65	13.13	15.71	16.06	16.63	15.84	9.27	4.39	1.61	1.25
FeO	12.53	16.22	10.19	19.13	29.81	17.34	15.05	8.03	11.79	18.82	16.67	20.74	20.46	20.96	20.55	20.73	19.55	16.08	18.59	11.49	19.76
Cr_2O_3	0.00	0.03	0.00	0.00	0.00	0.00	0.10	0.00	0.02	0.00	0.29	0.00	0.01	0.00	0.01	0.03	0.00	0.00	0.00	0.00	0.00
MnO	0.00	0.23	0.16	0.18	0.00	0.25	0.19	0.00	0.21	0.34	0.28	0.30	0.23	0.38	0.25	0.19	0.29	0.23	0.29	0.31	0.37
MgO	22.73	5.32	8.48	12.01	5.47	13.37	14.63	19.07	16.91	10.04	9.5	7.66	6.8	6.47	6.25	5.37	6.39	10.69	12.18	16.32	10.8
CaO	1.08	12.35	7.90	5.02	5.35	6.67	9.54	13.25	12.94	10.31	11.05	9.24	9.18	8.53	9.13	7.39	7.64	10.12	10.59	12.61	12.3
Na_2O	0.65	3.55	5.03	4.79	4.52	3.89	2.33	0.69	0.37	2.54	3.43	4.00	4.11	4.68	4.76	5.36	5.79	3.23	1.19	0.4	0.49
K_2O	0.20	0.51	0.23	0.00	0.09	0.12	0.19	0.00	0.09	0.54	0.61	0.72	0.58	0.71	0.47	0.67	0.52	0.39	0.17	0.08	0.11
F	0.00	0.00	0.00	0.00	0.00	0.00	0.00	0.00	0.00	0.00	0.18	0.00	0.00	0.00	0.00	0.00	0.00	0.00	0.00	0.00	0.00
Cl	0.00	0.02	0.00	0.00	0.00	0.00	0.00	0.00	0.00	0.00	0.00	0.04	0.00	0.00	0.00	0.00	0.01	0.00	0.00	0.00	0.00
Total	97.80	97.50	97.55	97.19	98.89	98.56	97.49	98.60	98.76	97.06	97.73	97.70	97.28	97.74	98.12	97.25	97.71	97.57	97.61	97.3	98.16

Mineral	Hbl-Act2	Act2	Bar	Win	Act1	Ed	Act2	Krs	Rbc	Bar	Act1	Act1	Ed	Act-Hbl2	Act2	Act1	Act-Hbl	Act-Hbl	Act-Hbl
Place	matrix	rim matrix	core	core	rim	core	rim	core in SrEp	core in Act1	core in Act1	rim rim Bar	core in Act2	core in Act2	rim	rim	rim Di1	core matrix	rim matrix	rim matrix
Locality	Ostrá breccia	Ostrá breccia	Šajby mylonite	Šajby mylonite	Šajby mylonite	Šajby mylonite	Šajby mylonite	Dobšinský potok	Dobšinský potok	Dobšinský potok	Dobšinský potok	Dobšinský potok	Dobšinský potok	Dobšinský potok	Dobšinský potok	Zadné Porče	Zadné Porče	Zadné Porče	Zadné Porče
Nappe	Rakovec	Rakovec	Rakovec	Rakovec	Rakovec	Rakovec	Rakovec	Dobš. Group	Dobš. Group	Dobš. Group	Dobš. Group	Dobš. Group	Dobš. Group	Dobš. Group	Dobš. Group	Jedľovec	Jedľovec	Jedľovec	Jedľovec
Event	M1b	M1b	M1a	M1a	M1a	M1b	M1b	M1a	M1a	M1a	M1a	M1a	M1b	M1b	M1b	M1a	M1b	M1b	M1b
SiO_2	48.30	54.24	50.29	53.75	56.56	45.66	55.17	40.38	53.59	46.11	54.16	56.04	53.88	52.47	53.21	54.14	49.85	54.04	52.43
TiO_2	0.02	0.06	0.05	0.04	0.02	0.06	0.07	4.63	0.02	0.09	0.01	0.02	0.01	0.01	0.02	0.00	0.09	0.06	0.01
Al_2O_3	5.95	2.45	4.24	1.33	0.19	7.35	1.17	14.76	0.39	7.3	1.82	0.69	6.21	3.98	0.86	1.25	6.39	3.29	1.05
FeO	20.11	16.19	21.56	21.29	9.38	22.98	13.37	12.6	30.57	22.63	15.84	8.39	11.48	15.94	17.92	15.4	15.05	10.3	20.04
Cr_2O_3	0.00	0.00	0.00	0.01	0.00	0.00	0.05	0.03	0.00	0.00	0.00	0.01	0.20	0.01	0.00	0.02	0.00	0.09	0.00
MnO	0.31	0.27	0.23	0.27	0.28	0.27	0.4	0.18	0.23	0.41	0.28	0.15	0.29	0.30	1.19	0.51	0.42	0.43	0.9
MgO	9.81	12.6	9.56	9.97	18.48	8.41	15.44	12.3	4.39	7.94	13.5	18.82	12.99	14.25	12.07	13.58	12.79	16.43	10.34
CaO	11.05	11.7	8.08	5.34	13.05	9.61	12.24	11.65	0.9	9.77	10.98	12.84	9.80	10.78	12.45	12.44	12.14	12.43	12.32
Na_2O	1.67	1.27	3.02	4.03	0.28	2.8	0.54	2.02	6.52	2.63	1.25	0.2	0.31	0.44	0.24	0.24	0.88	0.7	0.18
K_2O	0.59	0.13	0.39	0.24	0.01	0.75	0.08	0.3	0.00	0.79	0.16	0.03	2.53	0.12	0.24	0.04	0.22	0.07	0.1
F	0.00	0.00	0.00	0.00	0.00	0.00	0.00	0.00	0.00	0.00	0.00	0.00	0.00	0.00	0.00	0.00	0.00	0.00	0.00
Cl	0.00	0.00	0.00	0.00	0.00	0.00	0.00	0.00	0.00	0.00	0.00	0.00	0.01	0.01	0.00	0.00	0.01	0.00	0.00
Total	97.80	98.91	97.42	96.26	98.25	97.89	98.48	98.82	96.61	97.67	98.00	97.18	97.49	98.30	98.2	97.6	97.84	97.75	97.37

Inštrukcie autorom

Etika publikovania, záväzná pri publikovaní v časopise Mineralia Slovaca: *www.geology.sk/new/mineralia_etika_publikovania*

1. Geovedný časopis Mineralia Slovaca publikuje scientometricky hodnotné recenzované pôvodné vedecké články s vysokým citačným potenciálom. V úvode príspevku musí autor jasne deklarovať, čím konkrétnym je jeho príspevok prínosný pre rozvoj geovied. Rešeršné štúdie sa publikujú len ojedinele.

2. Články na publikovanie (manuskripty) sa do redakcie zasielajú poštou (dva vytlačené exempláre a CD so všetkými súbormi v editovateľnej podobe) alebo e-mailom (editovateľné súbory a kompletná verzia vo formáte PDF).

3. Súčasne s článkom je potrebné redakcii poslať autorské vyhlásenie o originalite textu a obrázkov. Kópie obrázkov z iných publikácií musia byť legalizované získaním práva na publikovanie. Vyhlásenie musí obsahovať meno autora (autorov), akademický titul a trvalé bydlisko.

4. Rozsah manuskriptu na publikovanie je najviac 25 rukopisných strán (MS Word, Times New Roman, veľkosť písmen 12 bodov, riadkovanie 1,5) vrátane literatúry, obrázkov a vysvetliviek. V prípade veľkého odborného prínosu sú v ojedinelých prípadoch povolené aj dlhšie články.

5. Články sú publikované v angličtine alebo v slovenčine. Články v slovenčine musia obsahovať anglický preklad názvu, abstraktu, kľúčových slov, resumé a popisov k obrázkom a tabuľkám. Články písané v angličtine musia obsahovať slovenské resumé.

Text

1. Abstrakt stručne sumarizuje článok. Môže mať najviac 200 slov a nemá obsahovať citácie. Počet kľúčových slov je maximálne 6. Text má mať úvod, charakteristiku (stav) skúmaného problému, použitú metodiku, nové zistenia, ich interpretáciu, diskusiu, záver a zoznam literatúry. Východiskové údaje musia byť zreteľne odlíšené od interpretácií. V texte musia byť odvolávky na všetky použité obrázky a tabuľky.

2. Hierarchiu nadpisov v texte je potrebné vyznačiť ceruzkou na ľavom okraji strany manuskriptu: 1 – najvyššia, 2 – nižšia, 3 – najnižšia.

3. V texte sa uprednostňuje citácia v zátvorke, napr. (Dubčák, 1987; Hrubý et al., 1988), pred formou ... podľa Dubčáka (1987).

4. Pozícia obrázkov a tabuliek v texte sa označí. Nie je vhodné, aby text v editore MS Word obsahoval vložené obrázky, ale náhľadová verzia v pdf ich má obsahovať.

5. Grécke písmená treba identifikovať na ľavom okraji slovom (napr. sigma). Potrebné je odlišovať pomlčku od spojovníka. Symboly, matematické značky, názvy skamenelín a pod., ktoré sa majú vysádzať kurzívou, autor v rukopise podčiarkne vlnovkou.

Obrázky a tabuľky

1. Ilustrácie a tabuľky vysokej kvality bývajú publikované buď **na šírku stĺpca (81 mm), alebo strany (170 mm).** Optimálna veľkosť písma a čísiel v publikovaných obrázkoch je 2 mm. Články v slovenčine musia mať popisy v obrázkoch a tabuľkách v slovenčine, záhlavie tabuliek a texty pod obrázkami a tabuľkami sú v slovenčine a angličtine. Články v angličtine majú všetky texty v angličtine. **Maximálny rozmer ilustrácie a tabuľky vytlačený v časopise je 170 x 230 mm.** Väčšie (skladané) ilustrácie sú publikované len v ojedinelých prípadoch.

2. Pri počítačovej tvorbe obrázkov odporúčame používať programy s vektorovým zobrazením (Corel Draw, Adobe Illustrator a pod.). Čiary tzv. vlasovej hrúbky, softvérová alebo rastrová výplň plôch (napr. v Corel Draw) nie sú prípustné. Výplne v obrázkoch musia pozostávať zo samostatne vysádzaných objektov.

3. Ilustrácie vrátane fotografií musia obsahovať **grafickú mierku** v centimetrovej či metrovej škále, prípadne sa rozmer zobrazených objektov vyjadrí v popise obrázka. Mapy a profily musia mať aj **azimutálnu orientáciu** a jednotné vysvetlivky, ktoré sa uvedú pri prvom obrázku. Zoskupené obrázky, napr. fotografie a diagramy, sa uvádzajú ako jeden obrázok s jednotlivými časťami označenými písmenami (a, b, c atď.).

4. Pri zasielaní fotografií vo forme počítačových súborov (formáty JPG alebo TIF) sa požaduje rozlíšenie minimálne 600 DPI. Publikovanie farebných ilustrácií môže byť spoplatnené.

Literatúra

1. Minimálne 50 % citácií musí reprezentovať publikácie od roku 2000. V zozname literatúry sa v abecednom poradí uvádza len literatúra citovaná v danom článku.

2. Spôsob uvádzania literatúry v zozname literatúry

Knižná publikácia: Gazda, L. & Čech, M., 1988: Paleozoikum medzevského príkrovu. *Bratislava, Alfa, 155 s.*

Časopis: Vrba, P., 1989: Strižné zóny v metapelitoch. *Miner. Slov., 21, 135 – 142.*

Zborník: Návesný, D., 1987: Vysokodraselné ryolity. *In: Romanov, V. (ed.): Stratiformné ložiská gemerika. Špec. publ. Košice, Slov. geol. spol., 203 – 215.*

Manuskript: Radvanský, F., Slivka, B., Viktor, J. & Srnka, T., 1985: Žilné ložiská jedľoveckého príkrovu gemerika. Záverečná správa z úlohy SGR--geofyzika. *Manuskript. Spišská Nová Ves, archív Št. Geol. Úst. D. Štúra, 28 s.*

3. Pri článku viac ako dvoch autorov sa v texte cituje iba prvý autor s dodatkom et al., ale v zozname literatúry sa uvádzajú všetci.

Instructions to authors

Publication ethics, being obligatory for publishing in the journal Mineralia Slovaca: *www.geology.sk/new/mineralia_publikation_ethics*

1. Geoscientific journal Mineralia Slovaca publishes scientometrically valuable original peer-reviewed scientific articles with a high citation potential. In the introduction of each article the author(s) must clearly declare, which innovative data the paper brings for the development of geosciences. The retrieval studies are published only exceptionally.

2. The articles for publishing (manuscripts) must be sent to Editorial Office by post (two printed copies and CD with editable files), or by e-mail (editable files plus complete preview version in PDF format).

3. Simultaneously with the article the Editorial Office must receive the author´s proclamation that no part of the manuscript was already published and figures and tables are original as well. Copied illustrations from other publications must contain a copyright.

4. The extent of the manuscript for publishing is limited to 25 manuscript pages (MS Word, 12 points Times New Roman, line spacing 1.5) including figures, tables, explanations and references. In the case of contribution with a high scientific value, the longer manuscripts for publishing are exceptionally permitted.

5. Articles can be published in Slovak or English languages. The title, abstract, key words, shortened text (resumé), as well as description to figures and tables in Slovak articles are published also in English. Articles published in English contain Slovak resumé.

Text

1. Abstract briefly summarizing the article is limited to 200 words, no references are allowed. The maximum number of key words is 6. Text of the article has to contain the introduction, characterization (state) of investigated problem, applied methodology, obtained new data, discussion, conclusion and references. The obtained data must be distinctly separated from interpretations. All applied figures and tables must be referred in the text.

2. The hierarchy of headings in the manuscript must be indicated by a pencil note: 1 – highest level, 2 – lower, 3 – lowermost level.

3. The references in the text prefer parentheses, e.g. (Dubčák, 1987; Hrubý et al., 1988). The form "according to Dubčák (1987)" should be used only exceptionally.

4. Position of figures and tables must be indicated in the manuscript. Editable text of manuscript sent to editorial office must be without figures and tables, though the preview PDF has to contain them in a correct position.

5. Greek letter in the text must be identified at the left margin of the text (e.g. sigma). The text should strictly distinguish the dash from hyphen. Symbols, mathematic signs, names of fossils, etc., which should be printed in italics, must be underlined by the wavy line in the manuscript.

Figures and tables

1. The high quality figures and tables can be published either in **maximum width of column (81 mm) or page (170 mm).** The optimum size of letters and numbers in the camera-ready figure is 2 mm. Articles published in Slovak contain the Slovak descriptions in figures and tables, the tables headings and descriptions beneath figures and tables are in Slovak and English. English articles contain all texts in English. **Maximum dimension of figures and tables in the journal is 170 x 230 mm. Larger (fanfolded)** illustrations are published only exceptionally.

2. For figures drawing the editorial office recommends the vector graphics editors (Corel Draw, Adobe Illustrator, etc.). The very thin lines (hair lines), the pre-defined software or raster fillings of polygons (e.g. in Corel Draw) are not allowed. The filling must consist from separately set objects.

3. Each illustration including photographs must contain graphic (metric) scale, eventually the dimensions of visualized objects have to be stated in the describing text to figure. Maps and profiles must contain also the azimuth orientation, their detail explanations are stated at the first figure. Grouped figures, e.g. photographs and diagrams, are compiled as one figure with separate parts designated by letters (a, b, c, etc.).

4. The photographs sent as JPG of TIF files are required for having minimum 600 DPI resolution. Publishing of colour illustrations can be charged by a fee.

References

1. Minimum 50 % of referred works must represent contemporary publications after 2000. The references in alphanumeric order encompass only literature cited in the article.

2. Examples of referring:

Book: Gazda, L. & Čech, M., 1988: Paleozoic of the Medzev nappe. *Bratislava, Alfa, 155 p.*

Journal: Vrba, P., 1989: Shear zones in the metapelite complexes. *Miner. Slov., 21, 135–142.*

Anniversary volume: Návesný, D., 1987: High-potassium rhyolites. *In: Romanov, V. (ed.): Stratiform deposits of Gemericum. Spec. publ. Košice, Slov. geol. soc., 203–215.*

Manuscript: Radvanský, F., Slivka, B., Viktor, J. & Srnka, T., 1985: Vein deposits of the Jedľovec nappe of Gemericum. Final report from the project SGR-geophysics. *Manuscript. Spišská Nová Ves, Archive Št. Geol. Úst. D. Štúra, 28 p.*

3. The article with more than two authors is referred by the name of the first author with the amendment et al., but the list of references contains names of all authors.

Ďalšie informácie/Further information: mineralia.slovaca@geology.sk; zoltan.nemeth@geology.sk

OBSAH – CONTENT

PÔVODNÉ ČLÁNKY – ORIGINAL PAPERS

Plašienka, D.
The Carpathian Klippen Belt and types of its klippen – an attempt at a genetic classification
Karpatské bradlové pásmo a typy jeho bradiel – pokus o genetickú klasifikáciu

Pelech, O., Józsa, Š. & Fajdek, P.
Fold deformation of the Fatricum – a case study from the Banka section (Považský Inovec Mts., Slovakia)
Vrásová deformácia fatrika – prípadová štúdia z profilu Banka (Považský Inovec, Slovensko)

Csibri, T., Lačný, A., Putiška, R., Dostál, I. & Kušnirák, D.
The depth range and possible continuation of the Havranická jaskyňa cave system revealed by geological methods and electrical-resistivity tomography (ERT), the Malé Karpaty Mts., Slovakia
Hĺbkový rozsah a možné pokračovanie jaskynného systému Havranickej jaskyne, zistené geologickými metódami a elektrickou odporovou tomografiou (ERT), Malé Karpaty

Teťák, F.
Simple processing and retilting of the oriented lineations and its application in paleocurrent analysis
Jednoduché spracovanie a sklápanie usmernených lineácií a jeho aplikácia pri paleoprúdovej analýze

Radvanec, M. & Németh, Z.
Variscan epidote-eclogite, blueschists and pumpellyite-actinolite facies Cpx/Sr-rich epidote-metagabbro blocks exhumed in Carboniferous, with Permian amphibolite facies overprint (Gemeric unit, Western Carpathians)
Variská metamorfóza exhumovaných blokov metagabra bohatého na Cpx a Sr epidot v karbónskej epidotovo-eklogitovej fácii, fácii modrých bridlíc a pumpellyitovo-aktinolitovej fácii s permským prepracovaním v amfibolitovej fácii (gemerikum, Západné Karpaty)

Indexed / Abstracted / Accessed by SCOPUS and EBSCO
Indexované / abstraktované / sprístupňované databázami SCOPUS a EBSCO

www.geology.sk/mineralia